THE MODELLING OF CAKING IN BULK LACTOSE

A thesis presented partial fulfilment of the requirements for the degree of
Doctor of Philosophy in Process and Environmental Technology at Massey University

John Bronlund

B. Tech (Hons)

1997

J. Bronlund

THE MODELLING OF CAKING IN BULK LACTOSE

1 I give permission for my thesis to be made available to readers in Massey University Library under conditions determined by the Librarian.

2 I agree that my thesis, or a copy, may be sent to another institution under conditions determined by the Librarian.

3 I agree that my thesis may be copied for Library use.

Signed 

Date 22nd October 1997

Name and Address Date

ABSTRACT

Caking during storage is a serious problem for manufacturers of bulk lactose. This study was carried out to investigate the causes of caking and identify solutions as to how such problems can be eliminated.

The mechanisms for caking in crystalline lactose powders were identified. Liquid bridging between adjacent particles was shown to occur in high relative humidity environments (>80% RH) These liquid bridges could form crystalline solid bridges if the material was subsequently dried out. The potential mechanism of amorphous lactose flow and bridging in conditions where the glass transition temperature is exceeded was shown to be insignificant in predominantly crystalline lactose powders (<5% amorphous lactose) The presence of amorphous lactose is still important as the amorphous matrix acts as a sink of moisture, which can be released upon crystallisation. This increases the moisture available in the system which can contribute to caking by the liquid bridging mechanism. Both of these mechanisms involve changes in the local temperature and moisture conditions within the bulk powder. Such changes were known to be caused by moisture migration under the influence of a temperature gradient.

A model which describes the transport of moisture in one dimension as a result of temperature gradients was developed and validated. The microscopic scale processes of liquid bridging and amorphous lactose moisture relations were included into this model. The model predictions agreed well with experimental trials for completely crystalline lactose powders. Comparison of model predictions for the case where amorphous lactose was present on the surface of the particles showed some inadequacies exist in the model. These were the rate of amorphous lactose crystallisation and the assumption of instantaneous equilibrium between the crystallising amorphous matrix and the air present in the interstices of the bulk lactose.

Using the model it was shown that for expected storage conditions, the product should be stored with a water activity below 0.57 a_w if no amorphous lactose is present and below 0.25 a_w if it is present. If these prescribed limits are met then the goal of producing caking free lactose powders can be achieved.

ACKNOWLEDGEMENTS

I always used wonder why research into industrial problems satisfies the requirements for a Doctorate in Philosophy.

Then I found a definition for Philosophy;

> *Philosophy, is like a blind man, in a dark room, looking for a black cat that isn't there.*

Then I realised that this was the ideal qualification for this kind of research.

When it comes to lactose caking, I have been that blind man in the dark room. This is not to say that I didn't get any help during my search for the alleged black cat. Indeed there have been many people who have helped and encouraged me along the way.

Tony Paterson, my principal supervisor, has spent many hours over the last few years helping me ponder the riddles of what is lactose. My other supervisors, Dr Richard Archer, Dr Dong Chen and Professor Ray Winger were also of great help, particularly at the two ends of the whole exercise. Dr Jim Hargreaves's initial work into lactose has also been invaluable to this work. Also thanks to Aaron O'Donnell for all his work in searching for the same lactose cat.

John Alger, Bruce Collins and Don McLean have aided me in the design and manufacture of many cat searching devices. Thank you all very much.

I would like to thank Ma and Pa Bronlund, my family and friends who have listened and encouraged me to complete this thesis. This was mostly in the form of questions like "Is your thesis finished yet John?".The people responsible for asking such questions know who they are and many will be hearing similar questions from me in the near future. Special thanks to Jules, Kath, Dave, Kim, Lynley, Stacey, Mike, Clint, Ross, Silvia and Inge.

Thanks to Marcel Gesterkamp, Stephen Kellam, David Hall, and John Thomas at (or once with) The Lactose Company of New Zealand at Kaponga for all their valuable assistance and financial backing for this project.

Most thanks of all goes to Susie, without whose love and support, none of this would have been possible. With this thing now complete we can breath a combined sigh of relief.

At the end of this work there was still no sign of the Black Cat, but I did find a small hard deposit of a white powdery substance in one corner.

TABLE OF CONTENTS

ABSTRACT III

ACKNOWLEDGEMENTS V

TABLE OF CONTENTS VII

LIST OF FIGURES XII

LIST OF TABLES XVII

CHAPTER 1
PROJECT OVERVIEW

1.1 PROBLEM DEFINITION 1.1

1.2 PROPOSED CAKING MECHANISMS 1.2
1.2.1 HUMIDITY CAKING 1.2
1.2.2 AMORPHOUS LACTOSE CAKING 1.2

1.3 MOISTURE MIGRATION 1.2

1.4 OVERALL PROJECT AIMS 1.3

CHAPTER 2
PHYSICAL PROPERTIES OF LACTOSE

2.1 LACTOSE CHEMISTRY 2.1

2.2 LACTOSE FORMS 2.1
2.2.1 CRYSTALLINE LACTOSE 2.1
2.2.2 AMORPHOUS LACTOSE 2.3
2.2.3 PARTIALLY AMORPHOUS LACTOSE 2.3

2.3 CHARACTERISATION OF LACTOSE POWDERS 2.5
2.3.1 PARTICLE SIZE DISTRIBUTION 2.5
2.3.2 DENSITY 2.5
2.3.2.1 Particle Density 2.5
2.3.2.2 Bulk Density, Tapped Density and Porosity 2.6

2.4 THERMAL PROPERTIES 2.7
2.4.1 SPECIFIC HEAT CAPACITY 2.7
2.4.2 EFFECTIVE THERMAL CONDUCTIVITY 2.7
2.4.2.1 Experimental Measurement of Effective Thermal Conductivity 2.7
2.4.2.1.1 Measurement by the Infinite Cylinder Method *2.9*
2.4.2.1.2 Measurement by the Guarded Hot Plate Method *2.12*
2.4.2.2 Summary of Lactose Thermal Conductivity Measurements 2.13

2.5 PROPERTIES OF LACTOSE SOLUTIONS 2.13
2.5.1 SOLUBILITY 2.13
2.5.2 SURFACE TENSION 2.14

2.6 CLOSURE 2.15

CHAPTER 3
MOISTURE RELATIONS IN LACTOSE

3.1 INTRODUCTION 3.1

3.2 THE DEGREE OF BINDING OF MOISTURE IN LACTOSE 3.1
3.2.1 CHEMICALLY BOUND MOISTURE 3.1
3.2.2 PHYSICALLY ADSORBED MOISTURE 3.2
3.2.3 BOUND AND FREE MOISTURE USED IN THIS WORK 3.3

3.3 MOISTURE SORPTION ISOTHERMS 3.3
3.3.1 PUBLISHED LACTOSE ISOTHERM DATA 3.4
3.3.1.1 Crystalline Lactose 3.4
3.3.1.2 Amorphous, Spray-dried and Freeze-dried Lactose 3.5
3.3.2 EXPERIMENTAL MEASUREMENT OF LACTOSE ISOTHERM DATA 3.6
3.3.3 α-LACTOSE MONOHYDRATE 3.7
3.3.4 β-LACTOSE 3.14
3.3.5 AMORPHOUS LACTOSE 3.16
3.3.6 MIXTURES OF CRYSTALLINE AND AMORPHOUS LACTOSE 3.18

3.4 RATES OF MOISTURE SORPTION ON TO LACTOSE 3.20
3.4.1 SORPTION ON TO α-LACTOSE MONOHYDRATE 3.21
3.4.2 SORPTION ON TO AMORPHOUS LACTOSE 3.22
3.4.3 SORPTION ON TO MIXTURES OF CRYSTALLINE AND AMORPHOUS LACTOSE 3.28

3.5 MOISTURE CONTENT DETERMINATION 3.31

3.6 WATER ACTIVITY MEASUREMENT 3.33

3.7 PROPERTIES OF AMORPHOUS LACTOSE 3.34
3.7.1 GLASS TRANSITION TEMPERATURE 3.34
3.7.2 VISCOSITY OF AMORPHOUS LACTOSE 3.36
3.7.3 QUANTIFICATION OF AMORPHOUS LACTOSE IN LACTOSE POWDERS 3.37
3.7.4 CRYSTALLISATION OF AMORPHOUS LACTOSE 3.38
3.7.4.1 Product of Amorphous Lactose Crystallisation 3.38
3.7.4.2 Crystallisation Kinetics 3.41
3.7.4.2.1 Polymer Crystallisation Kinetics 3.41
3.7.4.2.2 Prediction of Crystallisation Rate in Amorphous Lactose 3.43
3.7.4.2.2.1 Sorption-desorption phenomena 3.46
3.7.4.2.2.2 β to α-lactose conversion 3.47
3.7.4.2.2.3 Crystallisation rate 3.49

3.8 EFFECTIVE MOISTURE DIFFUSIVITY IN A PACKED BED OF LACTOSE 3.54

3.9 CLOSURE 3.55

CHAPTER 4
MODELLING HEAT AND MOISTURE TRANSPORT IN BULK LACTOSE

4.1 INTRODUCTION 4.1

4.2 FORMULATION OF TRANSPORT MODEL 4.1
4.2.1 CONCEPTUAL MODEL 4.1
4.2.2 ASSUMPTIONS 4.2
4.2.3 VALIDITY OF ASSUMPTIONS 4.2
4.2.3.1 Local Thermal Equilibrium 4.2
4.2.3.2 Local Moisture Equilibrium 4.3
4.2.3.3 Negligible Convection 4.4
4.2.3.4 Negligible Heat and Moisture Transport Due to Changes in Air Density 4.4
4.2.3.5 Mode of Moisture Movement 4.5
4.2.3.6 Other Assumptions Made 4.5
4.2.4 MATHEMATICAL FORMULATION 4.6

4.3 NUMERICAL SOLUTION OF TRANSPORT MODEL 4.6
4.3.1 SELECTION OF NUMERICAL SOLUTION METHOD 4.6
4.3.2 NUMERICAL SOLUTION 4.7

4.4 MATHS CHECKING 4.8
4.4.1 CHECKS AGAINST PREVIOUSLY VALIDATED SOLUTIONS 4.8
4.4.2 NUMERICAL ERROR CHECKING 4.9
4.4.3 MATHS CHECKING SUMMARY 4.9

4.5 MATHEMATICAL MODEL EVALUATION 4.10
4.5.1 MODEL PREDICTIONS 4.10
4.5.1.1 Temperature 4.10

4.5.1.2 Water Vapour Concentration 4.11
4.5.1.3 Absolute Humidity 4.11
4.5.1.4 Relative Humidity 4.12
4.5.1.5 Moisture Content 4.13
4.5.2 Heat Losses Due to Thermal Expansion 4.14
4.5.3 Experimental Data Collection 4.14
4.5.3.1 Experimental Apparatus Design 4.14
4.5.3.2 Experimental Data Collection 4.16
4.5.4 Model Prediction Accuracy 4.19
4.5.4.1 Temperature Prediction Accuracy 4.19
4.5.4.2 Surface Relative Humidity Prediction Accuracy 4.20

4.6 Closure 4.27

Chapter 5
Caking Mechanisms

5.1 Introduction 5.1

5.2 Caking Mechanism Overview 5.1
5.2.1 Humidity Caking 5.2
5.2.2 Amorphous Sugar Re-Crystallisation 5.3
5.2.3 Alternative Mechanisms 5.4
5.2.4 Effect of Pressure and Crystal Contact Area 5.4

5.3 Caking Mechanisms Under Consideration in this Work 5.5

5.4 Caking Strength Measurement 5.6
5.4.1 Caking Strength Requirements for this Work 5.7
5.4.2 Available Strength Measurement Methods 5.7
5.4.2.1 Tensile Strength 5.7
5.4.2.2 Shear Strength and Cohesion Tests 5.8
5.4.2.3 Compaction and Compressibility Measurements 5.8
5.4.2.4 Other Methods 5.9
5.4.3 Method Development 5.9
5.4.4 Method Performance 5.10

5.5 Caking by Liquid Bridging and Subsequent Drying 5.12
5.5.1 Mechanism Overview 5.12
5.5.2 Liquid Bridging 5.12
5.5.3 Solid Bridging 5.16
5.5.4 Summary of the Liquid Bridging and Drying Caking Mechanism 5.17

5.6 Caking due to Amorphous Lactose Flow and Crystallisation 5.18
5.6.1 Mechanism Overview 5.18
5.6.2 Rubber Bridging and Sticking 5.19
5.6.3 Relative Rates of Amorphous Flow and Crystallisation 5.20
5.6.3.1 Sticking of Thin Layers of Amorphous Lactose 5.21
5.6.4 Relevance of Amorphous Lactose to Caking in Bulk Lactose 5.24

5.7 Closure 5.24

CHAPTER 6
PREDICTION OF CAKING IN BULK LACTOSE

6.1 INTRODUCTION 6.1

6.2 CAKING IN PURELY CRYSTALLINE LACTOSE POWDERS 6.1
6.2.1 OVERVIEW OF CAKING IN CRYSTALLINE LACTOSE 6.1
6.2.2 INCLUSION OF STRENGTH PREDICTION INTO THE TRANSPORT MODEL 6.1
6.2.3 EXPERIMENTAL DATA COLLECTION 6.3
6.2.4 EVALUATION OF CAKING STRENGTH PREDICTIONS 6.5
6.2.5 INVESTIGATIONS OF CONDITIONS REQUIRED FOR LUMPING IN BULK LACTOSE 6.6
6.2.6 AVOIDANCE OF LUMPING IN PURELY CRYSTALLINE LACTOSE 6.10

6.3 CAKING IN FRESHLY MILLED OR DRIED LACTOSE CONTAINING AMORPHOUS LACTOSE **6.10**
6.3.1 OVERVIEW OF REQUIREMENTS FOR AMORPHOUS LACTOSE RELATED CAKING 6.10
6.3.2 MODIFICATIONS TO THE TRANSPORT MODEL TO INCLUDE THE EFFECTS OF AMORPHOUS LACTOSE 6.11
6.3.3 THE EFFECT OF AMORPHOUS LACTOSE MOISTURE BINDING CAPACITY ON MOISTURE MIGRATION 6.12
6.3.4 PREDICTIONS OF MOISTURE TRANSPORT WITH AMORPHOUS LACTOSE CRYSTALLISATION 6.13
6.3.4.1 Crystallisation to Anhydrous Lactose Product 6.13
6.3.4.2 Crystallisation to α-Lactose Mono-hydrate 6.15
6.3.5 EXPERIMENTAL VALIDATION 6.16
6.3.6 MODEL PREDICTION ACCURACY 6.21
6.3.7 AVOIDANCE OF AMORPHOUS LACTOSE RELATED CAKING IN BULK LACTOSE 6.24

6.4 CLOSURE **6.25**

CHAPTER 7
CONCLUSIONS AND SUGGESTIONS FOR FUTURE WORK

7.1 CONCLUSIONS **7.1**

7.2 SUGGESTED FUTURE RESEARCH **7.2**

REFERENCES **8.1**

APPENDIX A-1 NOMENCLATURE **A1.1**

APPENDIX A-2 PSYCHROMETRIC PROPERTIES OF AIR **A2.1**

APPENDIX A-3 TRANSPORT MODEL FORMULATION **A3.1**

APPENDIX A-4 FINITE DIFFERENCE APPROXIMATIONS **A4.1**

APPENDIX A-5 PROGRAM SOURCE CODE **A5.1**

LIST OF FIGURES

Figure 2.1 α-Lactose chemical structure. 2.1
Figure 2.2 Muta-rotation between lactose forms 2.1
Figure 2.3 Electron micrograph of α-lactose monohydrate at 2000x magnification 2.3
Figure 2.4 Electron micrograph of β-lactose at 2000x magnification 2.3
Figure 2.5 Electron micrograph of *supertab* lactose at 100x magnification 2.3
Figure 2.6 Particle size distributions of lactose powders 2.5
Figure 2.7 Typical heating curve for an infinite cylinder full of bulk lactose . . . 2.10
Figure 2.8 Semi-log plot of lactose cylinder heating time temperature history . . 2.10
Figure 2.9 Solubility of lactose as a function of temperature 2.14
Figure 2.10 Surface tension of saturated solutions of lactose 2.15

Figure 3.1 Literature isotherm data for α-lactose monohydrate 3.5
Figure 3.2 Summary of amorphous lactose isotherm data from the literature . . . 3.6
Figure 3.3 Moisture sorption isotherm of α-lactose monohydrate 3.8
Figure 3.4 Third stage sorption isotherm model predictions for α-lactose monohydrate 3.10
Figure 3.5 Moisture content versus capillary radius for special dense α-lactose monohydrate 3.13
Figure 3.6 Capillary condensation isotherm for α-lactose monohydrate 3.14
Figure 3.7 Observed weight change of β-lactose after storage above saturated salt solutions for 1 month 3.16
Figure 3.8 Moisture sorption isotherm for amorphous lactose 3.18
Figure 3.9 Effect of small amounts of amorphous lactose on the sorption isotherm of α-lactose samples as predicted from the additive isotherm model 3.19
Figure 3.10 Sorption isotherm of *supertab* lactose 3.19
Figure 3.11 Sorption rates measurement apparatus 3.20
Figure 3.12 Rates of sorption of moisture on to crystalline lactose 3.21
Figure 3.13 Comparison of observed moisture content with that predicted from bulk air relative humidity 3.22
Figure 3.14 Rate of moisture sorption on to spray dried amorphous lactose subjected to a step change in relative humidity from 0 to 43.5% RH 3.23
Figure 3.15 Comparison of experimental sorption rates with analytical solution . 3.25
Figure 3.16 Comparison of moisture diffusivity of some foods as a function of moisture content 3.26
Figure 3.17 Predicted rates of moisture sorption into varying thicknesses of amorphous lactose 3.30
Figure 3.18 Comparison of drying techniques for the measurement of moisture content in α-lactose monohydrate 3.31
Figure 3.19 Glass transition temperature of amorphous lactose as a function of moisture content 3.35

Figure 3.20 Dependence of viscosity on temperature above glass transition temperature predicted by the WLF equation 3.36
Figure 3.21 Isothermal DSC plot for amorphous lactose at 65°C and 0.22 a_w ... 3.45
Figure 3.22 DSC plot showing desorption of water of crystallisation from crystallisation product 3.45
Figure 3.23 Comparison of moisture sorption results for amorphous lactose from Niediek (1982) and isotherm determined from this work at 20°C ... 3.46
Figure 3.24 Conversion of β to α-lactose monohydrate as indicated by moisture uptake for β and *supertab* lactose 3.47
Figure 3.25 Predicted conversion from β to α-lactose after one month 3.48
Figure 3.26 Moisture content change in amorphous lactose during crystallisation 3.50
Figure 3.27 Crystallinity as a function of time during amorphous lactose crystallisation 3.50
Figure 3.28 Avrami plot for amorphous lactose crystallisation 3.51
Figure 3.29 Prediction of crystallisation progress using Avrami equation 3.52
Figure 3.30 Comparison of crystallisation times between this work and the literature 3.52
Figure 3.31 Avrami model predictions of time to reach 90% crystallinity 3.53

Figure 4.1 Conceptual model for heat and moisture transport in bulk lactose ... 4.1
Figure 4.2 Temperature time profile for the heating of a 100mm slab 4.10
Figure 4.3 Temperature profile through lactose slab 4.11
Figure 4.4 Water vapour concentration time profile within the slab 4.11
Figure 4.5 Humidity time profile for lactose slab 4.12
Figure 4.6 Relative humidity profile development through the lactose slab 4.13
Figure 4.7 Moisture content profile development through the lactose slab 4.13
Figure 4.8 Transport model validation experimental rig 4.16
Figure 4.9 Experimental temperature profiles for a 78mm lactose slab 4.17
Figure 4.10 Experimental surface relative humidity profile for a 78mm slab ... 4.18
Figure 4.11 Experimental temperature profiles for a 100mm lactose slab 4.18
Figure 4.12 Experimental surface relative humidity profile for 100mm slab 4.19
Figure 4.13 Predictions for 78mm slab temperature profiles 4.20
Figure 4.14 78mm slab surface relative humidity profile predictions 4.21
Figure 4.15 Effect of porosity on surface relative humidity predictions 4.21
Figure 4.16 Effect of diffusivity on surface relative humidity predictions 4.22
Figure 4.17 Effect of initial temperature on surface relative humidity predictions 4.23
Figure 4.18 Effect of initial water activity on surface relative humidity predictions 4.23
Figure 4.19 Effect of slab thickness on surface relative humidity predictions ... 4.24
Figure 4.20 Sorption isotherm model fitting limits 4.24
Figure 4.21 Effect of changing isotherm shape on surface relative humidity predictions 4.25
Figure 4.22 Best attempt at surface relative humidity predictions 4.26
Figure 4.23 Model predictions for 100mm slab experimental temperature profiles 4.26
Figure 4.24 Model predictions for 100mm slab experimental surface relative humidity profiles 4.27

Figure 5.1 Humidity caking mechanism 5.5
Figure 5.2 Amorphous related caking mechanism 5.6
Figure 5.3 Strength measurement apparatus 5.10
Figure 5.4 Typical force distance profiles for lactose samples using multi pin penetrometry method 5.11
Figure 5.5 Powder strength after one day equilibration time 5.13
Figure 5.6 Powder strength after ten days equilibration time 5.13
Figure 5.7 Powder strength after fifty days equilibration 5.14
Figure 5.8 Powder strength after one day as a function of moisture content 5.15
Figure 5.9 Solid bridge strength as a function of equilibrium relative humidity prior to drying 5.17
Figure 5.10 Comparison of solid bridge strength to originating liquid bridge strength 5.17
Figure 5.11 Comparison of sticking and crystallisation times in amorphous lactose 5.20
Figure 5.12 Additive isotherm method for quantification of amorphous lactose content of freshly milled lactose sample 5.22
Figure 5.13 Freshly milled lactose strength compared with purely crystalline powder strength stored over saturated salt solutions for one week 5.22
Figure 5.14 Strength of freshly milled lactose compared with strength of crystalline lactose stored for fifty days over saturated salt solutions 5.23

Figure 6.1 Typical strength development in a 100mm lactose slab subjected to a 20°C temperature gradient 6.2
Figure 6.2 Typical strength profile through lactose slab at steady state when a 20°C gradient has been applied 6.3
Figure 6.3 Experimentally measured steady state strength profiles through lactose slabs with applied temperature gradients for approximately one day 6.4
Figure 6.4 Predicted and experimentally measured strength profiles for lactose slab experiments 6.5
Figure 6.5 Strength profile for slabs of increasing thickness as a function of the fractional position into the surface 6.6
Figure 6.6 Effect of initial product water activity on cold surface strength and relative humidity 6.7
Figure 6.7 Typical relative humidity profile for the cooling of a lactose slab from one side 6.8
Figure 6.8 Maximum strength as a function of initial water activity 6.8
Figure 6.9 Temperature profile through lactose slab cooled evenly from both sides 6.9
Figure 6.10 Strength profile through slab cooled evenly from both sides 6.9
Figure 6.11 Comparison of moisture migration rates for increasing amorphous lactose fractions 6.12
Figure 6.12 Predictions of moisture transport with crystallisation for powder containing 2.5% amorphous lactose at 20°C after subjection to 20°C temperature gradient 6.14

Figure 6.13 Moisture migration in a lactose slab starting at a water activity of 0.25 a_w showing no signs amorphous lactose crystallisation 6.14
Figure 6.14 Moisture migration with amorphous lactose crystallisation to α-lactose monohydrate 6.15
Figure 6.15 Steady state amorphous lactose fraction profile through the lactose slab 6.16
Figure 6.16 Hammer mill arrangement 6.16
Figure 6.17 Method used to raise water activity of lactose slab 6.17
Figure 6.18 Schematic of rig used to provide constant RH air 6.18
Figure 6.19 Experimental temperature profiles for 78 mm lactose slab containing 4.5% amorphous lactose 6.19
Figure 6.20 Experimental surface relative humidity profiles for a 78 mm lactose slab with 4.5% amorphous lactose initially present 6.19
Figure 6.21 Two-point isotherm results for lactose samples taken before and after the slab experiment 6.20
Figure 6.22 Comparison of experimental and predicted temperature profiles with amorphous lactose present 6.21
Figure 6.23 Comparison of experimental and predicted surface relative humidity profiles with amorphous lactose present 6.22
Figure 6.24 Comparison of predictions for crystallisation to α-lactose monohydrate with 20 and 50 nodes 6.24

LIST OF TABLES

Table 2.1 General properties of α-lacose monohydrate and β-lactose anhydride . . 2.2
Table 2.2 Summary of crystalline lactose used in this work 2.2
Table 2.3 Amount of amorphous lactose present on various industrial lactose samples 2.4
Table 2.4 Particle density of the various crystalline lactose forms 2.6
Table 2.5 Bulk density, tapped density and porosity of lactose powders 2.6
Table 2.6 Solutions for the temperature change in an infinitely long cylinder 2.9
Table 2.7 Summary of thermal conductivity measurements by infinite cylinder method 2.11
Table 2.8 Summary of thermal conductivity measurements by guarded hot plate method 2.12

Table 3.1 tss-Isotherm parameters for α-lactose monohydrate 3.10
Table 3.2 GAB isotherm parameters for amorphous lactose 3.17
Table 3.3 Summary of amorphous lactose layer thickness estimates for different lactose grades 3.28
Table 3.4 Constants n and K for the Avrami equation 3.42
Table 3.5 Effective moisture diffusivity models for flow in porous media 3.55

Table 4.1 Summary of isotherm model parameters for limiting cases 4.25

Table 5.1 Comparison of multi point penetrometer readings with observational tests 5.11

Table 6.1 Summary of experimental conditions for strength profile measurement of lactose slabs under the influence of a temperature gradient 6.4

CHAPTER 1

PROJECT OVERVIEW

1.1 PROBLEM DEFINITION:

Caking in bulk lactose during storage is a very serious problem in the New Zealand dairy industry. At the onset of this project the mechanism of the caking of bulk lactose had not been identified although research and experience had highlighted the following observations which are of interest to the caking problem;

- caking is promoted by conditions of high temperature, moisture and pressure.
- interaction between lactose and free moisture is required before caking is observed.
- moisture gains and losses from the bag to the ambient are thought to be negligible.
- moisture migration occurs within the bulk lactose.
- lactose is packed above ambient temperature which will set up a temperature gradient within the bag.
- lactose bulk bags (900kg) take approximately twelve days to cool (from 40°C to 20°C) after packing.
- incipient caking is often evident within 12 days of packing but the product may get harder subsequently.
- during shipment to northern hemisphere countries, lactose may be subjected to elevated temperatures or subjected to very low temperatures on the wharf after the product is unloaded.
- milling causes many fines to be deposited on the larger crystals. This provides a large surface area for crystal contact.
- voids which contain free moisture are present in the lactose. They are thought to be formed during rapid crystallisation. Upon milling and crystal fracture this moisture is released.
- literature suggests that rapid drying and milling can cause amorphous lactose to be produced which may contribute to the caking problem.

From these observations and a preliminary survey of literature, two main mechanisms for the caking of bulk lactose were hypothesised. These were humidity caking, and amorphous lactose crystallisation.

1.2 PROPOSED CAKING MECHANISMS:

1.2.1 HUMIDITY CAKING:

When lactose crystals are exposed to high relative humidity for a period of time, moisture is adsorbed, resulting in a thin layer of syrup on the crystal surfaces. When enough free moisture is present liquid bridges can form between adjacent crystals. Liquid bridges give some strength to the bulk lactose and are the cause of lumping.

When this "humidified" lactose is then exposed to low humidity, moisture will be desorbed. Upon the loss of this moisture, crystallisation occurs which replaces the liquid bridges with solid bridges, which cement the larger crystals together. This results in caked lactose. The extent of the caking depends on how much moisture is adsorbed and desorbed.

1.2.2 AMORPHOUS LACTOSE CAKING:

During the drying and milling processes a thin layer of amorphous lactose is thought to form. This amorphous lactose can exist in two forms; glass or rubber. In the glass phase the viscosity is so high that molecular mobility is not possible, and in the rubber phase the molecules are capable of movement, flow and crystallisation. The temperature at which the glass form becomes a rubber is known as the glass transition temperature (T_g). Moisture can act as a plasticiser which decreases the glass transition temperature.

Flow of the amorphous lactose is thought to form a rubber bridge joining adjacent crystals if the glass transition temperature is exceeded. If the lactose stays above the glass transition temperature then crystallisation of the amorphous lactose will occur and a solid bridge and hence caking will result.

1.3 MOISTURE MIGRATION:

It is widely known that moisture migration can occur within a bulk powder when a temperature gradient is applied. Moisture is transported from regions of high temperature to regions of low temperature. This can result in parts of a bag becoming wet, even when initially the whole product was apparently dry.

Both of the hypothesised caking mechanisms described above are greatly influenced by free moisture. Therefore detailed knowledge of how moisture behaves within cooling or warming bulk lactose was required if an understanding of the caking problem was to be achieved.

1.4 Overall Project Aims:

The overall aims of this research were to;

- develop an understanding of the moisture relations of the different forms of lactose and moisture relations in bulk lactose.
- develop an understanding of amorphous lactose and its interactions in bulk lactose.
- identify the caking mechanism(s) responsible for the caking of bulk lactose.
- to mathematically model and experimentally validate heat and moisture transfer in bulk lactose and to use this model to help understand caking phenomena in bulk lactose.
- to mathematically model and experimentally validate caking in bulk lactose.
- to offer solutions to industrial lactose caking problems.

CHAPTER 2

PHYSICAL PROPERTIES OF LACTOSE

2.1 LACTOSE CHEMISTRY

In solution, lactose can occur in both the α (see Figure 2.1) and β isomeric forms. The designations refer to the orientation of the hydroxyl group on the number one carbon of the glucose moiety of the lactose molecule (see Figure 2.2) [Jenness and Patton 1959].

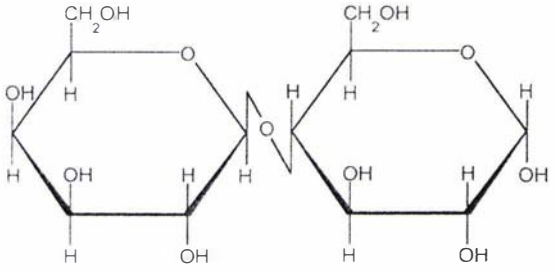

Figure 2.1 - α-Lactose chemical structure

Figure 2.2 - Muta-rotation between lactose forms

The inter-conversion between the α and β forms is termed muta-rotation, the rate of which is dependent on both temperature and solution composition. Muta-rotation occurs continuously and an equilibrium position will be eventually established. At 20°C the ratio of β/α in solution is 1.59 in pure water [Lowe 1993].

2.2 LACTOSE FORMS

Lactose powders can be either crystalline, amorphous or a mixture. Crystalline forms have very ordered molecular structure, where amorphous lactose has a largely disordered molecular structure and can be visualised as a very concentrated lactose solution. It is possible to produce several different crystalline forms. The different lactose forms and methods of manufacture are discussed by Hargreaves (1995). Discussion here will be limited to the α-lactose monohydrate and β-lactose anhydride crystal forms as well as to amorphous and partially amorphous lactose powders, as these are the lactose forms of most interest commercially and are important in caking phenomena.

2.2.1 CRYSTALLINE LACTOSE

The majority of commercially produced lactose is α-lactose monohydrate ($C_{12}H_{22}O_{11}.H_2O$). It is prepared by crystallisation from aqueous solution below 93.5°C. α-Lactose monohydrate may form many crystal shapes depending on the crystallisation

conditions, although most common are the prism and tomahawk shapes [Nickerson 1974].

When lactose crystallisation occurs above 93.5°C, the crystals formed are β-lactose anhydride. β-Lactose is much sweeter and much more soluble than α-lactose monohydrate, and therefore has a good market for uses when dissolution of large amounts of lactose is necessary. When crystallised from water the most common crystal shape is an uneven sided diamond [Nickerson 1974]. Commercially available β-lactose is produced by extrusion or roller drying and typically contains 70% in the β-form and 30% in the α-form, although commercial grades with higher β-content are available [Wade and Weller 1994]. Some commercially produced β-lactose also contains significant quantities of amorphous lactose. General properties of α-lactose monohydrate and β-lactose are given in Table 2.1 below.

Table 2.1 General properties of α-lactose monohydrate and β-lactose anhydride [adapted from Harper 1992].

Properties	α-Lactose monohydrate	β-Lactose anhydride
Molecular weight [g/mol]	360	342
Melting point [°C]	202	252
Boiling point [°C]	Disintegration not far above melting	
Heat of combustion [kJ/kg]	16,106	15,465
Heat of solution [kJ/kg]	-50.24	-9.62

The crystalline materials used in this work are listed in Table 2.2 below.

Table 2.2 Summary of crystalline lactose used in this work

Name	Lactose form	Supplier	Lot No.
Special Dense (Refined hydrous)	α-lactose.H_2O	Lactose Company of New Zealand	4030125 157
100 mesh (Refined hydrous)	α-lactose.H_2O	Lactose Company of New Zealand	4030821 101
200 mesh USP/NF/BP/EP (Refined hydrous)	α-lactose.H_2O	Lactose Company of New Zealand	5060302 116
300 mesh USP/NF/BP/EP (Refined hydrous)	α-lactose.H_2O	Lactose Company of New Zealand	5011103 127
Beta lactose (200 mesh)	78% β-lactose 22% α- lactose.H_2O[1]	Sigma L-3750	73H0314

[1] Anomeric ratio determined by polarimetry (see method in Hargreaves 1995)

Electron micrographs of 200 mesh samples of α-lactose monohydrate and β-lactose are shown as Figure 2.3 and Figure 2.4. These figures show that there are many fines and asperities present in the samples and that there is very little physical difference between the α and β lactose forms discernable from direct observation.

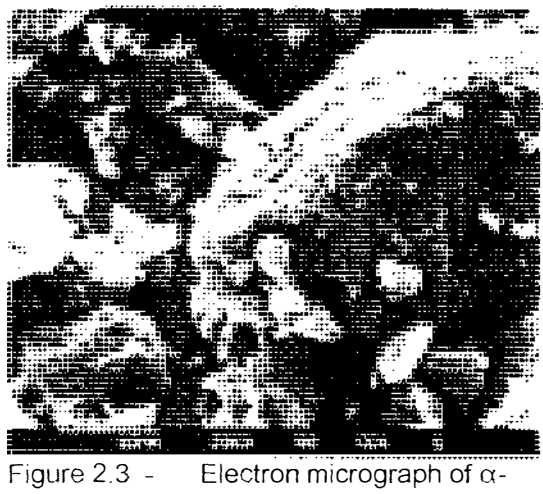

Figure 2.3 - Electron micrograph of α-lactose monohydrate at 2000x magnification

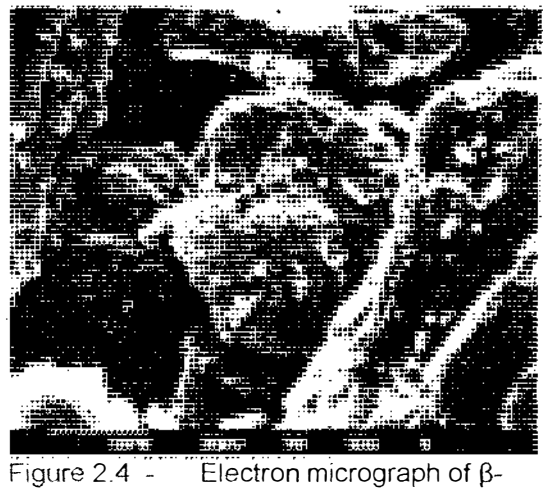

Figure 2.4 - Electron micrograph of β-lactose at 2000x magnification

2.2.2 AMORPHOUS LACTOSE

When a lactose solution is dried rapidly, the viscosity increases so quickly that crystallisation cannot take place. The resulting dry lactose is in the same disordered state as it was in solution except the mobility of the lactose molecules is very limited [Nickerson 1974].

The amorphous lactose used in this work was spray dried amorphous lactose produced at the New Zealand Dairy Research Institute by Dr R Lloyd and Dr XD Chen. Details of the manufacturing method used can be found in Lloyd *et al.* (1996).

2.2.3 PARTIALLY AMORPHOUS LACTOSE

A spray dried lactose product provided by the Lactose Company of New Zealand called "*Supertab*" has been used in this work. The product is approximately 90% crystalline in the α-lactose monohydrate form with 10% amorphous lactose present. It is used primarily for direct tableting in the pharmaceutical industry. Figure 2.5 is a scanning electron micrograph of *supertab* lactose which shows how *supertab* is comprised of small lactose crystals stuck together by amorphous lactose to form a spherical particle, resulting in a relatively porous structure.

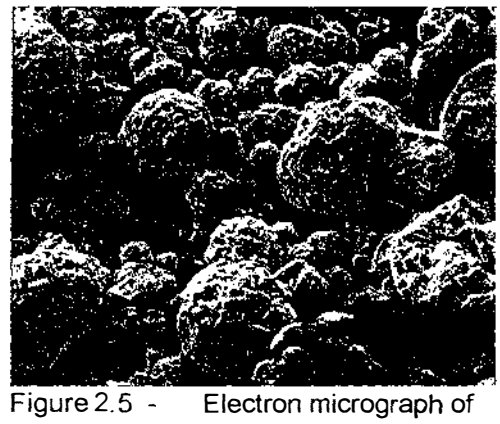

Figure 2.5 - Electron micrograph of *supertab* lactose at 100x magnification

Literature suggests that the processes of fast drying and milling can produce a layer of

Table 2.3 Amount of amorphous lactose present on various industrial lactose samples.

Sample	Amorphous lactose content [%]
Drier feed	0[1], 0[2]
Drier discharge	1.3[1], 1.6[2]
Drier fines discharge	0.9[1], 1.2[2]
ACM mill feed	0.6[1]
ACM mill discharge	1.9[1]
BM1 mill feed	0.5[1]
BM1 mill discharge	2.2[1]
BM2 mill feed	0.5[1]
BM2 mill discharge	2.9[1], 0.6[3]
100 mesh refined product	3.4[2], 0.3[3]
200 mesh refined product	4.1[2], 2.7[3], 1.8[3], 1.9[3], 0.4[3]
300 mesh refined product	6.1[2], 2.4[3]
Supertab	6.7[3], 6.2[3], 9.1[4]

[1] From Hargreaves (1995), [2] Samples collected from the Lactose Company of New Zealand 11/11/1994, [3] Samples collected from the Lactose Company of New Zealand 8/8/1995, [4] Bagged sample in stock 18/12/1995.

amorphous lactose on the outside surface [Roth 1976]. Hargreaves (1995) developed a technique utilising nuclear magnetic resonance which is able to quantify small amounts of amorphous lactose present in lactose samples. Results using this method on samples provided by the Lactose Company of New Zealand are listed in Table 2.3.

It is clear from these results that amorphous lactose can be present in crystalline lactose, particularly if the sample has been heavily milled. In general, the higher the degree of milling, the higher the amount of amorphous lactose present on the sample. It is also evident from these results that there is a large amount of variability between similar samples collected at different times (eg. the 200 mesh sample results). This is likely to be due to variability in the temperature and water activity history of the samples. Until recently, no humidity control of the process air streams has been present in the Lactose Company of New Zealand plant at Kapuni, Taranaki. This has meant that on some days adventitious partial conditioning of the product prior to packing may have occurred and hence different amounts of amorphous lactose are observed.

Two other methods of identifying and quantification involve moisture release upon crystallisation of the amorphous part of the lactose particle. These will be discussed in greater detail in Chapter 3.

2.3 CHARACTERISATION OF LACTOSE POWDERS

2.3.1 PARTICLE SIZE DISTRIBUTION

The particle size distributions of the lactose powders investigated in this work are summarised in Table 2.3. The analysis of the typical samples of special dense, 100, 200, 300 mesh and *supertab* lactose powders were measured by the Lactose Company of New Zealand using a Coulter LS100 particle size analyser. The particle size distribution of beta lactose was determined by Malvern laser scattering particle size analyser by the New Zealand Dairy Board, Product Evaluation Centre, Mt Eden, Auckland.

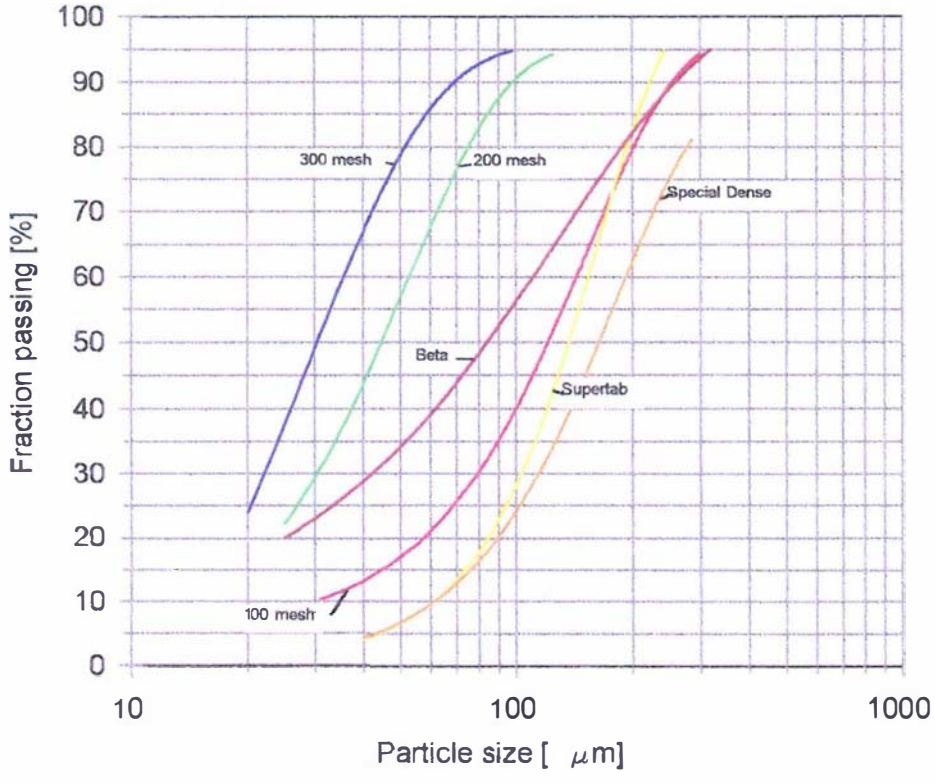

Figure 2.6 - Particle size distributions of lactose powders.

2.3.2 DENSITY

2.3.2.1 PARTICLE DENSITY

Berlin *et al.* (1971) measured the particle density of the three major crystalline lactose forms pycnometrically, by helium displacement. Weast and Astle (1979) reported the particle density of the α-lactose monohydrate and β-lactose forms although the measurement method was not given. Buma (1965) reported values for the density of lactose as measured by centrifugation in carbon tetrachloride liquid paraffin solutions and by air pycnometry. Herrington (1934) also published the densities of anhydrous α-lactose and β-lactose. These results are summarised in Table 2.4 below.

Table 2.4 Particle density of the various crystalline lactose forms.

Lactose form	Particle density [kg/m³]	Reference
α-Lactose monohydrate	1535	Berlin *et al.* (1971)
	1525	Weast and Astle (1979)
	1545	Buma (1965)
Anhydrous α-lactose	1547	Berlin *et al.* (1971)
	1545	Buma (1965)
	1544	Herrington (1934)
β-Lactose	1576	Berlin *et al.* (1971)
	1590	Weast and Astle (1979)
	1590	Buma (1965)
	1588	Herrington (1934)

In this work the value given by Berlin *et al.* (1971) for α-lactose monohydrate and the value given by Buma (1965) and Weast and Astle (1979) for β-lactose will be used because they are the most consistent among the range of values reported.

2.3.2.2 Bulk Density, Tapped Density and Porosity

The bulk density of the lactose powders used in this work are listed in Table 2.5 along with what was termed the "tapped density" by Wade and Weller (1994).

Table 2.5 Bulk density, tapped density and porosity of lactose powders

Name	Bulk density [kg/m³]	Porosity (untapped)	Tapped density [kg/m³]	Porosity (tapped)
Special Dense	800	0.49	925	0.40
100 mesh	750	0.51	932	0.39
200 mesh	600	0.61	890	0.42
300 mesh	500	0.67	856	0.44
Supertab	650	0.58	720	0.53
Beta lactose[1]			780	0.51

[1] particle density calculated as a mass ratio of α and β particle densities in fraction 22% α-lactose monohydrate and 78% β-lactose.

The tapped density is the bulk density of powders after tapping the volumetric cylinder against a hard surface until no further volume change is observed. Bulk density

is the density of the powder without any compaction applied to the sample. It can be seen from the data that for the finer powders up to 40% reduction in volume can occur by compaction of the powder.

In a packed bag the bulk density will approach the tapped density figures listed here due to the compaction action of the weight of other bags in a pallet or due to the large weight of lactose contained in a 900kg bulk bag.

2.4 THERMAL PROPERTIES

2.4.1 SPECIFIC HEAT CAPACITY

The specific heat capacity of solid α-lactose monohydrate is given by Jenness and Patton (1959) as 1252 J/kg°C. The specific heat capacity of β-lactose is given by Jenness and Patton (1959) as 1193 J/kg°C.

2.4.2 EFFECTIVE THERMAL CONDUCTIVITY

The most simple way of modelling the transport of heat through bulk lactose is to treat the lactose air mixture as an effective medium. An effective medium is where the two phase system of air and solid particles is approximated as being one phase with effective physical properties. For this reason, the effective thermal conductivity of bulk lactose was required. This can be approached in two ways. The first approach is to model the effective thermal conductivity as a function of the solid lactose thermal conductivity and the porosity of the powder.

There have been many models published in the literature aimed at achieving this. Shrotriya *et al.* (1991) described a model which can be used to predict the thermal diffusivity of a porous medium. Nimick and Leith (1992) provide a model for prediction of the effective thermal conductivity of an effective medium. Deng *et al.* (1992) provide a model for the case where the solid phase is a mixture of two different granular materials. A detailed analysis of thermal conductivity in porous media is given by Bauer (1993), discussing the validity of assumptions of pore type and size distribution. Bauer offers a general approach for prediction of thermal conductivity of porous media.

The second approach is to directly measure the effective thermal conductivity experimentally. In this study direct measurement was employed due to the unavailability of solid lactose thermal conductivity data.

2.4.2.1 EXPERIMENTAL MEASUREMENT OF EFFECTIVE THERMAL CONDUCTIVITY

Measurement techniques for the determination of the effective thermal conductivity of porous materials can be categorised into three groups. These are steady state, quasi-steady state and transient methods. In general, steady state methods such as the guarded hot plate method are unsuitable for food materials because of long temperature equilibration times and moisture migration in the sample (Sweat 1986). In spite of this, several researchers have used steady state methods to determine the thermal

conductivity of porous media. MacCarthy and Fabre (1989) measured the effective thermal conductivity of different grades of sucrose using a guarded hot plate. The results ranged from 0.094W/mK for icing sugar, to 0.164 W/mK for medium grade sucrose. Pham and Willix (1989) and Willix and Lovatt (1995) used a guarded hot plate method to measure the thermal conductivity of various foodstuffs including lactose powder. The inclusion of lactose powder in their work was made at my request and will be discussed in greater detail below.

Murakami and Okos (1989) suggested the use of the temperature history method for experimental determination of the thermal diffusivity of fine porous materials or powders. It is also evident from the literature that transient methods have been widely used for the determination of thermal transport properties in food and porous materials.

The measurement of thermal conductivity from the time taken for heat dissipation has been used by a number of researchers. Thorne (1989) describes a method where heating is applied to foodstuffs through a small thermistor. The same thermistor is then used to record the rate of heat dissipation. This is then used to estimate the thermal diffusivity. The results were reproducible although further evaluation of the method was required. Nimick and Leith (1992) measured the effective thermal conductivity of fused silica powder using an adaption of the needle probe technique. This used a thin heating probe inserted into the bulk powder. Power was applied to the thermal probe for ninety seconds and the external surface temperature of the heater was recorded as a function of time. This was used to calculate the effective thermal conductivity of the powder.

Kent *et al.* (1984) compared the use of five transient heating methods for the determination of the thermal conductivity and diffusivity of various food samples, including whole milk powder. Three used methods based on the heated probe with cylindrical symmetry. The other two methods used symmetry about a central plane.

Shrotriya *et al.* (1991) and Deng *et al.* (1992) both used a parallel wire method for measuring the thermal conductivity of a porous media. These used two thermocouples positioned at some radial distance from a heating wire. The resulting temperature profile was used to calculate the effective thermal conductivity.

Voudouris and Hayakawa (1994) mathematically analysed the suitability of the point source probe for simultaneous determination of thermal conductivity and diffusivity of foods. They concluded that results were in good agreement with published values of thermal conductivity but the method was best suited to products with high thermal diffusivity.

Scotter and Horne (1985) used a transient method based around the heating profile of an infinite cylinder to measure the thermal diffusivity of soil. From this the effective thermal conductivity was calculated.

Two experimental methods for determining the effective thermal conductivity of bulk lactose were carried out. These are the transient heating or cooling rates of an infinite cylinder filled with lactose using the method given by Scotter and Horne (1985) and a guarded hot plate method [Willix and Lovatt (1995)].

2.4.2.1.1 MEASUREMENT BY THE INFINITE CYLINDER METHOD

The conduction of heat through an infinite cylinder can be described by Eq (2.1) [Carslaw and Jaeger (1959)].

$$Y = 1 - 2\sum_{n=1}^{\infty} \frac{\exp(-\beta_n^2 . \alpha t/r^2)}{\beta_n J_1(\beta_n)} \qquad (2.1)$$

For $\alpha t/r^2 > 0.15$ only the first two terms of the series are significant and the solution can be evaluated by noting $\beta_1=2.405$, $\beta_2=5.520$, $J_1(\beta_1)=0.519$ and $J_2(\beta_2)=-0.340$. From this solution, Table 2.6 was constructed. The thermal diffusivity can be estimated from the time required to achieve a given temperature change from experimental time-temperature profiles.

Table 2.6 Solutions for the temperature change in an infinitely long cylinder

1-Y	$\alpha t/r^2$
0	0
0.175	0.10
0.34	0.15
0.50	0.20
0.72	0.30
0.84	0.40

An infinite cylinder of lactose was approximated by filling a 300mm long, 80mm diameter copper tube with special dense grade lactose (Lactose Company of New Zealand). The cylinder was tapped against the table regularly during filling. Three thermocouples were axially centred in the lactose, approximately one third, one half and two thirds of the way down the copper tube. Two additional thermocouples were taped to the inside surface of the copper tube with aluminium foil tape. The ends were well insulated with polystyrene, to ensure one dimensional heat transfer, and sealed water tight.

The cylinder was allowed to stand for approximately one hour to ensure uniform initial temperature before being submerged into a constant temperature water bath (Grant W38 with KD temperature controller). The surface and centre temperatures were recorded using a Intellution FIX data-logging station until the centre temperature reached the water bath temperature.

Temperature driving forces of 15-25°C were used for both heating and cooling runs in the range 15-40°C. An example time-temperature profile for heating of a cylinder is given in Figure 2.7. It can be seen from the plot that the two centre heating curves lie on top of each other indicating the absence of heat transfer down the tube length. This demonstrates the validity of using a solution for heat transfer in an infinite cylinder.

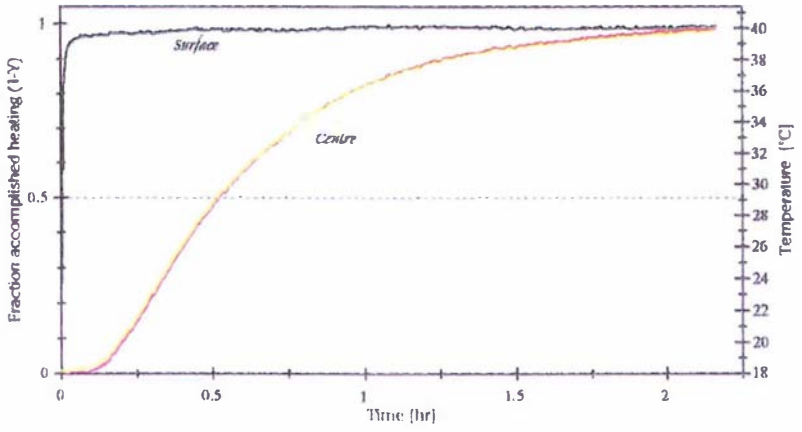

Figure 2.7 - Typical heating curve for an infinite cylinder full of bulk lactose.

The heating profile becomes linear if plotted on a semi-log scale as shown by Figure 2.8.

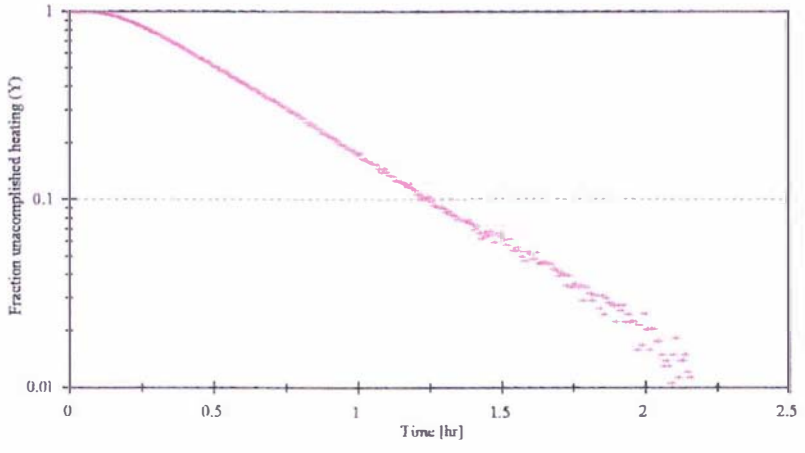

Figure 2.8 - Semi-log plot of lactose cylinder heating time temperature history

The linear section of this plot was then regressed to obtain the equation for the line of best fit and this used to calculate the time taken to achieved the degree of cooling as listed in Table 2.6. From this and the radius of the cylinder, the thermal diffusivity was determined. The thermal conductivity is then given by Eq (2.2).

$$\lambda = \alpha \rho c_p \tag{2.2}$$

A summary of all the thermal conductivity trials is given in Table 2.7.

Table 2.7 Summary of thermal conductivity measurements by infinite cylinder method

Sample	Heated/ Cooled	Porosity	Thermal Conductivity [W/mK]	± Uncertainty [W/mK]
Bagged (0.65 a_w)	Heated	0.43	0.17	0.02
Bagged (0.65 a_w)	Cooled	0.43	0.19	0.02
Bagged (0.65 a_w)	Heated	0.43	0.17	0.04
Oven dried	Heated	0.43	0.17	0.04
Oven dried	Cooled	0.43	0.21	0.02
Oven dried	Heated	0.43	0.18	0.02
<75μm	Heated	0.42	0.17	0.02
<75μm	Cooled	0.42	0.18	0.02
<75μm	Heated	0.42	0.17	0.02
105-150μm	Heated	0.43	0.17	0.02
105-150μm	Cooled	0.43	0.16	0.04
105-150μm	Heated	0.43	0.22	0.02
210-300μm	Heated	0.44	0.17	0.02
210-300μm	Cooled	0.44	0.18	0.02
210-300μm	Heated	0.44	0.17	0.02

It is well known that upon application of a temperature gradient to porous media, moisture migration will occur. In an effort to determine whether moisture migration is increasing the apparent thermal conductivity of the lactose as measured by the infinite cylinder method, the experiment was repeated using oven dried lactose. It can be seen from Table 2.7 that there is no significant difference between the measured thermal conductivity of dried lactose and lactose stored in ambient conditions (0.65 a_w). This indicates that the amount of heat transported with the diffusing water vapour is negligible compared with that transferred through conduction in the solid phase.

The effect of particle size on thermal conductivity was also investigated. The special dense lactose was sieved to obtain three separate fractions (<75, 105-150 and 210-300μm). Upon packing the cylinder however, the bulk density did not change significantly. As a consequence, the measured thermal conductivity was comparable with the values measured for whole special dense grade lactose powders.

The average thermal conductivity of tightly packed special dense lactose was 0.17 W/mK.

2.4.2.1.2 MEASUREMENT BY THE GUARDED HOT PLATE METHOD

Willix and Lovatt (1995) at the Meat Industry Research Institute of New Zealand included 100 and 200 mesh lactose powders (supplied by the Lactose Company of New Zealand) in their study of the thermal properties of foodstuffs. The guarded hot plate used a 200mm by 200mm measuring area. The lactose was poured into the apparatus in a free flowing manner to a depth of 20mm and levelled using a stainless steel straight edge. Additional lactose was then added and re-levelled with the straight edge sitting on two 0.65mm thick aluminium strips. This made the powder surface slightly proud of the surface to ensure good plate product contact. This treatment allowed some product compaction although the porosity of the product is likely to have remained high (Willix 1996).

Full details of the construction of the guarded hot plate apparatus used in this work are given by Pham and Willix (1989). Further details of the lactose loading method are given in Willix and Lovatt (1995).

The results of the experiments carried out by Willix and Lovatt (1995) are summarised in Table 2.8.

Table 2.8 Summary of thermal conductivity measurements by guarded hot plate method

Sample	Temperature [°C]	Thermal conductivity [W/mK]
100 mesh	-39.0	0.112
	-17.3	0.118
	-17.4	0.116
	-9.6	0.119
	-9.6	0.118
	2.6	0.107
	2.7	0.103
	16.3	0.104
	16.3	0.113
	25.1	0.120
	35.9	0.124
	36.0	0.123
200 mesh	-29.0	0.095
	17.0	0.097

It can be seen from this data that there is a large difference between the thermal conductivity measurements made by the infinite cylinder method and those made using a guarded hot plate. This is probably due to differences in porosity. As stated previously in the guarded hot plate measurements, the porosity of the samples (although not actually measured) was likely to have been relatively high. In the infinite cylinder method, the lactose was packed tightly to simulate industrial packing conditions.

If the parallel model for thermal conductivity given by Eq (2.3) is used [Murakami and Okos 1989], then the porosity change required to explain the difference in measured thermal conductivity can be calculated using Eq (2.4).

$$\lambda_{effective\ media} = (1-\epsilon)\lambda_{solid\ phase} + \epsilon\lambda_{gas\ phase} \tag{2.3}$$

$$\frac{1-\epsilon_{guarded\ hot\ plate}}{1-\epsilon_{infinite\ cylinder}} = \frac{\lambda_{guarded\ hot\ plate}}{\lambda_{infinite\ cylinder}} = \frac{0.12}{0.17} = 0.71 \tag{2.4}$$

This results in the porosity of the sample in the guarded hot plate apparatus being 0.52. This is reasonable as the porosity of 100 mesh lactose can range between 0.51 to 0.39 depending on the degree of compaction (see Table 2.5). This indicates that there is a large dependence of the effective thermal conductivity of porous materials on powder porosity. Because the infinite cylinder method measurements utilised tightly packed lactose, similar to the state of lactose in industrially packed lactose, those results have been used in subsequent work.

2.5 PROPERTIES OF LACTOSE SOLUTIONS

The properties of lactose solutions are required in understanding and interpreting moisture sorption phenomena.

2.5.1 SOLUBILITY

Figure 2.9 shows a diagram of the solubility of lactose as a function of temperature. It can be seen from the graph that the solubility of β-lactose is much greater than that of α-lactose. If α-lactose crystals are added to water an initial solubility limit is quickly reached. As muta-rotation occurs in solution α-lactose molecules will be converted to β-lactose and are then replaced by dissolution of more of the α-lactose molecules. Finally, equilibrium and a final solubility limit is reached. The concentration of the solution is a function of the alpha solubility limit and the equilibrium ratio of β:α lactose molecules [Lowe 1993].

If β-lactose crystals are added to water an initially high solubility is reached. As muta-rotation occurs α-lactose molecules in solution become supersaturated and crystallise out of solution. Eventually the solution will be at the equilibrium concentration and the β-lactose crystals will have been converted through solution to α-

lactose monohydrate crystals because it has the lower solubility limit.

Above 93.5°C β-lactose becomes the lactose anomer which has the limiting solubility and the opposite of the behaviour described above is observed.

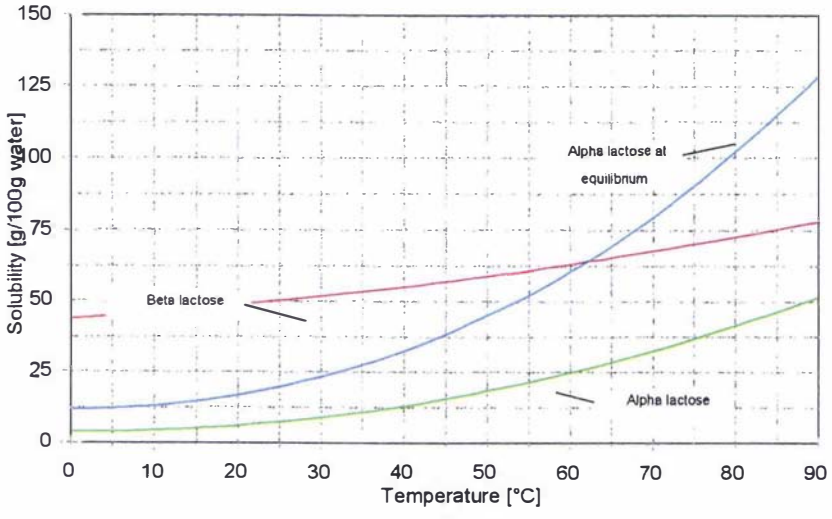

Figure 2.9 - Solubility of lactose as a function of temperature [Gerhartz 1988].

2.5.2 SURFACE TENSION

The surface tension of saturated lactose syrups was measured for use in the prediction of capillary condensation in lactose moisture systems. Saturated lactose solutions were made at 17, 30 and 40°C. Surface tension was measured using the capillary rise method [Adamson 1963]. This method was chosen over the numerous alternative surface tension measurement methods due to availability of equipment.

Glass capillaries of ~1mm diameter were clamped perpendicular to the surface of the lactose solution with the end slightly submerged. Fluid was sucked up the tube to ensure the inside walls of the capillary were wetted and therefore a zero contact angle was maintained while the measurement was being taken. The capillary fluid height (z) was then allowed to find its equilibrium level which was measured using a travelling microscope.

The surface tension was calculated from the capillary rise using La Place's equation Eq (2.5) [Adamson 1963].

$$\sigma = \tfrac{1}{2}\rho g z r \qquad (2.5)$$

The results of these experiments are summarised in Figure 2.10. The surface tension was found to change approximately linearly with temperature in the range 17- 40°C. A least squares fit resulted in Eq (2.6).

$$\sigma = 0.07021 - 0.000105\,T \quad (\pm 0.0017) \qquad (2.6)$$

The increase in the solubility of lactose with temperature is thought to be partly responsible for the decrease in surface tension with increasing temperature.

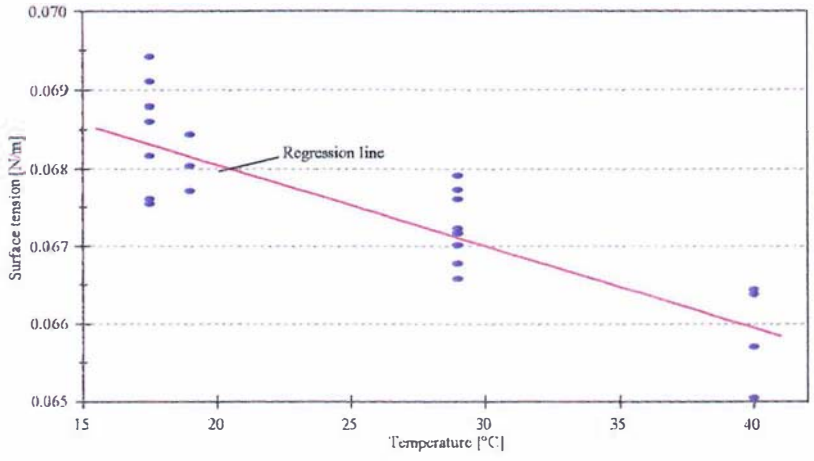

Figure 2.10 - Surface tension of saturated solutions of lactose

2.6 CLOSURE

The lactose powders used in this work have been characterised in terms of bulk properties, surface structure and particle size distribution. General properties of lactose have been summarised from literature or experimentally determined where literature data was unavailable or incomplete. This is not an exhaustive compilation of lactose properties but rather a list of those properties that describe the materials used in this work and that are important in the understanding and modelling of lactose caking phenomena.

One key group of properties which is of central importance in the understanding of caking phenomena was not discussed in this chapter. That group can be broadly described as moisture relations in solid phase lactose and because of its importance is the focus of the next chapter.

CHAPTER 3

MOISTURE RELATIONS IN LACTOSE

3.1 INTRODUCTION

A detailed knowledge of the relationships and interactions between moisture and the various lactose forms is essential to the understanding of caking phenomena. This includes understanding the differences between bound and free moisture, knowledge of the moisture sorption isotherm and sorption kinetics of lactose and the ability to accurately measure moisture content and water activity of lactose samples.

3.2 THE DEGREE OF BINDING OF MOISTURE IN LACTOSE

Water in powders can exist in many forms and can be classified according to degree of binding to the powder or its functionality. In addition, the functionality of the water can be described in terms of a single particle or as water in bulk powder [Kawamura 1991]. Broadly, moisture can be thought of as being chemically bound or physically adsorbed to a crystal.

3.2.1 CHEMICALLY BOUND MOISTURE

Chemically bound water is normally called crystal water or water of crystallisation. In α-lactose monohydrate, one water molecule is present for every molecule of α-lactose. This is further distinguished as being lattice water as it is required in the crystal lattice to maintain the integrity of the crystal structure. The lattice water can be removed by dehydration at 120°C [Stecher 1968] and can be seen as a single endotherm between 120-140°C by differential scanning calorimetry [Biliaderis 1990]. The heat of desorption of lattice water in α-lactose monohydrate is 51.46 kJ/mol of water removed [Berlin *et al.* 1971].

Buma (1965) measured the density of α-lactose crystals before and after dehydration of the lattice water (5%w/w) by centrifugation in carbon tetra-chloride liquid paraffin solutions. He showed that the densities were indistinguishable in magnitude (1545 kg/m^3). This indicates that substantial changes in the crystal lattice occurred upon desiccation.

Berlin *et al* (1971) explained the hydration phenomenon of α-lactose based on a mechanism put forward by Ladd and Lee (1965) and Ladd and Lee (1969). The anhydrous structure is first expanded and gaseous water molecules are accommodated so

that the resulting crystal structure is equivalent to that of the hydrate. In a second stage, the expanded lattice-water interaction occurs which may be stabilised through covalent bonding, hydrogen bonding or ion-dipole interaction energy. In α-lactose, hydrogen bonding formation is the most likely mode of interaction between the lactose and water.

β-Lactose does not have a hydrated crystalline form. This can be explained in terms of the hydration mechanism described above if it is considered that β-lactose has a higher melting point and higher density than α-lactose. This indicates a more compact crystal structure and requires a greater expenditure of enthalpy for expansion of the anhydrous crystal lattice than that required for α-lactose. This means it is energetically unfavourable for the formation of a hydrated crystalline β-lactose form.

3.2.2 PHYSICALLY ADSORBED MOISTURE

Adsorbed moisture is present on specific sites on the particle surface to form a monolayer and as subsequent additional layers. The water molecules can be attached to the crystal surfaces by van der Waals forces or hydrogen bonding. A delay in the removal of water as well as an increase in the heat of vaporisation calculated from the dehydration endotherm of a differential scanning calorimetry run, have been considered as an indication of stronger binding of water to a substance. Biliaderis (1990) suggests caution in these interpretations due to difficulties in interpolation of the baseline in estimating the heat of desorption and the fact that the process of moisture removal is very dependant on the mass transfer conditions.

Other methods by which the degree of binding of adsorbed moisture can be established are determination of unfrozen water, nuclear magnetic resonance, dielectric properties and measurement of vapour pressure [Karel 1975].

Unfreezable water is identified by comparing a differential thermal analysis plot with the known total water content of a food. The water unaccountable from the heat of fusion of the ice is then termed unfreezable water because it is evidently 'bound' by interaction with other food components. Franks (1991) argues that there are at least three reasons why such an analysis is incorrect. Firstly the ice melting endotherm is not equal to the latent heat of fusion of pure water as it contains a contribution from the heat of dilution of the concentrated solution into which the ice is melting. Secondly the area of the endotherm is incorrectly computed as no allowance is made to glass transition which must precede any melting. Thirdly freezing is nearly always incomplete as total freezing can only occur in systems where components other than water undergo complete eutectic crystallisation.

Proton magnetic resonance (NMR) is used routinely to determine the state of water in foods. Duckworth (1972) demonstrated using NMR that not all water present in foods is capable of acting as a solvent. Monolayer water does not act as a solvent nor does an additional fraction of water. He showed that each solute had a specific water activity at which it went into solution and that the presence of other insoluble components did not alter this value. For sucrose, this water activity was 0.82. This type of water has been termed non-solvent water. There have been no reports of the water activity where adsorbed moisture can act as a solvent for lactose systems.

The degree of binding of water to proteins, polymers and foods can be determined by dielectric measurements although quantification using this method is difficult [Karel 1975].

Karel (1975) suggests that the most successful method for studying properties of water involves preparation of sorption isotherms. The BET monolayer obtained from these isotherms is said to be strongly bound to specific sites on the surface of the particle. Such sites could be hydroxyl groups of polysaccharides or simple sugars, carbonyl and amino groups of proteins and others on which water can be bonded by hydrogen bonding, ion-dipole bonds or by other strong interactions. In lactose the monolayer water is likely to be hydrogen bonded to hydroxyl groups to the crystal surface.

It must be remembered, however, when using such an analysis that the BET isotherm equation describes physical adsorption of a vapour to a surface. Only when the equation is applied to isotherm data for such a system is interpretation of the BET monolayer value meaningful. Numerous occurrences of the application of the BET or GAB isotherms for systems when adsorption to the surface is coupled with diffusion from the surface into the product are found in the literature. This is not consistent with the mechanistic basis of the isotherm equation and therefore interpretation of the isotherm equation constants is inappropriate.

3.2.3 Bound and Free Moisture Used in this Work

It can be seen from this discussion that there are numerous interpretations made about how strongly bound water is in a particular food system. It is also evident that there is still some debate in the literature as to the validity of some of these interpretations. For the purposes of this work therefore, definitions of the concepts of bound and free moisture were made.

It is clear that when using an isotherm equation of mechanistic origin, some consideration of the function and degree of binding of water in the system must be made. In practical terms however, water that can be removed by placing lactose in a dry environment at moderate temperature is what is important in caking phenomena. For this reason water which can be removed by desiccation over phosphorous pentoxide over several weeks was termed "free moisture". Using this definition, lattice or crystal water in α-lactose monohydrate is not included as it is not removed until high temperature (120°C) is applied. Crystal water was termed "bound moisture". Monolayer moisture is termed free moisture using this definition.

3.3 Moisture Sorption Isotherms

The most commonly used and most effective physical method of assessing the state of water in food is measurement of water vapour in equilibrium with a given moisture content in solid at a constant temperature. The almost universally accepted convention is the use of the relative vapour pressure and it's designation as water activity Eq(3.1) [Karel 1989].

$$a_w = \frac{p_v}{p_w} = \textit{Equilibrium relative humidity} \qquad (3.1)$$

At constant temperature two phases such as air, and the powder exposed to it, are at equilibrium if their water activities are equal. The rates of transfer of water between the phases is proportional to the difference in vapour pressure between the two phases.

The relationship between the moisture content of a material and that of the gas phase at equilibrium are usually expressed in one of four ways (Karel 1989);

- Isotherms $M = f(p_v)$ at constant T
- Isobars $M = f(T)$ at constant p_v
- Constant activity curves $M = f(T)$ at constant p_v/p_w
- Isosteres $p_v = f(T)$ at constant M

The most common representation for food systems is the moisture sorption isotherm.

3.3.1 PUBLISHED LACTOSE ISOTHERM DATA:

3.3.1.1 Crystalline lactose:

Several researchers have published moisture sorption isotherms for α-lactose monohydrate. Figure 3.1 summarises the available data. This plot was constructed by scanning and digitising the graphs from the original papers and replotting the data. The data of Warburton and Pixton (1978) was reported on a free moisture basis rather than including the water of crystallisation present in α-lactose monohydrate in the moisture content determination. To allow comparison of this data with the other data reported in the literature, the water of crystallisation (5.26%) was added, before plotting on Figure 3.1.

It can be seen from Figure 3.1 that most researchers found that α-lactose monohydrate did not adsorb large amounts of moisture over the water activity range considered. All but Warburton and Pixton have included water of crystallisation in the moisture content analysis which probably accounts for the amount of scatter in the observed results. The amount of free moisture present on lactose is approximately 0.1% where the water of crystallisation makes up 5.26% moisture. It follows that if a small error in the total moisture content analysis is made this will be the same order of magnitude as the total amount of free moisture present in the sample

The effect of temperature in the range between 15 and 40°C on the moisture sorption isotherm of α-lactose monohydrate was required to model caking phenomena in bulk lactose. It can be seen that most of the literature data reported has been measured at room temperature although some attempts at investigating the effect of temperature on sorption phenomena has been attempted by Audu *et al.* (1978) and Loncin *et al.* (1968). These results show that investigation into the effect of temperature on sorption was required. The literature data also show that the effect of water activity values

approaching one has not been investigated. It was expected that the water activity of lactose at a cold surface in a bag would approach unity and therefore the available data were not adequate for the accurate modelling of caking in bulk lactose. Because of this it was decided to determine moisture sorption isotherms experimentally, as part of this work.

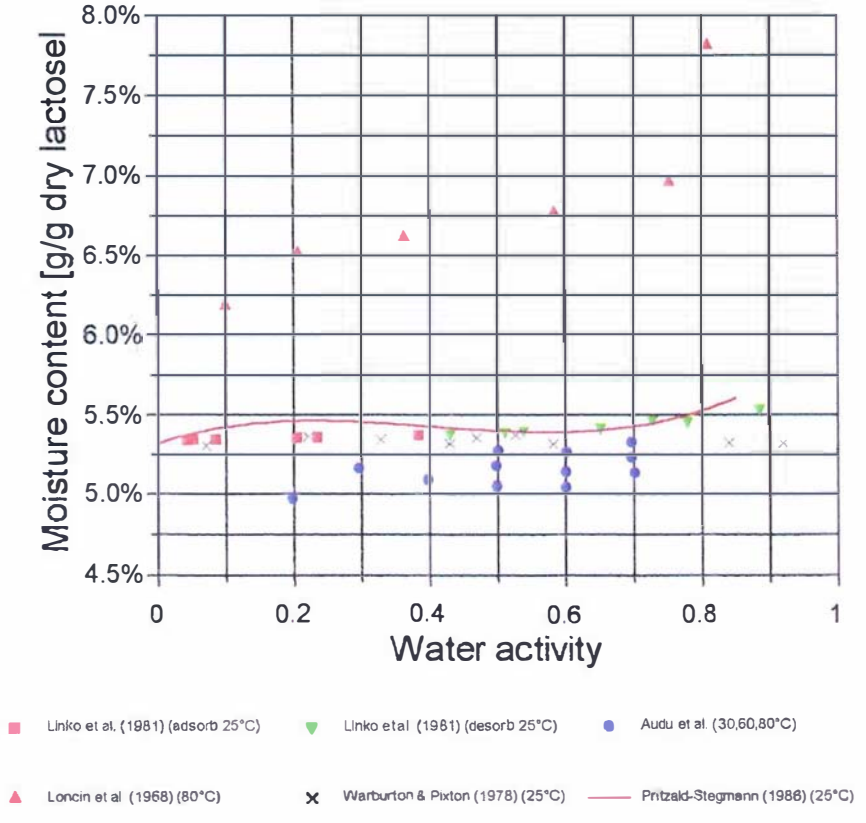

Figure 3.1 - Literature isotherm data for α-lactose monohydrate.

3.3.1.2 Amorphous, spray-dried and freeze-dried lactose:

Moisture sorption isotherm data for amorphous lactose have been published by numerous researchers. These data are summarised in Figure 3.2.

In most cases the isotherms show a step change in moisture content at about 0.4-0.6a_w. This decrease in moisture content is due to the crystallisation of amorphous lactose and the subsequent release of moisture. The available data show a great deal of scatter and do not show the effect of temperature on the sorption isotherm. Hargreaves (1995) also indicated that differences in glass transition temperature of amorphous lactose formed by spray drying and freeze drying can occur. For these reasons the moisture sorption isotherm for spray dried amorphous lactose was experimentally determined.

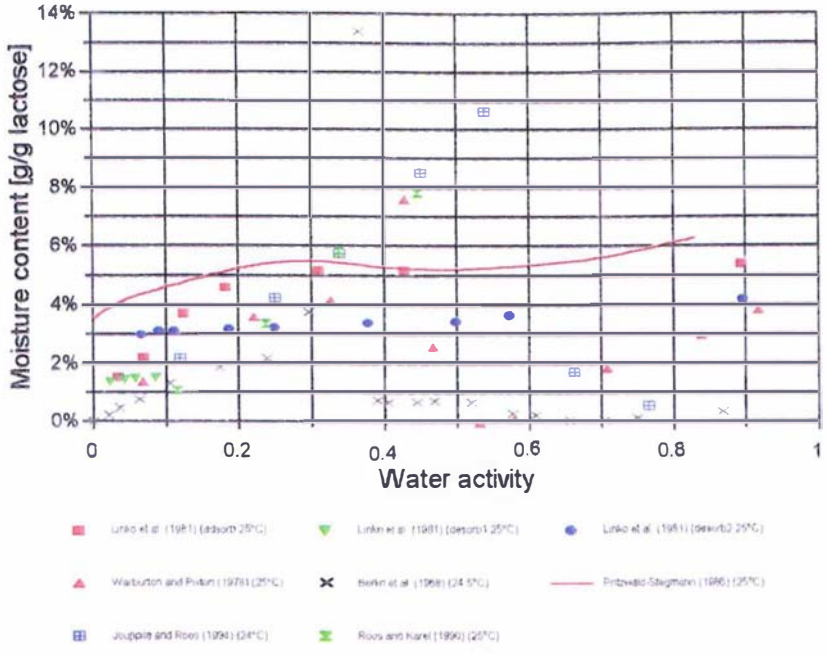

Figure 3.2 - Summary of amorphous lactose isotherm data from the literature.

3.3.2 EXPERIMENTAL MEASUREMENT OF LACTOSE ISOTHERM DATA:

Because previously published α-lactose isotherm data are of poor quality and does not encompass the full water activity range important in lactose caking problems, experimental data was generated. The effect of temperature on the sorption isotherm of α-lactose was also investigated in the ranges of 15-40°C because this had not been published in the literature and was required for this work.

The sorption isotherms of β-lactose were also measured because the product of amorphous lactose crystallisation at water activities below 0.55 a_w is reported to be β-lactose anhydride [Vuataz 1988]. Spray-dried amorphous lactose isotherms were measured to quantify the effect of temperature on sorption behaviour in the range 15-40°C.

Methods for obtaining moisture sorption isotherms for foods have been described by many researchers including Stitt (1958), Taylor (1961) and Smith *et al.* (1981). Many of theses methods have been reviewed by Gal (1975). In general the methods utilise one of three basic approaches.

- measurements of moisture content of samples in vacuum desiccators containing saturated salt solutions at atmospheric pressure, which give a certain relative humidity. Various authors have outlined which saturated salt solutions are required to maintain a given relative vapour pressure, [Richardson and Malthus 1955, Rockland 1960, Karel 1975 and Greenspan 1977].
- measurement of the vapour pressure of air in equilibrium with a food at a given moisture content, with a sensitive manometric system. [Taylor 1961].
- inverse gas chromatography where a column packed with the food powder as the stationary phase in gas chromatography. This technique allows investigation of

low water activity levels of up to one order of magnitude less than the other two techniques [Smith *et al.* 1981].

The first measurement approach was used in this work. Crystalline samples were left in ambient conditions (25°C, 75-90% RH), for approximately one month before the isotherm measurement. This was done to ensure that no amorphous lactose was present in the samples. Amorphous lactose samples were removed from vacuum sealed foil bags.

The sorption isotherms were determined using the static gravimetric method. Air tight plastic jars, containing saturated salt solutions placed inside temperature controlled rooms, were used to provide constant relative humidity and temperature environments. Stainless steel stands were used to hold the samples above the salt solutions. The values given by Greenspan (1977) were used for the equilibrium relative humidity of the saturated salt solutions.

Ten gram samples of lactose were placed inside the sealed plastic jars and allowed to equilibrate. The samples were covered air tight during weighing to ensure no weight gains or losses occurred. Care was taken to observe the onset of any mould growth in the samples placed in high relative humidity environments which might effect the results. The samples were weighed periodically over three months until constant weight was reached. Samples were returned to the sealed containers immediately after weighing.

Initial moisture contents for the samples were determined by desiccation over phosphorous pentoxide for three months. The isotherms were then determined from the weight change from the initial sample. In this way desorption occurred below the starting product water activity ($0.75a_w$) and adsorption above this value.

3.3.3 α-LACTOSE MONOHYDRATE:

The saturated salt solutions used in the determination of α-lactose monohydrate were;

LiCl	~	11%
$MgCl_2$	~	33%
$Mg(NO_3)$	~	54%
NaCl	~	75%
$(NH)_2SO_4$	~	81%
KCl	~	87%
KNO_3	~	94%
K_2SO_4	~	97%

These salts were chosen to concentrate on the high water activity end of the isotherms. The low water activity end was known to be reasonably level. Anular grade chemicals and distilled water were used for all salt solutions.

The raw data for all isotherms measured for α-lactose monohydrate are shown in Figure 3.3. The isotherm data shows that very little change in moisture content occurred in the lower water activity region (<0.85) for a large change in water activity. Only at water activities above 0.85 is appreciable free moisture present. The moisture content increases exponentially above this point and approaches an asymptote at a water activity of one.

Table 3.1 - tss-isotherm parameters for α-lactose monohydrate

Parameter	Value
M_o [g/g dry lactose]	2.5×10^{-4}
f	0.92
c	8.8
h	30

Each of these parameters has physical meaning when fitted to a particular system. M_o, commonly referred to as the BET monolayer value, is the moisture content at which a single layer of water molecules have been adsorbed to available sites on the crystal surface. As such it is commonly used as a measure of the specific surface area of a sample. To achieve this the cross-sectional area of water molecules adsorbed onto the lactose crystal surface must be known.

McClellan and Harnsberger (1967) published the cross sectional areas for various gases adsorbed to solid surfaces. The cross sectional area of water adsorbed varies from 8 Angstroms^2 per molecule onto charcoal to 31 Angstroms^2 per molecule onto silicon oxide. The area was approximately 10 - 13 Angstroms^2 per molecule for most substances listed.

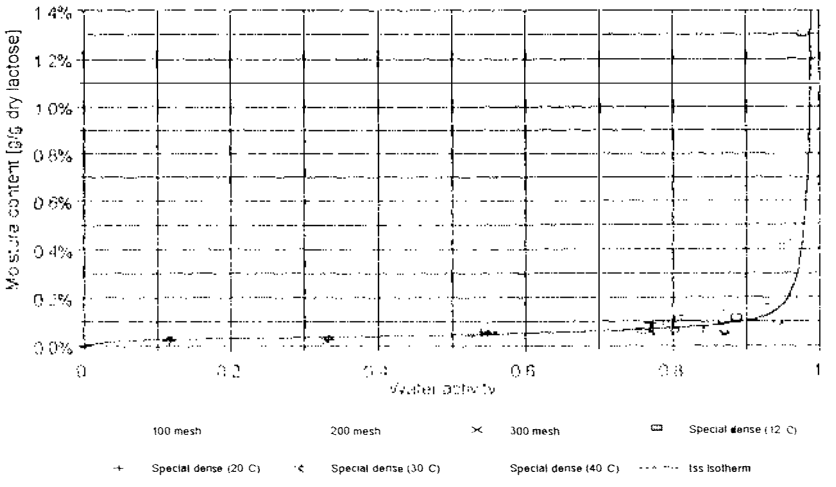

Figure 3.4 - Third stage sorption isotherm model predictions for α-lactose monohydrate.

Although no values for adsorption of water to sugars in general are given, the average cross-sectional area given above can be used as an estimate to allow calculation of the specific surface area of 150,000 m^2/m^3. A comparison can be made to specific surface areas for typical lactose powders of 36,000 for unmilled lactose to 320,000 m^2/m^3 for 300 mesh lactose, as measured by laser scattering. This indicates that the interpreted BET monolayer value is sensible for this system.

If total moisture content was used in the fitting of the BET monolayer, a value

equivalent to a specific surface area 200 times greater than predicted above, would result. This would then require the visualisation of lactose as a highly porous particle, which it is not. This illustrates that care is required when using isotherm equations with a theoretical basis.

The constant c, which is present in both the GAB and BET isotherms, is a constant dependant on the bonding energy of the sorbent onto the solid surface. Brunauer *et al.* (1938) shows that Eq (3.5) applies;

$$c \simeq e^{\frac{(E_1 - E_L)}{RT}} \tag{3.5}$$

That is, the difference in bonding energy between the monolayer adsorbed molecules and the molecules adsorbed on subsequent layers (E_1 - E_L) is approximately equal to $RT\ln(c)$. In the case of the model fitted here, (E_1 - E_L) = 5.30 kJ/mol. The latent heat of evaporation of water (E_L) ≈ 45 kJ/mol. This means the monolayer water is approximately 10% more strongly bound than free moisture. This again seems a sensible result.

The GAB constant f is a constant which is dependent on the energy of bonding of the second to ninth layers of adsorbed molecules on the surface. Anderson (1946) shows that the energy of bonding of these layers is equal, given by Eq (3.6).

$$f \simeq e^{\frac{(E_{2-9} - E_L)}{RT}} \tag{3.6}$$

If f = 1 then the GAB model simplifies to the BET model. If f >1 then this results in infinite sorption at a value of water activity less than 1 which is physically unsound. It follows therefore that $f \leq 1$. This means that the energy of bonding of the second to the ninth layers is less than the latent heat of vaporisation of free moisture. Anderson (1946) explains this by showing that because $f < 1$, the entropy of adsorption in the second to ninth layers is more negative than the entropy of vaporisation. This means that these layers are more ordered than pure liquid phase.

Chirife *et al.* (1992) showed that there is perhaps a correlation in the values of f in the GAB isotherm and the type of adsorbent. Proteins showed a narrow range of f values from between 0.82 - 0.88 while starchy based materials showed f values in the range 0.7 - 0.77. The f value estimated in this work is 0.92, which means the energy of bonding of the water molecules adsorbed in the second to ninth layers is equal to approximately 44.8 kJ/mol. This is 0.5% lower than the latent heat of vaporisation of pure water and indicates that the water molecules on the second and subsequent layers are relatively unstructured.

The fourth parameter in the tss isotherm (h) is a parameter which describes the number of water layers that need to be present, before the moisture can behave as free moisture [Timmermann 1989]. Because the moisture in lactose does not exhibit free behaviour until a water activity of higher than 0.85 is achieved, it makes sense that the value of h for this system is large (ie. 30). An estimate of h can be made by considering the space that an individual water molecule takes up. By approximating the water molecule as being spherical, Eq (3.7) was formulated to allow the diameter to be calculated.

$$d_{H_2O} = 2\left(\frac{3M_r}{4000\,\pi\,N_A\,\rho_w}\right)^{1/3} \tag{3.7}$$

For water at 20°C Eq (3.7) gives the diameter of a water molecule as being 0.39 nm. The thickness of the water layer on the outer surface of the crystal can be calculated from Eq (3.8) if a uniform monolithic layer is assumed.

$$x_w = \frac{M\rho_s}{A_s\rho_w} \tag{3.8}$$

At a water activity of 0.85 this calculates out to be 5 to 43 μm thick for the range of specific surface areas measured for lactose (36,000 to 320,000 m^2/m^3). This gives a range of values for h of 13 to 110. This analysis suggests that the fitted value of 30 is sensible.

It can be seen that in the fitting of the tss isotherm, care has been taken to observe that the physical basis for the isotherm was appropriate for the system under consideration and that the physical constants resulting from the model fitting are sensible.

A second, fundamentally derived model, which can be applied to the crystalline lactose system was given by Zsigmondy (1911), who used the concept of capillary condensation to describe the exponential increase in moisture content as the water activity approaches unity. Capillary condensation is the process where direct condensation can occur, due to surface tension effects, in the capillaries formed by the contact points between particles. In the capillary, the pressure is less than atmospheric pressure. This results in the saturated vapour pressure above the liquid surface being less (at the same temperature) than in the vapour pressure in the bulk air. If the pressure is lowered enough to cause the vapour pressure to be greater than the saturated partial pressure above the capillary surface, then condensation will occur, even if the bulk air relative humidity is below 100%. The water vapour pressure at which capillary condensation will occur is dependant on the capillary radius and is given by the Kelvin equation Eq (3.9) [Adamson 1963].

$$a_w = \frac{p_v}{p_w} = e^{\frac{2\sigma\cos\theta V_0}{r_k R(T+273.15)}} \tag{3.9}$$

When capillary size reaches molecular dimensions the Kelvin equation no longer applies and is, therefore, only suitable for water activity values greater than 0.8.

By using the Kelvin equation, the capillary radius (r) was calculated from the water activity for the isotherm data collected for special dense α-lactose monohydrate. A plot of moisture adsorbed versus capillary radius was then plotted (Figure 3.5). As all data used in this analysis was for the same size distribution, the geometry and packing characteristics should be similar between samples. This should result in the capillary radius versus moisture content plot being independent of temperature. It can be seen from Figure 3.5 that no dependance on temperature was observed in the range investigated.

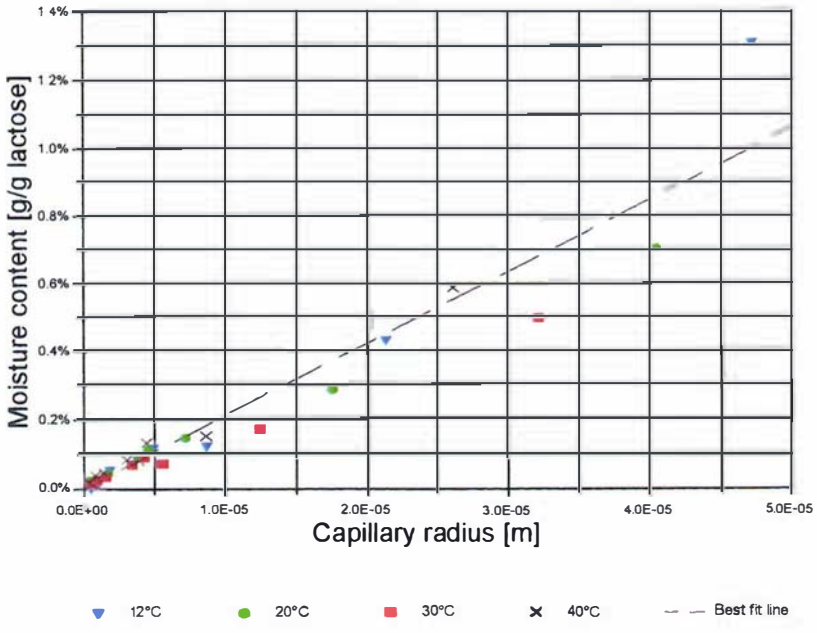

Figure 3.5 - Moisture content versus capillary radius for Special Dense α-lactose monohydrate.

A linear regression line was fitted to the water activity data values greater than 0.8 which is the region where the Kelvin equation applies, giving Eq (3.10).

$$M = 212\, r_k \tag{3.10}$$

From this relationship, the Kelvin equation, and surface tension data given in Chapter 2, an isotherm was predicted (Figure 3.6).

It can be seen from the plot that the predicted isotherm gives good predictions in the high water activity regions but the model is not mechanistically valid in the lower water activity regions.

In spite of the sound fundamental basis of the capillary condensation isotherm approach, the third stage sorption isotherm model developed by Timmermann was adopted in subsequent work. This is due to the applicability of the model over the whole water activity range while maintaining a plausible fundamental basis.

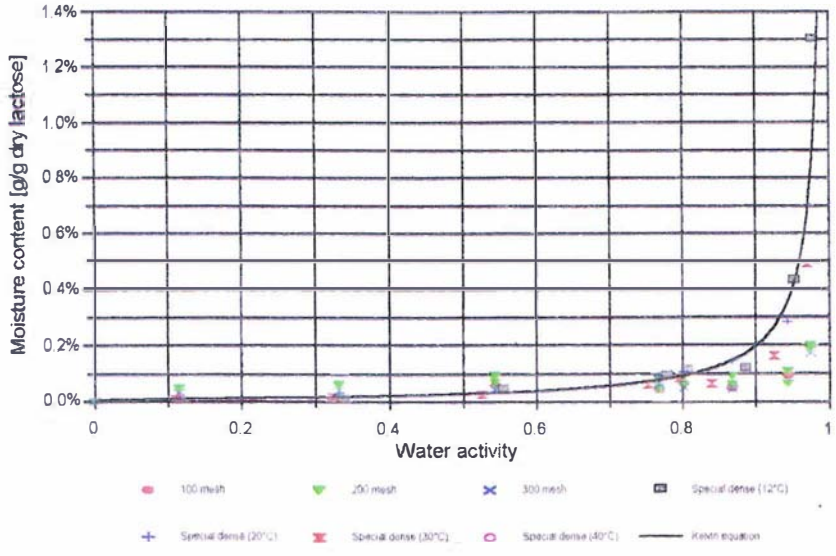

Figure 3.6 - Capillary condensation isotherm for α-lactose monohydrate.

3.3.4 β-LACTOSE:

The moisture sorption isotherm of β-lactose was determined because it has been reported to be the product of amorphous lactose crystallisation at low water activity (<0.55) by Vuataz (1988). If the thin layer of amorphous lactose present on milled lactose is crystallised to β-lactose then the sorption properties of the resulting crystal will be governed by β-lactose.

β-Lactose (Sigma lactose-3750) which consisted of 78% β-lactose and 22% α-lactose monohydrate, as determined by optical activity, was used in this work. Approximately 5 grams were suspended above saturated salt solutions for a period of one month in the same manner described above for α-lactose monohydrate isotherm determinations. The salts used to construct the β-lactose isotherm were;

LiCl	~	11%
$MgCl_2$	~	33%
$Mg(NO_3)$	~	54%
NaCl	~	75%
$(NH)_2SO_4$	~	81%
KCl	~	87%
KNO_3	~	94%
K_2SO_4	~	97%

It was anticipated that the isotherm for β-lactose would be similar to that of α-lactose monohydrate as the particle size distribution and particle density are similar. It was expected that β-lactose would behave as an inert solid and not adsorb large amounts of water until the capillary region is reached. For these reasons the salts were chosen to ensure more data points at high water activity. Desiccation over phosphorous pentoxide for one month was used to determine the free moisture content of the initial sample. The

isotherm points were then calculated from the observed weight gain in the samples. All measurements were conducted at 20°C.

The moisture sorption isotherm for β-lactose, calculated by weight change, is shown in Figure 3.7. It can be seen that the data suggest large quantities of moisture are adsorbed at high water activity. This corresponds to some 100 times more moisture than is adsorbed in α-lactose monohydrate for the same water activity. An explanation for this phenomenon was required before a good understanding of moisture sorption phenomena could be gained.

One explanation is that the β-lactose crystals are highly porous and therefore the specific surface area available for sorption is orders of magnitude higher than for α-lactose monohydrate. The scanning electron micrographs shown in Chapter 2 (Figures 2.3 and 2.4) show no evidence that β-lactose exists as highly porous particles. This means another explanation had to be found.

Troy and Sharp (1930) stated that solid β-lactose crystals can be converted to α-lactose monohydrate in the solid state above 0.65 a_w. The solubility of β-lactose at room temperature is approximately 50g per 100g or water. The solubility of α-lactose at the same temperature is approximately 7g per 100g of water. If this is considered, it is possible to understand how such a conversion in the solid state is possible.

If there is free moisture on the surface of a β-lactose crystal which is capable of acting as a solvent, then β-lactose will dissolve to form a saturated β-lactose solution. As muta-rotation will occur in solution, some β-lactose will convert to α-lactose in solution. As this occurs, more β-lactose will be dissolved from the surface to replace that lost by muta-rotation. It follows that, in time, the surface solution will become highly supersaturated with respect to α-lactose and the spontaneous crystallisation of α-lactose monohydrate will proceed. It follows then that β-lactose will dissolve preferentially to α-lactose and, through muta-rotation in the surface solution, it will be converted to crystalline α-lactose monohydrate. It should be possible to observe this phenomena if β-lactose is continually dissolved into a quantity of water. Solid α-lactose monohydrate will crystallise out. This conversion has been shown to occur in β-lactose based whey powders by Sharp and Doob (1941).

If α-lactose monohydrate is heated above 93.5°C in a moist environment, the reverse phenomenon occurs and was observed by Gillis (1920), Sharp and Hand (1939) and Olano *et al.* (1983). This is because the relative solubility of α-lactose and β-lactose, and the equilibrium position above 93.5°C favours the formation of β-lactose. The reverse reasoning to that applied above is then true.

This phenomenon of β-lactose to α-lactose monohydrate conversion in the solid state at water activity values above 0.65 could then explain the observed β-lactose sorption isotherm. When one mole of β-lactose is converted to α-lactose monohydrate then one mole of water is also bound as water of crystallisation. If this process is occurring during equilibration for the isotherm measurements, then it will show as weight gain even though this moisture is not free.

To check this hypothesis, a β-lactose sample was suspended above a saturated potassium chloride solution. After two weeks a sample was taken and the anameric ratio of the sample was measured by polarimetry, as was a sample which had not undergone the hydration treatment. The results showed an increase in the α-lactose content from approximately 22.8% α-lactose to 43.2% α-lactose, an almost doubling in α-lactose content with no change in the control sample.

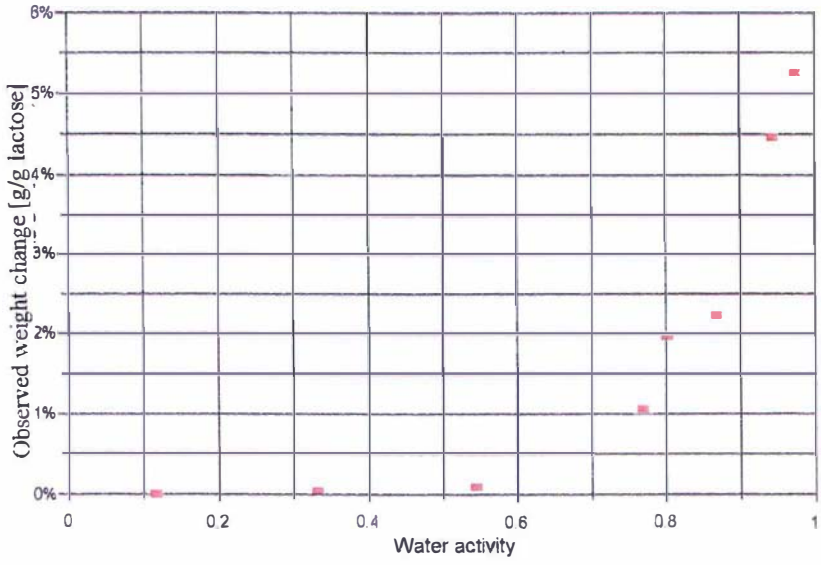

Figure 3.7 - Observed weight change of β-lactose after storage above saturated salt solutions for one month.

This increase in α-lactose content would result in the uptake and binding of water of crystallisation. The 19.4% increase in α-lactose observed would have resulted in a 1.1% increase in weight due to conversion of anhydrous β-lactose to α-lactose monohydrate. This is approximately half the observed weight gain shown in the β-lactose isotherm for a sample stored at 85%RH. It must be remembered that this preliminary test of the hypothesised β to α conversion in the solid state was using two weeks equilibration time where the isotherm measurements were taken over a one month period. It should be also noted that the observed weight gain in the β-lactose sample equilibrated over potassium sulphate ($0.98a_w$) suggests nearly complete conversion of β-lactose to α-lactose monohydrate had occurred.

This hypothesis therefore looks to explain the observed sorption phenomena of β-lactose, although a detailed investigation as to the extent and the rates of the transformation are required.

This discussion results in identifying that the measured data do not constitute a moisture sorption isotherm for β-lactose as a chemical transformation is occurring during the hydration. The rate of this transformation is thought to be dependant on the amount of moisture present and on temperature. For this reason the y-axis of Figure 3.7 is labelled as observed weight change rather than moisture content.

3.3.5 AMORPHOUS LACTOSE:

The moisture sorption isotherm data in the literature (Figure 3.1) shows a lot of scatter and does not demonstrate the effect of temperature on sorption behaviour. For these reasons the moisture sorption isotherm of amorphous lactose was measured as part of this work. The static gravimetric method outlined above for the crystalline isotherm determination was used, except emphasis was placed on measuring equilibrium moisture content at water activity values in the range $0\text{-}0.6a_w$. Above this range, crystallisation

occurs, and therefore isotherm data is not meaningful. The salt solutions used were;

LiCl	~	11%
KCH_2COO	~	23%
$MgCl_2$	~	33%
K_2CO_3	~	43%
$Mg(NO_3)$	~	54%

The raw results for the isotherm are shown in Figure 3.8 along with data collected by Jouppila and Roos (1993). The results do not shown any significant influence of temperature on the isotherm shape in the range investigated (15-40°C). Because the driving force for crystallisation increases with temperature, the maximum water activity at which a reading could be taken, reduced with temperature. This meant that at a water activity of $0.54a_w$ only the sample equilibrated at 12°C was achieved.

Jouppila and Roos (1993) fitted the GAB isotherm (3.11) to their isotherm data and it is also plotted on Figure 3.8. It can be seen that there is little difference between the data collected by Jouppila and Roos and that collected in this work. The GAB constants were adjusted to improve the fit to the spray dried amorphous lactose isotherm data after removing the three experimental outlying data points. Table 3.2 summarises the GAB model parameters fitted in this study along with those specified by Jouppila and Roos (1993).

$$M = \frac{M_0 c f a_w}{(1 - f a_w)[1 + (c-1) f a_w]} \qquad (3.11)$$

Table 3.2 GAB-isotherm parameters for amorphous lactose.

Parameter	This work	Jouppila and Roos (1993)
M_o [g/g dry lactose]	0.0488	0.0491
f	1.16	1.18
c	3.23	4.33

If these constants are interpreted as having physical meaning, it is evident that the GAB model is not consistent with the mechanistic basis of the isotherm model. A GAB constant f of greater than unity, as shown in Table 3.2, suggests that an asymptote will occur at a water activity less than one, which is a physical impossibility. The BET monolayer value is very high, which suggests a very large internal surface area and therefore the particle must be seen as a very porous particle. The time taken for absorption of moisture into the particle, shown in the following section however, suggests that diffusion is the mode of moisture uptake into the internal water sorption

sites and physical adsorption of water vapour occurs only on the outer particle surface. Because the GAB model describes absorption of a water vapour on to a surface and not a diffusion governed sorption process, it is not mechanistically applicable to amorphous lactose. The GAB model, with the fitted constants summarised in Table 3.2, will be used in this work for convenience, although it is stressed that no physical meaning can be attributed to any of the fitted parameters.

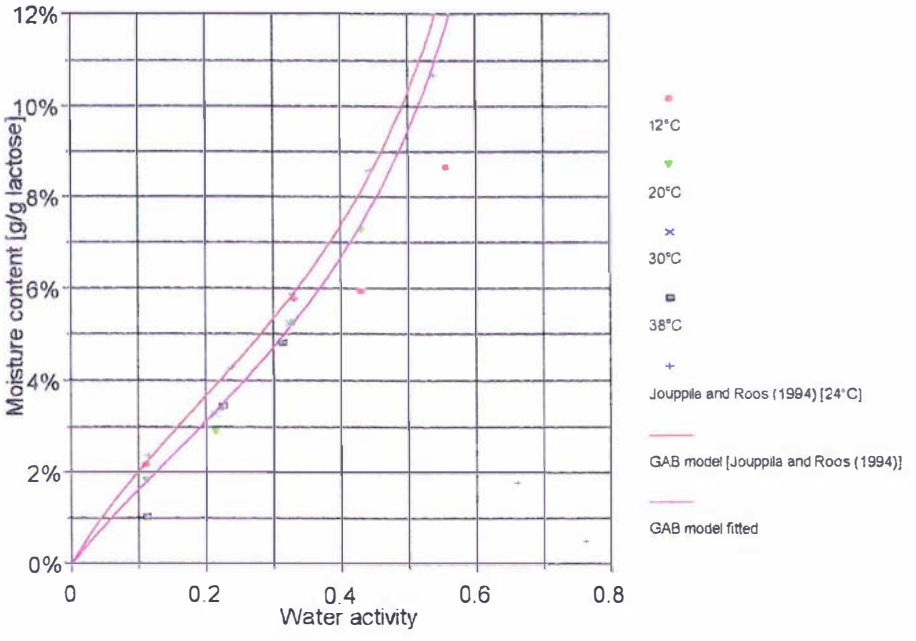

Figure 3.8 - Moisture sorption isotherm for amorphous lactose

3.3.6 MIXTURES OF CRYSTALLINE AND AMORPHOUS LACTOSE:

Because of the large moisture holding capacity of amorphous lactose, the effect of even small amounts of amorphous lactose is significant, in terms of increasing the free moisture available for spoilage and caking problems. In the water activity region where amorphous lactose is likely to be present (0-0.5) the amount of moisture adsorbed onto the crystalline surface is small.

The amorphous lactose layer, thought to be present on the outside of the particle, can absorb moisture throughout the whole amorphous mass. In this case the sorption isotherms for the individual components can be assumed to be additive on a mass basis. This will result in the isotherms shown in Figure 3.9.

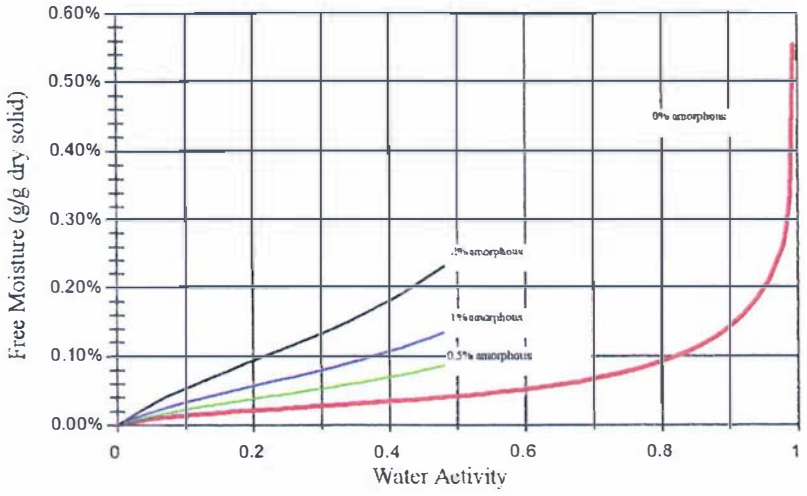

Figure 3.9 - Effect of small amounts of amorphous lactose on the sorption isotherm of α-lactose samples as predicted from the additive isotherm model.

The additive sorption isotherm model has been applied to explain the sorption isotherm of *Supertab* lactose, of which the amorphous lactose content, as quantified by the NMR technique developed by Hargreaves (1995), was found to be 9%. The result can be seen in Figure 3.10. It can be seen that very good agreement between the measured isotherm and the predicted additive isotherm was achieved. Further comparison of this model with varying amorphous lactose contents must be carried out before complete validation of the model can be achieved.

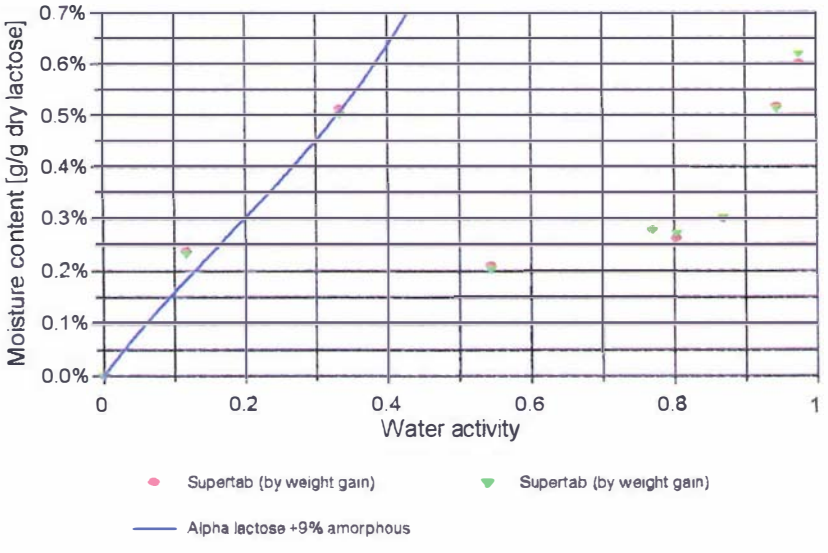

Figure 3.10 - Sorption isotherm of *supertab* lactose.

The effect of amorphous lactose on the isotherm illustrates the difficulties in using a moisture content measurement for use in understanding caking problems. If the amount

of amorphous lactose is unknown, then the moisture content measurement does not explain how resistant the product is to caking.

3.4 RATES OF MOISTURE SORPTION ON TO LACTOSE:

The rate of sorption of moisture on to both crystalline and partially crystalline lactose is necessary for the mathematical modelling of moisture transport in bulk lactose. Knowledge of the sorption rates will also improve the understanding of lactose drying, conditioning and caking phenomena. To achieve such an understanding, the rates of moisture sorption onto purely crystalline lactose and spray dried amorphous lactose were determined experimentally.

A Mettler AE200 analytical balance equipped with an RS232 interface connected to a 386 IBM compatible computer was used to data-log the change in weight of a lactose sample when applied to a step change in ambient relative humidity. The sample was surrounded by a 1 litre plastic bottle which had the bottom removed. Attached around the base of this surround was 5mm plastic tubing with holes drilled at regular intervals providing a manifold for air distribution around the sample. The top of the surround had a 15mm opening to allow air to escape. Air supplied from a Hycal water vapour generator was introduced into the chamber. Relative humidity and temperature of the air inside the chamber were also recorded using a Grant Squirrel data logger series 1000. This set up can be seen in Figure 3.11.

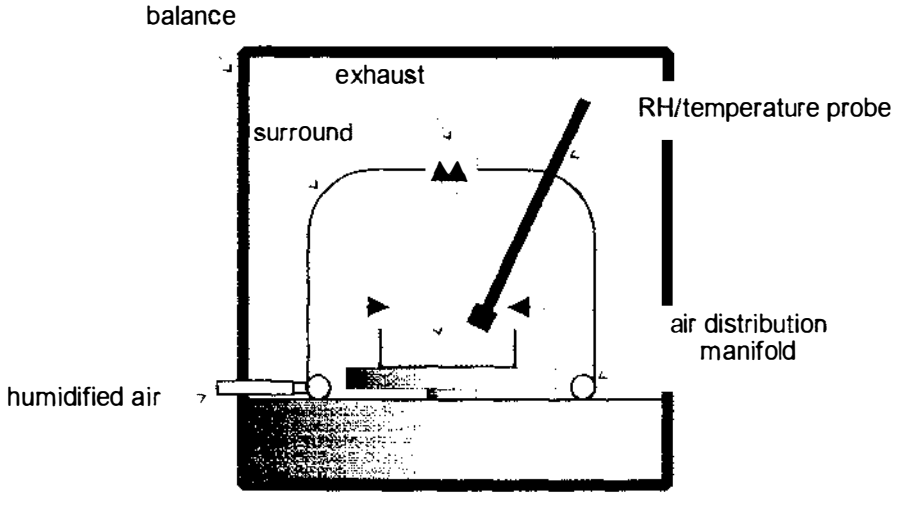

Figure 3.11 - Sorption rate measurement apparatus

The dew point generator was switched on to allow the chamber to reach a steady state condition. The sample was placed into the apparatus in an aluminium moisture dish as a thin layer of up to 3mm deep. In this way a step change was applied to the sample. The balance reading was data-logged along with the chamber relative humidity and temperature.

3.4.1 SORPTION ON TO α-LACTOSE MONOHYDRATE:

Crystalline 200 mesh lactose, which had been conditioned at high relative humidity to ensure no amorphous lactose was present, was used for the sorption rate experiments. The sample was allowed to reach equilibrium at 20% relative humidity at 30°C as indicated by constant weight. The water vapour generator was then changed to achieve a 90% relative humidity condition in the sample chamber. Figure 3.12 shows the change in relative humidity and moisture content of the lactose sample with time.

The variability in the relative humidity evident in Figure 3.12 was caused by small variations in the temperature of the controlled temperature room. It is evident in these results that there is a close coupling between a relative humidity rise and a subsequent moisture content rise. It should be noted that the relative humidity range investigated is in the exponential portion of the moisture sorption isotherm and therefore it is expected that large moisture content changes occur as a result of small relative humidity changes above 80% RH.

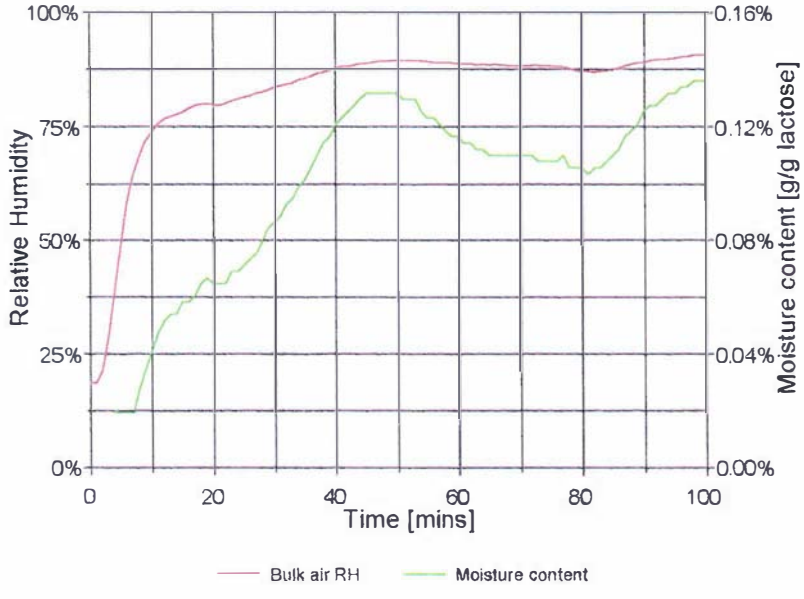

Figure 3.12 - Rates of sorption of moisture onto crystalline lactose.

Because the rate of moisture sorption is of the same order of magnitude as the change in relative humidity in the bulk air, it is difficult to see the sorption process alone. To show that the sorption of moisture on to crystalline lactose is fast, the predicted moisture content based on the recorded sample chamber relative humidity was compared against the moisture content observed in the experiment. In this way the bulk conditions and the state of the lactose can be compared directly. This is shown as Figure 3.13. At the beginning of the trial, there was a slight delay in the response of the lactose weight to that of the air relative humidity. This is due to the time taken for diffusion of water vapour through the lactose bed.

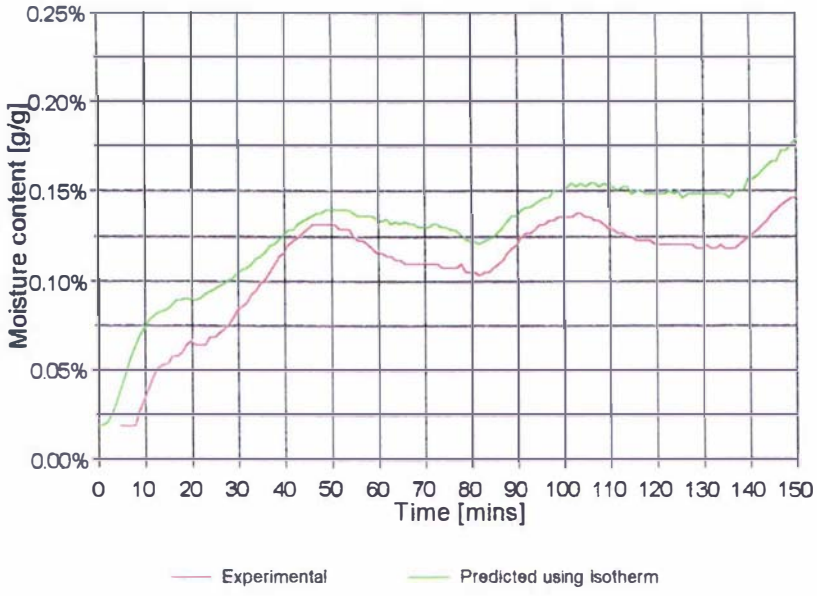

Figure 3.13 - Comparison of observed moisture content with that predicted from bulk air relative humidity.

It is clear from this plot that the rate of sorption of moisture on to crystalline lactose is fast. This is consistent with what is expected for physical adsorption onto a surface. If a Sherwood number of two is assumed, which corresponds to a stagnant system and hence the slowest system, then it can be predicted that the time constant for this process is of the order of less than a second (see Section 4.2.3.2). It is evident that it can be assumed that the state of moisture in the voidage of lactose and the solid crystalline lactose phase are in equilibrium as long as thermal equilibrium has been reached. This equilibrium assumption was used in further modelling of moisture transport in crystalline lactose.

3.4.2 SORPTION ONTO AMORPHOUS LACTOSE:

Amorphous lactose is much more hygroscopic than crystalline lactose and, as such, has very different moisture sorption behaviour. Amorphous sugars have a large number of internal sites where moisture can be attached. In this way the amount of moisture that can be sorbed in amorphous lactose is much larger than that found on crystalline lactose. It was important to describe the rate of sorption of moisture into an amorphous lactose particle. Knowledge of sorption rates into purely amorphous samples will improve understanding of amorphous lactose crystallisation phenomena and allow the prediction of sorption rates on to partially amorphous lactose particles.

The experimental methodology outlined above for the measurement of sorption rates onto crystalline lactose samples was adopted for the quantification of sorption kinetics of amorphous lactose. A sample of spray-dried amorphous lactose was equilibrated over phosphorous pentoxide for one month to ensure a completely dry sample prior to the sorption experiments. This sample was then placed in the rate measurement apparatus and the water vapour generator was set to give a chamber relative humidity of 43.5%

RH at 30°C. The weight of the sample was then logged and the moisture content change with time was calculated. The change in moisture content of the amorphous sample can be seen in Figure 3.14.

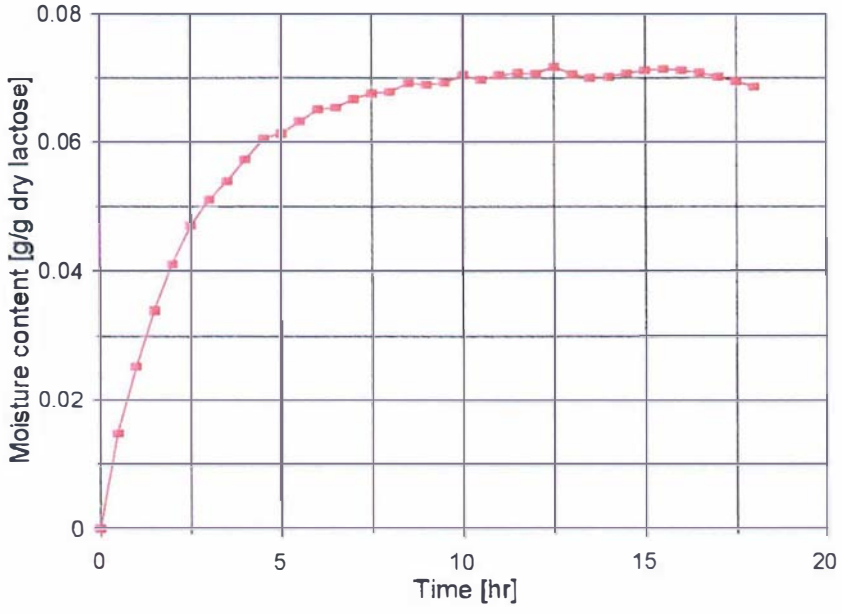

Figure 3.14 - Rate of moisture sorption onto spray dried amorphous lactose subjected to a step change in relative humidity from 0 to 43.5% RH.

Because the time for sorption is much greater than that for pure adsorption onto a surface (see Section 3.4.1) it is clear that this is not the controlling mechanism for the moisture sorption process on to amorphous lactose. Several researchers interpret the high BET monolayer value obtained from amorphous glass isotherms as indicating large internal surface areas, suggesting a highly porous structure (Berlin *et al.* 1973, Niediek and Babernics 1979 and Flink 1983). In the case of amorphous lactose however, it is clear that diffusion into the surface is the mode of moisture absorption into the particle. Adsorption of moisture is occurs only to the outer surface.

The rate of moisture gain shown in Figure 3.14 is the result of two competing rates. Firstly, diffusion of water vapour must occur from the bulk air into the thin lactose bed. Secondly the water vapour is absorbed into the amorphous lactose particles. In order to estimate the diffusivity of moisture in the amorphous lactose particle it was therefore required to somehow differentiate between these two rate processes.

The rate of sorption into the spherical amorphous lactose particles can be approximated as a reversible first order approach to an equilibrium moisture content.

$$\frac{d\xi}{dt} = D'(\xi_{eq} - \xi) = D'(\gamma C - \xi) \qquad (3.12)$$

where ξ is the mass average concentration of absorbed moisture in the amorphous particle, ξ_{eq} is the moisture concentration in equilibrium with the air moisture

concentration, C. D' is a constant to do with the rate of diffusion of moisture in the amorphous lactose and γ is a constant to relate the concentration C to ξ_{eq}. It can be shown that Y, the fractional unaccomplished change, can be related to the constant D' and to the Fourier number by the following relationship.

$$Y = e^{-D't} = \sum_{m=1}^{\infty} \frac{6}{(\pi . m)^2} e^{-(\pi . m)^2 Fo} \tag{3.13}$$

If the second and subsequent terms are ignored (true for larger Fo), then it can be shown that $D' \approx \pi^2 D/R^2$, where D is the diffusivity of moisture in the amorphous matrix and R is the particle radius.

The problem then lies in how to deal with the diffusion through the lactose particle bed. By using Eq (3.12) to describe the rate of sorption into the amorphous particle, the experiment can be mathematically represented as;

$$\frac{\partial C}{\partial t} = D_a \frac{\partial^2 C}{\partial x^2} - \frac{\partial \xi}{\partial t}$$

$$\frac{\partial \xi}{\partial t} = D'\gamma C - D'\xi \tag{3.14}$$

with boundary conditions and initial conditions given by;

$$\frac{dC}{dx} = 0 \qquad for \quad x = 0$$

$$C = C_b \qquad for \quad x = z \tag{3.15}$$

$$C = C_0 \quad and \quad \xi = \gamma C_0 \quad for \quad t = 0$$

This problem was solved analytically by Mikhailov and Ozisik (1985) This is given as;

$$Y = \frac{2}{\gamma} \sum_{m=1} \frac{[\gamma \cdot (1 - e^{-(\mu_m^2 D_a)(D'z^2)}]^2}{\zeta_m^2 [\gamma + (1 - (\mu_m^2 D_a)(D'z^2)]^2} \cdot e^{-\mu_m^2 t} \tag{3.16}$$

where ζ_m is the roots of $J_{3/2}(\zeta) = 0$. And μ_m is given by;

$$\mu_m^2 = \frac{1}{2} \left[\frac{D'z^2}{D_a} \cdot (1+\gamma) + \zeta_m^2 \pm \sqrt{\left[\frac{D'z^2}{D_a} \cdot (1+\gamma) + \zeta_m^2\right]^2 - \frac{4 D'z^2 \zeta^2}{D_a}}\right] \tag{3.17}$$

By approximating the moisture sorption isotherm of amorphous lactose as a straight line it was found that the constant γ = 18,789. The diffusivity of moisture in air was calculated from the expression given by Shah *et al.* (1984) multiplied by the porosity of the bulk powder. It was calculated to be 1.1×10^{-5} m^2/s. The roots to the Bessels function (ζ) were calculated using MATLAB version 5. The solution was then used to generate a plot of Y versus time. The only unknown in the system was the parameter D', and this fitted by minimising the sum of the squares of the differences between the predicted and experimental curves. This can be seen in Figure 3.15.

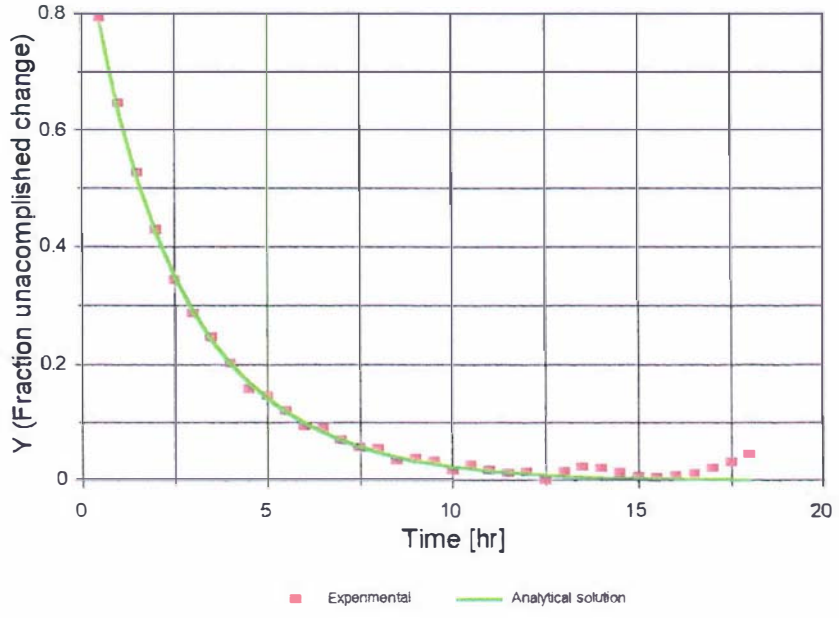

Figure 3.15 - Comparison of experimental sorption rates with analytical solution.

From this comparison it was found that the value of D' was 9×10^{-4} s^{-1}. By using the average particle size of 32μm, as measured by Lloyd *et al.* (1996) the diffusivity of moisture in the amorphous matrix was estimated at 2.33×10^{-14} m^2/s.

It is important however, to interpret this diffusivity measurement correctly. Measurements of moisture losses or gains, as determined from drying or adsorption rate curves, incorporate numerous transport mechanisms. Luikov (1980) specifies ten separate mechanisms for moisture movement that can be contributing to a diffusion co-efficient as measured from drying curves. These include molecular diffusion, mixing, recirculation, closed pores, dispersion, pore diffusion, surface diffusion etc.

It is desirable to be able to predict the magnitude of the moisture diffusivity in amorphous lactose at different temperatures and moisture content. To hypothesise what would happen to diffusivity in different conditions, it was necessary to look at the effect of these conditions on each of the mechanisms of moisture absorption separately.

Many researchers report experimental evidence of the moisture content affecting the diffusivity of moisture in foods as determined by drying kinetics [Fish 1958, Bruin and Luyben 1980, Luyben *et al.* 1980, Colin and Rasmuson 1988, Wang and Fang 1988, Tong and Lund 1990a, 1990b, Karel and Saguy 1991, Leslie *et al.* 1991, Vagenas and

Karathanos 1991, Xiong *et al.* 1991, Pel *et al.* 1993, Aguilera and Stanley 1990, Maroulis *et al.* 1995, Noel *et al.* 1995] or that the diffusivity of other solutes is a function of concentration [Al-Duri and McKay 1992].

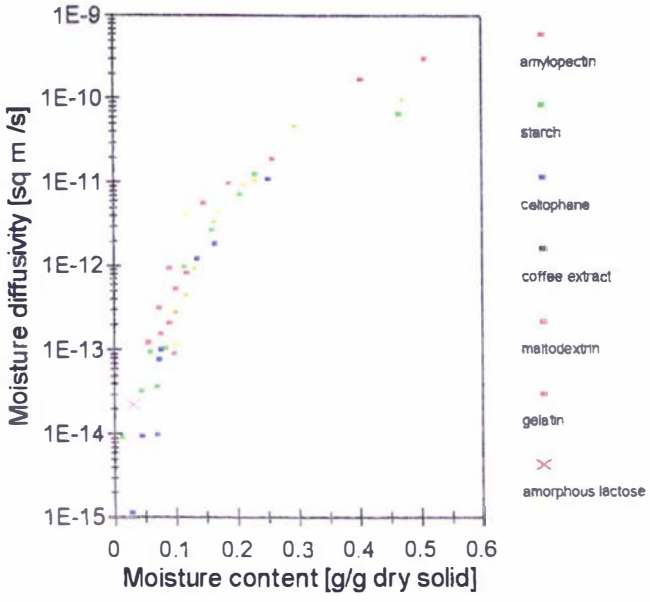

Figure 3.16 - Comparison of moisture diffusivity of some foods as a function of moisture content (from Bruin and Luyben 1980).

A typical illustration of how the apparent diffusivity of moisture in foods depends on moisture content in given by Bruin and Luyben (1980), which is shown here as Figure 3.16. The moisture diffusivity of spray-dried amorphous lactose measured in this work is also plotted on this graph. It can be seen that this data point continues the trend evident for moisture diffusivity in food materials as a function of moisture content.

The trend shown by these experimental observations is discussed by King (1968), who attributes the change in behaviour, to changes in the predominant mode of moisture transport. For example, capillary effects may predominate at high moisture content but at low moisture content there is not enough full pores for capillarity to contribute to the rate of moisture uptake by the porous food material.

Leslie *et al.* (1991) showed an increase in porosity in starch based materials as moisture content decreased. This was then used to explain the associated increase in effective diffusivity observed with decreasing moisture content. This is an example of how structural changes associated with the drying process can effect the moisture transport phenomena to produce a result that it opposite to what is normally expected in food systems.

It is clear from the literature that the amount of moisture in the system will influence whether capillarity, surface diffusion or pore diffusion is the controlling mode of moisture transport through the pore structure of the amorphous particle. It is equally evident that structural changes in the system caused by moisture or heating effects may affect the rate at which moisture is absorbed into the particle. In the case of amorphous sugars, this could include collapse phenomena which results in reduced porosity in the particle and as a consequence, reduced importance of pore diffusion. Crystallisation

phenomena may also be occurring within the amorphous matrix, which may release more moisture into the system and hence effect the absorption rate.

The effect of temperature on moisture diffusivity in porous media is often modelled using the Arrhenius relationship [Madamba *et al.* 1996, Tong and Lund 1990a,b, Karel and Saguy 1991] or by a modified Arrhenius relationship incorporating a factor accounting for the degree of binding of moisture in the system [Xiong *et al.* 1991]. The main reason for the increase in moisture absorption rates at higher temperature is the increased moisture holding capacity of hot air. In this way more moisture can be transported by the mechanism of pore diffusion.

The "solid" regions of the porous amorphous particle are regions of supersaturated sugar solution in either the glass or rubbery states. As such, molecular diffusion into these regions is molecular diffusion of water into a highly viscous concentrated liquid. The Stokes-Einstein equation has been developed from the hydrodynamical theory for moisture diffusivity in liquids [Welty *et al.* 1984] and can be used to relate the diffusivity to the viscosity of the liquid (see Eq (3.18)).

$$D = \frac{\kappa(T+273.15)}{6\pi r\eta} \tag{3.18}$$

Many other equations of this nature can be found in the literature to describe the relationship between diffusivity, temperature and viscosity [Welty *et al.* 1984, Reid *et al.* 1987, Sinnott 1989, Bird *et al.* 1960]. If such relationships are applicable to highly concentrated solutions around the glass transition temperature, then diffusivity should be proportional to free volume. Vrentas and Duda (1979) suggest that the best models for prediction of molecular diffusivity in polymer solutions are those based on free volume considerations.

Because the WLF model has been shown to describe the change in viscosity with temperature and moisture content around the glass transition temperature of sugar solutions it may be argued that the WLF model can be used to describe the change in moisture diffusivity. Karel and Saguy (1991) take this approach to allow the prediction of shelf life in food systems.

Le Meste *et al.* (1991) and Noel *et al.* (1995) argue that this is not the case and that viscosity and diffusivity are relatively decoupled properties. This is based largely around comparison of the magnitude of the change in viscosity between a dilute sugar solution and a solution near its glass transition temperature, when compared to the change in moisture diffusivity. A 12 log cycle change in viscosity gives only a 4 log cycle change in diffusivity. It should be pointed out however that the sugar solution near the glass transition temperature is likely to be porous and that the molecular diffusion processes under consideration may be several orders of magnitude less than the distances used in calculation of the effective diffusivity from drying kinetics.

To summarise this discussion it is suggested that direct comparison of apparent diffusivity values with dilute solution moisture diffusivity data using the Stokes-Einstein equation is not sensible as the Stokes-Einstein equation applies only for the molecular diffusion mode of moisture transport. Unless the distance for diffusion by this mode is quantified, accurate molecular diffusivity data cannot be achieved from drying studies.

It seems, from a brief revue of the literature, that the factors effecting the overall rate

of moisture sorption into amorphous lactose are very complex with a large degree of interaction. Because of this, it is suggested that more experimental data collection is required before further insight into the mechanisms of moisture sorption in amorphous lactose can be arrived at.

3.4.3 SORPTION ONTO MIXTURES OF CRYSTALLINE AND AMORPHOUS LACTOSE:

With a preliminary estimate for the diffusivity of moisture in amorphous lactose, it was possible to predict the sorption rates of mixtures of amorphous and crystalline lactose particles. In particular it is desirable to predict the rate of moisture uptake onto a lactose crystal with a layer of amorphous lactose present on the outside of the particle, such as is brought about during the flash drying and milling processes.

If it is assumed that the amorphous lactose present on a particle is evenly distributed on the surface of the crystal, then the thickness of the amorphous layer can be found from the measured specific surface area of the powder, using Eq (3.19).

$$x_{amorphous} = \frac{a\,\rho_c}{A_s \rho_a} \tag{3.19}$$

The amorphous lactose particle density (ρ_a) was calculated from the bulk density reported by Lloyd *et al.* (1996), assuming a porosity of 0.4. The specific surface area of typical grades of lactose powders were measured by a laser scattering technique, as part of the particle size distribution measurements discussed in Section 2.3.1. The estimates of typical amorphous lactose contents were taken from Table 2.3. The estimates of amorphous layer thickness as calculated using Eq (3.19) are summarised in Table 3.3 below.

Table 3.3 Summary of amorphous lactose layer thickness estimates for different lactose grades

Lactose sample	A_s [m^2/m^3]	a (%)	$x_{amorphous}$ [μm]
Special dense	36,200	1	0.56
100 #	86,700	2	0.46
200 #	275,400	4	0.29
300 #	319,400	6	0.38

It should be noted that these estimates are meant as guidelines only. The particle size prior to milling, will change the amount of milling needed to achieve the desired mesh size. Conditions in the drier can change from day to day and therefore the degree of flash drying can change. The storage conditions can allow amorphous lactose crystallisation.

Each of these factors will effect the amount of amorphous lactose present on a lactose sample.

In spite of this, the above calculations can be used as a guide to the thickness likely to be present on lactose powders. It is clear from the estimates in Table 3.3, that the powders with high amorphous lactose content also have high specific surface area. These effects largely cancel each other, resulting in a reasonably consistent amorphous lactose layer thickness. It is also evident from these calculations, that the amorphous layer is very thin (~ 0.3 to 0.6μm). With the amorphous layer thickness and the measured moisture diffusivity in amorphous lactose, it was possible to predict the time required for sorption to take place.

For most of the particle size distribution it is safe to assume that the thickness of the amorphous layer on the particle is much less than the particle radius. This being the case it is then possible to model the amorphous layer as an infinite slab of thickness $2x_{amorphous}$. The inside boundary between the amorphous layer and the crystalline surface is a symmetry boundary condition, as no moisture diffusion can occur past the crystalline surface. The outer surface of the amorphous layer can be assumed to be in equilibrium with the ambient air. The model is mathematically expressed as Eq (3.20).

$$\begin{aligned}
&\frac{\partial C}{\partial t} = D\frac{\partial^2 C}{\partial x^2} && for\ 0 < x < x_{amorphous} \\
&\frac{\partial C}{\partial x} = 0 && for\ x = x_{amorphous} \\
&x = f(RH) && for\ x = 0 \\
&x = x_i && for\ 0 \le x \le x_{amorphous} \quad and \quad t = 0
\end{aligned} \tag{3.20}$$

Crank (1975) gives an analytical solution to this problem which can be written as Eq (3.21).

$$Y = \frac{8}{\pi^2} \sum_{m=0}^{\infty} \frac{1}{(2m+1)^2} \exp\left[-\frac{(2m+1)^2 D t \pi^2}{4x_{amorphous}^2}\right] \tag{3.21}$$

This solution was used to evaluate the time sorption of moisture. Figure 3.17 shows the effect of amorphous lactose layer thickness on the time taken for sorption. It can be seen from this graph that because the layer is so thin, the time taken for sorption is short. This has obvious importance in the handling of the product prior to bagging, especially in situations where a large amount of air contact is occurring. The time taken for absorption into a packed bed of the powder will be much larger due to the coupled diffusion processes of diffusion through the bed, and absorption into the amorphous lactose layer.

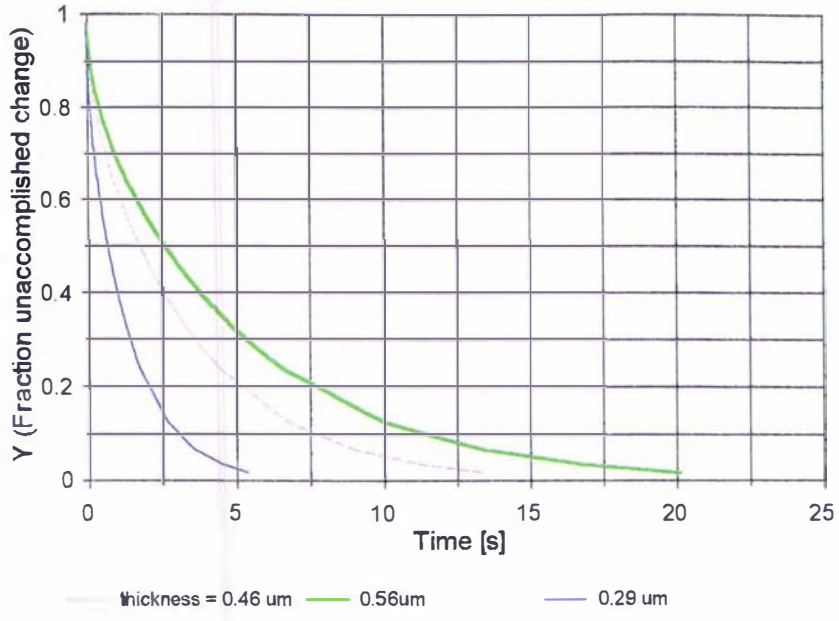

Figure 3.17 - Predicted rates of moisture sorption into varying thicknesses of amorphous lactose.

It must be remembered however, that when amorphous lactose surfaces are placed in conditions of high ambient humidity, crystallisation phenomena are also occurring which may release moisture and effect the sorption rates. In this case, the sorption rate will appear slower than predicted, depending on how fast the crystallisation rate is. This is because the outer surface of the amorphous layer will reach high moisture contents much faster than further into the amorphous layer. This may cause crystallisation and hence the expected steady state moisture content is reduced due to the depletion of the amorphous lactose present. Because the diffusivity of moisture in amorphous lactose is controlling the rate of adsorption, it appears that the rate of sorption is slower than predicted using the model developed above. The time taken until the rate of crystallisation overtakes the rate of sorption is however still expected to be similar to that predicted by the sorption model above.

The model used above for the prediction of sorption rates in mixed amorphous and crystalline particles is not yet validated. Sorption rates for samples with varying amorphous lactose contents are needed to achieve this. The diffusivity of moisture in amorphous lactose used in the construction of Figure 3.17 is that measured in this work. As such, the effect of temperature and moisture content has not been included, due to unavailability of data. If diffusivity is a function of temperature and moisture content, then the analytical solution used above is not applicable, as constant properties are not observed. If this is true then a numerical solution to the problem is required.

3.5 MOISTURE CONTENT DETERMINATION

There are two main reasons to measure the moisture content of lactose samples. The first is to satisfy product specifications. The specification will state what moisture content determination method is to be used and what results are acceptable. The second and most important reason is to give information on what is occurring in lactose. Hopefully this information can be related to quality problems like caking and mould growth, and solutions to reducing quality problems can be identified. As stated previously it is "free" surface moisture, not "bound" crystal water that contributes to caking related phenomena. With this in mind, this section will discuss the merits and demerits of the common methods of moisture determination.

Moisture content measurement in α-lactose monohydrate is difficult. This is because of the different characteristics of the two types of moisture present in the powder, that is "bound" and "free" moisture. The differences between these types of moisture have been highlighted above. The difficulties arise because of the "bound" water of crystallisation comprising 5% (g/g dry solid) is two orders of magnitude greater than the "free" moisture we are interested in, which comprises about 0.05% (g/g dry solid).

The most widely accepted method for "free moisture" in food science research is vacuum desiccation over phosphorous pentoxide for at least one month. Phosphorous pentoxide maintains an absolute humidity of 0.0193 mg water per kg of dry air and is therefore an excellent desiccator [Grayson 1979]. It will remove only free moisture as no extra energy is applied to the sample to overcome the activation energy required to break the relatively strong bonds holding the water of crystallisation within the lattice structure. This method was used in construction of the sorption isotherms presented in this report. Due to the long time requirements, this method is not applicable for routine industry based measurements and another quicker method must be identified.

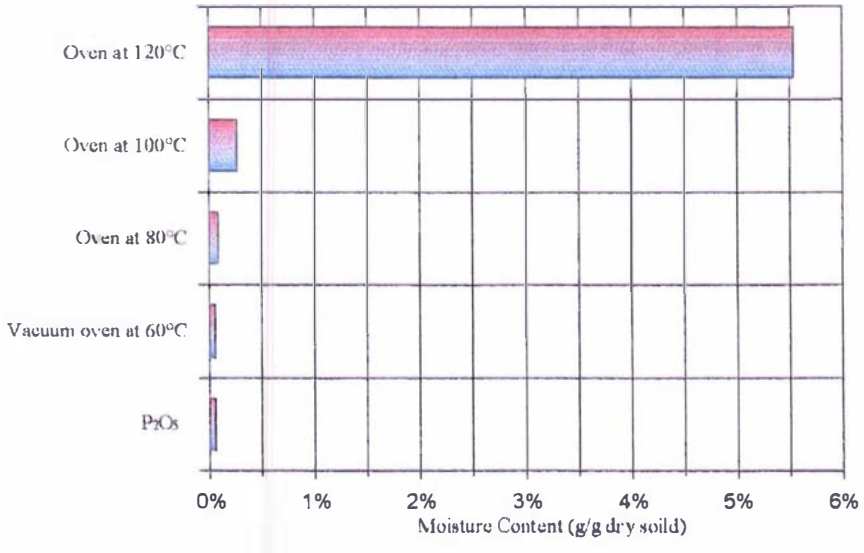

Figure 3.18 - Comparison of drying techniques for the measurement of moisture content in α-lactose monohydrate. Comparison included oven drying at 80, 100 and 120°C for 2 hours, 60°C at 700 mm Hg vacuum for 3 hrs and desiccation over phosphorus pentoxide for 2 weeks.

It is possible to remove the bound water if the water molecules receive enough energy. An anhydrous crystal form is produced if the lactose is dried at 120°C [Stecher 1968]. For this reason, moisture content determination methods based around oven drying can be prone to large errors. If the oven drying method removes even 1% of the bound water of crystallisation, the moisture content calculated from the observed weight loss will over estimate the "free" moisture content by 100%. This can be demonstrated by the results of moisture content measurements taken on the same sample using oven drying at varying temperatures (see Figure 3.18).

It can be seen that as temperature increases, more and more "bound" moisture is removed. As a consequence, the oven method lactose moisture content measurements are seldom repeatable and often meaningless when used to explain caking and spoilage related phenomenon. The vacuum oven drying method, which dries the samples at 60°C gives sensible results which agree favourably with the phosphorous pentoxide desiccate method. This indicates that at this low temperature, only "free" surface moisture is removed. The vacuum oven drying method is therefore, an acceptable method for routine free moisture content determinations.

One might argue, that if drying at 120°C removes all of the "bound" moisture, then this method can be employed and the theoretical "water of crystallisation" can be subtracted off to give an estimate of the "free" moisture present. This is true in theory but in practice, the error inherent in the oven method is typically of the same order of magnitude as the free moisture we having to measured. For example to employ this method, the oven drying measurement must report a result of say 5.010±0.005% to achieve a free moisture measurement of 0.010±0.005%. Clearly, this is not a realistic expectation.

A similar argument can be applied to the Karl Fischer technique. In this method the entire sample is dissolved and all the moisture is released. The amount of moisture released is then determined by titration. It follows that this is a measurement of the total moisture content, including water of crystallisation. The accuracy of the Karl Fischer technique does not allow the free moisture content to be determined.

It should be also evident from this discussion that even if one were content to measure the total moisture content, the accuracy of the oven drying and Karl Fischer methods, mean that only very large changes in the free moisture content will be observable. This means that the water activity must be greater than 0.8. This corresponds to a very wet product which is not expected in industrial lactose production after drying Therefore, these techniques are not useful in efforts to understand product moisture relations in the dryer and downstream processes.

Other moisture content determination techniques exist but similar accuracy problems limit their usefulness. Of the methods discussed here, the most accurate is the phosphorous pentoxide desiccation method. This is not suitable for routine measurements due to long time requirements. Almost as good as this method is vacuum oven drying at 60°C. The results of this technique were very similar to the desiccation method. The vacuum oven drying method can be used in routine measurements to provide useful information regarding caking related phenomena.

The effect of even small amounts of amorphous lactose can have a profound affect on the measured moisture content. This means that even if a good technique for "free" moisture content measurement has been used, the results explain nothing about the state of amorphous lactose in terms of the rate of crystallisation, unless the amorphous lactose

content is also known. This is a difficult property to measure and at present only an NMR technique is available [Hargreaves 1995]. Moisture content measurements for samples which contain amorphous lactose therefore provide very little information which can be related to spoilage or caking problems in bulk product.

An alternative measurement which is of use for such considerations is water activity.

3.6 WATER ACTIVITY MEASUREMENT

The shape of the sorption isotherm for crystalline lactose (Figure 3.3) shows that water activity measurements are much more sensitive than moisture content measurements. The low slope of the isotherm at low water activity values means that while a moisture content measurement on a batch of samples may show only small differences of 0.01%, the samples in the batch may have water activities which may vary by up to 0.1. The moisture content can be predicted from the water activity reading using the sorption isotherm for the product being measured.

The sorption behaviour of amorphous lactose means that if the pure amorphous lactose isotherm is known, the water activity of the whole product will allow the estimation of the moisture content of the amorphous fraction without knowledge of how much amorphous lactose is present. This is useful, as from this information the glass transition temperature can be calculated and it can be shown whether the amorphous lactose is in a condition where crystallisation will occur or not. If amorphous lactose crystallisation is occurring, the rate of crystallisation can also be estimated. This analysis can not be achieved with a moisture content measurement of a lactose sample alone.

It follows from this discussion that the method of choice for identifying the state of moisture relations in lactose powders is by measurement of water activity and not by moisture content.

A review of the different techniques for measurement of water activity has been conducted by Troller (1983). This discusses various methods including bi-thermal equilibration, vapour pressure manometer, hair hygrometer, isopiestic hygrometry, electrical hygrometers, psychometry, dew point measurement and freezing point depression. The equilibration time, reliability, cost and maintenance requirements of each instrument are compared.

As discussed previously, water activity is the relative humidity of air which is in both thermal and moisture equilibrium with the product of which the water activity is being measured. There are many methods available for measurement of the psychrometric properties of air so it follows that water activity can be best measured by allowing the product to come to equilibrium with some air and then measure the relative humidity of this air. This is the basis of most water activity measurement devices.

In electronic water activity meters, equilibration times of down to five minutes are reported. This would make such meters suitable for routine laboratory analyses. The problem is however, that five minutes is not likely to be sufficient time for equilibrium to be reached. In a sealed vessel containing a 50mm deep bed with a stagnant head space above it, three hours are needed before a steady state relative humidity is achieved. For these reasons careful assessment must be made before purchase of a water activity meter. If long equilibration times are required for accurate water activity measurement, the number of analyses that can be achieved using one water activity meter would be only a

few per day.

One alternative to an electronic water activity meter is a water activity kit developed by the CSIRO in Sydney, Australia [Steele 1989]. In this method, the product is sealed in a glass jar with a petrie dish containing a liquid which is allowed to come into equilibrium with the sample and air in the jar for sixteen hours. After equilibrium has been reached, the refractive index of the liquid is measured using a refractometer. This takes approximately one minute. Using this method, long equilibrations can be used to ensure accurate measurements and as many samples as there are jars available can be performed. The only major drawback is that it takes sixteen hours until the result is known.

In this work a water activity meter was developed based on a Hycal capacitance type relative humidity probe which was sealed into the screw cap lid of an air tight glass bottle. All readings were taken at constant temperature (25°C) by submerging the sample container in a water bath. The relative humidity measurement was recorded on a chart recorder to give a visual indication of when equilibrium had been reached. Once a steady state measurement was observed the water activity was read. This can take up to three hours for a lactose sample.

3.7 PROPERTIES OF AMORPHOUS LACTOSE:

Due to the importance of amorphous lactose on the moisture relations of lactose and on caking phenomena it is necessary to characterise the properties of amorphous lactose.

3.7.1 GLASS TRANSITION TEMPERATURE:

The glass transition temperature for a given material with varying moisture content can be predicted using the Gordon and Taylor equation Eq (3.22) originally formulated for T_g prediction of mixtures of polymers [Slade and Levine 1991, Roos and Karel 1991a, 1991b, 1991c, 1993].

$$T_g = \frac{w_1 T_{g1} + k w_2 T_{g2}}{w_1 + k w_2} \qquad (3.22)$$

where k = constant for material, w_1, w_2, T_{g1} and T_{g2} are mass fractions and glass transition temperatures (dry) of components 1 and 2 respectfully. Johari *et al.* (1987) and Mayer (1988) predicted the glass transition temperature of pure amorphous water to be at -135°C. Dry lactose has a glass transition temperature of 101°C. Values of k for amorphous lactose have been determined to be 7 [Roos and Karel 1991c], 6.7 [Jouppila and Roos 1994] and 6.56 [Roos 1993].

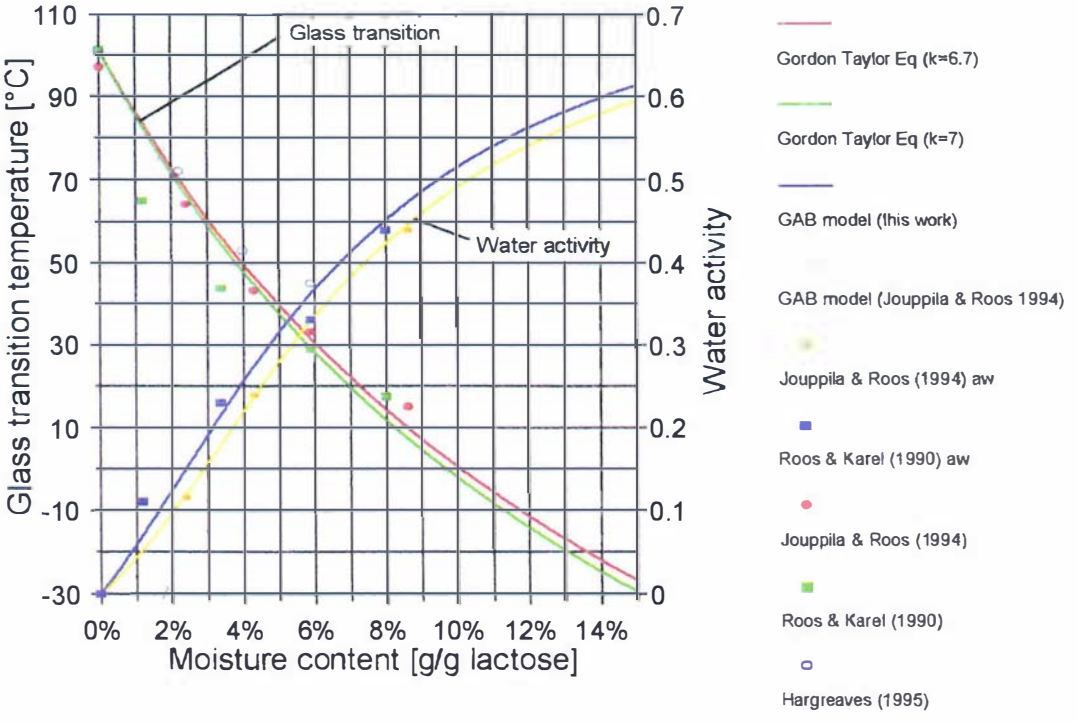

Figure 3.19 - Glass transition temperature of amorphous lactose as a function of moisture content.

This relationship can be seen in Figure 3.19 in the moisture content range of interest to this work. This plot highlights the extreme dependancy of the glass transition temperature on the moisture content of amorphous lactose. The measured glass transition temperatures are reported to ±5 °C in some cases [Hargreaves 1995] and depend on the scanning rate used in the differential scanning calorimeter run. It can also be seen from Figure 3.19 that the value of the constant (k) in the Gordon and Taylor equation gives quite different glass transition temperature predictions in the moisture content area of interest (4-12%). In this moisture content range the best predictions are for the lower constant value (k = 6.7) given by Jouppila and Roos (1994). The value given by Roos (1993) (k = 6.56) is not based on experimental data for amorphous lactose but predicted from data for many sugars and extrapolated to include amorphous lactose. For this reason it was not used in subsequent work.

The moisture content prediction is also critical with respect to an accurate prediction of the glass transition temperature from a water activity measurement. The isotherm given by Jouppila and Roos (1994) predicts a slightly higher moisture content for the same water activity than the isotherm determined in this work. This results in a difference in moisture content of up to 1% which in turn corresponds to a difference in glass transition temperature of up to 5 °C. This has obvious significance with respect to the prediction of crystallisation rate and other molecular mobility limited processes. The isotherm measured in this work was used in subsequent calculations to estimate the glass transition temperature of amorphous lactose.

3.7.2 VISCOSITY OF AMORPHOUS LACTOSE:

The viscosity of amorphous lactose is important when considering the bridging of amorphous lactose between adjacent particles forming sticky agglomerates. The WLF or Williams-Landel-Ferry equation relates relaxation time of mechanical properties to the temperature above the glass transition temperature (T_g) [Williams *et al.* 1955]. Viscosity is a property which is governed by the relaxation of the amorphous structure. The equation is given by Eq (3.23).

$$\log\frac{\eta}{\eta_g} = \frac{C_1 (T - T_g)}{C_2 + (T - T_g)} \qquad (3.23)$$

Williams *et al.* (1955) reported average constants (C_1 and C_2) to be 17.44 and 51.6 respectively and to apply for many materials. Soesanto and Williams (1981) found these universal constants to be adequate to describe the temperature dependence of viscosity of sugar solutions at temperatures above the glass transition temperature. Williams *et al.* (1955) state however that the universal constants should only be used as a last resort for describing relationships where no reliable data are available from any other source. Because no viscosity data for amorphous lactose exists above the glass transition temperature and because the universal constants were shown to be adequate for sucrose solutions [Soesanto and Williams 1981] these values will be used in this work. From (3.23) and the universal constants Figure 3.20 was constructed.

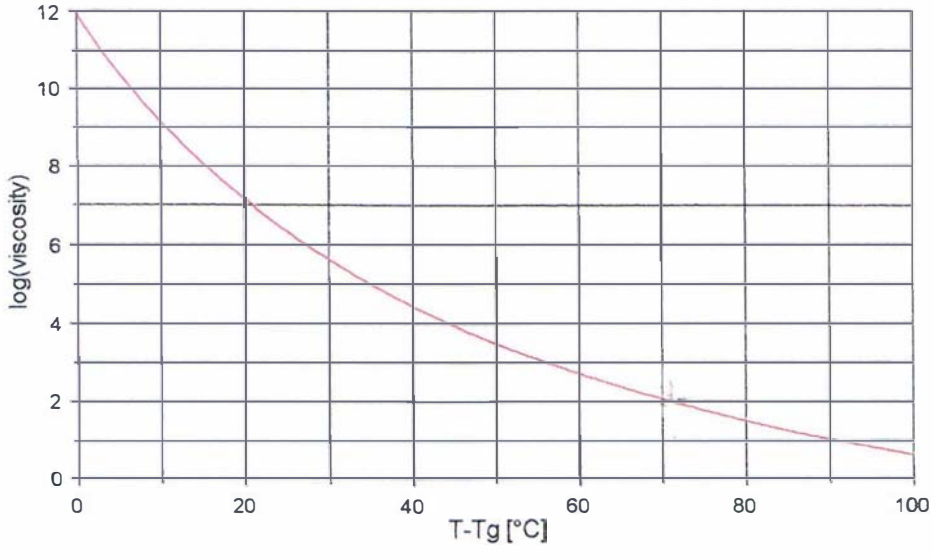

Figure 3.20 - Dependence of viscosity on temperature above glass transition temperature predicted by the WLF equation.

3.7.3 QUANTIFICATION OF AMORPHOUS LACTOSE IN LACTOSE POWDERS

Some method of quantification of the amount of amorphous lactose present in lactose powders was required, in order to model the moisture movement and caking phenomena in bulk lactose. Three methods of quantifying low levels of amorphous lactose have been reported in the literature. Hargreaves (1995) developed a low resolution nuclear magnetic resonance method. This is expensive to carry out as specialist equipment and operators are required. Hargreaves also showed that polarimetry can be used, if some equilibrium ratio of α and β lactose is assumed. The background levels of β-lactose, in the crystalline lactose portion are also needed. Buckton and Darcy (1995) developed a method which used very accurate gas adsorption equipment. A dry lactose sample was made to undergo crystallisation at 90% RH where it was expected that the product of crystallisation would be α-lactose monohydrate. The sample was then subjected to dry conditions again. The weight increase in the sample was assumed to be due to an increase in water of crystallisation associated with the newly formed α-lactose monohydrate crystal.

Two new methods of identifying and quantifying the amount of amorphous lactose in a predominately crystalline lactose sample were hypothesised as part of this work and further developed in other projects [O'Donnell (1997), Paterson *et al.* (1997)].

The first method uses the additive isotherm developed for mixtures of crystalline and amorphous lactose samples (see Section 3.3.6). Samples of the powder to be tested were placed in desiccators kept, at 0 and 33% RH using phosphorous pentoxide and a saturated solution of magnesium chloride. The moisture content was evaluated from the weight changes after two weeks equilibration time and the amorphous lactose content was determined using the additive isotherm Eq (3.24).

$$M_{mixture} = M_{crystalline} + a.M_{amorphous} \qquad (3.24)$$

where the moisture contents of the crystalline and amorphous phases were evaluated using the moisture sorption isotherm equations of each phase at 0.33 a_w (Eq's (3.2) to (3.4) and (3.11)) .

The second method makes use of the moisture release that occurs during crystallisation. A sample of lactose was sealed into a 20 ml Kimex tube with a Hycal dew point probe attached, so the water activity of the product could be measured. The initial water activity was recorded and then the sample was heated, in a water bath to 90°C, to cause any amorphous lactose on the sample to crystallise. This was indicated by a increase in the measured headspace relative humidity. The sample was cooled back to ambient temperature and the final water activity of the sample recorded. An increase in water activity of the sample was taken to indicate the presence of amorphous lactose. If an assumption on the product of crystallisation is made, an estimate of the quantity of amorphous lactose present can be made. Paterson *et al.* (1997) and O'Donnell (1997) showed that the predictions made by assuming either, complete crystallisation to an anhydrous product, or complete crystallisation to a hydrous product, fell either side of the amorphous content of the samples as measured by the additive isotherm method, polarimetry and NMR. Because of this, the method was used, only as a test for the presence of amorphous lactose in a sample, as a result could be obtained within a few hours.

3.7.4 CRYSTALLISATION OF AMORPHOUS LACTOSE:

3.7.4.1 Product of amorphous lactose crystallisation:

The work of Vuataz (1988), studying the role of water activity and temperature in lactose crystallisation has been widely used in discussion of the crystallisation product of amorphous lactose. Very little direct investigation of the crystallisation product has followed, in spite of the significance of this in interpreting and establishing the mechanisms for amorphous lactose crystallisation kinetics.

Vuataz (1988) measured the rate of sorption of moisture in spray-dried milk powders and observed moisture loss, due to amorphous lactose crystallisation, at humidities greater than 39.1% RH at 25°C. The product was determined using near infra red spectroscopy. For water activity values of 0.391 and 0.493, the crystallisation product was shown to be β-lactose. At a water activity of 0.572, the product was α-lactose monohydrate. It should be noted that the near infra red spectra are difficult to interpret and this method has not been used in any subsequent work.

Vuataz (1988) continued the investigation by crystallising spray dried milk samples at 80°C and 98°C. He concluded that at 0.55 a_w and 80°C a phase change from amorphous lactose to β-lactose occurred after about three minutes followed by conversion to α-lactose monohydrate after about sixteen minutes. At the same water activity but at 98°C, amorphous lactose first crystallises to α-lactose monohydrate in one minute but then converts to β-lactose after about sixteen minutes. At higher water activity (0.58 a_w) α-lactose monohydrate crystallisation occurs at low temperature and β-lactose crystallisation occurs at high temperature (>93.5°C).

There are many other observations of amorphous lactose crystallisation in the literature although not all researchers have directly investigated the crystallisation product.

Herrington (1934) observed amorphous lactose crystallisation in humidified environments by measuring the weight change of an amorphous lactose sample placed in high humidity environment. No effort to measure or control the level of relative humidity in the balance chamber was taken, but the results show that when the maximum amount of moisture adsorbed was high, the crystallisation time was reduced and α-lactose monohydrate was the crystallisation product. In runs where the maximum amount of moisture was not as high, crystallisation times become longer and a mixture of α-lactose and β-lactose were produced.

Sharp and Doob (1941) suggest the product of crystallisation in whey powders is the crystal form that is previously present in the powder. That is, if the powder has predominantly crystalline β-lactose in the solid phase, the amorphous lactose will crystallise to the β-form. If α-lactose is present in the crystalline fraction, then the amorphous lactose will crystallise to the α-form. These conclusions were drawn from measured changes in the anameric ratio with temperature at constant relative humidity. Upon investigation of the data it is difficult to see the justification for such a conclusion. The small changes in α-lactose content could be explained by experimental uncertainty. The data of Sharp and Doob do however show strong evidence that crystalline β-lactose will convert to α-lactose monohydrate if placed in environments of above 65% relative humidity, as first stated by Troy and Sharp (1930).

Sharp (1938) developed a seeding test to detect the presence of a α-lactose

crystalline surface or a β-lactose surface. The method involved making a slightly supersaturated solution of lactose at temperature above and below 93.5°C. Seed crystals were then added to the lactose solutions. If the seed crystals are β-lactose then growth would be observed in the supersaturated solution above 93.5°C but not in the solution below 93.5°C. The reverse observation was found to be true for α-lactose crystal seeds. Sharp (1938) then used this technique to test the crystalline form present on the surface of industrially produced α-lactose monohydrate crystals. Surprisingly, these crystals tested positive for the presence of β-lactose. When the same crystals were moistened with a small amount of water before being added to the seeding test, they indicated no β-lactose present. The small amount of water added was enough to dissolve the crystalline β-lactose present on the α-lactose crystal surface. The presence of β-lactose on the crystal surface was explained by the crystallisation of β-lactose from a small amount of amorphous present on the surface due to rapid drying. Sharps' observation indicates that amorphous lactose can crystallise to β-lactose even when the main crystalline form present in the sample is α-lactose monohydrate. This observation disagrees with the conclusions given by Sharp and Doob (1941). Sharp (1938) found that tests on spray-dried milk powders which have caked due to amorphous lactose moisture adsorption and crystallisation usually showed the presence of β-lactose.

Bushill *et al.* (1965) report that amorphous lactose obtained by freeze and spray-drying lactose solutions crystallises as a mixture of α-lactose monohydrate and β-lactose when exposed to air of a fairly wide range of humidities. Under similar conditions the amorphous lactose present in spray-dried milk powders crystallise to α-lactose monohydrate although it can crystallise to an anhydrous molecular compound consisting of α-lactose and β-lactose in a molar ratio of 5:3. This was identified using x-ray diffraction techniques. Jouppila *et al.* (1997) have recently reported the existence of this product in spray dried milk powder.

Berlin *et al.* (1968) measured the moisture sorption isotherm for freeze-dried lactose at 24.5°C. This shows crystallisation of the amorphous lactose occurred above 0.375 a_w. The crystallisation product has a total moisture content of 1% for 0.375 a_w to 0.85 a_w, indicating the formation of β-lactose or a mixture of α-lactose and β-lactose.

Warburton and Pixton (1978) showed a similar observation when they measured the change in weight of lactose glasses at different relative humidities. The results show crystallisation occurred at 0.45 a_w and an anhydrous product was produced. Their results also show the expected rise in weight which would result from the conversion of β-lactose to α-lactose monohydrate at high water activity.

Linko *et al.* (1982) measured the isotherm of amorphous lactose by dehydrating over phosphorous pentoxide then hydrating to a water activity of 0.9 and measuring moisture content by weight change and water activity using a relative humidity probe. The accuracy of the isotherm is questionable as no note of the equilibration time for the water activity measurement is given, and more sorption, followed by crystallisation and moisture release is expected at high water activity. It is unlikely equilibrium was reached in this experiment and therefore, what was measured as water activity can not be called water activity by definition. The result is interesting however, as the second desorption isotherm curve shows evidence of crystallisation, as indicated by a drop in the moisture content of the sample. The product moisture content, as measured by weight gain, is below the water of crystallisation content of pure α-lactose monohydrate (≈ 5.26% w/w). This suggests that some β-lactose was formed due to the crystallisation of

amorphous lactose.

Niediek (1982) measured the rate of sorption of moisture onto amorphous lactose with a sensitive balance. At 60°C and at a relative humidity of 46.8%, the lactose adsorbed a maximum of 4.6% moisture before crystallisation occurred in one- two hours. The resulting moisture content, as measured by weight change, was 0.8% which suggests the formation of β-lactose. At 30°C and 50% relative humidity the maximum moisture content reached was 10% and crystallisation occurred within ten hours. The crystallised product had a moisture content of 3.5%, indicating a mixture of the α- and β-lactose forms.

Wursch *et al.* (1984) looked at crystallisation of spray-dried milk powders with a moisture content of 3.14% stored at different temperatures. No change was observed in moisture content, lactose content or anameric ratio after 60 days for those samples stored at 45°C. At higher temperature significant lactose losses occurred, caused by extensive Maillard reaction reaching 21% lost after two months at 60°C. Lactose crystallisation accompanied the lactose losses by Maillard reaction. A reduction in α-lactose content and an increase in β-lactose was observed. This result was confirmed by x-ray diffraction. It was also shown that the rate of crystallisation to β-lactose at 60°C increased with increasing moisture content. At 6.1% moisture content, lactose started to crystallise to the β-anameric form but after two days α-lactose monohydrate was formed progressively. Wursch *et al.* (1984) suggested protein in milk powders may be important in favouring β-lactose crystallisation.

Saito (1985) reported that crystallisation to β-lactose proceeded very slowly in whole milk powder at 37°C, when humidity was low enough to inhibit the crystallisation of α-lactose monohydrate. X-ray diffraction analysis confirmed that β-lactose alone, was in the crystalline state in whole milk powder stored at 37°C for 5 months at an relative humidity of less than 20%.

Labrousse *et al.* (1992) investigated collapse and crystallisation in amorphous lactose matrix and showed that crystallisation of lactose in a lactose-gelatin matrix occurred rapidly above 52% relative humidity at 25°C as indicated by moisture loss. The final equilibrium moisture contents of those samples which crystallised ranges from about 1 to 2.5%. This indicates that complete crystallisation of amorphous lactose to α-lactose monohydrate did not occur, even when placed in relative humidity environments of up to 85%.

Jouppila and Roos (1994) measured the sorption isotherm of amorphous lactose by weight change and found that no measurements for water activity values above 0.55 a_w were possible because crystallisation at 24°C occurred before equilibrium moisture content was achieved. The moisture contents of the crystallised samples were approximately 2% at 0.66 a_w and <1% at 0.76 a_w. This indicated the product of crystallisation in these samples was β-lactose or a mixture of the α-lactose and β-lactose forms.

If the amorphous lactose structure is considered, it is evident that both α-lactose and β-lactose are highly supersaturated. If the mobility of the molecules are high enough, they should both spontaneously nucleate and crystallisation will proceed. In the case of β-lactose, there is nothing to stop this occurring if the molecules are able to move and arrange themselves into the ordered crystal lattice structure. α-Lactose monohydrate crystals, however, require lattice water to keep the structure stable. This is only possible if there is enough water present in the amorphous matrix.

Walstra and Jenness (1984) report that it is possible to produce a stable (S) anhydrous α-lactose crystal form by crystallisation from a supersaturated solution of lactose in ethanol. It is conceivable that such a product could be formed during the crystallisation of amorphous lactose at low water activity. In both ethanol solutions and dry amorphous lactose there is not enough moisture present to support the formation of α-lactose monohydrate crystals. The stable (S) α-lactose will dissolve preferentially to α-lactose monohydrate and therefore in high water activity conditions, it is likely that it will be converted into the hydrous form, in much the same way that β-lactose has been shown to do.

A general mechanism of the amorphous crystallisation phenomena, that fits most of the observations reported in the literature can be hypothesised. Either β-lactose or (S) α-lactose anhydride crystal forms will form during the crystallisation of amorphous lactose at low water activity (<0.55). At high water activity, there is enough water present to form α-lactose monohydrate crystals. If a crystallisation experiment is carried out at high water activity (>0.55), then until the product reaches that high water activity, the product may be partially crystallising to form an anhydrous product. As moisture is released during this process, or further absorption takes place, the crystallisation to α-lactose monohydrate may proceed. In conditions of high water activity, the solid state conversion of the anhydrous to the hydrous forms will also occur. The final product, will therefore be, a mixture of the anhydrous and hydrous lactose forms in different proportions depending on the conditions of the experiment.

3.7.4.2 Crystallisation kinetics:

A kinetic model for the crystallisation of amorphous lactose was required for the modelling of caking phenomena in bulk lactose. Since the application of glass transition related relaxation phenomena to food systems, there have been many efforts to use models originally developed for polymer systems to describe phenomena in food systems. The glass transition temperature has been used to describe collapse [To and Flink 1978a,b,c, Tsourouflis *et al.* 1976], sticking (Wallack and King 1988), crystallisation [Roos and Karel 1992] and caking [Aguilera *et al.* 1995, Peleg 1993] of amorphous sugar systems. Because these models were originally developed for polymer systems, it is useful to begin with the polymer science literature.

3.7.4.2.1 POLYMER CRYSTALLISATION KINETICS

The progress of crystallisation is dependant on the formation of stable nuclei and the ability of molecules to move about and build on these nuclei. When a molten polymer is cooled below its melting point to a constant temperature, the rate of crystallisation is at first slow. The rate then accelerates to a maximum and then slows again as it approaches equilibrium. The rate of crystallisation is therefore sigmoid in shape as a function of time.

Avrami (1939, 1941) developed Eq (3.25) to describe this phenomena which has become known throughout the polymer science field as the Avrami equation.

$$Y(t) = 1 - e^{-Kt^n} \qquad (3.25)$$

The constant (K) contains nucleation and growth parameters. The value of n is dependant on the mechanism of nucleation and of the form of crystal growth. Theoretical values of n and K are summarised in Table 3.4

Table 3.4 Constants n and K for the Avrami equation.

Form of Growth	Type of nucleation			
	Heterogenous (fixed number of nuclei)		Homogenous (fixed nucleation rate)	
	n	K	n	K
Interface controlled spherulitic	3	$4\pi/3v^3N\rho^*$	4	$\pi/3v^3J\rho^*$
Diffusion controlled spherulitic	3/2		5/2	
Discoid	2	$\pi bv^2N\rho^*$	3	$\pi/3v^2J\rho^*$
Fibrillar	1	$fvN\rho^*$	2	$f/2vJ\rho^*$

b = thickness of platelet; f = cross section of rodlet; ρ^* = relative density (ρ_c/ρ); N = number of nuclei per unit volume; J rate of nucleation per unit volume; v = rate of crystal growth.

The number of nuclei (N) in an isotactic polystyrene system was found by Boon (1966, 1968) to be a function of temperature. The maximum number was at the glass transition temperature, and decreased exponentially with increasing temperature, to be very few at the melting point of the polymer. This would result in the conclusion that at the conditions of interest, (ie. a very supersaturated solution at or near the glass transition temperature) the number of nuclei should be high and not a rate limiting phenomenon in the crystallisation of amorphous lactose.

In unrestrained crystallisation processes, the crystallisation starts from a number of point nuclei, and progresses in all direction at an equal linear velocity (v). In isothermal crystallisation, the radius will increase at a constant rate. The rate of growth however, is very dependant on temperature. At the melting point and at the glass transition temperature, its value is close to zero. The maximum growth rate is observed between these two extremes, usually midway for most polymers.

The basic equation for the linear growth rate is a function of the diffusive transport processes and the free energy of formation of a surface nucleus of critical size. It is given as Eq (3.26) [Van Krevelen 1990].

$$v = v_o \, e^{-\frac{E_D}{R(T+273.15)} - \frac{W^*}{k(T+273.15)}} \qquad (3.26)$$

The first term in the exponential represents the ability of molecules to join the growing crystal, so is related to molecular mobility. The second term represents the surface nucleation phenomena. The WLF equation, Eq (3.27), can be used to represent the first term, as mobility is well defined by this relationship near the glass transition temperature [Van Krevelen 1990].

$$\frac{E_D}{R(T+273.15)} \gg \frac{C_1}{R((C_2+T)-T_g)} \qquad (3.27)$$

The second term is a function of how supercooled the solution is. In the area of interest to this work, it is safe to assume that the degree of super-saturation or super-cooling is very high and it is only mobility which is controlling the rate of crystallisation of amorphous lactose. This being the case, the second exponential term tends to zero and can be ignored.

3.7.4.2.2 PREDICTION OF CRYSTALLISATION RATE IN AMORPHOUS LACTOSE

The mobility of the lactose molecules is related to the viscosity of the amorphous sugar, and since viscosity changes above the glass transition temperature are adequately described by WLF kinetics [Soesanto and Williams 1981], it follows that the use of WLF kinetics to describe crystallisation phenomena should also be possible. Roos and Karel (1990, 1991a) have used this approach to describe the crystallisation of amorphous lactose. Progress of crystallisation was followed using isothermal differential scanning calorimetry (DSC). The resulting crystallisation curves for lactose equilibrated above phosphorous pentoxide were slightly skewed, indicating that the Avrami polymer crystallisation model did not apply. Crystallisation kinetics for samples equilibrated at 0.23 and 0.33 a_w were even more skewed and the time required for crystallisation reduced with increasing moisture content, even when the same driving force for crystallisation was used ($T - T_g$). The time taken for crystallisation (peak time) was then fitted as a function of ($T - T_g$) and found to follow the WLF relationship.

In explaining the results obtained by Roos and Karel, it is necessary to understand what experimental technique was used in the collection of crystallisation data. Amorphous lactose was analysed in pans using isothermal DSC. The heat given off during the crystallisation was recorded and used as a measure of the progress of crystallisation. As such it is evident that if the product of crystallisation is anhydrous, then moisture will be released during the crystallisation. If the samples were in sealed pans then this moisture will be released and taken up by the remaining amorphous lactose. This will increase the moisture content, decreasing the glass transition temperature, and therefore increasing the rate of crystallisation. Although this explanation is given by the authors, the data are still presented as following WLF kinetics for the initial T-T_g driving force used in the experiments.

Although such data are useful in characterising the time for crystallisation in a closed system, such analysis clearly is not a sensible approach for describing the mechanism behind the crystallisation phenomena. If this is to be done, the fate of moisture in the system must be considered. In the dried lactose samples even a small amount of moisture present in the sample could be the cause of the skewness in the crystallisation kinetics data observed by Roos and Karel. This may mean that the Avrami equation used to describe polymer crystallisation is not necessarily inadequate for the description of amorphous lactose crystallisation.

Avranitoyannis and Blanshard (1994) showed that for a completely dry sample of amorphous lactose, the Avrami equation can be used to predict the kinetics of crystallisation. It was found that there was a change of mode of crystallisation from homogenous to heterogenous nucleation as temperature increased. It should be noted

however, that the time taken for crystallisation (600 days at $(T-T_g)$ = 40°C) were orders of magnitude different from those observed by Roos and Karel (1991a) (20 minutes in similar conditions). The reason for this is not clear.

Because of the difficulties in firstly producing dry amorphous lactose, and then in controlling the crystallisation product at the high temperatures required to induce crystallisation once it has been obtained, it is desirable to avoid using dry amorphous lactose in studies of crystallisation kinetics.

This raised the idea of using the sealed DSC pans with known initial amorphous lactose moisture content, and following the progress of crystallisation using isothermal DSC. The data provided could then be analysed after first making some assumption as to the fate of moisture released during the crystallisation. Using this assumption, the glass transition temperature could be predicted as a function of crystallinity and the Avrami equation fitted using the differentiated form Eq (3.28).

$$\frac{d(1-Y)}{dt} = nKY\left[\frac{-\ln(Y)}{K}\right]^{\frac{n-1}{n}} \tag{3.28}$$

From the DSC data the parameters $d(1-Y)/dt$ and Y are known at any time. The Avrami coefficient n can be assumed and K found as a function of time. This can then be fitted as a function of $T-T_g$.

To investigate this technique for analysis of amorphous lactose crystallisation kinetics, a series of stainless steel DSC pans were filled with amorphous lactose which had been equilibrated over saturated salt solutions to give water activities of 0.22 and 0.33 a_w. The pans were hermetically sealed inside controlled temperature and relative humidity rooms set to within 2% RH from the desired water activity of each sample. This was done to minimise moisture uptake or desorption during the filling and sealing of the pans. The pans were then used in an isothermal DSC run to follow the progress of crystallisation. The crystallisation product was investigated by measurement of the melting temperature of the sample after the isothermal run. This proved to be difficult as the sample decomposes at about 200°C, which releases gasses which cause the pressure in the pan to build up and lift the lid off making investigation of the crystallisation product impossible.

A typical isothermal DSC plot is shown as Figure 3.21. The second peak evident in Figure 3.21 is thought to be due to the solid state conversion of β to α-lactose·H_2O. This hypothesis was confirmed when attempting to determine the melting point of the crystallisation product. A small hole was punched in the top of the sealed DSC pan to allow gasses and water vapour to escape during the heating phase of the DSC run. It was found that a endothermic peak, starting at 115°C and ending at 160°C occurred. This was thought to be caused by the removal of the water of crystallisation of any α-lactose·H_2O product that formed during the isothermal crystallisation (Figure 3.21). The magnitude of the heat of desorption was shown from the DSC plot to be 145.6 J/g of sample present. This figure compares well with the data given by Berlin *et al.* (1971) of 12.3 ± 0.7 kcal/mole of water desorbed or 142.9 ± 8.1 J/g of α-lactose·H_2O. This suggests that the product of crystallisation at 65°C with an initial water activity of 0.22 a_w was α-lactose monohydrate. It would be expected that the product of crystallisation would be β-lactose anhydride under these conditions if the released moisture was allowed to escape during the crystallisation.

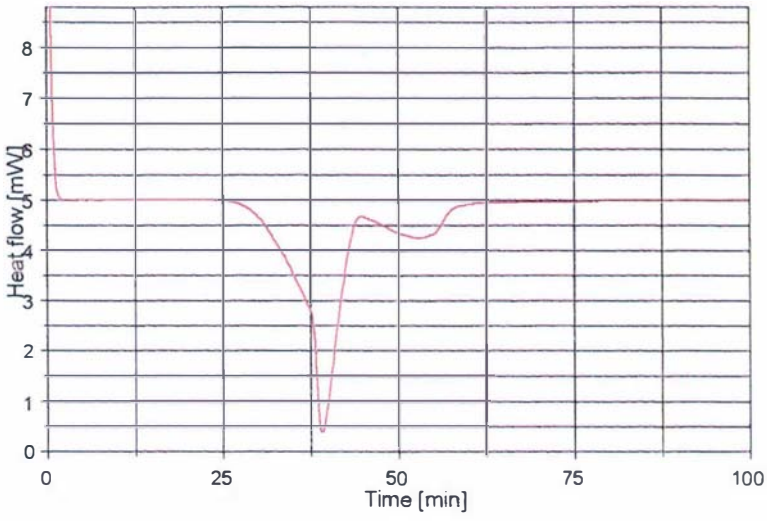

Figure 3.21 - Isothermal DSC plot for amorphous lactose at 65°C and 0.22 a_w.

This suggests that the analysis of isothermal DSC plots is very difficult because several phenomena are important and can occur simultaneously during the experiment. Each of these phenomena are important in predicting caking phenomena. They are;

❶ sorption/desorption
❷ β to α-lactose conversion
❸ crystallisation

Because of the importance of each of these phenomena they are discussed in more detail below.

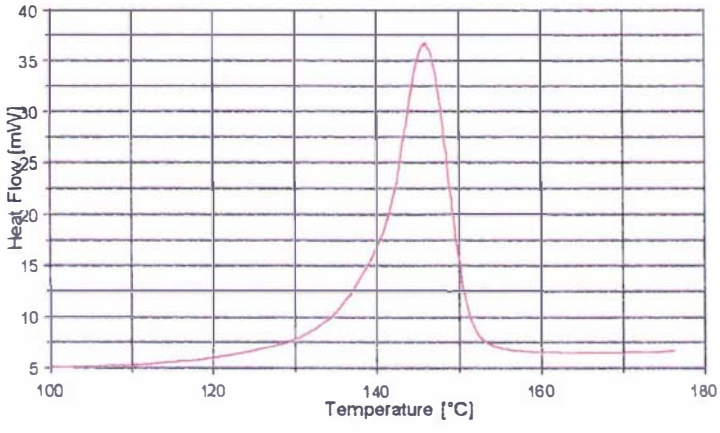

Figure 3.22 - DSC plot showing desorption of water of crystallisation from crystallisation product.

3.7.4.2.2.1 Sorption - desorption phenomena

To eliminate sorption/desorption effects in attempting to measure crystallisation kinetics, the rate of sorption must be an order of magnitude faster than crystallisation. This can be seen in reported results from Niediek (1982) when compared with the moisture sorption isotherm found in this work (Figure 3.23).

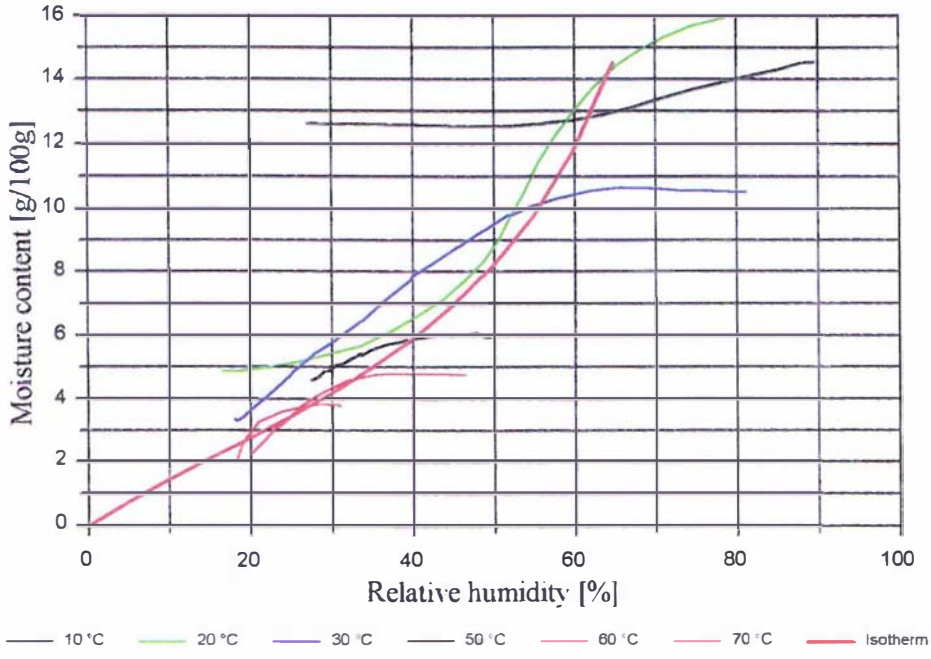

Figure 3.23 - Comparison of moisture sorption results for amorphous lactose from Niediek (1982) and isotherm determined from this work at 20°C.

Niediek (1982) measured the maximum amount of moisture that could be adsorbed in amorphous lactose at different temperatures. Figure 3.23 shows that as the temperature increased, the amount of moisture that could be sorbed was reduced. Up to the point where the isotherms plateau, the results follow the isotherm determined in this work. The plateau is caused by the fact that crystallisation begins to occur faster than the sorption rate after a critical moisture content is reached. In Niediek's data the value of T-T_g ranges between 20 to 30°C.

The magnitude of the sorption rate into amorphous lactose at 30°C was determined and discussed in Section 3.4.2 which suggests that crystallisation must proceed at a rate slower than about 1-2 hours. If this condition was met in an experiment, then sorption/desorption effects did not need to be considered in the analysis of the crystallisation data.

3.7.4.2.2.2 β to α-lactose conversion

The discussion of crystallisation products above suggests that a combination of α-lactose monohydrate and β-lactose are formed during amorphous lactose crystallisation. It has been found by Troy and Sharp (1930) and by results in this work, that solid state conversion of β to α-lactose can occur. Using this explanation to describe the results of the β-lactose moisture sorption isotherm the amount of conversion that occurs at different water activity values can be seen for equilibration of approximately one month. This can be seen as Figure 3.24.

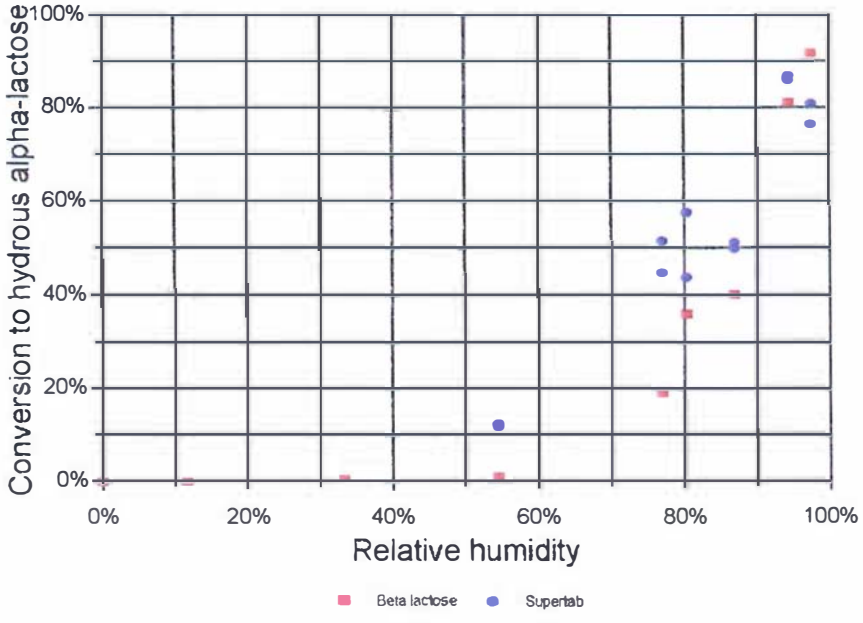

Figure 3.24 - Conversion of β to α-lactose monohydrate as indicated by moisture uptake for β and *Supertab* lactose.

Also plotted on Figure 3.24 is the conversion of β to α-lactose monohydrate, calculated from the amorphous lactose crystallisation product at high water activity from the moisture sorption isotherm for *Supertab*. The amount of moisture, bound in the crystallisation product of the *Supertab* material was found by drying each sample over phosphorous pentoxide for two weeks. The difference between the initial isotherm weight gain and the free moisture content indicated the amount of moisture present in the crystallisation product.

These results suggest that, if amorphous lactose crystallisation results in the production of β-lactose in a moist environment, then some of this β-lactose is converted to the α-lactose form, at a rate depending on the available moisture present. As a consequence of this it was desirable to establish a kinetic model for the crystallisation of amorphous lactose to β-lactose. A kinetic model for the solid state conversion of β to α-lactose is also required to describe the uptake of moisture into the α-lactose crystal lattice. This is of particular importance as this phenomenon will act to remove free moisture from the bulk lactose system.

A simple attempt at modelling the rate of conversion of β to α-lactose can be achieved by assuming an excess of β-lactose exists in the free moisture layer on the

surface of the crystal and that it is saturated with respect to β in solution. If this is the case and a seed for α-lactose crystallisation exists then the rate of crystallisation of α-lactose is the same as the rate of muta-rotation between the α and β-anomers is solution. Using crystallisation kinetics given by Thurby and Nicholson (1976) this can be expressed as Eq (3.29).

$$k_2 C_\beta - k_1 C_\alpha = k_{cryst} (C_\alpha - C_{\alpha_{sol}})^{1.5} \qquad (3.29)$$

The parameters k_1, k_2, C_β and $C_{\alpha sol}$ were obtained from Lowe (1993). The value k_{cryst} was obtained from Thurby and Nicholson (1976). Once this equation was solved with respect to the concentration of α-lactose in the surface solution, then the rate of dissolved α-lactose removal from the solution into the crystalline form could be obtained from Eq (3.30).

$$(1-Y) = M \cdot t \cdot k_{cryst} \cdot (C_\alpha - C_{\alpha_{sol}})^{1.5} \qquad (3.30)$$

Y is the fraction of conversion uncompleted. This is a function of the moisture content of the lactose and the temperature of storage. Figure 3.25 shows this relationship when based on the moisture sorption isotherm for α-lactose monohydrate.

It can be seen from comparing Figure 3.25 with Figure 3.24 that the same order of magnitudes are predicted even though several important phenomena are ignored in the simple model used here. Some of these phenomena include the removal of water from the system during the crystallisation of α-lactose monohydrate and the depletion of the β-lactose crystal. More research is required into the solid state conversion of β to α-lactose if progress into the prediction of crystallisation phenomena is to be made in the future..

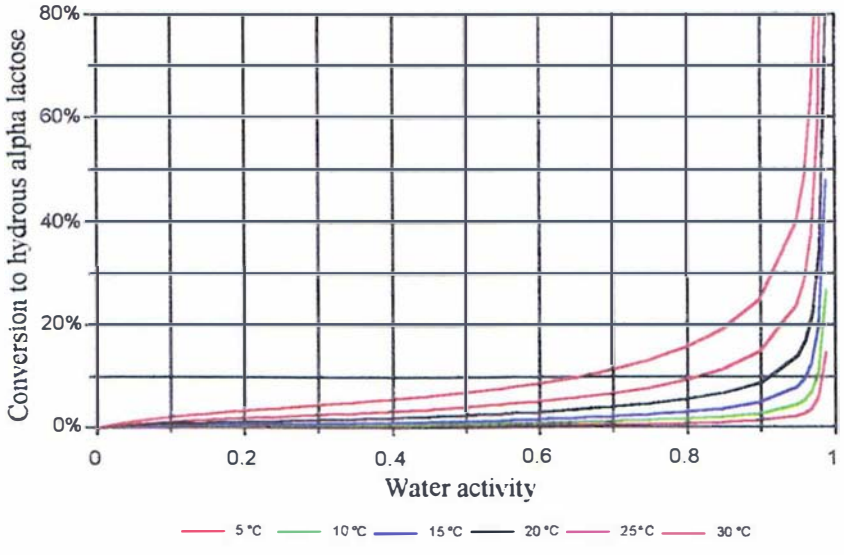

Figure 3.25 - Predicted conversion from β to α-lactose after one month.

To ensure the solid state β- to α-lactose conversion did not interfere with the crystallisation phenomena, crystallisation experiments targeted low water activity environments, where the rate of β- to α-lactose conversion is negligible, due to the deficiency in available water.

3.7.4.2.2.3 Crystallisation rate

To evaluate the rate of crystallisation, an experiment which removed the secondary effects of unknown crystallisation product, sorption rates and the conversion of β to α-lactose was designed. For these reasons, the crystallisation rate at 30°C and relative humidity environments of around 45% were investigated. Under these conditions the adsorption time was expected to be of the order of one day and the crystallisation time approximately one month. The crystallisation product was expected to be β-lactose, and the rate of solid state conversion to α-lactose monohydrate was expected to be negligible. Lower temperature or relative humidity would result in extended crystallisation times and make experimental measurement impractical.

The progress of crystallisation can be followed by recording the weight change with respect to time, for a dried sample subjected to these conditions. To achieve this, samples of amorphous lactose which had been equilibrated over phosphorous pentoxide for four weeks, were placed on to the sorption rate measurement device outlined in section 3.4 above. The chamber relative humidity was then changed to the required value using the dew point generator. The sample weight was data-logged every thirty minutes for a period of approximately one month. These data were expressed as the change in moisture content and can be seen in Figure 3.26 which shows the results for two samples subjected to 45% RH and 43.5% RH at 30°C for approximately one month.

It can be seen from Figure 3.26 that the product of crystallisation is anhydrous as the final moisture content is approximately 0%. This confirms the hypothesis that, under the conditions of the experiment, β-lactose or stable anhydrous α-lactose crystallisation products were produced.

The sample placed in higher relative humidity has a slightly faster rate of crystallisation, but both experiments show curves of similar shape. The initial adsorption can be seen to take approximately one day. When this is compared to the gradual decrease in moisture content with time over the next 25 days, it validates the assumption that in the range of conditions investigated, sorption phenomena are much faster than crystallisation.

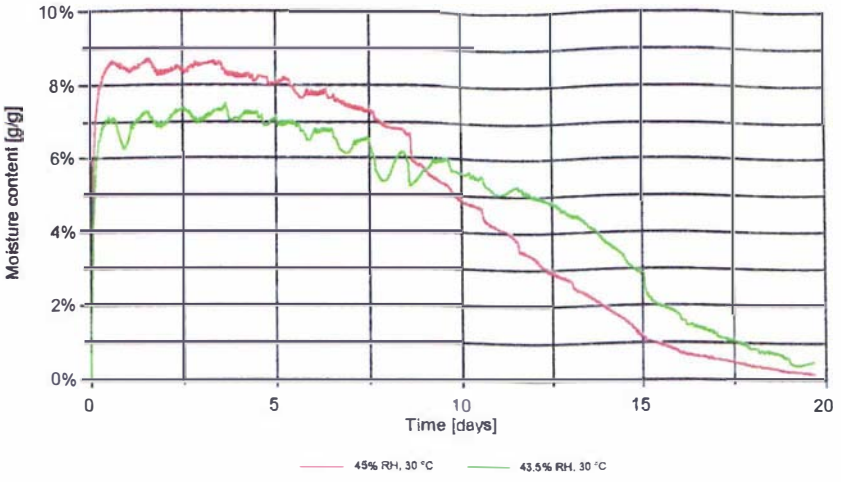

Figure 3.26 - Moisture content change in amorphous lactose during crystallisation.

When these data are then converted to crystallinity versus time (Figure 3.27) the shape of the graph appears relatively symmetrical.

This symmetry suggests that the rate of crystallisation is not a function of $(T\text{-}T_g)$ alone, and that the history of the amorphous lactose (crystallinity) is also important in describing the crystallisation process. The Avrami equation, discussed above, has been used in the past to describe crystallisation kinetics similar to those observed in this work [Avranitoyannis and Blanshard 1995].

By linearising the Avrami equation Eq (3.25) the following results;

$$\log(-\ln(Y)) = \log(K) + n\log(t) \tag{3.31}$$

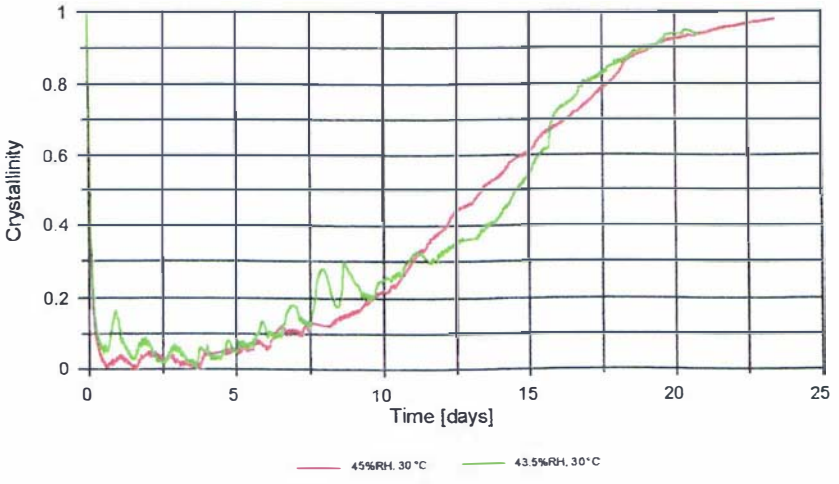

Figure 3.27 - Crystallinity as a function of time during amorphous lactose crystallisation.

When the data for the experimental trials are plotted in this form, straight lines result with slope equal to three (Figure 3.28). This suggests that the Avrami equation can be used to describe amorphous lactose crystallisation under these conditions. As previously discussed, the Avrami number equal to three suggests linear growth in three dimensions is occurring.

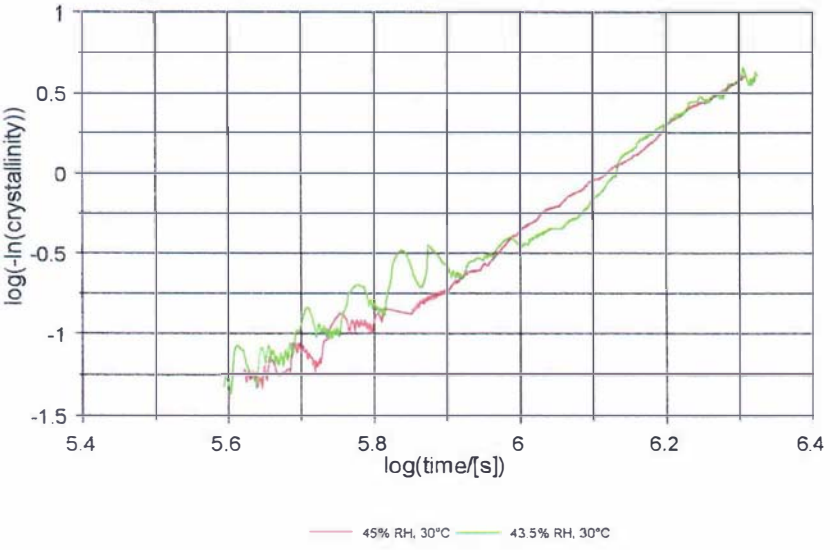

Figure 3.28 - Avrami plot for amorphous lactose crystallisation.

For amorphous lactose in an environment of 45% RH the rate constant is 4.5×10^{-19} s^{-3} while at 43.5% RH the rate constant is slightly less at 4.3×10^{-19} s^{-3}. These rate constants were obtained by nonlinear regression to the Avrami equation.

The predictions for the experimental data collected in this work using the Avrami equation and these fitted constants can be seen in Figure 3.29. This graph shows good predictions of the time taken for crystallisation.

The experimental technique for determination of crystallisation kinetics of amorphous lactose developed here offers a relatively limited window of conditions which can be investigated. Beyond this window, analysis becomes much more complicated because consideration to the role of sorption and desorption rates, β to α-lactose conversion and other phenomena playing an important role in the overall crystallisation phenomena. For this reason it is desirable to compare results with those shown in the literature for the time taken to achieve crystallisation.

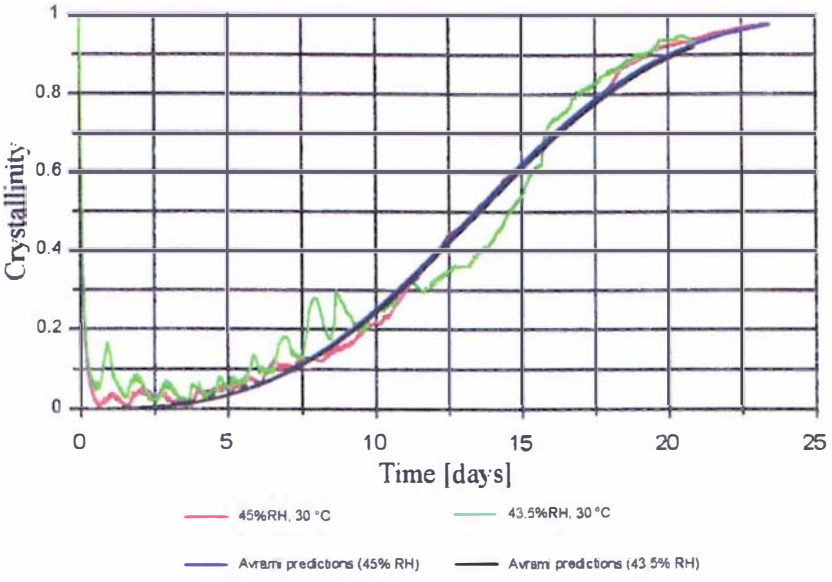

Figure 3.29 - Prediction of crystallisation progress using Avrami equation.

Roos and Karel (1990 & 1992) gave the time taken for crystallisation as a function of the driving force for molecular relaxation (T-T_g). This can be seen along with the data measured in this work taken as the time to achieve 90% crystallinity in Figure 3.30. It is evident from this curve that the crystallisation time is reasonably well predicted by the WLF relationship, indicating that molecular mobility is likely to be rate governing with respect to the rate of crystallisation.

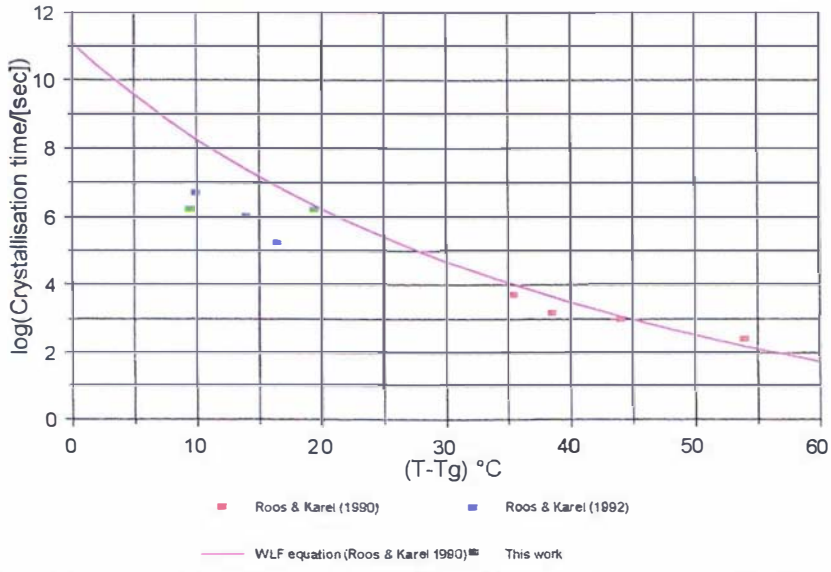

Figure 3.30 - Comparison of crystallisation times between this work and the literature.

The problem then arises of how to predict the rate of crystallisation using the Avrami model at different moisture contents and temperature (hence T-T_g). As discussed previously, the rate of nucleation is not thought to be rate limiting due to the large degree of super-saturation or undercooling present in amorphous lactose samples. For linear growth, the rate constant (K) can be predicted as a function of (T-T_g) using (3.26). Incorporating the effect of three dimensional growth (from Table 3.4) it follows that the rate constant relationship to (T-T_g) is of the form;

$$K = \frac{4\pi N \rho^{*}}{3}\left(e^{-\frac{C_1}{R(C_2+T-T_g)}}\right)^3 v_o^{\,3} \qquad (3.32)$$

If the constants are all lumped together this becomes Eq (3.33).

$$K = C_3'\left(e^{-\frac{C_1}{R(C_2+T-T_g)}}\right)^3 \qquad (3.33)$$

If this relationship is fitted to the available experimental data, including those provided by Roos and Karel (1990,1992) the values for C_1, C_2 and C_3 can be evaluated from the time to reach 90% crystallinity using the Avrami equation. From such an analysis the value of C_1 was 3.54×10^4, C_2 was 108.4 and C_3 was evaluated to be 3×10^{27} s^{-3}.

When the time taken to achieve 90% crystallinity is plotted as a function of T-T_g Figure 3.31 results.

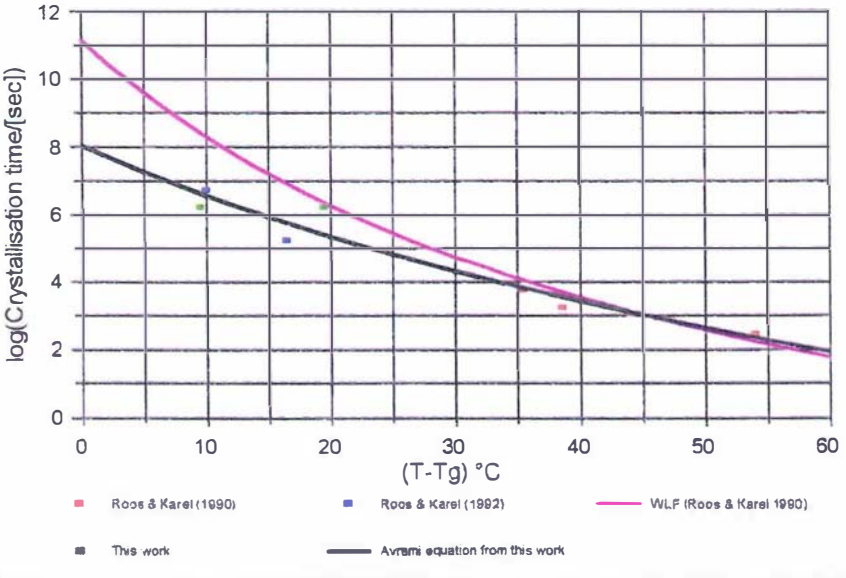

Figure 3.31 - Avrami model predictions of time to reach 90% crystallinity.

This curve looks to give better fit to the crystallisation times for the high T-T_g region of the curve than does the simple WLF model using the universal constants and also offers the advantage that the actual rate of crystallisation can be predicted as a function of time. It is apparent that more crystallisation data is required for the intermediary T-T_g region. This experiment could be achieved by equilibrating lactose samples above salts solutions at low temperature and then increasing temperature to give the desired T-T_g. In this way the effect of adsorption kinetics can be nullified.

The final model used in subsequent work is Eq (3.28), where $n = 3$ and Eq (3.33) where $C_1 = 3.54\times10^4$, $C_2 = 108.4$, $C_3 = 3\times10^{27}$ s^{-3} and R=8.314. Additional consideration to the rate of conversion of the β-lactose form to α-lactose monohydrate is required due to the associated moisture uptake and hence, removal from the free moisture pool in the bulk lactose system. Similarly the rate of uptake of moisture into the amorphous lactose layer present on industrial lactose powders requires consideration in order to give accurate crystallisation predictions.

3.8 EFFECTIVE MOISTURE DIFFUSIVITY IN A PACKED BED OF LACTOSE:

The diffusivity of moisture in air can be estimated with the following correlation (Shah *et al.* 1984);

$$D = 1.7255\times10^{-7}(T + 273.15) - 2.552\times10^{-5} \quad (3.34)$$

The diffusivity of moisture through a bulk porous media is less than for air due to the reduced area available for the transport of the vapour and the effects of constrictivity (δ) and tortuosity (τ_2) in the media. For this reason an "effective" moisture diffusivity is defined. Collin and Rasmuson (1988) summarise a number of correlations used to predict effective diffusivity in soils and other unsaturated porous materials. The simplest of correlation ignores the effects of tortuosity and constrictivity or the partial filling of the pores with moisture and is written as;

$$D_{eff} \quad \epsilon D \quad (3.35)$$

This estimate represents the maximum moisture diffusivity possible in the bulk porous media. Collin and Rasmuson (1988) concluded that the most suitable correlation for prediction of moisture diffusivity in soils was that derived by Millington and Shearer (1971). A summary table of the estimated effective diffusivity of lactose is given as Table 3.5 below.

Due to the homogeneity of lactose the effective moisture diffusivity in bulk lactose is likely to be in the higher end of the range predicted by these correlations. As a first approximation the simplest estimation of effective moisture diffusivity was used with a porosity (ϵ) of 0.4.

Table 3.5 - Effective moisture diffusivity models for flow in porous media

Model	Equation	δ/τ_2	D_{eff} (m^2/s)
Simple approximations	ϵD	-	1.04×10^{-5}
	$(\delta/\tau_2)\epsilon(1-S)D$	0.5	5.18×10^{-6}
		1	1.04×10^{-5}
Currie (1961)	$(\delta/\tau_2)\epsilon(1-S)^4 D$	0.5	5.17×10^{-6}
		1	1.03×10^{-5}
Van Brake and Heertjes (1974)	$\frac{\epsilon(1-S)D}{\tau_2/\delta + 9.72S}$	0.5	5.15×10^{-6}
		1	1.02×10^{-5}
Millington and Shearer (1971)	$D(1-S)^2[\epsilon(1-S)]^{2f}$ $f = 0.67$ *for* $\epsilon = 0.4$	-	7.57×10^{-6}

3.9 CLOSURE:

The overall moisture relations of lactose are central to the caking of lactose powders and have been discussed in depth in this chapter. Moisture sorption isotherms, sorption kinetics and amorphous lactose crystallisation have been highlighted within the chapter as being especially important in subsequent chapters.

Equations have been formulated to allow adequate mathematical description of these phenomena in the modelling of moisture movement and caking in bulk lactose. The modelling of moisture movement in bulk lactose due to a temperature gradient is the subject of the next chapter.

CHAPTER 4

MODELLING HEAT AND MOISTURE TRANSPORT IN BULK LACTOSE

4.1 INTRODUCTION

Moisture migration within bulk powders, due to temperature gradients are commonly associated with caking problems during storage [Lyle 1957]. It is the process where moisture from hot sections of the bulk powder is transported by water vapour diffusion to cooler parts, increasing local moisture content and causing caking problems to occur.

Bulk storage temperature differences of up to 20°C, can occur during the manufacture of lactose in industry. Similar temperature gradients occur during shipping through the tropics where the product is reheated.

Because both of the proposed caking mechanisms are sensitive to the presence of free moisture, moisture migration plays a significant part in caking problems in stored lactose. For this reason, it was important to be able to predict how moisture migration occurs in a cooling bag. To achieve this, a mathematical model was developed to predict the moisture movement caused by a temperature gradient, so it could be used to investigate its effect on caking phenomena.

This chapter describes the formulation, implementation and validation of a mathematical model which describes one dimensional moisture migration, due to an imposed temperature gradient.

4.2 FORMULATION OF TRANSPORT MODEL

4.2.1 CONCEPTUAL MODEL

The physical situation to be modelled is illustrated in Figure 4.1 below;

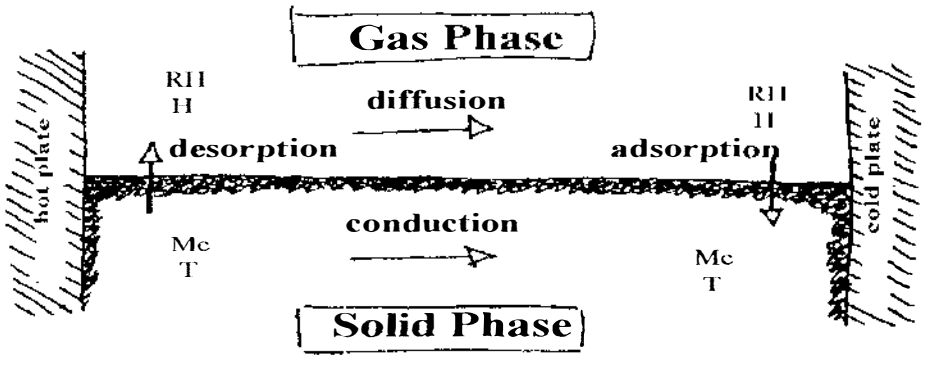

Figure 4.1 - Conceptual model for heat and moisture transport in bulk lactose.

The physical basis of the model can be summarised as;

- one dimensional heat and moisture transport through a packed bed of lactose.
- initially the lactose has a constant moisture content throughout the bed.
- a temperature gradient is applied across the bed.
- the solid and gaseous phases are considered as continua with interaction over adjacent interfaces.
- moisture diffusivity and thermal conductivity are treated as effective properties of the porous matrix

4.2.2 ASSUMPTIONS

The main assumptions made for the model are;

- all moisture transfer occurs by diffusion in the gas phase.
- all phases are in local thermal equilibrium.
- all phases are in local moisture equilibrium.
- the gas phase can be considered as ideal.
- all free moisture is present at the lactose crystal surface.
- the void volume is completely mixed.
- heat and moisture transport by convection is negligible.
- no gravitational effects are present.
- the voidage volume change with increasing moisture content is negligible.
- enthalpy and moisture transport due to air expansion with temperature is negligible.
- heat of crystallisation and dissolution is negligible.
- crystal surface dissolution occurs instantaneously.

4.2.3 VALIDITY OF ASSUMPTIONS

4.2.3.1 LOCAL THERMAL EQUILIBRIUM

The validity of this assumption was proven by calculating the time constant for the process of convective heat transfer from the particle surface to the pore air phase. By ignoring diffusion of moisture, and assuming negligible heat is transferred in the gas phase, a heat balance in the gas phase was written as;

$$\epsilon . V . \rho_a . \frac{\partial h_g}{\partial t} = (1 - \epsilon) . V . A_s . h_c . [T_s - T] \qquad (4.1)$$

By making the approximation;

$$\frac{dh_g}{dt} = c_{p_a} . \frac{dT}{dt} \qquad (4.2)$$

and assuming c_{pa}, ρ_a and h_c are constant in the temperature range of interest and taking Laplace transforms of Eq (4.1) gives;

$$T(s) = \frac{T_s(s) + \tau . T(0)}{\tau . s + 1} \tag{4.3}$$

where the time constant (τ) is given by;

$$\tau = \frac{c . \rho_a . c_{p_a}}{(1 - c) . A_s . h_c} \tag{4.4}$$

Eq (4.3) is of the form typical of a first order process. If standard lactose properties are used and a surface heat transfer coefficient (h_c) of 3W/m^2°C (for stagnant air) [McCabe and Smith 1984] the first order time constant (τ) is of the order of less than a second. Therefore the assumption of local thermal equilibrium is valid as the model is run for periods of over 10 hours.

4.2.3.2 Local Moisture Equilibrium

In a similar manner to above, the validity of the assumption of local moisture equilibrium was shown by calculating the magnitude of the first order time constant of the sorption process. A mass balance on the solid phase was written as;

$$(1 - c) . V . \rho_s . \frac{\partial M}{\partial t} = k_g . A_s . (1 - c) . V . (P_v - P_s) \tag{4.5}$$

By assuming the moisture sorption isotherm is linear (true for the water activity range 0.1 - 0.8), and using the value for saturated vapour pressure obtained from the literature (25°C) [Cooper and Le Fevre 1969], the following expression was derived;

$$P_s = P_w . A_w = 2.2 \times 10^6 . M \tag{4.6}$$

Substituting Eq (4.6) into Eq (4.5) and by assuming k_g and ρ_s are independent of temperature, and taking laplace transforms gives;

$$M(s) = \frac{P_v(s) + \tau . M(0)}{\tau . s + 1} \tag{4.7}$$

Equation (4.7) is of the typical form for a first order system. The first order time constant (τ) for the system is given by Eq (4.8).

$$\tau = \frac{\rho_s}{2.2\times10^6 k_g A_s} \qquad (4.8)$$

If standard lactose properties are used and a surface mass transfer coefficient (k_g) of 1.8×10^{-6} s/m (from Sherwood number ($_{Nsh}$) of 2 for negligible flow past a particle of average size, McCabe and Smith 1984) the first order time constant (τ) is of the order of less than a second. This shows that the sorption process occurs very quickly and the assumption that local moisture equilibrium between the solid and the gas phases is valid.

4.2.3.3 Negligible Convection

Natural convection can be neglected if the Rayleigh number is less than $4\pi^2$ (Bear and Bachmat, 1991).

$$N_{Ra} = \frac{\rho_a.g.\alpha.K.L.\Delta T}{\lambda.\mu} \qquad (4.9)$$

If convection is unimportant in the worst case situation that occurs in industry, then convection will not play an active role in the transport of moisture and heat in the simplified one dimensional case. The worst case scenario consists of lactose powder, recently packaged into a $1m^3$ cubic bulk bag placed in a store room.

The properties for lactose in this situation are;

α = 1/298 K (1/T)
μ = 1.8×10^{-5} Pa.s
ΔT = 20°C (immediately after bagging)
L = 1m (dimension of a bulk bag)
K = 1.98×10^{-7} m^2 (Hodges 1992)

This gave $N_{Ra} = 0.05$, which is much less than the critical Rayleigh number ($4\pi^2$) and therefore natural convection is not significant in the transport of heat and moisture in bulk lactose under the types of conditions under consideration.

4.2.3.4 Negligible Heat and Moisture Transport Due To Changes in Air Density

Upon heating a node of fixed volume, the air density will decrease and air will flow out of that fixed volume carrying heat and moisture with it. Because of this, a heat and moisture transport term due to air expansion and contraction with changing temperature should be included in the model. It was assumed that the amount of heat and moisture transported in this way was negligible. Having made this assumption, rather than making a further assumption that air density was constant in the temperature range of

interest (15 - 40°C), it was desirable to allow it to change with temperature. As a result, if air density is allowed to change and no effort made to account for the air that expands over the boundaries of the node of fixed volume, then moisture and dry air balances over the whole system will result in a net loss of air and moisture. Some heat will be associated with the air lost from the system and therefore a total heat balance over the system will also show a discrepancy. Quantification of the amount of moisture and heat lost from the system was required to show how significant this effect was.

The driving force for moisture diffusion in the porous system was expressed as a water vapour concentration (kg water vapour/ m^3 dry air) and absolute humidity was back calculated from water vapour concentration. This means the only way the total amount of moisture in a node of fixed volume could change was by the processes modelled (diffusion and condensation). For this reason no moisture was overlooked by the model and the total moisture in the system is accounted for. The balance equation for moisture in the system was written in terms of a moisture concentration (kg water vapour/ m^3 air) and only dry air was lost.

The effect of thermal expansion at heated parts of a porous slab and contraction at parts of the slab undergoing cooling, will promote extra moisture movement in the direction of the temperature gradient (hot to cold).

Quantification of the significance of heat losses and gains in dry air to the system by thermal expansion and contraction was most easily achieved by checking the effect of the assumption that they are negligible, after a working simulation was completed. Once the model was formulated, and numerically solved, a running total of the dry air lost, along with the heat lost with this air, was made using a simple dry air mass balance at each time step. This heat loss term was then be compared with the total heat entering over the boundaries. The results of this test are discussed in Section 4.5.2.

4.2.3.5 MODE OF MOISTURE MOVEMENT:

Other modes by which moisture transfer in the lactose bed can occur are surface diffusion, capillary action and diffusion through the lactose particles themselves. The structure of the lactose crystal is very ordered and contains few spaces in the crystalline matrix where free moisture can be present. Because of this, diffusion through the particle is not significant.

Because the free moisture in the lactose system exists on the surface of the crystal particles, a thin film of saturated lactose syrup is present. This film is likely to be concentrated at contact points between adjacent particles due to surface tension forces. It can be seen from the moisture sorption isotherm that the amount of free moisture present in atmospheres of less than 95% relative humidity is very small, consisting of only a few mono-layers thick. It was concluded that flow of moisture by surface diffusion would be insignificant.

4.2.3.6 OTHER ASSUMPTIONS MADE

All other assumptions made are reasonable assumptions necessary to enable a simple model formulation.

4.2.4 MATHEMATICAL FORMULATION

Details of the mathematical formulation of the conceptual model described above can be found in Appendix A3. The mathematical model is summarised as transport equations (4.10) and (4.11),

$$\frac{\partial Q}{\partial t} = D_{\epsilon} V_{\epsilon} \frac{\partial^2 [H \rho_a h_v]}{\partial x^2} + \lambda_{\epsilon} V_{\epsilon} \frac{\partial^2 T}{\partial x^2} \qquad \text{for } t>0 \text{ and } 0<x<L \tag{4.10}$$

$$\frac{\partial W}{\partial t} = D_{\epsilon} V_{\epsilon} \frac{\partial^2 [H \rho_a]}{\partial x^2} \qquad \text{for } t>0, \text{ and } 0<x<L \tag{4.11}$$

with initial conditions given by (4.12) and (4.13),

$$T = f(T_{initial}) \qquad \text{for all } x \text{ at } t=0 \tag{4.12}$$

$$W = f(RH_{initial}) \qquad \text{for all } x \text{ at } t=0 \tag{4.13}$$

and boundary conditions given by (4.14) and (4.15).

$$h_c (T - T_a) = 0 \qquad \text{for } t>0 \text{ at } x=0, L \tag{4.14}$$

$$\frac{\partial (H \rho_a)}{\partial x} = 0 \qquad \text{for } t>0 \text{ at } x = 0, L \tag{4.15}$$

Algebraic equations describing the psychometric properties of air and water are listed in Appendix A-2. System input values and equations describing lactose properties and moisture relations of lactose are discussed and listed in Chapters 2 and 3.

4.3 NUMERICAL SOLUTION OF TRANSPORT MODEL

4.3.1 SELECTION OF NUMERICAL SOLUTION METHOD

The model summarised in Section 4.2.4, shows the solution of two coupled partial differential equations was required. One equation describes the transport of heat and the other the transport of moisture through the lactose slab. Some algebraic equations used in the model are non linear. The complexity of the model makes the analytical solution difficult and, with the advent of inexpensive computing facilities, the model was best solved numerically.

The most common methods available for the numerical solution of partial differential equations are;

- Explicit finite difference schemes
- Implicit finite difference schemes (eg. Lee's or Crank-Nicholson)
- Finite elements methods

Each of these methods have advantages and disadvantages. The explicit finite difference scheme is the easiest method to implement as the predictions of the dependent variables are made based on known values. If changes in the dependent variable are occurring quickly, this method can lead to instability problems and an implicit finite difference scheme should be used. In an implicit scheme the predictions of the dependent variable is based not only on known values but also future values of the dependent variable. This results in a series of equations which must be solved simultaneously. When dealing with a coupled system a sparse matrix results, which is usually solved iteratively. In the case where the system behaves non-linearly, solution of simultaneous equations in this manner is difficult.

Finite element methods are more difficult to implement and most often an existing package is used. This method is especially useful for solution of problems where the geometry of the system is irregular.

In the case of solution of the transport model, formulated in Section 4.2.4 above, changes occur relatively slowly. Total equilibration for a 100mm slab of lactose with a 20°C temperature gradient applied to it is in the order of 12 hours. This suggests that the extra complexity involved in implementing an implicit scheme, over a more simple explicit scheme was not warranted. The non-linearity inherent in the system, makes implementation of an implicit scheme difficult in any case.

Because the system is of regular geometry and changes occur relatively slowly, the finite elements method offers no real advantages over the explicit finite difference scheme. For these reasons the explicit finite difference scheme was used to solve the transport model.

4.3.2 NUMERICAL SOLUTION

The equations representing the lactose slab were solved using an explicit finite difference scheme. The lactose slab was divided into several nodes where the content of each node was considered uniform. By discretising the continuous system in this way, a series of equations which describe transport of heat and moisture between adjacent nodes were derived.

The partial differential equations were approximated using the expanded Taylor series and these equations, together with the boundary conditions, initial conditions and algebraic equations, which characterise the system, were solved in a Borland C++ program.

The formulation of the finite difference equations for the system can be found in much greater detail in Appendix A4.

The program was written using object orientated programming techniques. Object orientated programming offers many advantages over conventional "top down" programming. The first and most important of these advantages is that by treating each item in the real world as a separate subject, the program is more closely representing

the actual situation. By treating each node as a separate object which interacts with neighbouring nodes or boundaries, the lactose slab is simulated more closely. Other advantages include easier debugging, more control over what can affect an object, easily understood code, code reuse and greater flexibility.

One example of the flexibility given by object orientated programming could be if the system was changed so it also contained a heating source in the centre of the slab. With an object orientated program all that would be required is the inclusion of an extra heating term in the equation describing heat transfer in the centre node. As nothing else has changed in the system no other changes are required. With top down programming a lot of rewriting and restructuring would normally be required.

A copy of the source code for the program is included with this thesis as Appendix A5.

4.4 MATHS CHECKING

4.4.1 CHECKS AGAINST PREVIOUSLY VALIDATED SOLUTIONS

After a model has been implemented in a numerical solution, checks must be made to ensure that what has been implemented numerically is what was actually formulated. This is done by comparison against an existing solution which has already been validated. Due to the complexity of the transport model formulated here, a direct comparison like this could not be made. If the model was simplified by turning off moisture or heat transport, then individual parts of the model could be checked separately.

Moisture transport was switched off by making the binary moisture diffusivity of water vapour in air equal to zero. As diffusion is the only method by which moisture is transported in the model, only heat transfer by conduction will occur. This reduced the transport model to the simple one dimensional heat transfer by conduction in an infinite slab case. If the surface heat transfer coefficients were set very high then the temperature history of the slab could be predicted using the Fourier solution for heat conduction in an infinite slab. The predictions by this method were compared to the transport model predictions for the case of a 100mm lactose slab of initially uniform temperature (20°C), heated on both sides by a step change on the surface to 40°C. During a simulation of over eight hours, the maximum difference in any nodes between the two models was 0.06°C. This shows the heat conduction part of the transport model is a reasonable representation of the actual system.

A similar comparison was performed against a previously validated finite difference model for heat conduction in an infinite slab with convection occurring at the slab boundaries, (RADS, Cornelius 1991). The same situation described above was simulated with both surface heat transfer co-efficients set to 10W/m^{2}K. The maximum difference observed during an eight hour simulation was 0.045°C at the centre of the slab, and 0.14°C at the slab surfaces. This showed the term describing convection at the lactose slab surfaces, had been correctly implemented in the transport model.

In much the same way as the heat transport portion was checked above, the moisture transport part of the transport model was also to have been checked. In practise

however, this was difficult. With an analytical solution, the moisture concentration changes by diffusion only. With the transport model, the water vapour concentration changes also because of the equilibrium relationship between the gas phase and solid phase within a particular node. Therefore, this condensation/evaporation process was disabled before a comparison with the analytical solution was made.

To disable the evaporation/condensation process required reformulation and could not be done by simply changing system input data. To reformulated the model for the purpose of checking the models mathematical correctness defeats the whole purpose of the check. For this reason no comparison against existing models was carried out for the moisture transport portion of the transport model, and this was compared directly against experimental results.

4.4.2 Numerical Error Checking

The fundamental principle which forms the finite difference numerical scheme, used in this work to solve the coupled heat and moisture transport equation, is the discretisation of both time and space, by cutting the continua of time and space into a series of time-steps and nodes, over which the properties of the material are averaged. As the time-step approaches zero and the number of nodes approaches infinity, the real continua are more closely modelled. This has the effect of rapidly increasing simulation time and introduces rounding errors which accumulate in the calculated results. Some trade off is therefore required so numerical errors are at acceptable levels and simulation times are also sensible.

A series of simulations were run using typical values for system inputs. The time-step in these runs was changed from 1 second to 10 seconds and the number of nodes in a total slab thickness of 100 mm was changed in the range 5 to 20 nodes. The temperature and relative humidity predictions for nodes at 0, 20, 40, 60, 80, and 100 mm were compared. For these positions the maximum temperature and relative humidity difference compared with the run with 20 nodes and a 1 second time step were compared for each time-step. From these results it was shown that the error in using only 5 nodes lead to differences in predictions of up to 20% RH than that predicted using 20 nodes. The effect of time-step had less influence on predictions. This analysis showed that 20 nodes and a 5 second time-step was required to achieve accurate predictions. The simulation time for these settings is of the order of 2 minutes per hour of real time simulated. This was acceptable for the investigation of caking carried out in further work.

4.4.3 Maths Checking Summary

The model describing the transport of heat and moisture through a slab of bulk lactose developed in this work was shown to give accurate predictions when compared against existing solutions. This indicated that the implementation of the formulated model was performed correctly.

Checks on the level of numerical errors accumulating in the solution of the model indicated that a minimum of twenty nodes and time steps of less than five seconds are required to obtain accurate predictions.

4.5 MATHEMATICAL MODEL EVALUATION

Using the guidelines for the number of nodes and time step summarised above, the model was evaluated for its ability to predict heat and moisture migration in real systems.

4.5.1 MODEL PREDICTIONS:

The first stage in the validation of any mathematical model is to ensure that the predictions made are sensible. To do this, plots of profiles through the lactose slab were constructed for each of the physical properties of interest (ie. temperature, relative humidity, absolute humidity, water vapour concentration and moisture content) as well as the time history of these properties. For this investigation a simulation was performed for a 100 mm lactose slab initially at 20°C and 60% RH, which was heated from one side to 40°C while maintaining the other side constant at 20°C.

4.5.1.1 TEMPERATURE:

The temperature history profile for the slab is seen in Figure 4.2.

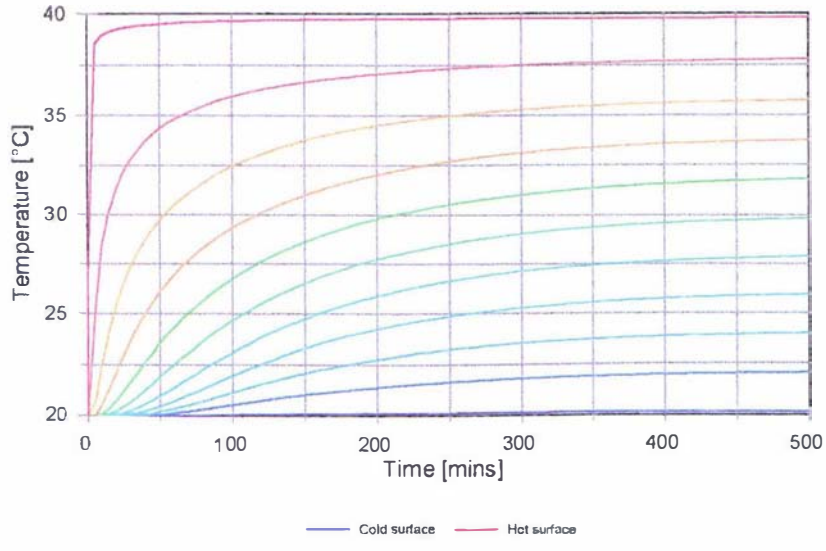

Figure 4.2 - Temperature time profile for the heating of a 100mm slab.

The profile of temperature across the lactose slab at different times approaching steady state can be seen in Figure 4.3. Several interesting effects can be seen in this plot. The steady state temperature profile was linear throughout the lactose slab. Because thermal conductivity is independent of moisture content, and temperature, a linear temperature gradient resulted. This indicates a sensible temperature prediction.

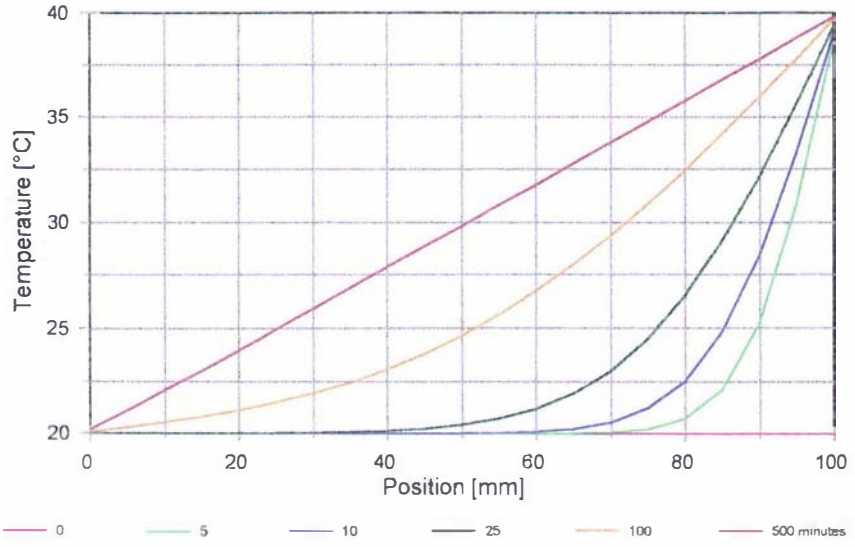

Figure 4.3 - Temperature profile through lactose slab.

4.5.1.2 WATER VAPOUR CONCENTRATION:

The water vapour concentration at times approaching steady state can be seen in Figure 4.4. Water vapour concentration gradients are the driving force for moisture diffusion. At steady state there is no moisture diffusion occurring so by definition the gradient through the lactose slab should be zero. Figure 4.4 shows that as time approaches infinity the difference in water vapour concentration between the hot and cold surface approaches zero.

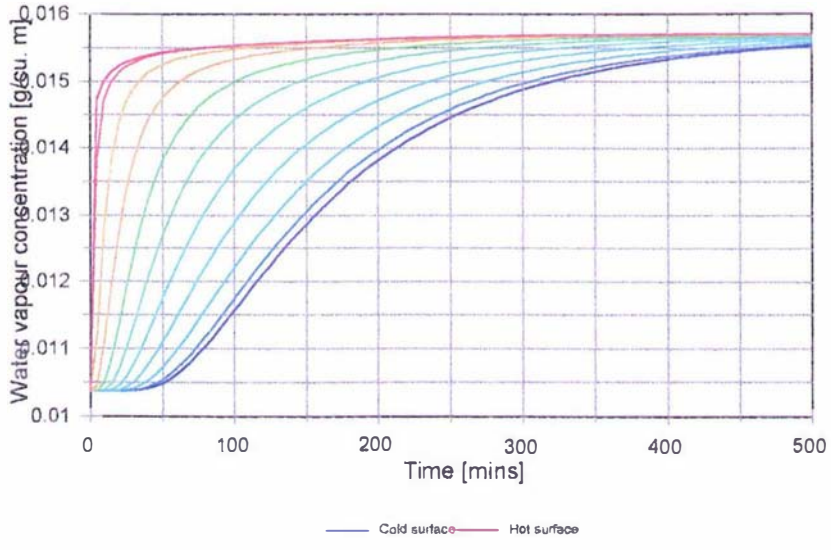

Figure 4.4 - Water vapour concentration time profile within the slab.

It can be seen from Figure 4.4, that the steady state water vapour concentration increases from the initial value. In this simulation the average slab temperature was increased. This resulted in a net increase in the amount of moisture present in the voidage volume due to the extra moisture holding capacity of the warmer air. This indicates that sensible predictions for the change in void space moisture content were achieved using the model.

4.5.1.3 ABSOLUTE HUMIDITY:

Figure 4.5 shows the profile of absolute humidity in the lactose slab. It can be seen from this plot that the steady-state condition resulted in a slight difference in humidity across the slab. This difference is the result of the temperature gradient and its effect on air density in the voidage. The result given in Figure 4.5 was therefore, what was expected.

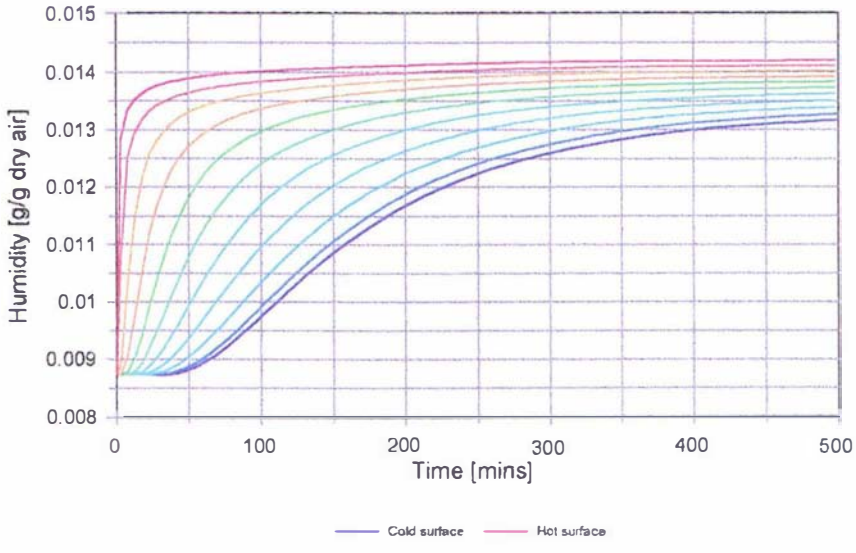

Figure 4.5 - Humidity time profile for the lactose slab.

4.5.1.4 RELATIVE HUMIDITY:

Figure 4.6 shows the relative humidity profile through the lactose slab. It can be seen that immediately after the temperature gradient is applied the hot side relative humidity drops. The relative humidity front then moves through the lactose slab until steady state is reached. The steady state relative humidity profile is nearly an inverse relationship to temperature. The slight nonlinearity was due to the nonlinear relationship of saturated vapour with temperature.

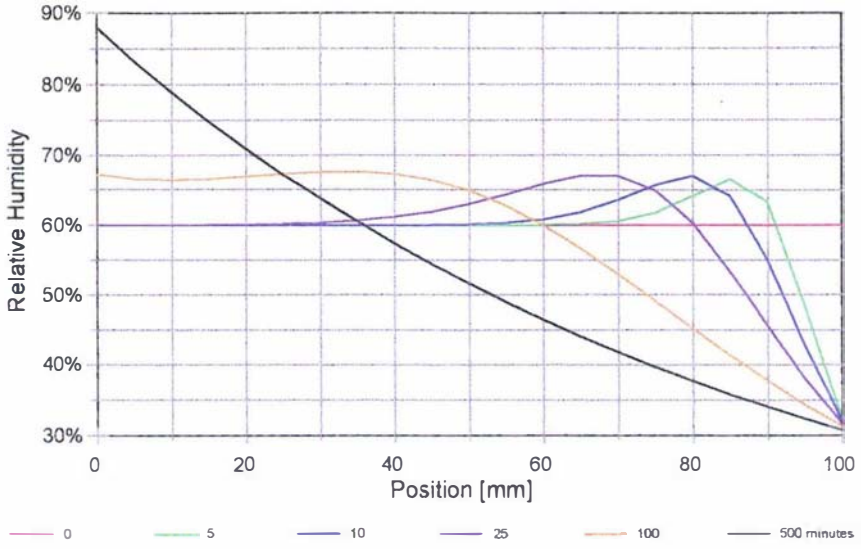

Figure 4.6 - Relative humidity profile development though the lactose slab.

4.5.1.5 MOISTURE CONTENT

Figure 4.7 shows the moisture content of the lactose profile at different times approaching steady state in the lactose slab. It can be seen that a front of moisture moves through the lactose slab. At steady state, the moisture content profile approaches the shape of the sorption isotherm. This is because of the near linearity of the RH profile and the observed independence of sorption behaviour with temperature.

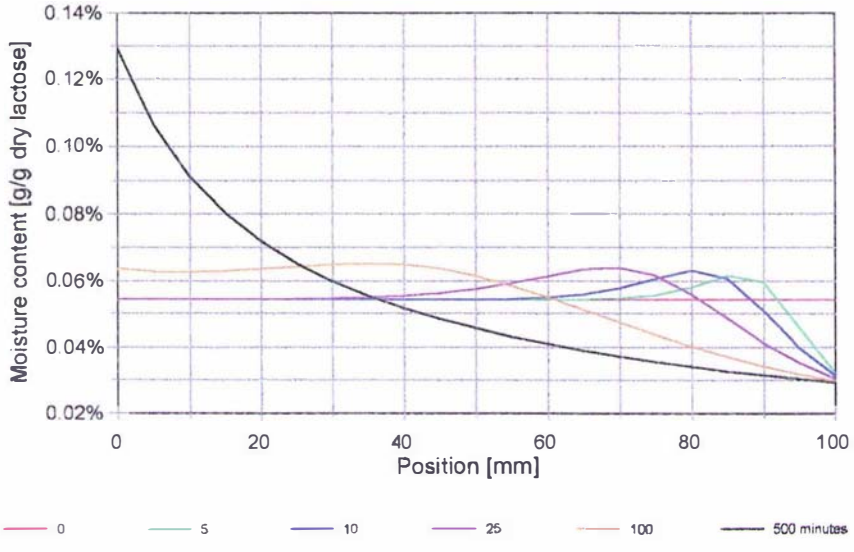

Figure 4.7 - Moisture content profile development through the lactose slab.

4.5.2 HEAT LOSSES DUE TO THERMAL EXPANSION:

Because air density was allowed to change as a function of temperature, without the inclusion of a transport term for that thermal expansion in the model, inconsistencies occurred. If a node of lactose underwent heating, a net loss of dry air resulted. If the node was cooled, a net gain of dry air resulted. The dry air gained and lost from the system contains heats and therefore a total heat balance did not work. Quantification of the significance of these heat losses and gains was required, to assess whether these effects were significant.

The amount of heat lost at time step (n) with changing temperature in a node due to air expansion is given by Eq. (4.16)

$$[Heat\ lost]_n = c_p V \sum_0^n \rho_n - \rho_{n-1} | T_n \qquad (4.16)$$

A negative heat loss indicates the gain of heat associated with cooling.

To assess whether this heat loss was significant it was compared it to the amount of heat flowing through the node. This can be expressed as Eq (4.17)

$$Total\ heat\ flow = \sum_0^n |Q_n - Q_{n-1}| \qquad (4.17)$$

A measure of the significance of heat losses was given by the accumulated Heat losses/Total heat flow in each node. This calculation was performed for a 100 mm slab of lactose initially at 20°C which had one boundary, step changed to 40°C while the other was kept at 20°C. Initial water activity was 0.67 and thermal conductivity was 0.175 W/mK. The ratio of heat losses to heat flow was at a maximum of 0.03% throughout the whole slab. This showed that the assumption that negligible heat is transferred by thermal expansion, is valid, and that the mass lost is also negligible.

4.5.3 EXPERIMENTAL DATA COLLECTION

The true test of validity of a model is its performance against reality. To validate the transport model one dimensional heat and moisture transport data was required. The thermal conductivity of lactose is only half an order of magnitude greater than that of any insulation material available. Therefore a great deal of care and consideration was taken in the design of the experimental apparatus to ensure the collection of good, one dimensional heat and moisture transport data.

4.5.3.1 EXPERIMENTAL APPARATUS DESIGN

The greatest difficulty in the collection of one dimensional heat and mass transport data is ensuring the transport is only in one dimension. This problem is more pronounced by the fact that the thermal conductivity of lactose is only about five times the thermal conductivity of polystyrene. Cleland *et al.* (1994) have shown, from finite

difference simulations for heat transfer in slabs, that to ensure one dimensional heat transfer, the dimension where transport is not desired must be at least three times the dimension of interest. If the measurements are then made in the centre of such a slab then edge effects are not important.

This limit restricts the thickness of slab possible for investigation. Three slab thicknesses where investigated in this work; 78, 100 and 150 mm. The edges of the slab were provided by high density polystyrene. The top and bottom boundaries of the lactose slab were heated or cooled with constant temperature plates. These were hollow stainless steel plates which were kept at constant temperature by pumping water through them. The flow-rate through the plates was high enough to ensure no temperature difference occurred between the inlet and outlet. Baffles were included inside the plates to eliminate uneven temperature over the plate surface. Hot water was re-circulated from a Grant constant temperature water bath. Cold water from mains supply was used as this was reasonably constant in temperature. The experimental apparatus used, can be seen drawn in Figure 4.8.

Thermocouples were positioned diagonally across the slab so the heat transfer to each thermocouple was not interfered with by any others present in the slab. To enable the accurate positioning of the thermocouples, thirty gauge thermocouples were used. The more widely used twenty gauge thermocouples were found to be too large to give a small easily positioned thermocouple junction.

Also required for validation of the model was some measure of moisture movement through the lactose bed. Transient water vapour concentration measurements would have been ideal for this purpose but this is difficult to do in practise.

Relative humidity probes were used to measure relative humidity at each surface of the lactose slab. The probes were flush mounted into the stainless steel plates as seen in Figure 4.8. Each probe was covered with Wattman No 12 filter paper to avoid the blocking of the sintered stainless steel probe head with lactose powder.

The Hycal relative humidity probes used were chosen because of their small size. Despite this the probes were too large and had too high a thermal capacity to mount within the lactose slab, to allow measurement of moisture movement within the slab interior. Surface relative humidity data allowed the partial validation of the moisture transport part of the transport model. If the boundary relative humidity profiles were accurately predicted by the model then this was a good indication that predictions of RH profiles at interior nodes were also correct.

All temperature and relative humidity measurements were recorded using the FIX data-logging system.

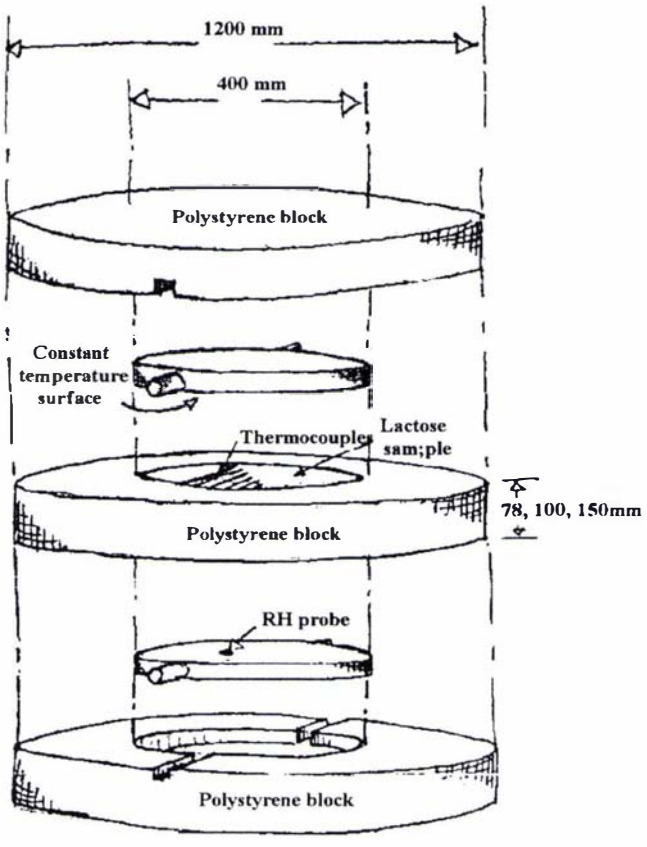

Figure 4.8 - Transport model validation experimental rig.

4.5.3.2 EXPERIMENTAL DATA COLLECTION

Experimental data for temperature and surface relative humidity was measured for slabs of thicknesses 78, 100 and 150 mm. The experimental rig was allowed to equilibrate at room temperature. The sample cavity was then filled with lactose power. This material was purely crystalline as it was equilibrated at atmospheric conditions (~70% RH) for at least two weeks prior to the experimental run. Under these conditions amorphous lactose will crystallise within one day (see Section 3.7.4.2).

The lactose was levelled off using a straight edge and the top heating plate was gently lowered on top of the lactose sample. It was then rechecked to ensure there were no air gaps between the plate and the lactose surface. Once the top plate was in position the covering polystyrene was put into place to minimise heat losses.

With the apparatus assembled, approximately 3-4 hours equilibration time was allowed to ensure a uniform temperature and relative humidity profile across the slab. Hot water was then pumped through the hot plate from a constant temperature water bath. At the same time, cold water from a tap supply, was run through the cold plate. These plates were maintained at constant temperature until steady state was reached. This was observed by plotting the relative humidity and temperature profiles using the FIX data logging software.

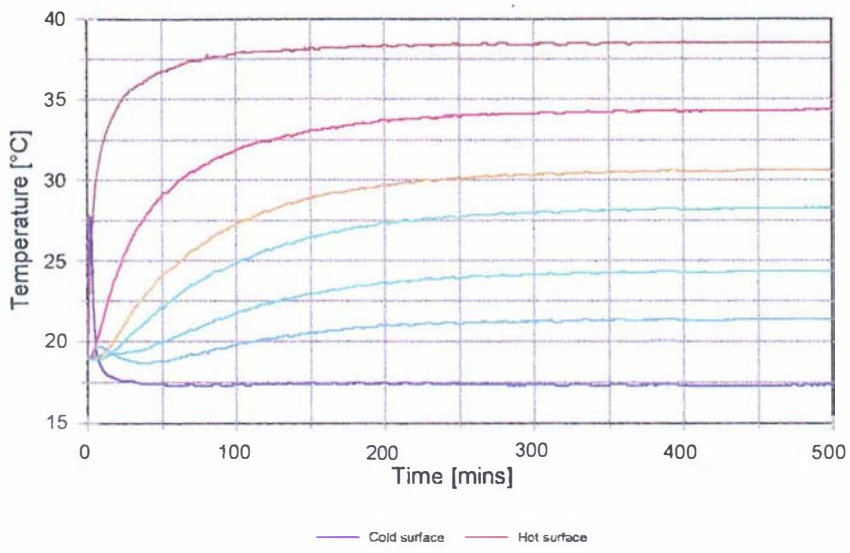

Figure 4.9 - Experimental temperature profiles for a 78mm lactose slab.

Typical results for the 78 mm slab experiment are shown in Figure 4.9 for the temperature profile and Figure 4.10 for surface relative humidity profile. Thermocouple positions were determined by assuming a linear temperature gradient across the slab at steady state and were back calculated from the thermocouple temperatures. The surface temperature profiles heated relatively slowly. This was due to the presence of water already present in the plates. Because of this, time was required to heat or replace this water. Steady state temperature profiles were seen after 200 minutes (~3 hours). The surface relative humidity profiles shown in Figure 4.10 were typical for the establishment of a steady state temperature gradient across a slab of lactose. There was an immediate drop in hot surface relative humidity caused by the temperature increase. A similar small change in cold side relative humidity was observed in some cases depending on the differences between the tap water temperature and the initial lactose temperature. This initial change was followed by a gradual change in relative humidity caused by the diffusion of moisture from the hot to the cold plate.

After approximately 600 minutes (10 hours), steady state was reached. This shows that the moisture transport process is slow compared to the transport of heat in the lactose system. The steady state, cold surface relative humidity, reached in most cases 95% RH, when the initial water activity of the product was around 0.6-0.7 a_w and a 20°C temperature gradient was applied. This corresponds to the exponential region of the moisture sorption isotherm. It was noted that there was no significant difference between experiments where the hot surface was on the top of the slab and those where the slab was heated from below. This reinforces the assumption that natural convection is not significant in the experimental system.

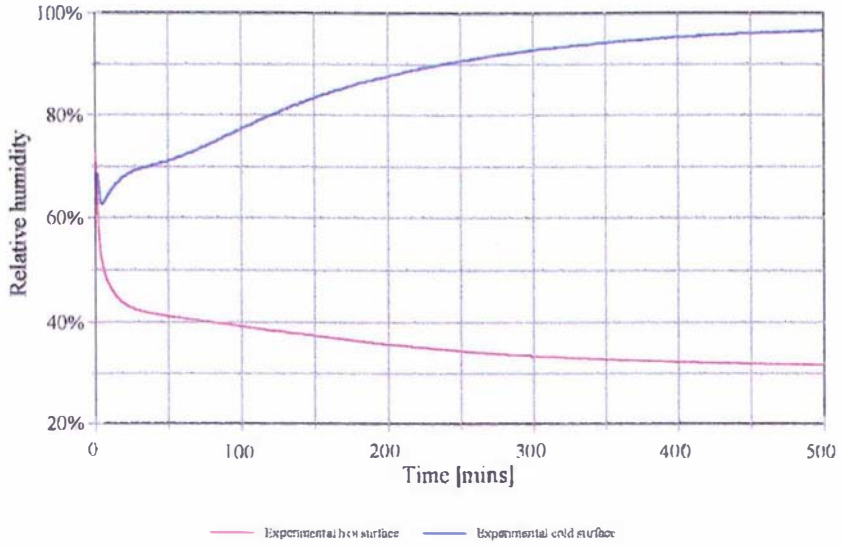

Figure 4.10 - Experimental surface relative humidity profile for 78mm slab.

Typical results for experiments using the 100 mm slab are shown in Figure 4.11 and Figure 4.12. These plots show similar trends to those observed in the 78 mm slab experiments.

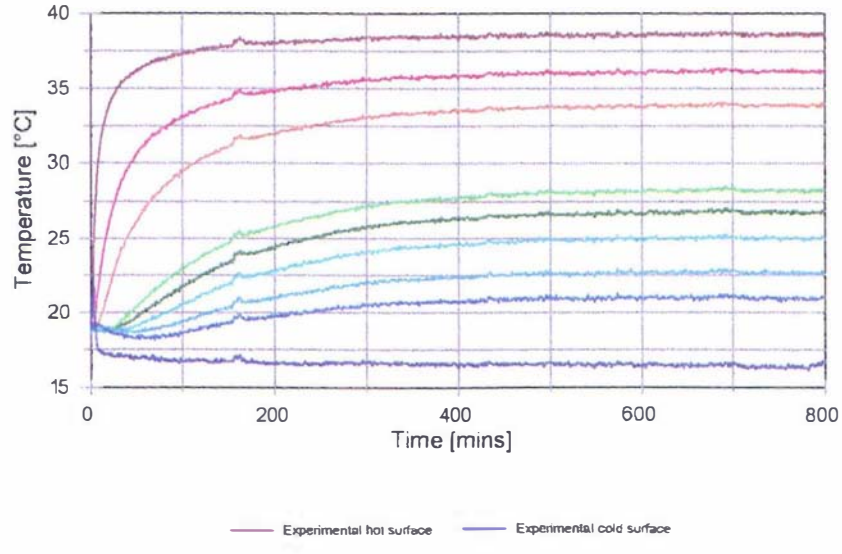

Figure 4.11 - Experimental temperature profiles for a 100mm lactose slab

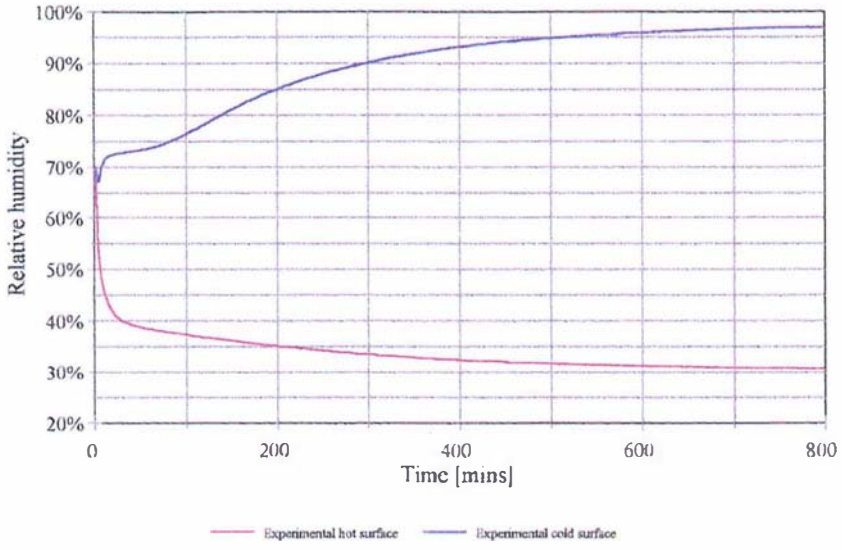

Figure 4.12 - Experimental surface relative humidity profile for 100mm slab.

4.5.4 MODEL PREDICTION ACCURACY

With the availability of experimental data for the application of temperature gradients to a lactose slab the model was then evaluated in terms of its ability to accurately predict the experimental results. Due to the relative rates of heat and moisture transport in the lactose system, the temperature predictions were first evaluated, followed by the relative humidity predictions. Special dense lactose was used for the testing of the model against experimental data.

4.5.4.1 TEMPERATURE PREDICTION ACCURACY

Because the experimental data was slightly variable and the surface heating rates were slowed due to the displacement of water already present in the plates, the actual measured surface temperature profiles were used to represent the ambient nodes in the model. The surface heat transfer coefficient was set to be high (150 W/m^2K) to simulate the good heat transfer conditions which existed for the plate-lactose contact. In this way, accurate surface temperature profiles were achieved and the ability of the model to predict internal heat transfer could be assessed.

The model was run in the manner described above with the following parameters;

Thermal conductivity	0.175 W/mK
Porosity	0.4
Effective diffusivity	ϵD_{air}
Slab thickness	0.078 m
Initial water activity	0.68
Initial temperature	19.5°C
Fitted isotherm (see Table 3.1)	

Figure 4.13 shows the temperature predictions compared with the experimentally measured profiles.

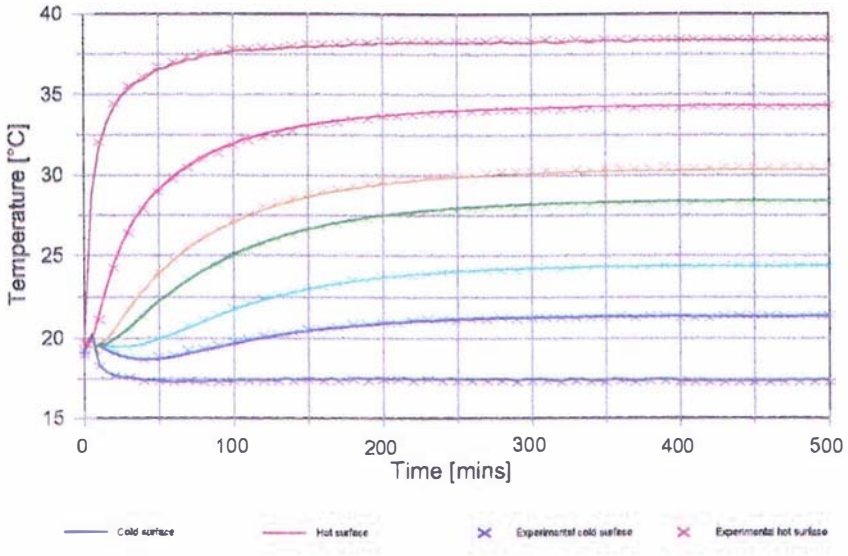

Figure 4.13 - Predictions for 78mm slab temperature profiles.

It can be seen from Figure 4.13 that excellent temperature predictions were achieved using these parameters. A sensitivity analysis was performed to determine which parameters have significant effect on temperature predictions. It was found that the range of thermal conductivity measured by the infinite cylinder method (see Section 2.4.3.1) resulted in differences in internal temperature of up to 3 °C. The final steady state temperatures were accurately predicted as was expected. The average thermal conductivity from the infinite cylinder experiment was found to give the best temperature predictions. The results given by the guarded hot plate method (see Table 2.8) were clearly too low to achieve accurate model predictions. The slab experiment proved to be the most useful method of establishing an accurate measure of effective thermal conductivity in lactose.

The other parameters did not significantly change model accuracy with respect to temperature profile predictions. This analysis showed that the uncertainty in the thermal conductivity parameter could always account for any lack of fit with respect to temperature predictions and therefore the heat transport portion of the model can not be shown to be invalid. The temperature predictions of the model were of suitable accuracy for the purposes of this work.

4.5.4.2 Surface Relative Humidity Prediction Accuracy

The surface relative humidity profiles for the 78 mm slab experiment along with the predicted profiles using the same parameters as above, are shown in Figure 4.14.

It can be seen from Figure 4.14 that the predicted relative humidity profiles are similar in nature, to the trends observed experimentally. Several parameters influence the degree of accuracy obtainable in predicting moisture movement rates in bulk lactose. These are; porosity, initial water activity, initial temperature, moisture

diffusivity, lactose slab thickness and the shape of the moisture sorption isotherm. To identify how significant these parameters are for prediction, a sensitivity analysis was carried out.

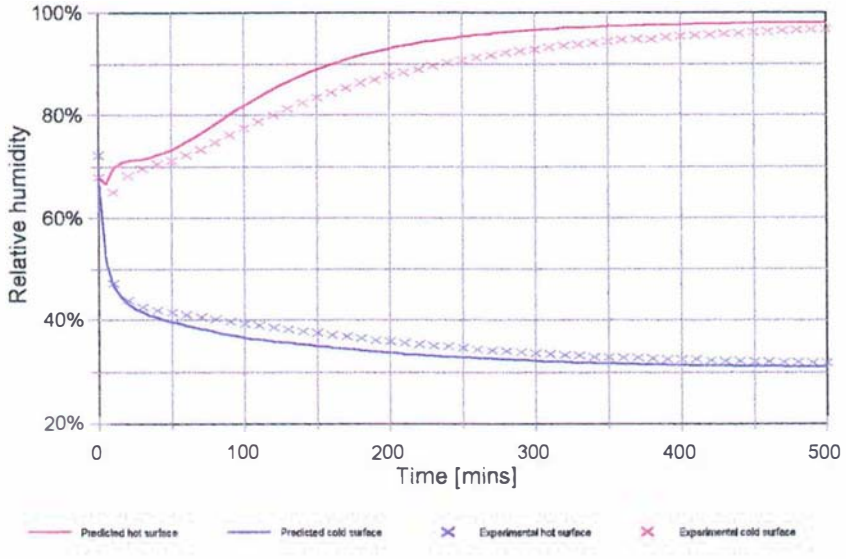

Figure 4.14 - 78mm slab surface relative humidity profile predictions.

The extremes of measured porosity were that of loose powder bulk density (0.49) and tapped density (0.40) as seen in Table 2.5. These were used to investigate the sensitivity of model performance on porosity. The effect of varying porosity can be seen in Figure 4.15.

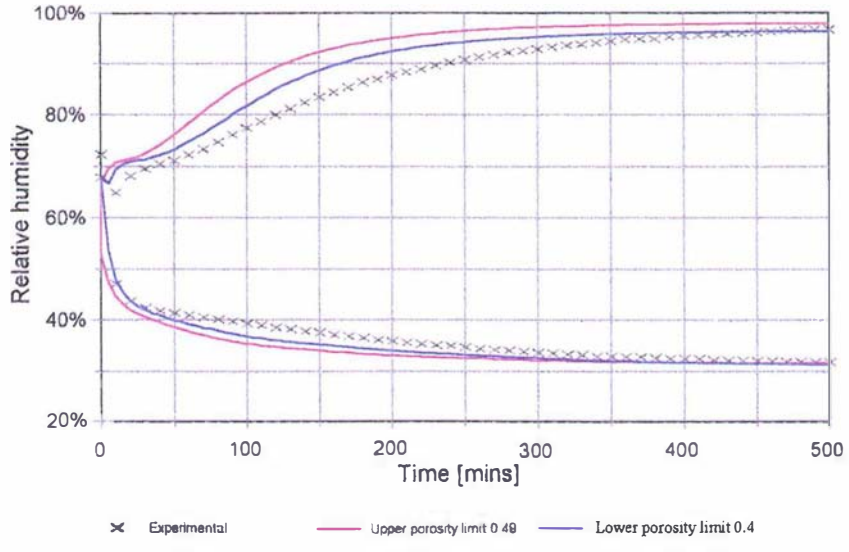

Figure 4.15 - Effect of porosity on surface relative humidity predictions.

This shows that the major effect of increasing porosity is to increase the rate of moisture migration. This is due to the simple model for effective moisture diffusivity in the porous matrix Eq (3.27). The results of the simulation were therefore expected however the prediction using the minimum porosity limit (0.40) did not accurately predict the experimental results. Porosity on its own does not account for the lack of fit of the model.

The results of the porosity analysis indicated that the rate of moisture movement is predicted to be faster than experimentally observed and therefore an investigation into the sensitivity of the moisture diffusivity parameter on model performance was undertaken. To do this the extreme estimates of diffusivity models discussed in Section 3.8 were used. This involved the use of the simple model for diffusivity given by Eq (4.18)

$$D_{effective} = \left(\frac{\delta}{\tau_2}\right) \epsilon D_{air} \qquad (4.18)$$

where δ/τ_2 is a parameter involving the tortuosity and constrictivity of the diffusion path and can range from 0.5 to 1.0. Figure 4.16 shows the prediction of surface relative humidity using δ/τ_2 of 0.5 and 1.0 for comparison.

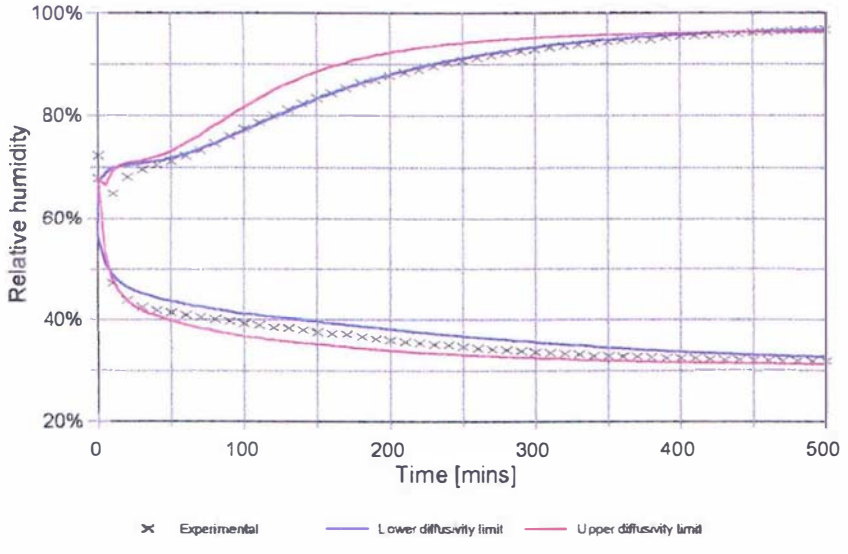

Figure 4.16 - Effect of diffusivity on surface relative humidity predictions.

This shows that the adjustment of the diffusivity parameter could allow very good cold surface predictions to be achieved. The hot surface relative humidity profile was not as well predicted however. The reason for the rapid drop in relative humidity on the hot side is the increase in temperature. This is then followed by the gradual diffusion of moisture toward the cold surface. It follows therefore that the magnitude of this temperature increase could have been influential on how accurate the hot surface relative humidity predictions were.

To assess this, an analysis on the sensitivity of the model on initial temperature was undertaken. Figure 4.17 shows predictions with initial temperature of 19 and 20°C. It

can be seen from this graph that the effect of initial temperature was as hypothesised above for the initial drop in relative humidity. There is a correspondingly higher increase in relative humidity on the cold surface due to the slightly higher temperature increase caused by a higher initial temperature.

The effect of initial product water activity can be seen in Figure 4.18.

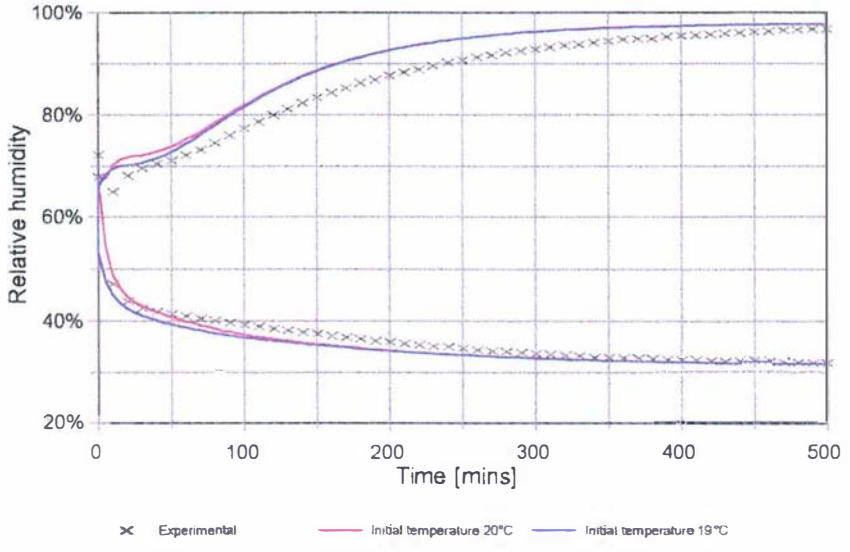

Figure 4.17 - Effect of initial temperature on surface relative humidity predictions.

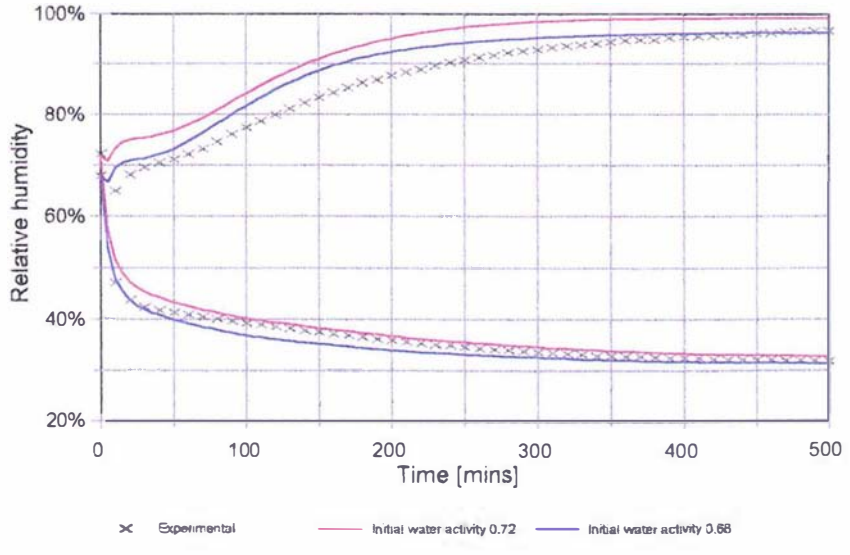

Figure 4.18 - Effect of initial water activity on surface relative humidity predictions.

This shows that the effect of changing initial water activity gives predictions which are shifted up or down without significantly changing the profile shape.

Due to the slightly irregular surface of the constant temperature plates, the lactose slab thickness could be measured only to the nearest millimetre. The effect of this on

relative humidity predictions can be seen in Figure 4.19. This plot shows that slab thickness has very little effect on predicted surface relative humidity profiles.

The most significant parameter with respect to surface relative humidity profile prediction is the shape of the moisture sorption isotherm for crystalline lactose. To investigate the sensitivity of the model on isotherm shape, the two extremes for sorption isotherms were fitted to the experimental isotherm data discussed in Section 3.3.3.1. These isotherm fits are shown in Figure 4.20

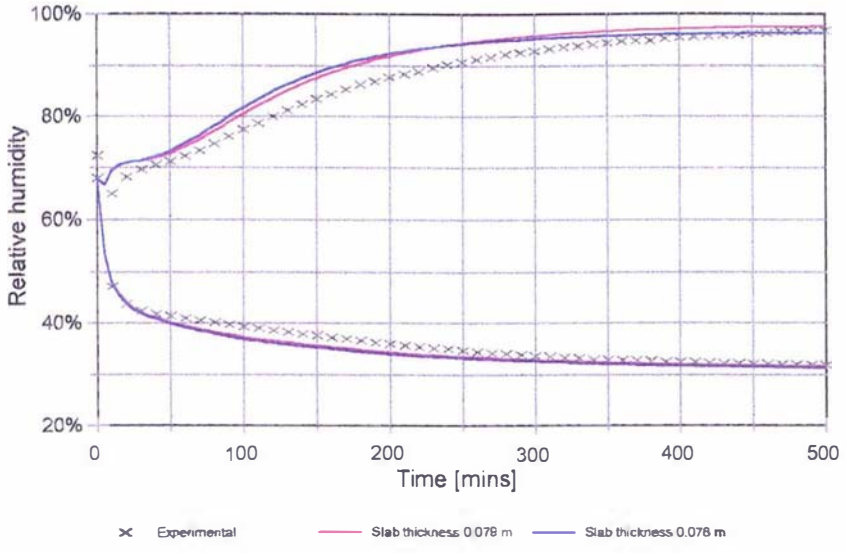

Figure 4.19 - Effect of slab thickness on surface relative humidity predictions.

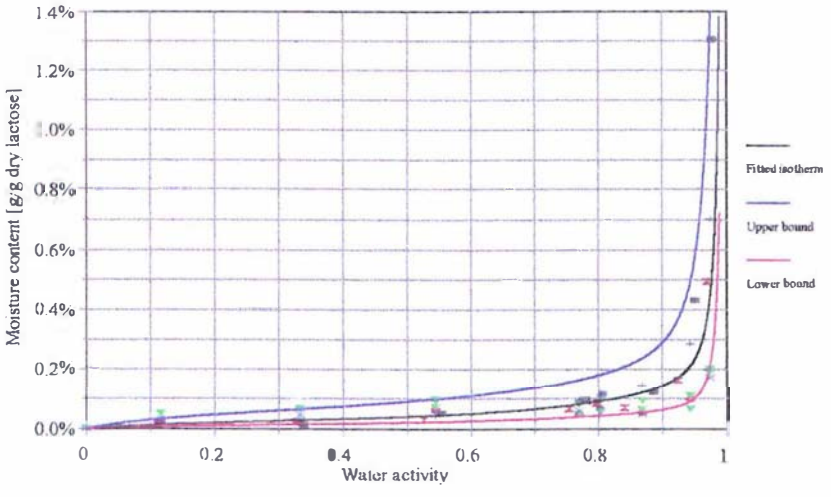

Figure 4.20 - Sorption isotherm model fitting limits. Note: the markers represent experimentally measured points. See Section 3.3.3 for further discussion.

Table 4.1 Summary of isotherm model parameters for limiting cases.

tss Isotherm parameter	Fitted isotherm	Lower limit	Upper limit
M_o[g/g dry lactose]	2.5e-4	1.5e-4	6.0e-4
f	0.92	0.82	0.85
c	8.8	8.8	8.8
h	30	20	15

The sorption isotherm parameters for these isotherms are summarised in Table 4.1 The model predictions using these two extremes are shown in Figure 4.21

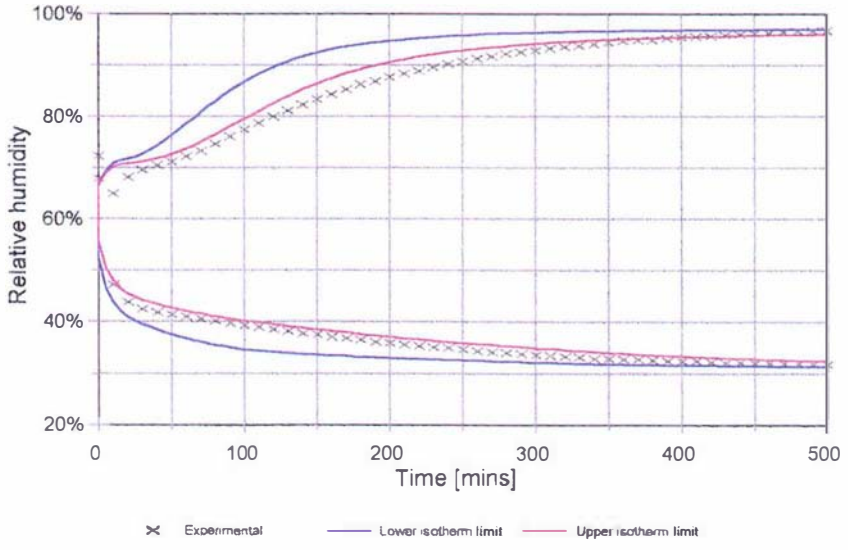

Figure 4.21 - Effect of changing isotherm shape on surface relative humidity predictions.

This plot shows that a large difference in model predictions can result from errors in the sorption isotherm model. In spite of the high sensitivity of the model to the sorption isotherm parameters, it was found that reasonable predictions could be made using the originally fitted isotherm parameters outlined in Section 3.3.3.1.

With the analysis of the sensitivity of the various parameters to prediction accuracy carried out, a best attempt for model predictions was attempted.

The model parameters used in this simulation are summarised below;

thermal conductivity	0.175 W/m^{2}K
porosity	0.4
δ/τ_2	0.7
slab thickness	0.078 m
initial water activity	0.68
initial temperature	19°C

These parameters resulted in the model predictions shown in Figure 4.22.

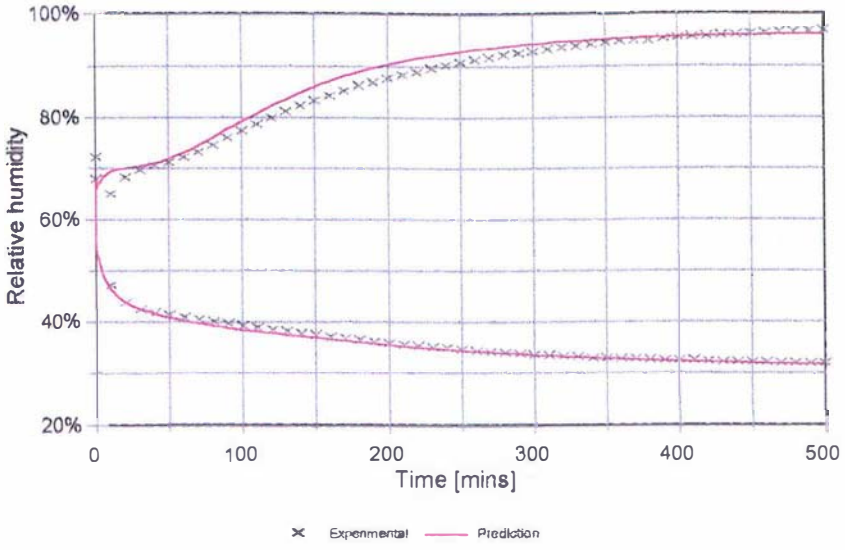

Figure 4.22 - Best attempt at surface relative humidity predictions.

Using the same values for porosity, thermal conductivity, diffusivity and sorption isotherm parameters, the prediction of the 100 mm experiment were carried out. These are shown as Figure 4.23 and Figure 4.24. It can be seen from these plots that the model gives good predictions of the experimental data collected

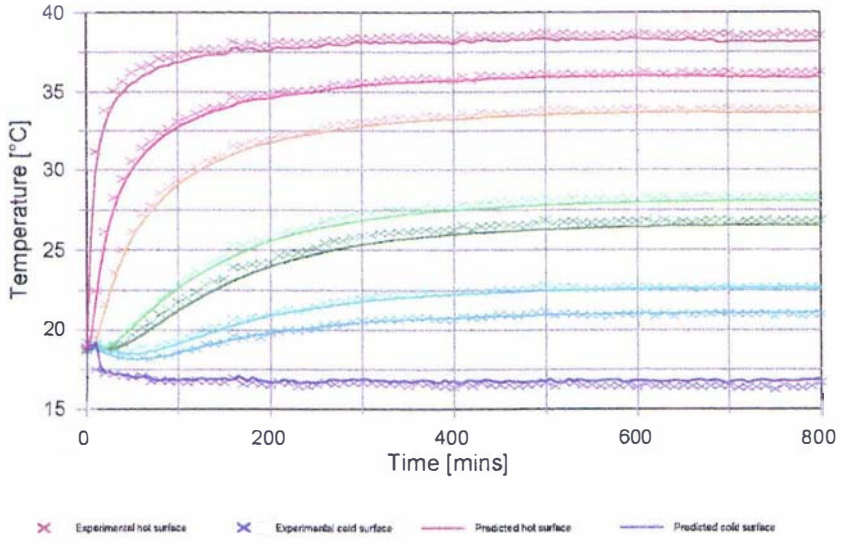

Figure 4.23 - Model predictions for 100mm slab experimental temperature profiles.

The predictions given by the transport model were of sufficient accuracy for the scope of this work. Further improvement in the model is not justified until the accuracy of the system parameters can be significantly improved.

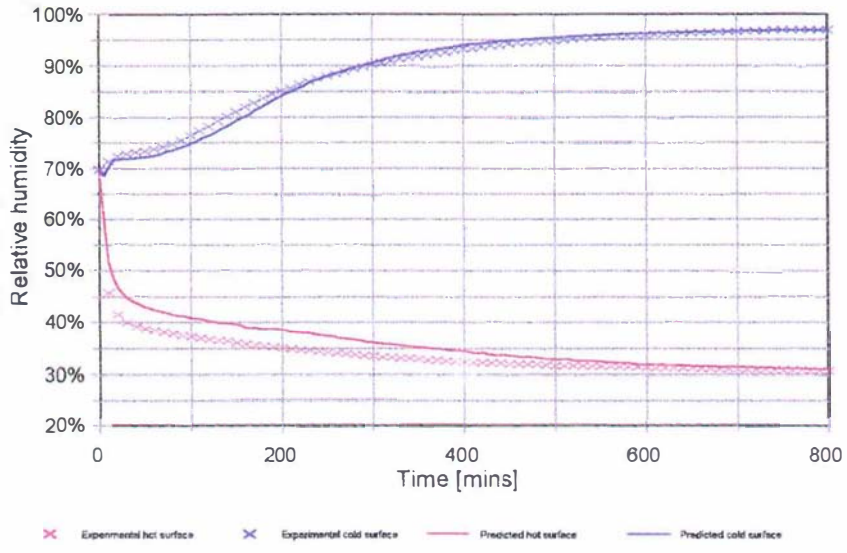

Figure 4.24 - Model predictions for 100mm slab experimental surface relative humidity profiles.

4.6 CLOSURE

The analysis of mathematical model accuracy, numerical error and model prediction accuracy undertaken shows that the mathematical model of the transport of heat and moisture due to temperature gradients, was of sufficient accuracy for the scope of this work. This model allowed the prediction of the local state of water within a bulk lactose slab. With such information it would be possible to describe the state of the lactose with respect to the tendency for caking problems within the slab. For this to be achieved knowledge of the extent of caking under different relative humidity conditions was required. This is the subject of the next chapter.

CHAPTER 5

CAKING MECHANISMS

5.1 INTRODUCTION

With the ability to predict how conditions within bulk lactose change with time due to temperature gradients, it was then necessary to determine the range of conditions under which caking is significant. Once this had been achieved, the mathematical model could be expanded to include caking phenomena and a model for caking in bulk lactose can be constructed. This would then allow the investigation of strategies to minimise caking of lactose in bulk storage. Such modifications to the model are outlined in Chapter 6. This chapter outlines the investigation of the conditions required for caking in bulk lactose powders.

5.2 CAKING MECHANISM OVERVIEW

Moisture has been known to be a principle factor in the caking and sticking propensity of food powders for many years [Nelson 1949]. Caking and sticking in powders are caused almost always by liquid bridging which may be followed by a re-crystallisation process. For liquid bridging to proceed, the surface of the crystals must be fluid at least at certain sites. Peleg (1983,1993) lists the mechanisms by which, this surface wetting may occur as;

1. moisture sorption, accidental wetting or moisture condensation that causes dissolution of the surface, and the formation of a saturated film around the particles.
2. liquefaction of the surface itself through the transition from the meta-stable glass state to the thermo-plastic rubbery state of amorphous sugars, by exceeding the glass transition temperature.
3. liberation of absorbed moisture, released by amorphous glass re-crystallisation.
4. melting of the surface (especially if fat compounds are present).

For the caking of sugars, two general caking mechanisms are evident, that of humidity caking and amorphous sugar re-crystallisation.

5.2.1 HUMIDITY CAKING

Many authors have hypothesised the caking mechanism in sugars [Moss *et al.* 1933, Nelson 1949, Meade 1963, McGinnis 1971, Pancoast and Junk 1980, Nicol 1991], onion powder [Peleg and Mannheim 1969, 1977], and fertilisers [Hardesty and Kumagai 1952, Kumagai and Hardesty 1956, Whynes and Dee 1957, Anonymous 1990a, Rutland 1991]. A detailed review of the earlier investigations into the caking of sucrose was carried out by Bagster (1970a, 1970b).

The basic mechanism presented by these researchers has been termed "Humidity Caking", and was summarised by Nelson (1949) as;

> "Powders, when exposed to conditions of high relative humidity will absorb moisture. A powder, will at equilibrium, give an equilibrium relative humidity, dependent on its moisture content. There exists what has been termed the critical relative humidity for adsorption to take place. This is the relative humidity at which pure sugar crystals change from a theoretically moisture free condition to a dissolved or liquid condition. For sucrose this value has been observed as being approximately 85%."

The moisture content of sucrose is typically between 0.02-0.06% (dry weight) [McGinnis 1971]. Nelson (1949) suggests that moisture contents above 0.06% lead to caking problems. Anonymous (1990b) suggested that for storage of sucrose, the equilibrium relative humidity should be kept below 65%, to avoid caking.

Bagster (1970a) suggested that most of the moisture stays at the surface in the case of a sucrose crystal. Solutes at the surface may then be dissolved to form a saturated solution. Irani *et al.* (1959) stated that caking propensity is directly dependant on the solubility of the material being caked. This would indicate an increase in caking strength with increasing temperature due to the increasing solubility with temperature.

It has been experimentally observed [Rumpf 1975, Schubert 1984] that where particles possess free liquid films on the surface, liquid bridges will form between adjacent particles as surface tension forces cause flow to occur toward the contact regions of two or more particles. Scoville and Peleg (1981) determined that liquid bridges are sufficient to alter the bulk properties of food powders. Nelson (1949) however stresses that caking does not occur until this moist sugar has lost excess moisture and the syrup film at the fused points of contact has re-crystallised to the crystal surface, causing the cementing together of adjacent particles.

Peleg and Mannheim (1969) observed that caking tendency of onion powders increased with temperature in the range 15-35 °C. They attributed the observation of shrinkage on caking to the inter-particle attraction caused by liquid bridging. These forces result in the formation of a closer matrix and hence shrinkage. It should be pointed out that these observations can be also explained by the amorphous glass re-crystallisation caking mechanism.

From the observations of Peleg and Mannheim (1977) and Scoville and Peleg (1981) it is clear that the physical properties of cohesion and bulk density are mainly attributed to the particle surface properties of the powder. This means flow-ability loss and caking will start even when the particle interior is relatively dry. Inter-particle cohesion in crystalline materials can develop with very minor, sometimes difficult to detect, changes in moisture content. The bulk properties of bulk density and compressibility, may be more sensitive indicators of such changes [Moreyra and Peleg 1981].

5.2.2 AMORPHOUS SUGAR RE-CRYSTALLISATION

Stickiness or cohesion in powders is a problem in the storage of amorphous sugar containing food powders [Downton *et al.* 1982, Wallack and King 1988, Noel *et al.* 1990, Roos and Karel 1993]. The characteristic sticky point of a particular material has been defined as "the temperature at which the force required to stir a food powder increases sharply" [Lazar *et al.* 1956]. Stickiness usually results in caking above the sticky point [Roos and Karel 1993].

The sticky point of a powder and caking tendency are moisture dependent phenomena [Notter *et al.* 1958]. Peleg and Mannheim (1973) indicated a relationship between caking and the cohesion of powdered sucrose. Moreyra and Peleg (1981) have conducted an investigation of the effect of water activity on the bulk properties of a number of powders including powdered sucrose. Their results have showed that the behaviour of sucrose changes markedly at 0.6 a_w. Flink (1983) points out that this observation could be due to transitions in the structure of the surface of the powder, first with collapse and then re-crystallisation of a thin layer of amorphous material formed during the milling process. Roos and Karel (1991a) observed that for a sucrose/fructose (7:1) mixture, the sticky point was close to the temperature corresponding to the end of glass transition.

Roos and Karel (1993) attributed the stickiness phenomena to glass transition. Above T_g increasing mobility may result in stickiness. Wallack and King (1988) used liquid bridge formation kinetics to determine the critical viscosity for stickiness. It was found to be around 10^6-10^8 Pa.s. Roos and Karel (1993) demonstrated that the viscosity for stickiness is equivalent to the viscosity of amorphous sugars at T-T_g value of 10-20°C.

Various additives, often of high molecular weight, have been used to combat stickiness in spray drying and in powders. When high molecular weight additives such as gums, proteins, or malto-dextrin are used as drying aids, they serve to increase the viscosity at a given moisture content and can raise viscosity sufficiently to avoid stickiness [Downton *et al.* 1982]. This could be the result of increasing the glass transition temperature of the mixture, or the additives could act as a moisture sink which means much more moisture is required to achieve a high water activity.

Downton *et al.* (1982) described the mechanism for the stickiness phenomenon. Moistening the particle surface reduces the viscosity. If two surfaces come into contact, they may or may not stick together, depending on whether sufficient liquid flow can occur to build a bridge between the particles that is strong enough to resist subsequent mechanical deformation. By dimensional analysis or simplistic energy balance Eq.(5.1) was formulated.

$$\eta = \frac{k'\sigma t}{d} \tag{5.1}$$

where k' is a dimensionless proportionality constant, σ is surface tension driving force, t is contact time, η is viscosity and d is distance over which flow must occur.

Peleg (1993) derived Eq.(5.2) for the temperature/moisture relationship of stickiness, collapse and glass transition.

$$\ln \frac{T - T_r}{T_0 - T_r} = -k''M \qquad (5.2)$$

where T is Temperature, T_0 is characteristic temperature corresponding to zero moisture content, T_r is reference temperature, M is moisture content (dry basis) and k'' is a constant. This is again evidence that stickiness, glass transition and caking are all attributed to the same phenomenon.

5.2.3 ALTERNATIVE MECHANISMS

Alternative mechanisms for caking of fertiliser caking include plastic deformation [Anonymous 1990a, Rutland 1991] and the formation of double salts [Anonymous 1990a]. Double salt formation occurs during storage of fertilisers when chemical reactions between different salts do not reach completion in the granulation process. The end result of these exothermic reactions can be extensive re-crystallisation, increased temperature and severe caking. Plastic deformation caking occurs in fertiliser storage when high pressure is applied.

5.2.4 EFFECT OF PRESSURE AND CRYSTAL CONTACT AREA

Flow-ability and caking is affected by the number of points of contact between crystals [Anonymous 1990b]. The number of points of contact is affected by;

- pressure
- crystal size (the smaller the crystal size the greater the number of points of contact)
- coefficient of variation (as this increases, the number of contact points will increase as fine particles will fill the interstices between the larger crystals).

Lyle (1956) and Pancoast and Junk (1980) also indicated the importance of face to face contact in the caking of sucrose. Pressure influences the severity of caking in that the greater the compression, the closer the contact between the crystals will become. This will result in a greater number of contact points and hence more adhesion between adjacent crystals [Bagster 1970b]. Nelson (1949) indicated that not only did pressure increase the number of points of contact between crystal faces, but makes more certain the fusing of any syrup film on the crystals

Bagster (1970b) states that smaller particles have a greater surface area per unit of bulk volume. Because of this there is more water associated with a bag of fine crystals at a given equilibrium relative humidity than for larger crystals. There is also evidence to suggest that the time to reach equilibrium in conditioning granulated sugar was less for finer particle sizes.

Irani *et al.* (1959) stated that the effect of extremely high pressures at points of contact can locally raise solubility of the material so that the resulting saturated solution may crystallise, upon flow to neighbouring positions, where pressure is lower.

5.3 CAKING MECHANISMS UNDER CONSIDERATION IN THIS WORK

Two caking mechanisms have been suggested from the literature. These have been termed humidity caking and amorphous sugar re-crystallisation. Humidity caking refers to the formation of liquid bridges at high relative humidity conditions. Due to capillary condensation effects, moisture is collected in the contact points between adjacent lactose particles. The high moisture content will allow dissolution of the surface of the crystal and the formation of a liquid bridge of saturated lactose solution. This state of inter-particle bonding will be termed in this work as lumping.

When lumped lactose material is then exposed to a lower relative humidity environment desorption will take place. This will result in the super-saturation of the dissolved lactose in the liquid bridge and therefore cause crystallisation. This will result in the formation of a solid bridge. The solid bridge has more strength than the liquid bridge present in lumped lactose. The presence of solid bridges is termed caked lactose. This process is illustrated in Figure 5.1.

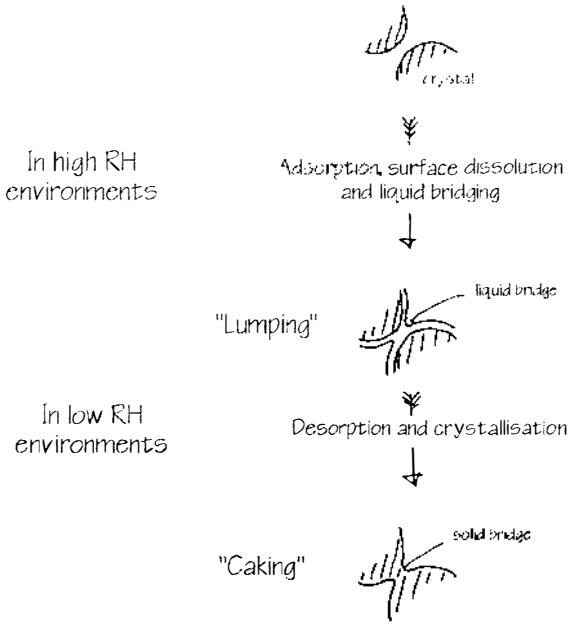

Figure 5.1 - Humidity caking mechanism.

Amorphous caking is thought to be brought about if significant levels of amorphous lactose are present on the outside surface of the lactose crystals. If, for whatever reason, the local moisture content and or the temperature in a bag of lactose cause the amorphous lactose to undergo a glass transition, then there is a capability for amorphous lactose to flow toward the inter-particle contact points due to surface tension forces. Such flow is sometimes called sticking [Lazar *et al.* 1956]. Sticking is essentially caused by liquid bridging, but differs from lumping described above, because of the increased viscosity of the amorphous lactose compared with a saturated lactose solution. This will result in an increased bonding strength of material in this form.

If the amorphous lactose remains above the glass transition temperature for extended

periods of time, crystallisation will occur. This would result in solid bridges as described above for humidity caking. It is expected that the solid bridges formed would exhibit stronger bonding strength than the rubber bridges caused by sticky amorphous lactose but this would depend on the relative sizes of the bridges. The amorphous lactose related caking mechanism is summarised in Figure 5.2.

If sticking does not occur when amorphous lactose is present, the amorphous lactose will act as a moisture source which will be released on crystallisation. The moisture sorption isotherm for a partially amorphous lactose sample shown in Figure 3.9 shows that if a sample containing 2% amorphous lactose undergoes crystallisation at 0.45 a_w to an anhydrous product, it will release enough moisture to result in product water activity of greater than 0.9 a_w. This moisture release would then contribute to the propensity of liquid bridging by the humidity caking mechanism described above.

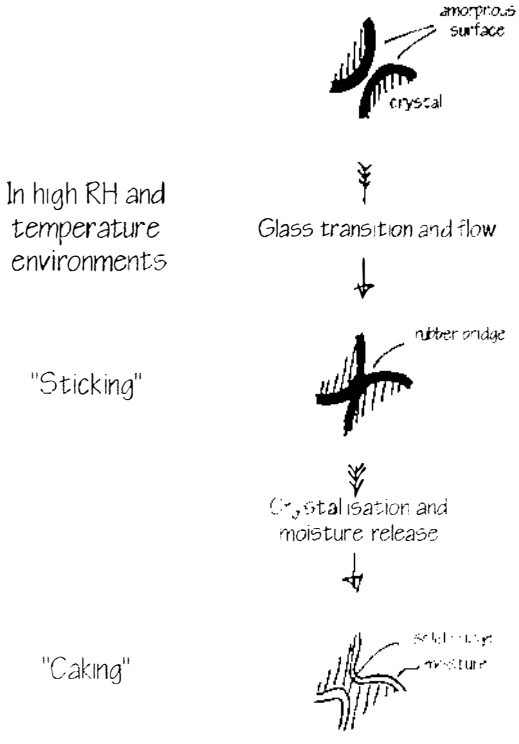

Figure 5.2 - Amorphous related caking mechanism.

5.4 CAKING STRENGTH MEASUREMENT

In order to determine which of the caking mechanisms contribute to caking problems under different conditions, some quantitative strength measurement was required. The development of such a measurement technique needed to consider the types of bonding forces which combine to give a powder an observed bulk strength, while also bearing in mind the practical requirements of any measurement technique which might be employed. These factors are discussed in more detail below.

5.4.1 CAKING STRENGTH REQUIREMENTS FOR THIS WORK

The strength of caked or lumped lactose powder is caused by either liquid bridges or solid crystalline bridges. The major difference between the humidity caking and amorphous lactose related caking mechanisms is the viscosity of the liquid bridges and the likely size of the resultant crystalline bridges. In either case, some form of bridges are the major reason for the increased strength of lumped or caked bulk powder.

A liquid bridge has strength due to the presence of capillary forces. These are made up of surface tension forces and the force due to differences in pressure inside and outside the liquid bridge [Schubert 1984]. Such forces are best measured as the tensile strength of the product. Schubert (1975) defines tensile strength as the 'unidirectional maximum tensile force per unit of the plane cross-sectional area of the bulk material at right angles to the direction of the tension when a locally constant, purely tensile stress prevails in the fracture cross-section of the material regarded as a continuum'.

As such, the method of characterising the relative strength of product in different conditions needed to be able to measure the strength of the liquid bridges or solid bridges inherent in the bulk media. The technique decided upon, also needed to meet the requirement of being suitable for use in measuring the strength of material packed into the experimental temperature gradient rig described in Section 4.5.3.1. This allowed the application of a temperature gradient to a packed lactose bed and the characterisation of the resulting strength profiles throughout the bed, due to moisture migration.

Any technique which required the removal of the product from the experimental rig would cause the disturbance of the liquid bridges giving the sample strength and therefore was not suited to this purpose. The technique also needed to be suitable for the strength determination of small samples which were equilibrated in desiccators at varying conditions.

5.4.2 AVAILABLE STRENGTH MEASUREMENT METHODS

Numerous methods can be found for the determination of the bulk strength of particulate materials. These can be characterised into several main categories including, tensile strength, shear strength, crushing strength and other miscellaneous measurement methods.

5.4.2.1 TENSILE STRENGTH

Tensile strength measurements have been made by Schubert (1975), Schubert *et al.* (1975) and Pietsch *et al.* (1969) for finely divided solids. The advantage of tensile strength measurement is the availability of theoretical relationships between tensile strength and the various kinds of binding mechanisms which have been developed by Rumpf (1961), Schubert (1975) and Pietsch *et al.* (1969).

Kawashima (1991) summarises several other researchers tensile strength measurement devices as does Schubert (1975). Hasegawa *et al.* (1985) detail two commercially available tension testers. Most methods involve the measurement of strength when the powder is pulled apart. For example the split table method makes use of a horizontal

platform on to which the powder is packed. Part of the platform is movable and is pulled from the remaining part, causing a breakage in the powder. The force required to separate the two portions is used as a measure of the tensile strength.

Each of the tension force methods are relatively simple, established techniques, however they were not suitable to testing in situ in the experimental temperature gradient rig.

5.4.2.2 Shear Strength and Cohesion Tests

Shear strength measurements are often used as measures of cohesion or flow-ability in powder systems. Jenike (1970) developed a shear cell which uses a split ring system into which the powder is packed. A loading force is applied to the top of the cell and the strength required to drag the top ring over the bottom ring is measured. Similarly an annular shear cell has also been developed [Walker 1967] which allows the accurate measurement of shear forces at low normal stresses. For the purpose of measurement of food powders, the annular shear cell is preferred, particularly for low strength powders such as soup mix and onion powders [Schubert 1987]. The annular shear cell is a complicated and expensive device however and simpler methods are often preferred by many researchers.

In spite of this, there are a number of researchers who have used shear measurements and many testers are commercially available. These include Nash *et al.* (1965) who use a method similar to the Jenike tester for investigating the effectiveness of anti-agglomerating agents in finely ground powders. Plinke *et al.* (1994) used the method of Peschl (1989) which is a rotational split level shear tester for measurement of shear strength in limestone. They found that the method agreed well with the more widely accepted Jenike and Gebhard techniques. Scoville and Peleg (1981), Moreyra and Peleg (1981) and Hollenbach *et al.* (1982) used a Jenike and Johanson flow factor tester to characterise the flow-ability of selected food powders. Hasegawa *et al.* (1985) review the operation of three commercially available shear strength testers for use in characterising powder beds.

The basic operation of any shear cell testers, effectively excludes the method for use in this work. All methods require one plane to be dragged across another plane of powder material. While such a setup is possible in small scale equilibrated samples, it is not easily achieved in the experimental temperature gradient rig, without the physical disruption of the system.

5.4.2.3 Compaction and Compressibility Measurements

Many researchers have used compression tests as a measure of the strength of particulate materials [Whynes and Dee 1957, Moreyra and Peleg 1981, Scoville and Peleg 1981, Hollenbach *et al.* 1982,1983, Abdel-Ghani *et al.* 1991, Riepma *et al.* 1992 and Morishma *et al.* 1993]. Each method is essentially a measurement of the crushing strength of a standardised pellet or sample. While such measurements are common and the availability of instruments such as an Instron universal testing machine are high, the action of the method is to measure a combination of forces including shear, tension,

particle breakage and compressibility. This is likely to cloud the strength measurement which is aimed at the measurement of the strength provided by bridge formation. The other difficulty with these methods is that the instruments are not suitable for measuring strength profiles through the lactose bed in the temperature gradient experimental rig.

5.4.2.4 OTHER METHODS

Several other alternative methods have been used in the past for the characterisation of the strength of powders. Abdel-Ghani *et al.* (1991) measured the effective elastic modulus by the method of indentation testing. Seville and Clift (1984) showed the effect of thin layers of liquid on the fluidisation characteristics of particles. It was shown that the fluidisation characteristics were dependent on inter-particle forces and liquid bridges present in the system. Kono *et al.* (1994) have used this as a basis for the measure of flow properties of powers by measuring the minimum fluidisation velocity and minimum bubbling velocity of the powder bed. The results showed this technique to be better than the Jenike shear cell which requires high normal loading to obtain accurate strength measurements

Penetrometry is a technique used extensively in the field of soil science for the characterisation of soil systems [McLaren and Cameron 1990]. Such measurements simply involve recording the force required to push a probe into the sample. Because the size and shape of the probe will be influential on the force recorded, it becomes an empirical measure. A multi-point penetrometer has been used by Baker and Mai (1982) for measuring the strength of top soil. The size of the pins which were pushed into the ground were approximately the same as the particulate system and the number of pins was increased until the force measurement device could accurately measure the applied force. In this way the forces broken by the penetrometer were the inter-particle forces under investigation rather than compressive strength commonly achieved with larger penetrometer probes.

Bagster (1970a) summarised some of the early techniques which have been used to quantify caking in powders. These range from largely qualitative observation based tests to the use of penetrometry. Irani *et al.* (1959) measured caking in fertilisers by measuring the weight of fertiliser retained on a particular sized screen.

From this review of strength measuring techniques for bulk powders and the unavailability of testing equipment capable of being utilised in the temperature gradient experimental rig, it was evident that a new strength measurement device or a modification to one of those discussed above needed to be developed for use in this work. The multi point penetrometry method was considered to be the most likely technique for this work. This was developed further and is discussed below.

5.4.3 METHOD DEVELOPMENT

A multi-point penetrometry technique, based around consideration of the device used by Baker and Mai (1982), was developed for the measurement of lactose caking strength. Thirty two, 1mm pins were pressed into a plastic disc in a regular circular pattern to a constant depth. If this is compared with the average particle size of 50-

100μm the pins are approximately one order of magnitude greater in size. Pins of this size were used to give enough strength so bending and dis-alignment of the pins did not occur. This meant that the action of the penetrometry method was a combination of breakage of inter-particle bonds and some compression of the sample. Each pin was filed flat to ensure a known contact area. The probe was then mounted on the arm of a stripped down beam balance which, through the counter weight system, allowed the probe to be set up weight-less above the lactose sample. Weights or water were then added to the top of the probe and the force-distance penetrated history was recorded. A breakthrough force was observed which was taken to be the characteristic strength of the material. The equipment can be seen in Figure 5.3 below.

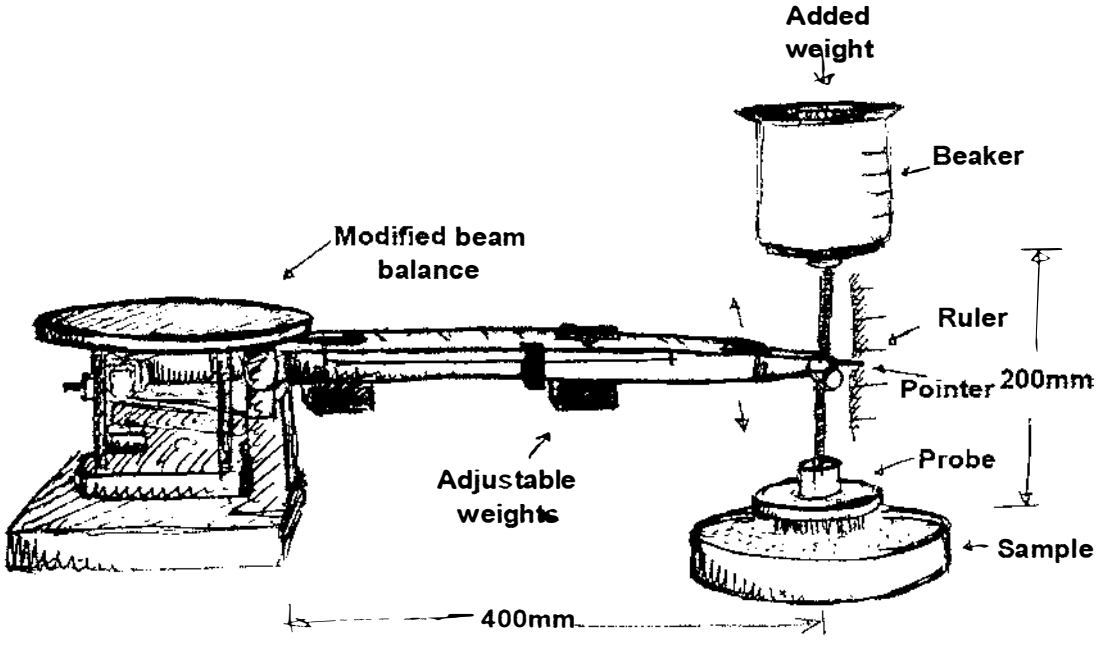

Figure 5.3 - Strength measurement apparatus

5.4.4 METHOD PERFORMANCE

Figure 5.4 shows typical penetration depth versus force applied curves, for lactose powders stored under 95% RH for one month at room temperature using this apparatus. It can be seen that initially there was penetration of up to 2 mm deep before the sudden breakthrough of the probe as the samples strength was exceeded.

This initial penetration was caused by the slight irregularity of the sample surface and the probe stoped this gentle penetration after all the probes pins were sitting on the sample surface. The weight for breakthrough of the surface, was expressed as a force per unit area of pins pushed into the sample.

The instrument was shown to be useful in characterising the strength of powders which are essentially free flowing through to solidly caked samples. The high strength powder, range could be improved in accuracy by reducing the number of pins present in the penetrometer probe.

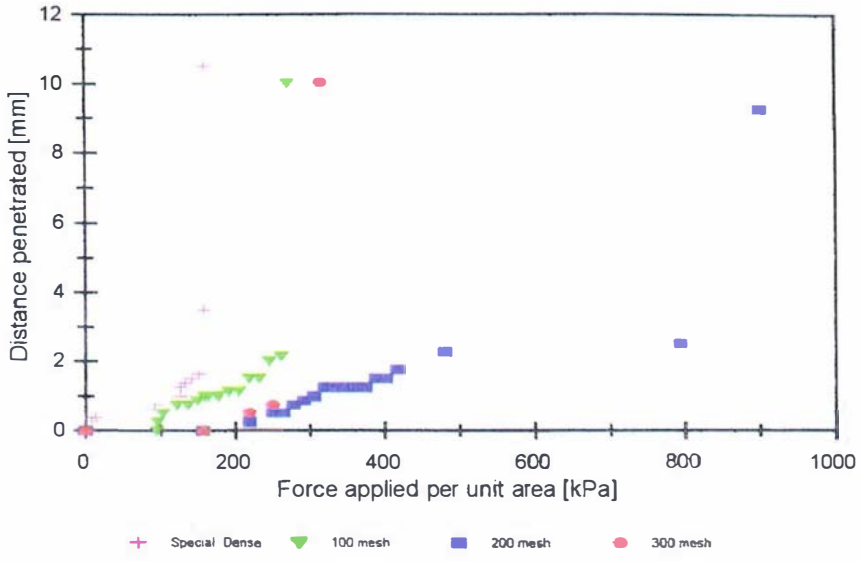

Figure 5.4 - Typical force distance profiles for lactose samples using multi pin penetrometry method.

In order to give some meaning to the strength measurements given by the penetrometer method, qualitative observational tests on the strength of the samples were also undertaken. From these tests, the following comparisons, were made.

Table 5.1 Comparison of multi point penetrometer readings with observational tests.

Strength [kPa]	Observation
0	Free flowing with no obvious strength
50	Lumps form which have very little strength and cannot be picked up without disintegration. Surface powders easily
100	Can just pick up lumps but are broken very easily. Powders easily.
200	Can pick up lumps and break into two. Still easily crushed and powdered.
400	Can pick up lumps and snap into parts. Has reasonable strength but still powders easily
800+	Strongly lumped material which can be broken but is difficult to crush. Powders easily.

This shows that lactose samples with strength measurements of less than 200 kPa. are either free flowing or will become so with minimal mechanical input. Samples with strengths ranging from 200 - 600 kPa. have intermediate strength, while samples with greater than 600 kPa. have large strength and are not easily crushed. Industrial caking problems were estimated to have strength of the greater than 400 kPa range of this scale.

5.5 CAKING BY LIQUID BRIDGING AND SUBSEQUENT DRYING

This section aims at investigating the mechanism sometimes referred to as humidity caking caused by the formation of and subsequent drying of liquid bridges in the powder. This was achieved by identifying which relative humidity conditions caused increased powder strength and what effect drying had on the caking strength.

5.5.1 MECHANISM OVERVIEW

The liquid bridging and subsequent drying mechanism was outlined in Figure 5.1 above. It involves the adsorption by capillary condensation of large amounts of moisture in high relative humidity conditions. Surface tension forces cause the formation of inter-particle liquid bridges which give the particle system strength and cause what is known as lumping in the bulk powder. Over a period of approximately three hours [Hodges *et al.* 1993] dissolution of the surface takes place due to the high moisture content. This results in the liquid bridge being comprised of a saturated solution of lactose. Solute effects are likely to increase liquid viscosity and slightly reduce surface tension from that of pure water (see Section 2.5.2).

If the liquid bridge is then dried out, due to the desorption of water in low relative humidity environments, the concentration of lactose in the liquid bridge will increase until super saturation occurs and crystallisation will proceed. This will result in the formation of a crystalline bridge which will be smaller in size than the liquid bridge originally present. The strength of this crystalline bridge per unit area will greatly exceed that of the liquid bridge.

5.5.2 LIQUID BRIDGING

The strength of liquid bridges was assessed for lactose samples under varying relative humidity conditions at room temperature (18°C). Plastic petri dishes of 75 mm diameter were packed 5 mm high with lactose powders. The samples were conditioned at ambient conditions to ensure no amorphous lactose was present. The top surface was levelled off using a straight edge to provide a flat surface from which the strength could be measured using the multi-point penetrometry method discussed above.

These samples were equilibrated in desiccators containing the following saturated solutions;

Potassium acetate	~ 23 % RH
Sodium bromide	~ 60 % RH
Sodium chloride	~ 76 % RH
Ammonium sulphate	~ 82 % RH
Potassium chloride	~ 86 % RH
Potassium nitrate	~ 95 % RH
Potassium sulphate	~ 98 % RH

Samples were removed from the controlled relative humidity environments after one day, ten days and fifty days of equilibration time and the strength determined using the

multi-point penetrometry method. Figure 5.5 shows the strength profile of lactose powders equilibrated for one day. This clearly shows the development of strength only under high relative humidity conditions.

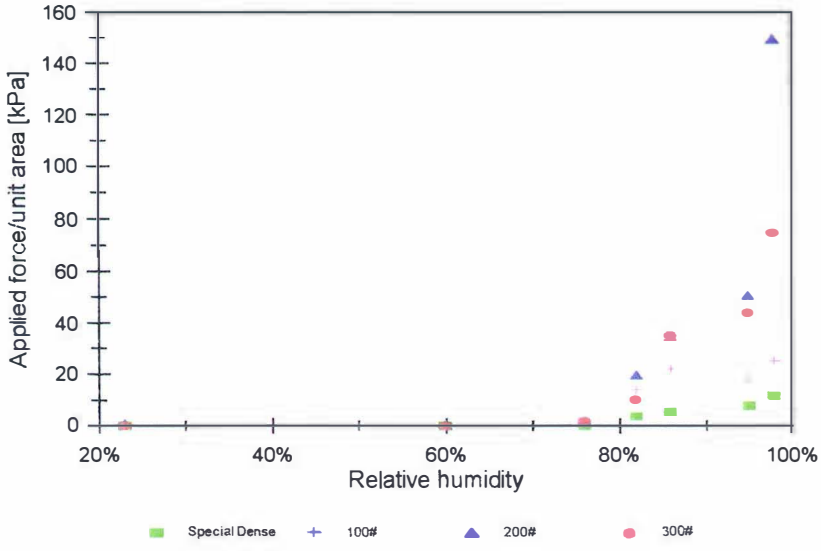

Figure 5.5 - Powder strength after one day equilibration time.

In this high relative humidity region, the material is weakly lumped, but could be picked up by hand (see Table 5.1). Although the strength of the lumped lactose in high relative humidity environments after one day is not great, these results are an indication of the region of water activity where lumping problems are likely to occur. This region of greater than 0.85 a_w corresponds to the region where capillary condensation can occur, in the pore size distribution which occurs in lactose samples. This is also an indication of the relative humidity conditions which are capable of forming a stable liquid bridge [Harnby *et al.* 1996].

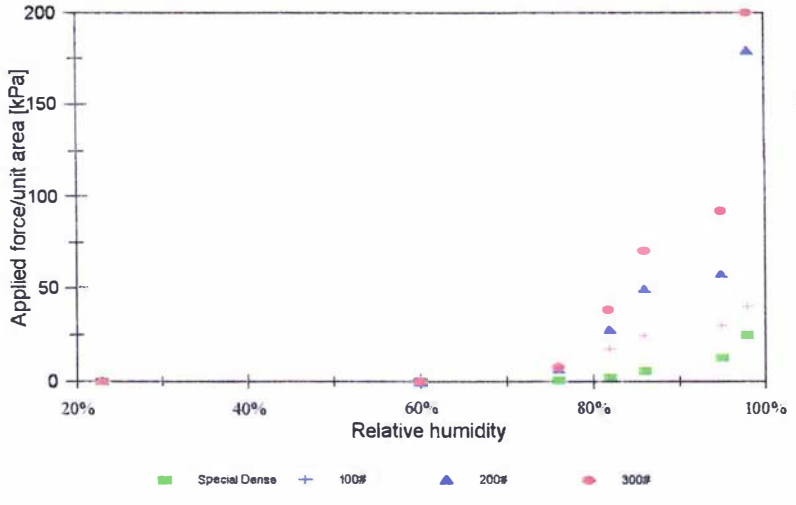

Figure 5.6 - Powder strength after ten days equilibration time.

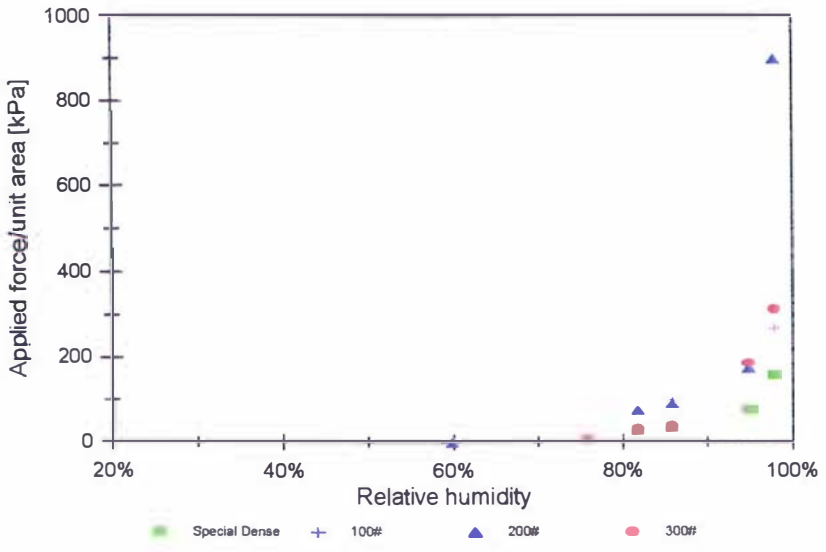

Figure 5.7 - Powder strength after 50 days equilibration.

Figure 5.6 and Figure 5.7 show the measured strength profiles for samples equilibrated for ten and fifty day periods. A similar trend to the results observed in Figure 5.5 is evident. After ten days there is a slight increase in sample strength at the high relative humidity region. After fifty days there is another increase in strength as well as a dramatic increase in strength in the 200 mesh sample. The samples stored in 95% and 98% relative humidity showed obvious shrinkage and reduction in porosity. This shrinkage is thought to be brought about by surface tension forces in the liquid bridges pulling the particles closer together.

There is some evidence of strength dependancy upon particle size. It can be seen from Figure 5.7 that special dense and 100 mesh lactose powders generally had lower strength than the finer 200 mesh and 300 mesh grades. This observation is consistent with the hypothesis that the number of contact points within the bulk solid increases with decreasing particle size. In this experiment the lactose powders were loosely packed and levelled off. The density measurements outlined in Table 2.5 suggest that large variations in bulk density are possible, particularly for the finer lactose grades. It follows that some of the scatter in results are due to variability in bulk density. This may explain the greater apparent strength of 200 mesh lactose as opposed to 300 mesh.

The strength of the powder material is brought about by the presence of liquid bridges. It is more informative to look at the powder strength as a function of the size and number of bridges present. Such a comparison is difficult to make for non-spherical, non-uniformly sized particles. Because the volume of liquid present in the system is proportional to the number and sizes of the liquid bridges it is useful to plot strength as a function of equilibrium moisture content. This can be seen as Figure 5.8.

Figure 5.8 shows an approximately linear relationship between bulk powder strength and sample moisture content. Except for the 300 mesh sample, the plot indicates a trend of increasing strength at the same moisture content as particle size decreases. It is sensible that the strength of the lactose is correlated to the moisture content as this corresponds to both the size and number of bridges present in the system.

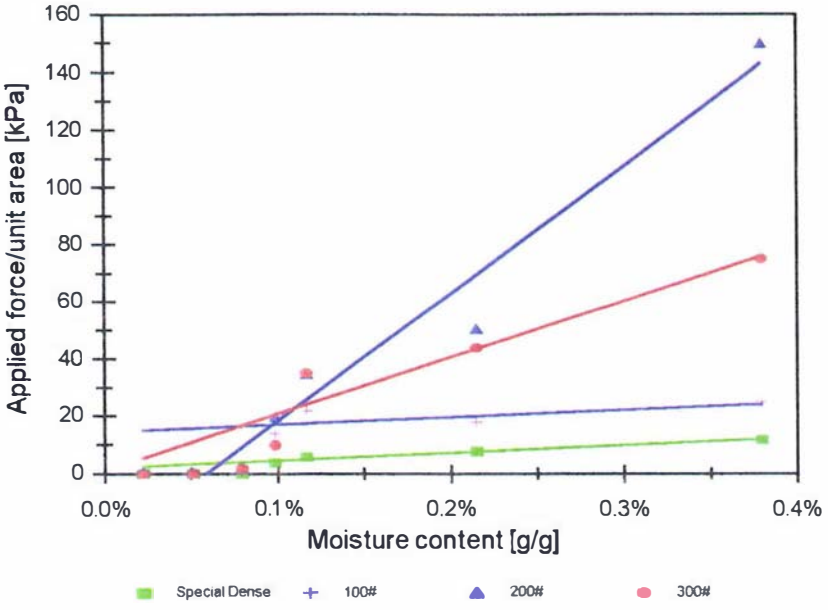

Figure 5.8 - Powder strength after one day as a function of moisture content.

Another approach to interpretation of the strength measurements made on lactose in this work is the comparison of strength to capillary radius. This is possible through the use of the Kelvin equation Eq.(3.7) discussed in Section 3.3.3.1. It was shown, for the moisture sorption isotherm results, that the capillary radius was approximately a linear function of the moisture content [Eq (3.8)] and as such will not show any trends different than Figure 5.8.

The strength of the bulk powder equilibrated under high relative humidity conditions increased with time. No clear trend was observed for rate of this observed increase in strength. It was shown in Section 3.4.1 that the rate of sorption of moisture on to crystalline lactose is fast and that it is safe to assume that the bulk air and lactose surface are in local moisture equilibrium. This being the case, it is difficult to see why the samples showed an increase in bulk strength over a one month equilibration period. One explanation is that strength is not simply caused by liquid bridging alone. In samples equilibrated for fifty days, evidence of extensive shrinkage was observed. Such shrinkage is thought to be due to the preferential dissolution of small crystals and growth of the larger crystals present in the system. Such behaviour is common in solution based crystalline systems.

In bulk powder samples it is common that larger particles are slightly separated by small asperities present on the surface of the crystals (see Figure 2.3). The separation of the larger crystals caused by these, would cause the strength of liquid bridges to be reduced as was shown by Schubert (1984). If these asperities are dissolved, in the surface moisture forming the liquid bridge in high relative humidity conditions, there would be some shrinkage occurring and a corresponding increase in bulk density.

This would have several implications with respect to strength of the powder sample. The distance between the particles would be reduced. This would result in stronger liquid bridges. Also occurring in the system is the growth of larger crystals caused by the dissolution of the small asperities. This growth is likely to occur in the liquid bridged

area due to the concentration of surface moisture to the contact points by surface tension forces. This may result in the formation of partial crystalline bridges. Because the samples in the experiment were not controlled at constant temperature, some growth may have occurred in the bridge area due to the cyclic heating and cooling of the sample because of the variable ambient storage temperature.

It follows from this discussion that the increased strength is thought to be due to the reduction in inter-particle distance caused by the dissolution of small asperities and the production of small crystalline bridges formed due to temperature fluctuations and preferential large crystal growth. This mechanism for increased strength can explain the measured strength of 200 mesh lactose after fifty days equilibration time (see Figure 5.7).

Although the irregularity of geometry and particle size coupled with variability in bulk density, depending on how tightly the particles are packed, make a generic mechanistically based strength prediction method difficult, a basic conclusion can be reached from the results discussed. High relative humidity conditions (>90% RH) or alternatively moisture contents above 0.4% must be reached before strong lumping will occur. For further work, a simple average linear correlation between lactose moisture content and bulk powder strength will be used to predict the extent of lumping due to liquid bridging after one days equilibration time. This can be expressed as Eq.(5.3)

$$Strength\ [kPa.] = 15900 \times M \tag{5.3}$$

5.5.3 SOLID BRIDGING

The drying of liquid bridges formed from saturated lactose solutions will cause the super-saturation and eventual crystallisation of the lactose surface solution. This will result in the formation of solid crystalline bridges. It is difficult to predict the strength of such a crystalline bridge. It is likely to be a function of the size of the original liquid bridge and of the concentration of the lactose solution. The concentration will be the solubility of lactose and therefore a function of temperature (see Figure 2.9).

To assess the strength of solid crystalline bridges, samples were equilibrated over saturated salt solutions for fifty days. The strength of the liquid bridges present in these samples were measured using the multi-point penetrometry method. These samples were then allowed to dry out in ambient air (~70%RH) for a period of seven days. Once dried out, the samples were measured for strength using the same technique as used above

Figure 5.9 shows the results of strength measurements as a function of the relative humidity conditions first equilibrated at. This plot shows samples which had high strength in the lumped form also gave high strength measurements once dried. The strength of the dried material generally had the same or greater strength than the originating liquid bridged material. This can be seen in Figure 5.10.

These results indicate that material in the lumped state will retain the same strength or greater strength once dried out. This shows that despite the much smaller bridges present in the solid form, the increased strength of these bridges compensates. To avoid the occurrence of caked product by this mechanism, it is necessary to avoid the onset of lumping. Investigation into how to achieve this goal is the focus of the next chapter.

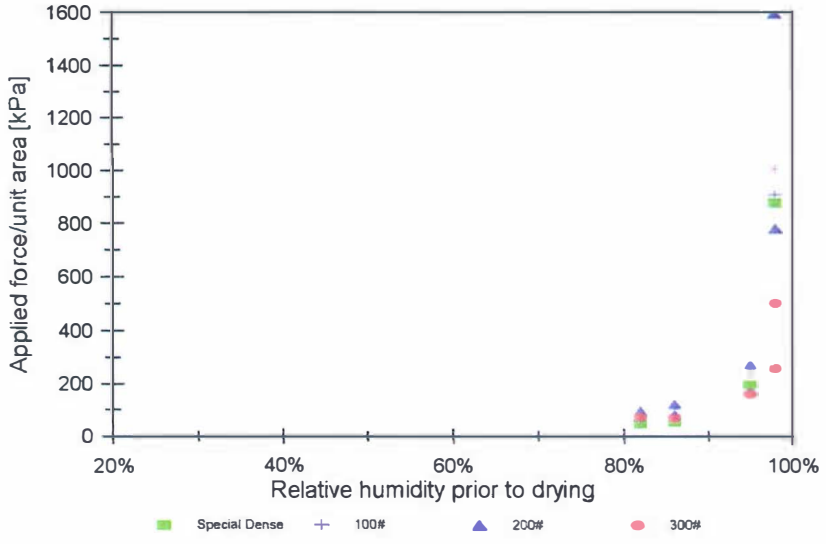

Figure 5.9 - Solid bridge strength as a function of equilibrium relative humidity prior to drying.

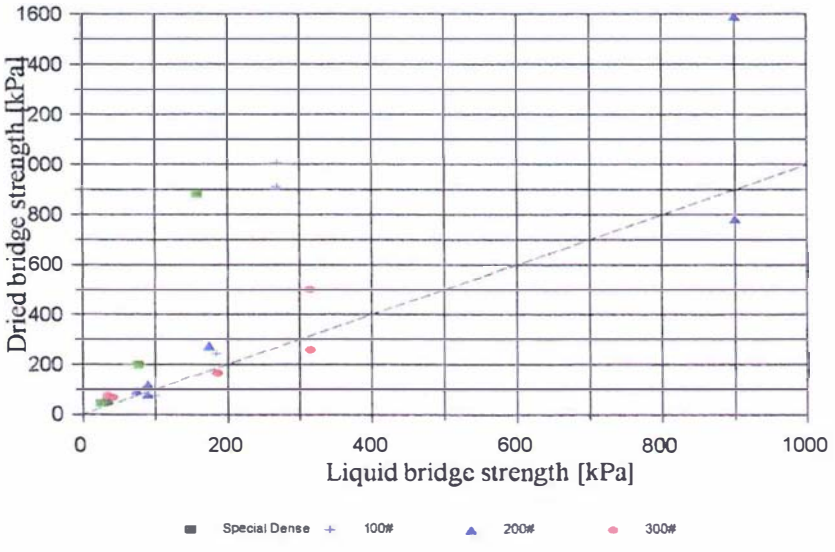

Figure 5.10 - Comparison of solid bridge strength to originating liquid bridge strength.

5.5.4 SUMMARY OF THE LIQUID BRIDGING AND DRYING CAKING MECHANISM

Liquid bridging causes significant lumping problems in bulk lactose at relative humidity conditions greater than 90% RH or local moisture contents of greater than 0.4%. Such conditions would also be favourable for mould growth and therefore should be avoided.

While it is evident that lactose is not bagged in such conditions, there are three basic

mechanisms by which high relative humidity conditions may subsequently exist in the bag. These are;

❶ moisture infiltration from ambient due to inadequate packaging.
❷ redistribution of moisture within the bag raising the local moisture content due to temperature gradients.
❸ the release of moisture due to amorphous lactose crystallisation.

Moisture infiltration from ambient is not of principle concern here as work has been undertaken by Lactose New Zealand to minimise this effect. The moisture transport model and the experiments used in validation of this model have clearly shown that such conditions are possible due to the temperature gradients expected in industrial product storage and shipping if the moisture content of the lactose at packing is too high. The release of moisture due to amorphous lactose crystallisation is the focus of the next section of this work.

If the conditions required for lumping of lactose do occur, then the strength provided by the liquid bridges has been shown to be retained or increased once the liquid bridges are dried out and solid crystalline bridges form. The strength of the liquid bridge is also likely to increase with increasing temperature due to the increase in solubility associated with that temperature increase. This is due to the greater amount of crystallisation which would result from the subsequent drying of a liquid bridge of higher lactose concentration.

5.6 CAKING DUE TO AMORPHOUS LACTOSE FLOW AND CRYSTALLISATION

This section investigates the mechanism of viscous flow of amorphous lactose above its glass transition temperature. This results in the formation of viscous liquid bridges which could be followed by crystallisation to give a caked product.

5.6.1 MECHANISM OVERVIEW

The amorphous lactose flow followed by crystallisation mechanism is summarised in Figure 5.2 above. It involves the presence of a thin layer of amorphous lactose on the outer surface of the crystalline lactose particles. Such layers have been identified to have been present on milled and quickly dried sugars [Roth 1976, Hargreaves 1995] and have been discussed in more detail in Section 2.2.3.

Due to moisture sorption or temperature rise in the amorphous layer, the glass transition temperature is exceeded. This results in the rapid reduction in viscosity allowing both viscous flow due to surface tension forces and crystallisation to proceed This is a two step process somewhat similar to that described by the mechanism of caking by liquid bridging and subsequent drying. The first stage of viscous flow is termed sticking and the second stage of crystallisation results in the formation of caked product. The major differences between the two hypothesised mechanisms is the mode in which the lactose crystal surface becomes capable of flow and the lack of reliance on subsequent drying to produce a solid bridge in the case of amorphous lactose crystallisation. Crystallisation is also likely to result in a subsequent increase in free moisture which would be available for moisture migration (see Section 3.7.3.1).

5.6.2 RUBBER BRIDGING AND STICKING

Downton *et al.* (1982) described the mechanism of sticking in hygroscopic amorphous powders. The driving force for the formation of bridges between adjacent particles is due to maintaining a minimum surface energy and is governed by the surface tension of the amorphous material present. The rate at which the bridges are formed is governed by the viscosity of the material. Downton *et al.* (1982) showed experimentally for a sucrose-fructose mixture, that the critical viscosity for sticking in a short time is in the range 10^6-10^8 Pa.s. This work was extended by Wallack and King (1988) to cover coffee extract and a mixture of malto-dextrin, sucrose and fructose. Results for these substances also fell in the critical viscosity range found by Downton *et al.* (1982). Wallack and King (1988) utilised the Frenkel model Eq. (5.4) for interpretation of experimental observations.

$$\left(\frac{r_b}{R_p}\right)^2 = \frac{3\,\sigma\,t}{2\,R_p\,\eta} \tag{5.4}$$

where r_b is the bridge radius. The Frenkel model is based on the formation of a liquid bridge by a coalescence process, driven by surface energy causing viscous flow. This model has been used as the basis for many attempts to describe agglomeration and sintering phenomena [Rosenzweig and Narkis 1981, Ristic and Dragojevic-Nesic 1987 and Wallack and King 1988].

The size of the inter-particle bridge required for sticking is an important parameter if the Frenkel equation is to be of use. Wallack and King (1988) measured this through the use of scanning electron microscopy. They found that a reasonable representation from sticking coffee extract particles was r_b/R equal to 0.1. This result can be used to predict the time for sticking to occur at any viscosity.

It is common for researchers into sticking and agglomeration of food powders to determine experimentally what has become known as the sticking temperature of a powder. The first such experiment as performed by Lazar *et al.* (1956). This involved the gradual heating of the sample in a test tube which is closed to the atmosphere and containing a stirrer. The stirrer was then turned by hand and the temperature at which the force required to turn the stirrer dramatically increased was recorded as the sticking temperature. Modifications to this technique and another similar method used by Tsourflis *et al.* (1976), have been used by many researchers to characterise the sticking temperatures of various food powders [Downton *et al.* 1981, Wallack and King 1988, Chuy and Labuza 1994].

Some researchers have made a link between sticking temperature and the glass transition temperature. For example, Roos and Karel (1993) demonstrated that sticking occurs at 10-20°C above the glass transition temperature. Chuy and Labuza (1994) found that such measurements depended upon the sample heating rate. In hindsight it becomes obvious that sticking temperature is essentially a meaningless measure of sticking unless the heating rate is also stated. In the extreme case of an infinitely slow heating rate, the sticking temperature would correspond to the glass transition temperature. The sticking phenomenon is a dynamic process, just as amorphous crystallisation is, and because of this time dependancy, it cannot be characterised

meaningfully by a single temperature.

Aguilera *et al.* (1995) have looked at the kinetics of caking of amorphous food powders using spray-dried fish protein hydrolyzate as a model system. They found that the onset of caking was a first order function with a time delay. The time delay was 5.6 ±0.19 hrs and was attributed to be due to the time taken for moisture diffusion into the outer layers of the particles. The first order function fitted is shown as Eq.(5.5).

$$1 - \frac{\phi(t)}{100} = e^{-(t-t_d)/\tau_c} \qquad (5.5)$$

where $\phi(t)$ is the caking index defined as the fraction of material which will not pass though a 125μm mesh and τ_c is the relaxation time for caking. The relaxation time for caking was found to fit the WLF function (Eq 3.16), where the adjustable parameters C_1 and C_2 were 11.16 and 10.7 respectively.

5.6.3 RELATIVE RATES OF AMORPHOUS FLOW AND CRYSTALLISATION

For sticking to occur, viscous flow must proceed at a rate faster than amorphous lactose crystallisation. To determine whether this is so in the case of amorphous lactose, the Frenkel equation was used along with the WLF viscosity prediction equation (Eq.3.16). The surface tension used was 0.066 N/m which corresponds to a supersaturated solution of lactose (see Figure 2.9). A key parameter, which is unknown in the lactose system, is the size of the bridge which will give the powder significant strength. For this investigation a range of r_b/R from 0.01 to 0.25 was used. The predictions of time for the relative rates of sticking and crystallisation as a function of T-T_g can be seen in Figure 5.11.

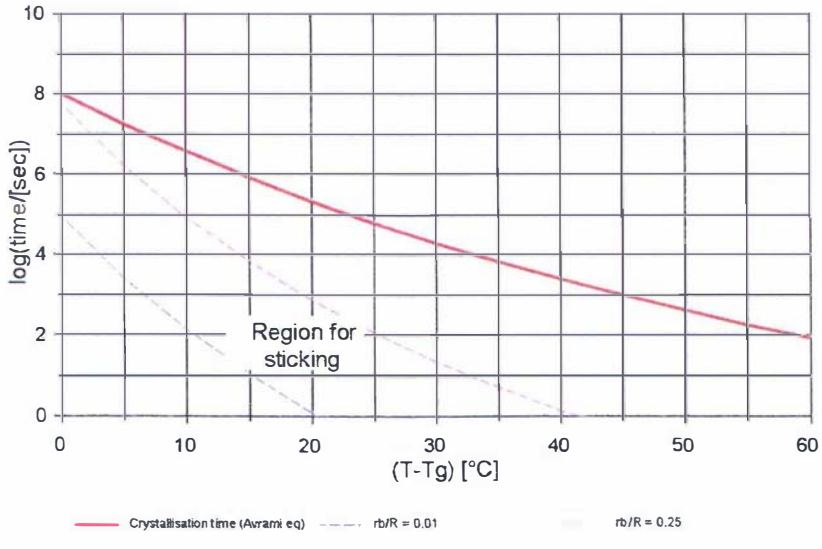

Figure 5.11 - Comparison of sticking and crystallisation times in amorphous lactose.

This plot shows that crystallisation is always proceeded by the sticking phenomena. Hence if crystallisation has occurred, rubber bridges should have already formed.

5.6.3.1 Sticking of Thin Layers of Amorphous Lactose

Sticking phenomena occur in spray or freeze-dried food powders such as lactose based infant powders [Chuy and Labuza 1994], coffee extract [Wallack and King 1988] and mixed sugar powders [Downton *et al.* 1982, Wallack and King 1988]. In these powders there are large quantities of amorphous sugar present. The question then arises that if there is a thin surface layer of amorphous lactose only, as is present in milled lactose, does sticking still play a significant role in caking?

Roth (1976) answered this question for the case of freshly milled icing sugar. Samples that had re-crystallised at 35% RH did not show any traces of solidification. He suggests that the amorphous surface layers (less than 100Å thick) are too thin to be in position to connect touching parts with a solid body bridge of sufficient strength during crystallisation. He went on to suggest that re-crystallisation lead indirectly to caking by releasing moisture to a point whereby the liquid bridging mechanism could proceed. In samples where significant strength was observed and shrinkage occurred it was shown that the shrinkage observed amounted to a reduction in contact area thickness of 1000Å. This corresponded to about ten times the thickness of amorphous surface layer present. This suggested that surface dissolution and liquid bridging were the major cause of caking in icing sugar in high relative humidity conditions.

To test to see if this is also the case for freshly milled lactose, an experiment was conducted which aimed at measuring the strength of lactose samples with amorphous lactose present after one week's exposure to environments of varying relative humidity. If sticking can occur with thin layers of amorphous lactose, then significant strength should be observed at intermediate relative humidity. If not, then results similar to those observed and reported in Section 5.4 for liquid bridged samples would be observed and high strength will result only above 90% RH.

Samples of coarse lactose were milled for five minutes in a Janke and Kunkel Analysenmuhle (A10) pin mill holding approximately 50 grams of lactose. Cooling water was used to ensure the milled lactose did not heat up during the milling process. The freshly milled sample was then transferred into petri dishes in the manner stated for the liquid bridging experiments (see Section 5.5.2). Samples were then equilibrated for one week above saturated salt solutions at 20°C. Samples were also equilibrated over phosphorous pentoxide and magnesium chloride to allow an estimation of amorphous lactose content using the combined sorption isotherm method (see Section 3.3.6). The salt solutions used were;

lithium chloride	~ 11% RH
potassium acetate	~ 22% RH
magnesium chloride	~ 33% RH
potassium carbonate	~ 43% RH
magnesium nitrate	~ 54% RH
sodium chloride	~ 76% RH
potassium chloride	~ 87% RH

After one weeks equilibration time, the samples stored for moisture isotherm determination were weighed and the moisture isotherm was calculated using the dried sample (P_2O_5) and the sample equilibrated over magnesium chloride (0.33 a_w). Under these conditions the rate of amorphous lactose crystallisation is negligible. The amorphous lactose content was determined using the additive isotherm method (see

Section 3.3.6). This analysis showed that 4% amorphous lactose was produced in the milling process. These results can be seen in Figure 5.12.

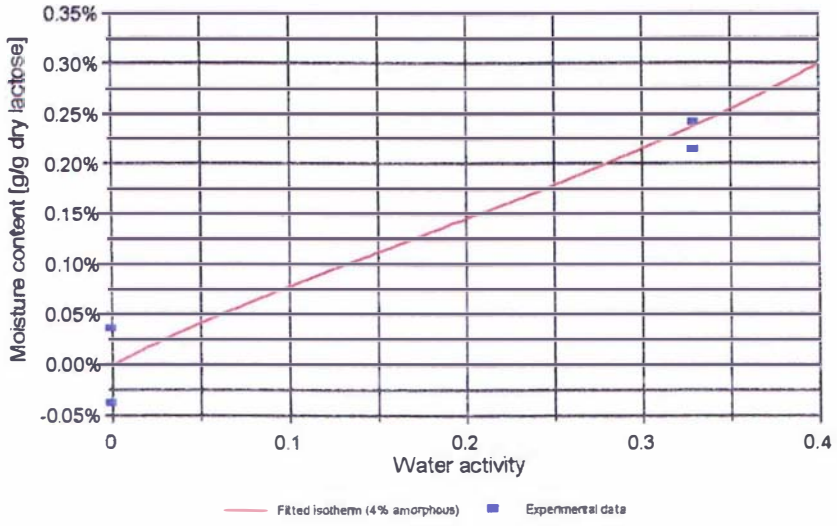

Figure 5.12 - Additive isotherm method for quantification of amorphous lactose content of freshly milled lactose sample.

After one week's equilibration time, the remaining samples were tested for strength using the multi-point penetrometry method. Figure 5.13 shows the results compared with the strength of liquid bridged purely crystalline lactose material after ten days equilibration time (from Section 5.5.2).

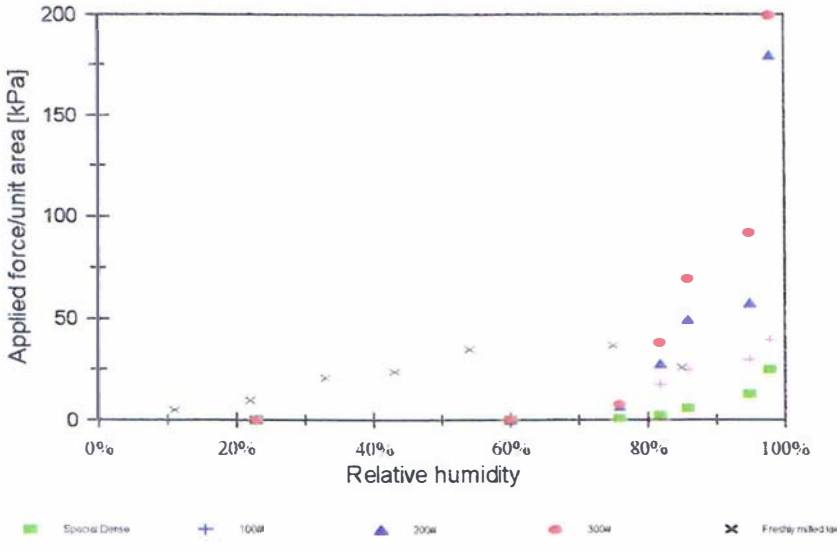

Figure 5.13 - Freshly milled lactose strength compared with purely crystalline powder strength stored over saturated salt solutions for one week.

This graph demonstrates that there is some extra strength in the freshly milled lactose samples compared with the conditioned powders. In the week's equilibration time, the samples equilibrated above 0.45 a_w crystallised and thereby released moisture. The samples below this value were all below the glass transition temperature. It is difficult

therefore to explain why the low water activity samples showed greater strength than the conditioned lactose samples. One possible explanation is that fast adsorption of moisture to the surface of the amorphous layer could have occurred during transfer of the powder to the petri dishes. This could have enabled sticking of the particles before storage above the salt solutions.

Because the glass transition temperature was not exceeded in these samples the amorphous lactose surface would not have been capable of flow, and therefore amorphous bridging should not have occurred. If amorphous lactose flow and crystallisation, did occur in the samples containing 4% amorphous lactose, it would have been expected to see a dramatic increase in strength at approximately 0.5 a_w. No such change was observed.

It should be noted that even though the amorphous lactose containing samples showed greater strength than the crystalline samples, the strength measured was not high. No sample showed any signs of bulk powder strength. There was no signs of lumping or caking in the samples. This can be seen more clearly if the results are plotted with the measured strengths of lactose samples equilibrated for fifty days as shown in Figure 5.14.

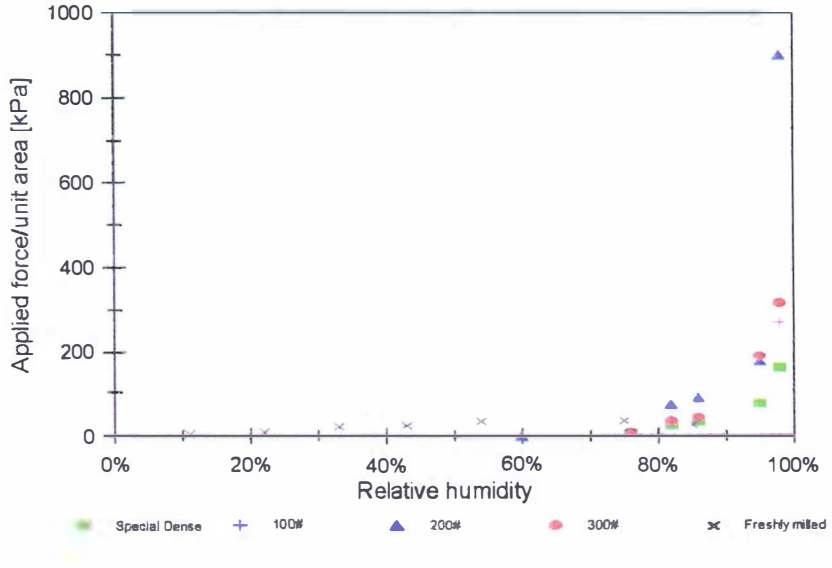

Figure 5.14 - Strength of freshly milled lactose compared with strength of crystalline lactose stored for fifty days over saturated salt solutions.

It is clear from this graph and Table 5.1 which shows a qualitative description of the scale of the multi-point penetrometry method, that no significant strength occurred due to amorphous lactose flow in conditions above the glass transition temperature. This finding is consistent with that reported for freshly milled icing sugar by Roth (1976).

This suggests that the role of amorphous lactose in the occurrence of caking in bulk lactose is due to increasing the moisture holding capacity of the powder and the subsequent release of this moisture if crystallisation proceeds. Roth (1976) also concluded that amorphous sucrose influences caking phenomena in icing sugar by this mechanism. This may be due to the amorphous sugar layer being too thin for flow to occur toward the inter-particle contact points.

5.6.4 Relevance of Amorphous Lactose to Caking in Bulk Lactose

It has been shown that there was a small increase in strength due to the presence of amorphous lactose. This extra strength was not significant with respect to lump formation or obvious signs of caking. If these strength measurements are compared with samples exhibiting even weak lumps, they become insignificant. This suggests that amorphous lactose flow does not contribute to caking in bulk lactose in the low amorphous lactose content range.

Amorphous lactose is important, because of its moisture binding ability and the possible release of this moisture if conditions are favourable for crystallisation. This will cause high local moisture contents which result in lumping by liquid bridge formation as described in Section 5.5. This moisture will be free for diffusion into other regions of the bulk lactose.

5.7 Closure

This work has showed that the main cause of caking is due to the formation of inter-particle crystalline bridges. Such bridges give the powder significant strength. These crystalline bridges occur though the formation of liquid bridges which have intermediate strength. Over time, the strength of these bridges increase dramatically. The mechanism for this is not clear although it is thought to be due to the dissolution of small inter-particle asperities allowing shrinkage of the bulk powder. This will also result in closer liquid bridges and possibly the formation of crystalline bridges due to the growth of larger crystals in the region of the liquid bridge. This mechanism is a function of the geometry and packing of the particles and is too complex to allow accurate modelling Such modelling was not required to achieve the purpose of this work.

The one day liquid bridge strength, although not high, is an indicator of the future formation of caked product if high water activity conditions are maintained. As a general rule, product with a water activity greater than 0.9 a_w is at high risk.

Amorphous lactose is important with respect to moisture binding and release during crystallisation and therefore was be included in the transport model to allow investigation into possible ways to avoid caking in industrial applications. The next chapter outlines the inclusion of these caking mechanisms into the overall transport model.

CHAPTER 6

PREDICTION OF CAKING IN BULK LACTOSE

6.1 INTRODUCTION

Chapter 4 outlined the development of the transport model describing the migration of moisture as a result of an imposed temperature gradient. With this model, good predictions for temperature and surface relative humidity profiles were achieved. Chapter 5 outlined experimental results characterising the conditions at which the mechanisms of caking by either liquid bridging or amorphous lactose flow can occur.

This chapter summarises the work in which the transport model and the conditions required for caking were coupled together. In this way, an overall model describing caking caused by temperature gradients was achieved. This is discussed at first with respect to purely crystalline lactose powders and then extended to the case where amorphous lactose is present.

6.2 CAKING IN PURELY CRYSTALLINE LACTOSE POWDERS

6.2.1 OVERVIEW OF CAKING IN CRYSTALLINE LACTOSE

Caking in crystalline lactose with no amorphous lactose present, occurs through the formation of liquid bridges. This was discussed in detail in Section 5.5 above. After one day, powder samples subjected to high relative humidity conditions (>85 %RH) showed significant strength using the multi-point penetrometer measurement method. Further equilibration for up to fifty days resulted in increased strength.

It was shown in the transport model validation experiments that such conditions could be achieved locally in product with a water activity of greater than 0.6 a_w when a 20°C/100mm temperature gradient was applied for 13 hours. This section outlines the prediction of bulk strength profiles through a lactose slab when a temperature gradient is applied.

6.2.2 INCLUSION OF STRENGTH PREDICTION INTO THE TRANSPORT MODEL

The transport model describing moisture migration due to temperature gradients, developed in Chapter 4, was modified to include the prediction of bulk powder strength. As discussed in Section 5.5.2, it is evident that bulk powder strength is a function of the

moisture content and geometry of the powder system. The strength measurement using the multi-point penetrometry apparatus for samples equilibrated in varying relative humidity conditions for one day, showed strength to be an approximately linear function of moisture content.

As the storage time increased, the measured powder strength also increased. No clear trend was observed for the rate of strength increase although this is thought to be due to the dissolution of small asperities in the powder allowing the shrinkage of the bulk powder and a corresponding reduction in inter-particle separation distance with the possible formation of small crystalline bridges. Such behaviour is dependent on the packing properties of the powder and particle size distribution. Increased pressure due to bag stacking might also be an important parameter in this phenomena. Such considerations are beyond the scope of this work although in spite of these phenomena, it can be seen that the one day strength profiles were due to liquid bridging, and lumping was observed. Even though these samples showed relatively weak strength (40-50 kPa.), the one day strength measurements can be used as an indication of serious caking problems, especially if the conditions causing the liquid bridges are maintained for long periods of time.

To allow the prediction of lumped lactose strength in the transport model, the simple correlation between liquid bridge strength and moisture content outlined in Section 5.5.2 was used. This equation was shown as Eq(5.3) in the previous chapter and represents an a generalised strength relationship for all lactose powder grades. With this relationship included as part of the transport model, the strength profile within the slab was able to be predicted. The time taken for the development of significant bulk powder strength was also able to be assessed.

A typical profile for the onset of liquid bridging due to the migration of moisture from the hot surface to the cold region under a temperature gradient is shown in Figure 6.1.

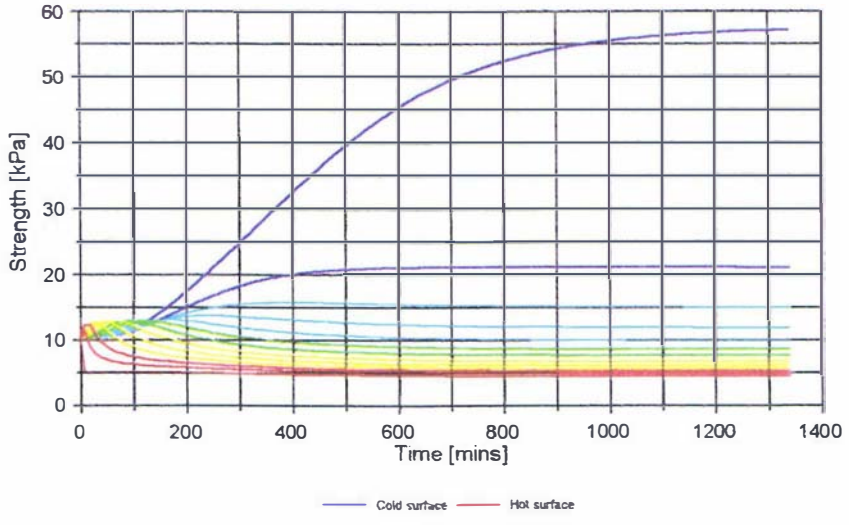

Figure 6.1 - Typical strength development in a 100 mm lactose slab subjected to a 20°C temperature gradient.

Because the strength of the powder was modelled as a function of the lactose moisture content, it can be misleading to interpret the flattening out of the surface relative humidity profile as the reaching of steady state conditions. At high water activity

conditions a very small change in relative humidity will result in a large change in product moisture content. This corresponds also to a large change in bulk powder strength. This is evident in Figure 6.1 by the long time required to reach constant strength. Apparent constant surface relative humidity predictions for this simulation were achieved after 1000 minutes.

Each line on the graph represents 4 mm depth into the slab. This shows that the gradient of strength across the slab is very steep on the cold surface. This feature can be seen more clearly in Figure 6.2.

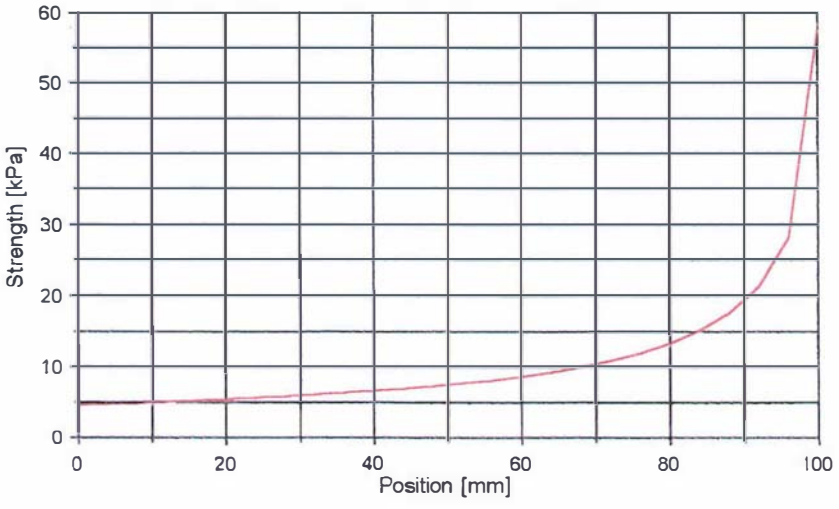

Figure 6.2 - Typical strength profile through lactose slab at steady state when a 20°C gradient has been applied.

6.2.3 EXPERIMENTAL DATA COLLECTION

The addition of strength predictions into the transport model was evaluated by comparison with experimentally measured strength profiles though a lactose slab. It was not possible to measure the strength profile though the slab as a function of both time and position due to the destructive nature of the strength measurement technique. Because of this, the strength profile was measured after steady state had been reached.

Several slab experiments were conducted using 100, 200 and 300 mesh grade lactose. The initial water activities of these products were greater than 0.6, indicating the absence of amorphous lactose in the samples. The lactose slab was allowed to equilibrate for 2-3 hours to ensure a uniform moisture and temperature initial condition throughout the slab. A temperature gradient was then applied across the slab in the same manner described in Section 4.3.2 for the transport model validation experiments, ensuring the cold surface was uppermost to allow strength measurements to be conducted. The temperature and surface relative humidity profiles were recorded using a FIX data logging station.

Once steady state had been reached, the apparatus was disassembled. The multi-point penetrometer was then used to measure the powder strength on the uppermost surface. The measurement was performed in the same manner as that described for strength measurements outline in Section 5.4.4 with the probe positioned into the sample cavity of the transport model validation rig.

Once the surface strength measurement was determined, the lactose was scraped away to a depth of 10 mm using a straight edge. The strength at this level was then measured. This was repeated until it was evident that the powder was free flowing and showed no significant strength.

The steady state strength profiles for 100, 200 and 300 mesh lactose slab experiments for a 100 mm thick slab, are shown in Figure 6.3.

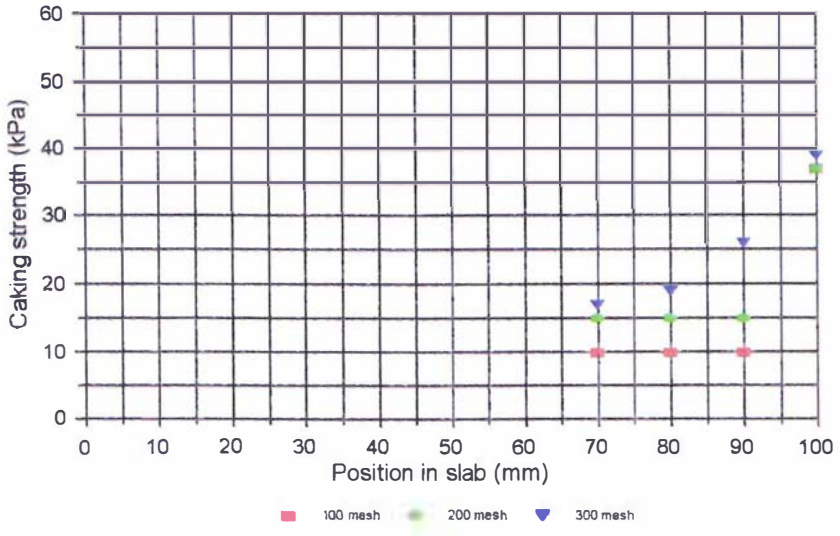

Figure 6.3 - Experimentally measured steady state strength profiles through lactose slabs with applied temperature gradients for approximately 1 day.

Starting water activity, temperature and applied hot and cold surface temperature are given in Table 6.1.

Table 6.1 - Summary of experimental conditions for strength profile measurement of lactose slabs under the influence of a temperature gradient.

Sample	Initial product water activity	Initial temperature	Hot side temperature	Cold side temperature
100 mesh	0.65	17.2 °C	39.2 °C	15.2 °C
200 mesh	0.64	15.5 °C	39.1 °C	15.3 °C
300 mesh	0.62	14.8 °C	39.4 °C	14.5 °C

It can be seen that only the outer 10-20 mm of the slab nearest the cold surface, showed any significant strength. It must be considered that because the depth of the slab has non-uniform moisture content and therefore non-uniform strength, the multi-point penetrometer measurements were an average strength of the first 5-10 mm into which the measurement is being taken. This is particularly significant at the cold surface where the gradient of moisture is very steep.

6.2.4 EVALUATION OF CAKING STRENGTH PREDICTIONS

To test the performance of the model in prediction of strength profiles in the lactose slab, the model was run for those conditions summarised in Table 6.1. The predicted steady state strength profile was then compared against the experimentally determined strength through the lactose slab.

Figure 6.4 shows the comparison between the experimental and predicted strength profiles at steady state.

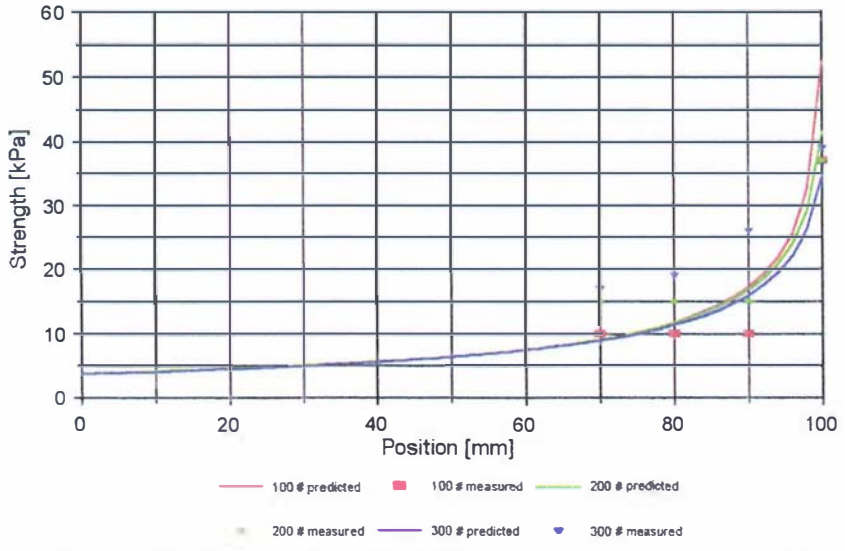

Figure 6.4 - Predicted and experimentally measured strength profiles for lactose slab experiments.

This graph shows the predicted strength approximates the measured strength profiles. Both measures reflect the steep gradient of strength at the cold surface. If further consideration is given to the interpretation of the measured strength profiles as being an average of the strength through the slab as being an average over a depth of 5-10 mm, it can be seen that the model is adequate for describing the onset of lumping by the liquid bridging mechanism. If the lactose is maintained at this level of liquid bridging for long periods (approaching one month), then the phenomena of small asperities dissolving , large crystal growth and bulk density reduction due to shrinkage will result in increased strength in these regions.

If the lactose is dried out by reversing of the direction or removal of the temperature gradient, small solid bridges will occur, of strength at least equal to that of the liquid bridges they formed from (see Section 5.5.3).

Accurate prediction of caking strength due to these phenomena was not pursued in this work because of their complex nature and reliance on characterisation of the geometry and packing arrangement of the particles. In spite of this, the onset of significant caking by this mechanism can be estimated from the magnitude of the liquid bridge strength incorporated into the transport model (>30 kPa). This was used in subsequent work as an indicator of potential caking problems.

6.2.5 INVESTIGATIONS OF CONDITIONS REQUIRED FOR LUMPING IN BULK LACTOSE

With the ability to predict the onset of significant strength in purely crystalline lactose, due to moisture migration caused by temperature gradients, an investigation into the bagging and storage conditions which cause caking was carried out. The effect of slab thickness was investigated by running the model at three different slab thicknesses (100, 200 and 500 mm). The other parameters in the model were maintained constant between simulations. The parameters used were;

slab thickness	100, 200 and 500 mm
initial temperature	20 °C
initial water activity	0.7
cold surface temperature	20°C
hot surface temperature	40°C

All other parameters were those determined in Section 4.5.4.2 for the best estimates obtained in the transport model validation. Figure 6.5 shows the predictions of strength profile for these simulations at steady state conditions.

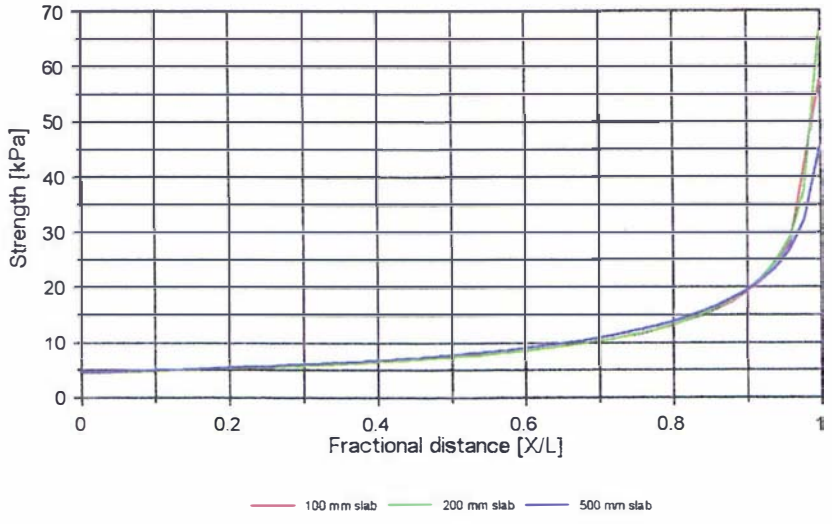

Figure 6.5 - Strength profile for slabs of increasing thickness as a function of the fractional position into the surface.

Figure 6.5 shows that the slab thickness does not significantly alter the shape of the steady state profile through the lactose slab. The increasing thickness does however, result in a correspondingly larger region in the slab where significant lumping caused by liquid bridging occurs. Figure 6.5 shows that the region with significant strength is at a fractional distance of approximately 0.96. This corresponds to a region 4 mm wide in the 100 mm slab, 8 mm in the 200 mm slab and 20 mm wide in the 500 mm slab. Because of the much larger distance over which the moisture migration must occur, the time taken to reach this steady state condition increases proportionally with the slab thickness.

The initial water activity of the product is an important parameter with respect to caking phenomena. Water activity is essentially an indirect measure of moisture and

therefore characterises the total amount of moisture in the lactose system. The effect of varying water activity in the range 0.5 to 0.8 a_w was investigated for the heating of a 20°C lactose slab from one side to 40°C while maintaining the other side at 20°C. Figure 6.6 shows the effect of initial product water activity on the steady state cold surface strength predicted.

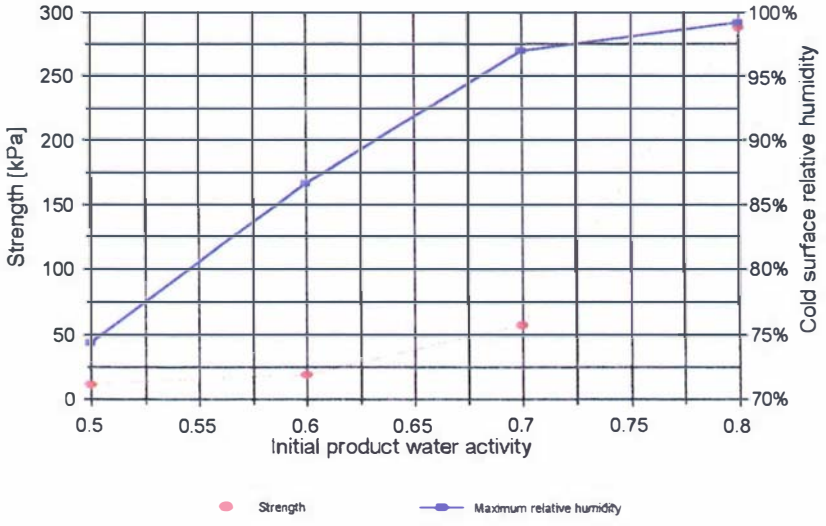

Figure 6.6 - Effect of initial product water activity on cold surface strength and relative humidity.

This analysis shows that for the case of heating the slab a maximum product water activity of 0.65 a_w must not be exceeded if caking problems are to be avoided in bulk lactose exposed to a 20°C temperature gradient for extended periods of time. The case of heating described above is analogous with the situation whereby a lactose bag is heated from some source. An example of this in industry, is the transporting or product by ship through the tropics.

The reverse case is true for the bagging of freshly manufacturing product. Due to drying and milling operations and hot transport air, the product is typically hotter than the storage warehouses where the product is placed post production. This results in the product being slowly cooled. This causes the migration of moisture towards the outside of the bag. An investigation into the critical water activity above which caking problems will result was undertaken for the case of cooling a 40°C lactose slab on one side to 20°C while maintaining the other at 40°C. A typical example of the surface relative humidity profile resulting from a simulation of this type is shown in Figure 6.7. This plot shows that initially a rapid increase in water activity occurs which is caused by the depletion of moisture from the surrounding lactose. After a period of approximately five hours the cold surface relative humidity decreases slightly again until an equilibrium position is reached.

Figure 6.8 shows the steady state relative humidity reached on the cold surface as a function of initial water activity. Also shown on this plot is the maximum relative humidity reached. This plot shows that for the case of application of a 20°C temperature gradient to a cooling lactose slab, an initial water activity of 0.57 a_w can not be exceeded.

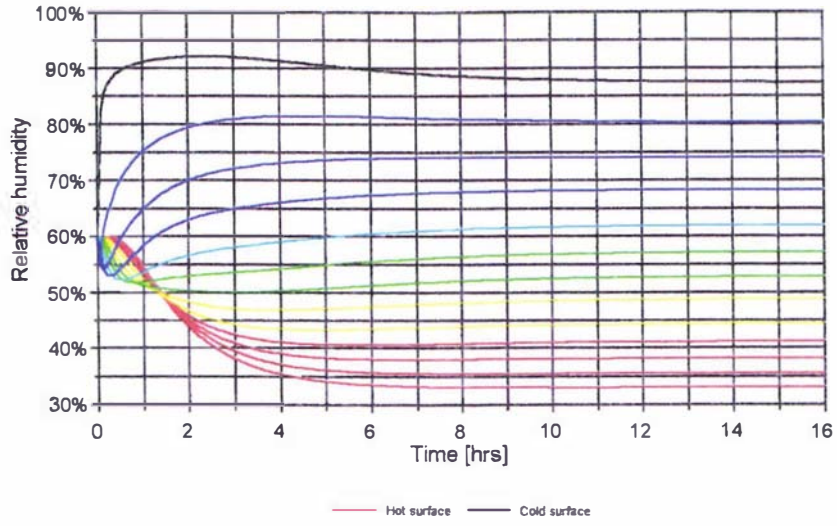

Figure 6.7 - Typical relative humidity profile for the cooling of a lactose slab from one side.

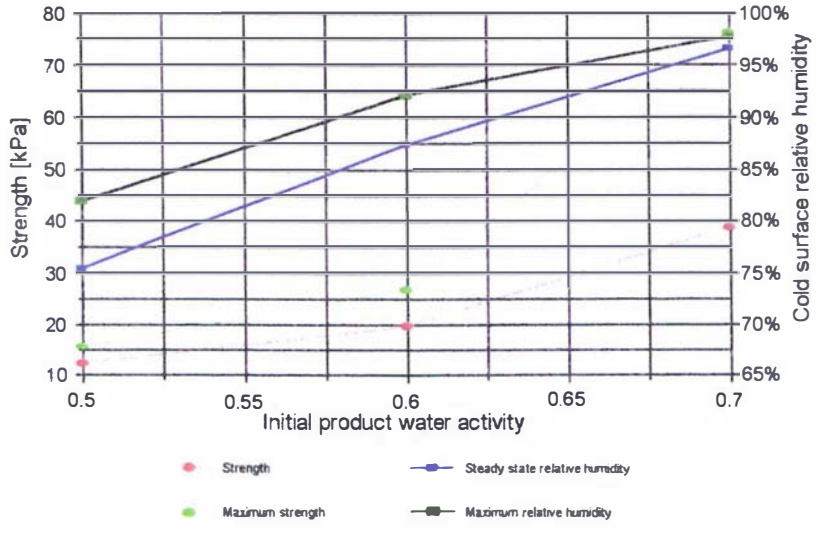

Figure 6.8 - Maximum strength as a function of initial water activity.

The above analyses investigated the effect of 20°C temperature gradients for heating and cooling of the slab from 20°C or 45°C. Investigation shows that heating a slab by 20°C as above but with the initial temperature of 15°C results in very similar strength profiles.

In the cooling of bulk bags of lactose a constant temperature is not maintained indefinitely nor is it a slab. Rather the bag is cooled in three dimensions. This case can be approximated with the transport model if both sides of the lactose slab are set to be colder than the initial lactose temperature. Predictions by this method will be an over prediction of caking, because in the real case the lactose is cooled from up to six sides of the lactose bag. The thickness of the lactose slab will vary depending on the pallet stacking arrangement of the bulk bag. If four bags are stacked together the slab thickness would be approximated by 2 m. If a single bulk bag is cooled then 1 m is the

most appropriate thickness for investigation using the transport model.

Figure 6.9 shows the temperature profile for the cooling of a slab of 1 m thickness from 40°C evenly from both sides to 20°C with an initial water activity of 0.7 a_w.

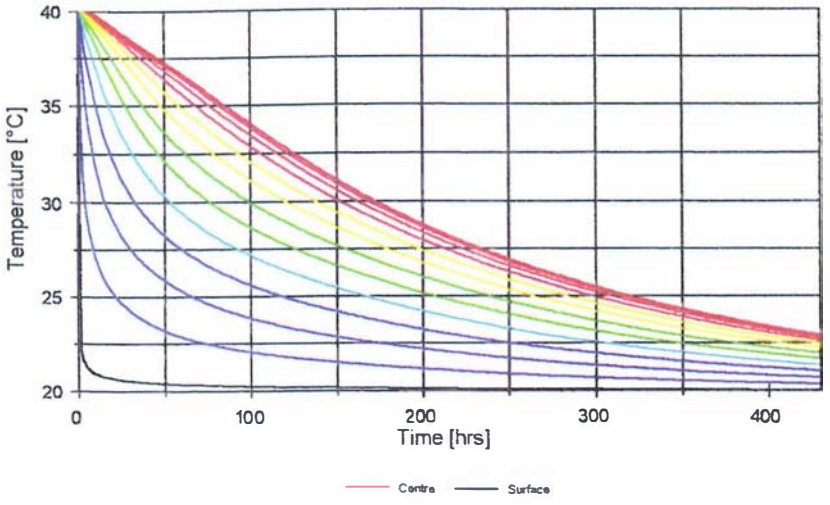

Figure 6.9 - Temperature profile through lactose slab cooled evenly from both sides.

It can be seen from this plot that significant temperature gradients are maintained for approximately 150 hours before the centre of the slab is cooled. Figure 6.10 shows the corresponding change in strength due to liquid bridging within the bag with time caused by the temperature gradient. It should be noted that the true strength of the powder will not decrease with time because the removal of moisture as the temperature gradient subsides will result in the formation of solid crystalline bridges. These solid bridges are as strong or stronger than the originating liquid bridge. Figure 6.10 indicates that in such a case the formation of liquid bridges which are subsequently dried out can occur. To avoid this occurring the lactose should be bagged at a water activity of less than 0.57 a_w.

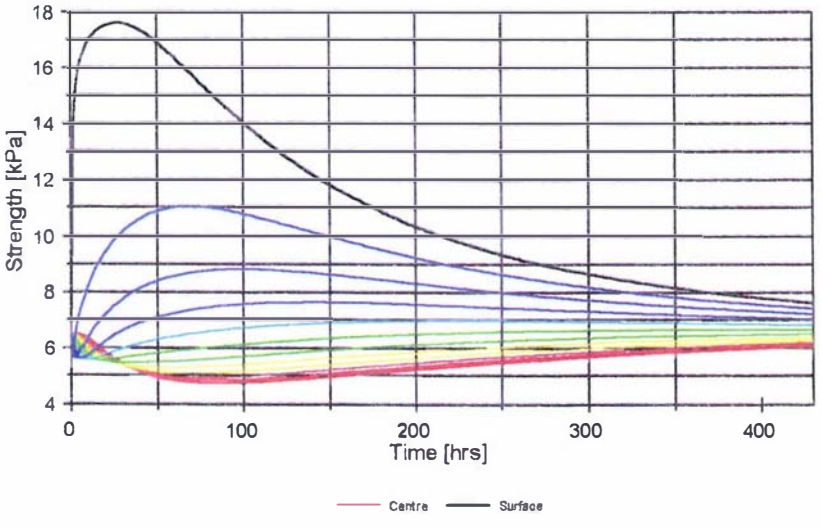

Figure 6.10 - Strength profile though slab cooled evenly from both sides.

6.2.6 Avoidance of Lumping in Purely Crystalline Lactose

The investigations carried out with the transport model have enabled the identification of bagging and storage conditions where lumping and caking by the mechanism of liquid bridging and subsequent drying can occur. It has also been possible to determine criteria for bagging and storage conditions which, if not exceeded, will not cause caking related problems. Caking problems should be avoided if the product is bagged at a water activity below 0.575 a_w, and if temperature gradients of over 20°C are avoided.

In general it is good practice to minimise both the temperature and water activity of the product at bagging. Because of the rapid rate of moisture sorption into crystalline lactose the effect of lowering product temperature must be carefully considered. If the product is in contact with large quantities of air during conveying then the lower temperature will result at the cost of increased product water activity. If a compromise must be made between lowering water activity or temperature, then greater weighting should be given to lowering the water activity as this has the greatest impact on the cause of caking problems.

6.3 Caking in Freshly Milled or Dried Lactose Containing Amorphous Lactose

6.3.1 Overview of Requirements for Amorphous Lactose Related Caking

In Section 5.6 it was shown that significant caking strength is not caused by the flow of the amorphous lactose surface in conditions where the glass transition temperature is exceeded. This does not mean the presence of amorphous lactose is unimportant with respect to caking phenomena. The total amount of free moisture present in a powder containing amorphous lactose can greatly exceed the free moisture present in a purely crystalline lactose sample. This extra moisture binding capacity was discussed previously in Section 3.3.6 and was shown graphically as Figure 3.9. The additive moisture sorption isotherm was added into the transport model so the effect of the amorphous lactose on the rate and extent of moisture migration within the bulk lactose could be predicted.

If the moisture migration through bulk lactose results in local conditions that exceed the glass transition temperature, crystallisation will proceed. The rate of crystallisation is a function of the difference between the temperature and the glass transition temperature of the amorphous matrix. The crystallisation kinetics have been studied as part of this work and were discussed in more detail in Section 3.7.4. Because the amorphous form of lactose can hold much more moisture than the crystalline form, moisture will be released upon crystallisation. The amount of moisture released will vary depending on the product of crystallisation. To assess the impact of crystallisation on caking propensity, the kinetics of crystallisation and the associated release of moisture were added to the transport model.

Details of how the moisture relations and crystallisation kinetics were included in the transport model are given in the next section.

6.3.2 MODIFICATIONS TO THE TRANSPORT MODEL TO INCLUDE THE EFFECTS OF AMORPHOUS LACTOSE

In the range of amorphous lactose fractions present on freshly milled or dried crystalline α-lactose mono-hydrate produced commercially (0-6%), the thickness of the amorphous lactose surface layer was calculated to be between 0 to 0.6μm. The time for sorption has been estimated at up to 20 to 30 seconds (see Section 3.4.3). As the time scale is small compared to that for moisture migration and heat conduction in the bulk lactose, the assumption of instantaneous moisture adsorption is valid for powders containing small amounts of amorphous lactose on the surface.

The local moisture content of the combined crystalline and amorphous particle was determined using the additive moisture sorption isotherm developed in Section 3.3.6. This can be summarised as Eq (6.1).

$$M = M_{crystalline} + a M_{amorphous} \tag{6.1}$$

where $M_{crystalline}$ and $M_{amorphous}$ are the moisture contents of the purely crystalline and amorphous lactose fractions given by Eqs (3.2-3.4) and Eq (3.9) respectively and a represents the amorphous lactose fraction. The transport model describes the change in the total amount of free moisture contained at any position in the lactose slab (see Eq 4.11). The distribution of this moisture between the solid and gaseous phases was obtained iteratively using Eq (6.1) above.

The differentiated form of the Avrami equation (Eq 3.28) was used to describe the rate of crystallisation in the amorphous component of the lactose particle. The Avrami equation rate constant (K), is a function of (T - T_g) and is given by Eq (3.32). The parameters used were $C_1 = 3.54\times10^4$, $C_2 = 108.4$, $C_3 = 3\times10^{27}$ and n=3. The equation was then solved at each time step using simple Euler numerical integration at each node of the lactose slab. The initial crystallinity of the amorphous layer was set to a small number (10^{-16}) to allow the onset of crystallisation once favourable conditions were achieved.

As the crystallinity of the amorphous layer increases, the amount of amorphous lactose and hence the moisture binding capacity of the combined particle is reduced. The amount of moisture released depends on the crystallisation product. This is discussed in detail in Section 3.7.4.1. For the modelling of amorphous lactose crystallisation in a lactose slab under the influence of a temperature gradient, both extremes were considered. Simulations were performed assuming an anhydrous β-lactose product as well as simulations assuming α-lactose mono-hydrate as the product of crystallisation. In both cases it was assumed that the moisture released was uninhibited and was redistributed evenly between the solid and gaseous phases.

6.3.3 THE EFFECT OF AMORPHOUS LACTOSE MOISTURE BINDING CAPACITY ON MOISTURE MIGRATION

Figure 6.11 shows predictions of the effect of changing amounts of amorphous lactose on the rate of moisture migration.

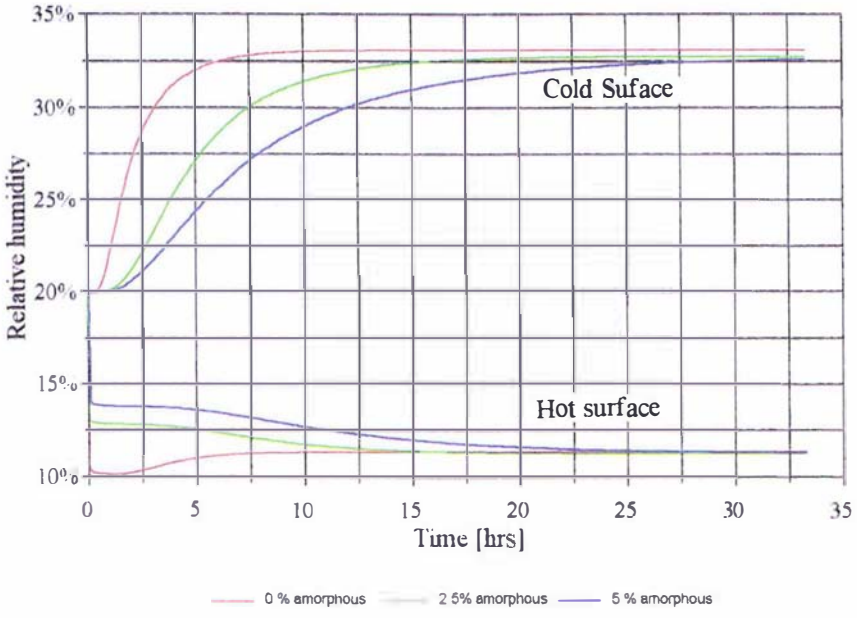

Figure 6.11 - Comparison of moisture migration rates for increasing amorphous lactose fractions.

In each case the starting water activity of the lactose slab was set to 0.25 a_w and the temperature was initially 20°C. One surface was maintained at 20°C and a step change to 40°C was applied to the other surface. These conditions were chosen so that no position in the slab ever reached conditions conducive to significant amorphous lactose crystallisation.

It can be seen from Figure 6.11 that the steady state water activity on both hot and cold surfaces are similar between simulations for varying amounts of amorphous lactose present. The rate that these steady state conditions are reached is notably different however. The increased binding capacity of the amorphous lactose slows the rate that steady state is reached. This is because more moisture must be transported to achieve a given change in surface water activity if amorphous lactose is present. This is a function of the shape of the combined crystalline and amorphous lactose moisture sorption isotherm.

It is evident from these results that the rate of moisture migration though a lactose slab under the influence of a temperature gradient is markedly effected by the amount of amorphous lactose present. It may be possible to exploit this behaviour and use it as the basis for a amorphous lactose fraction measurement method. To use the model to quantify the amount of amorphous lactose present, the moisture sorption isotherm data for both crystalline and amorphous lactose would have to be more accurately determined. Another approach might be to calibrate the technique against known lactose

samples. This method might offer advantages over the other techniques such as shorter measurement times than the additive isotherm method, cheaper than NMR and avoidance of crystallisation phenomena which are not known well enough to allow quantification of amorphous lactose using the controlled crystallisation method. Further research on the feasibility of this method is left for subsequent investigations.

6.3.4 Predictions of Moisture Transport with Amorphous Lactose Crystallisation

As discussed above, the prediction of crystallisation phenomena in the lactose slab will depend on the product of crystallisation. If β-lactose is formed, then all of the moisture associated with the amorphous fraction will be made available when crystallisation proceeds. If α-lactose mono-hydrate is formed, then large amounts of moisture will be bound as water of crystallisation (5% w/w) and therefore the total amount of free moisture in the system will be reduced. It is likely that some combination of these two extremes occurs in practise depending on the conditions of crystallisation. A more detailed discussion on crystallisation product was given in Section 3.7.4.1. The mechanism of solid state conversion of β-lactose to the α-lactose mono-hydrate crystal form was outlined in Section 3.7.4.2.2.2, and is likely to be significant at high water activity conditions.

The modelling of amorphous crystallisation in the bulk lactose slab described in this work was limited to the case of the formation of either α-lactose mono-hydrate or β-lactose product. No subsequent conversion of the β to α crystal forms was included into the model. While these assumptions over simplified the real phenomena occurring in the lactose slab, they represent the extremes of what can occur. In this way they were used to offer insight into how amorphous lactose contributes to caking in bulk lactose.

6.3.4.1 Crystallisation to anhydrous lactose product

The model was run for the case where all the moisture contained within the crystallising amorphous lactose was released into the surrounding bulk of the lactose powder. The amount of moisture contained within each node was calculated as described in Chapter 4. The difference was that the distribution of moisture between the solid and gaseous phases could change as crystallisation processed. The new crystallinity of the amorphous layer was calculated using the Avrami equation and the fraction of amorphous lactose remaining was used to calculate the new moisture sorption isotherm using the additive isotherm model. This was used to determine how the moisture contained in the node was distributed between the solid and gaseous phases.

Figure 6.12 shows predictions of what occurs in the lactose slab for a starting water activity of 0.35 a_w and with 2.5% amorphous lactose present on the surface of the lactose crystal. It can be seen from this figure that for the first 16 hours the relative humidity profiles are similar to that predicted from simulations where crystallisation did not occur. When the cold surface relative humidity reached 55%, crystallisation began to proceed. The model predicted a rapid release of moisture which caused a snowball effect to occur. This released moisture was then able to diffuse back through the slab causing more amorphous lactose to crystallise. Once all of the amorphous lactose had

crystallised, moisture migration occurred in the then completely crystalline lactose bed until a new equilibrium was reached. It is clear from Figure 6.12 that the overall water activity of the resulting product is much greater than the average starting water activity.

Figure 6.13 shows the prediction of relative humidity for a simulation using the same conditions as above but with a starting water activity of 0.25 a_w. This plot shows crystallisation did not occur in the time frame studied as the water activity did not reach a high enough level. The steady state cold side water activity of 0.45 a_w shown would be expected to crystallise in approximately 36 days. This would mean that crystallisation could still occur in an industrial product bagged at 0.25 a_w during storage and transport if the temperature gradient is maintained for extended periods of time. It is unlikely that temperature gradients would be maintained for this length of time.

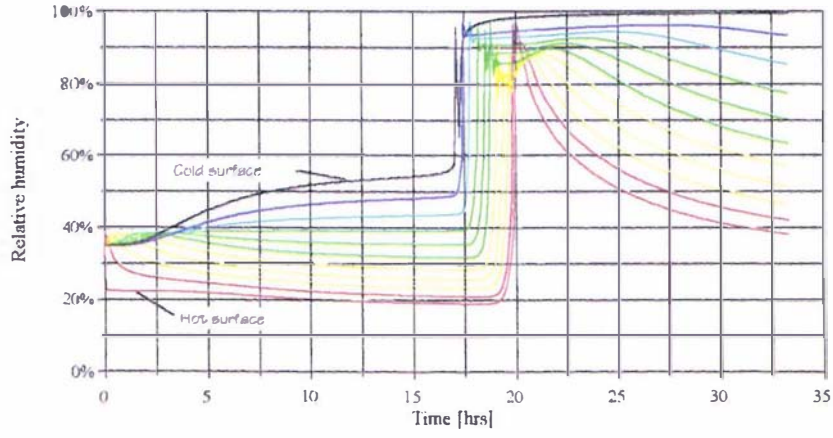

Figure 6.12 - Prediction of moisture transport with crystallisation for powder containing 2.5% amorphous lactose at 20°C after subjection to a 20°C temperature gradient.

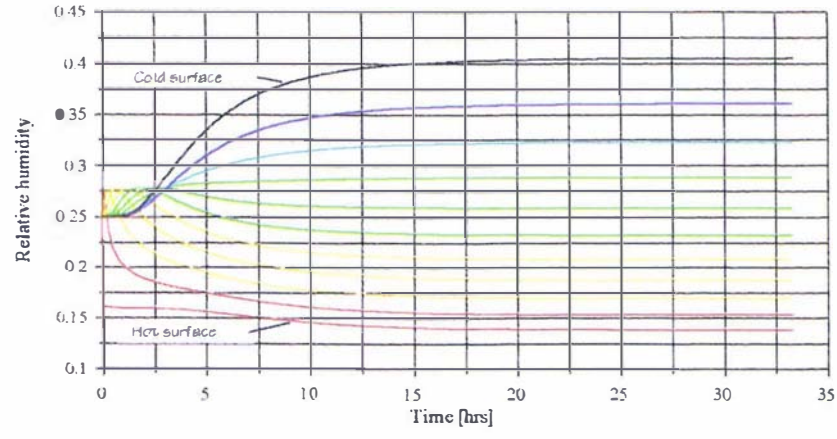

Figure 6.13 - Moisture migration in a lactose slab starting at a water activity of 0.25 a_w showing no signs of amorphous lactose crystallisation.

6.3.4.2 CRYSTALLISATION TO α-LACTOSE MONO-HYDRATE

The model was modified so that as the amorphous fraction underwent crystallisation, free moisture was removed from the system, being bound as crystal water. This was achieved by including a term for the uptake of bound water, as crystallisation proceeds into the moisture transport equation (Eq 4.11) resulting in;

$$\frac{\partial W}{\partial t} = D \epsilon V \frac{\partial^2 (H \rho_a)}{\partial x^2} - 0.0526 \rho_s V \frac{\partial a}{\partial t} \qquad (6.2)$$

where the water of crystallisation is 0.0526 kg water/kg amorphous lactose crystallised. The distribution of the water (W) between the solid and gaseous phases was the same as outlined above for crystallisation to an anhydrous product above. The rate of change of amorphous lactose content was estimated using the Avrami equation (Eq 3.26).

Figure 6.14 shows predictions of what occurs in the bulk lactose under the same conditions as used to generate Figure 6.12 but for α-lactose Mono-hydrate as the crystallisation product.

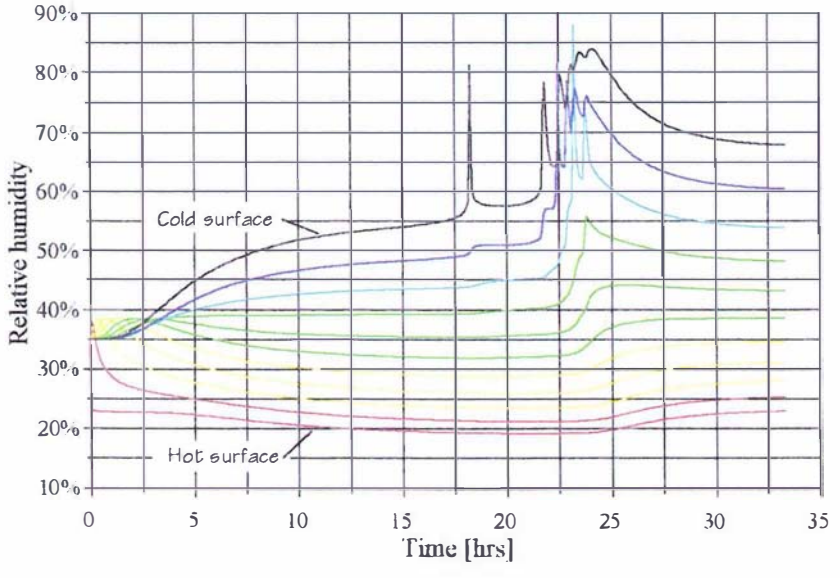

Figure 6.14 - Moisture migration with amorphous lactose crystallisation to α-lactose Mono-hydrate.

It can be seen from Figure 6.14 that the result is similar to that predicted for crystallisation to an anhydrous product. Crystallisation and moisture release proceeded when the cold surface water activity reached 0.55 a_w. Because some of the free moisture associated with the amorphous lactose was bound, the extent of moisture release was not as marked as that predicted for an anhydrous product. This reduction in the amount of free moisture occurred to such an extent that not all positions through the lactose slab reached a high enough water activity to allow crystallisation. This resulted in a steady

state position being reached where amorphous lactose was still present on the hot surface of the slab. This can be seen in Figure 6.15 which is a plot of steady state amorphous lactose content as a function of position through the lactose slab

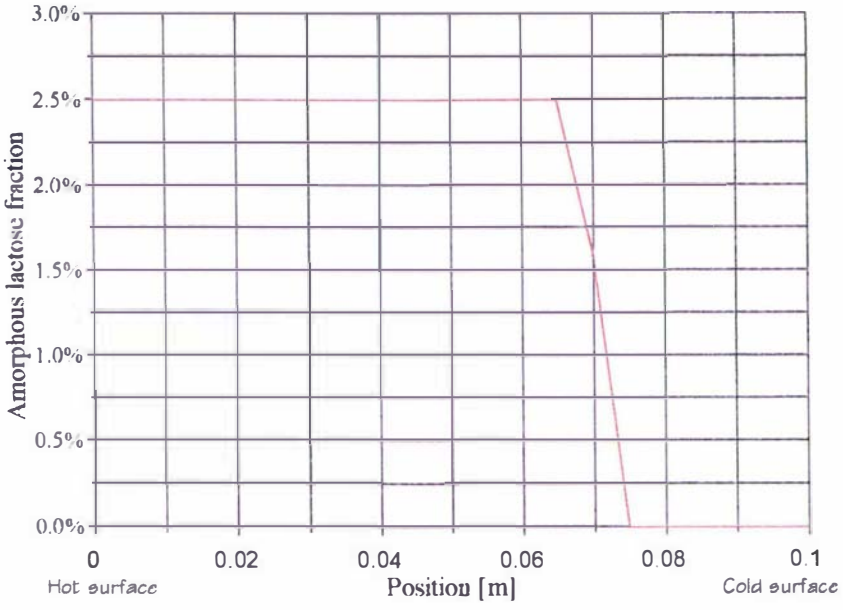

Figure 6.15 - Steady state amorphous lactose fraction profile through the lactose slab.

6.3.5 EXPERIMENTAL VALIDATION

Before the model could be used to make inferences on the impact of amorphous lactose on caking phenomena, the model was tested against experimentally collected data. To achieve this it was first necessary to obtain approximately 10 kg. of lactose powder which contained 2-5% amorphous lactose. This was achieved by milling 80 mesh product in a hammer mill. Figure 6.16 shows the hammer mill arrangement used.

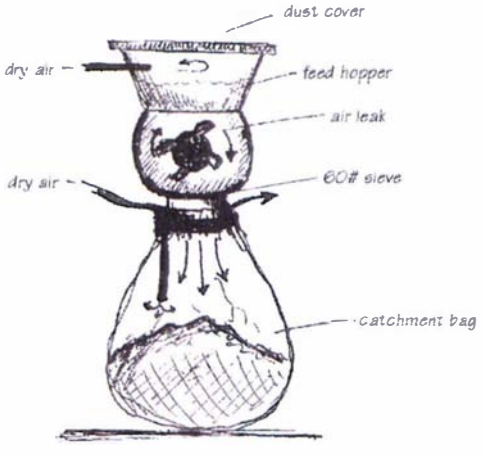

Figure 6.16 - Hammer mill arrangement.

The lactose material was added to the mill in batches and the top of the feed hopper sealed to eliminate the spreading of dust. Dry air was introduced into the feed hopper to help cool the mill and avoid moisture adsorption into any amorphous lactose produced in the mill. To escape the mill, the lactose had to pass through a 60 mesh screen. It was found that milling to this degree was sufficient to produce amorphous lactose in the desired range. Finer screens produced a much finer product but the extra milling resulted in the product heating up in the mill to a level where amorphous lactose crystallisation could potentially occur. The long time required for milling to a very fine powder was also inhibitory.

The milled lactose was caught in a plastic bag which was taped to the mill exit. An air stream was introduced to help cool the product and keep the water activity of the product at a low level. A relative humidity probe (Hycal) was used to monitor the relative humidity in the catchment bag to ensure conditions conducive to amorphous lactose crystallisation were not permitted. More details can be found in O'Donnell (1997) as the initial setting up of the mill was completed as part of his research.

Using this milling arrangement it was found that a product with water activity of approximately 0.2 a_w could be produced. Several batches of product were milled over a period of three days, providing the 10 kg. of lactose needed for the model validation experiment. Each of these batches were combined into a large plastic liner and mixed thoroughly.

The lactose was then quickly loaded into the slab experimental apparatus outlined in Section 4.5.3.1 using the 78 mm slab thickness. The water activity of the lactose was 0.2 a_w as indicated from the top and bottom surface relative humidity probes. A preliminary model simulation using the proposed experimental conditions showed that even under a 30°C temperature gradient, significant amorphous lactose crystallisation was not expected to occur. To allow crystallisation to proceed, the initial water activity of the product was therefore raised to 0.3.

Figure 6.17 shows how this was achieved using the experimental slab apparatus.

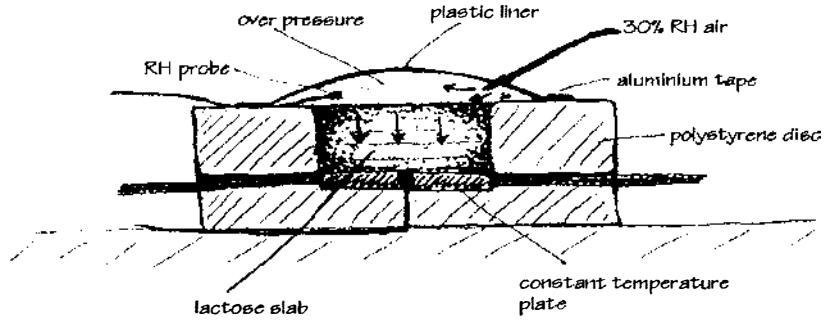

Figure 6.17 - Method used to raise water activity of lactose slab.

A plastic film was taped to the top of the exposed lactose slab. A supply of air was then introduced through the liner and a slight over pressure was applied. This promoted a slow permeation of air through the lactose slab. The air supply was maintained for approximately 4 days until the top and bottom surface relative humidity measurements were equal.

The 30% relative humidity air stream was provided by bubbling air through a series of water columns at approximately 3 atmospheres absolute pressure. In such an apparatus the air reaches saturation ($p_v = p_w$). When the air then passes through a pressure regulator thus dropping the pressure to 1 atmosphere absolute, the vapour pressure (p_v) drops to one third of the saturated vapour pressure (p_w). This results in an air stream controlled at approximately 33% relative humidity. This means that by adjusting the pressure of the air supplied to the water columns, any desired relative humidity air stream could be achieved. A schematic diagram of the apparatus is given as Figure 6.18.

The device used in this work was designed and built for use in fruit weight loss experiments (see McGuire 1997).

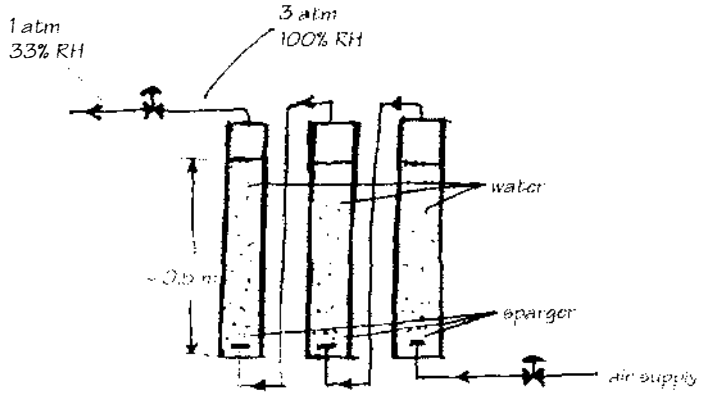

Figure 6.18 - Schematic of rig used to provide constant RH air

Once the water activity of the lactose powder was raised to approximately 0.3 a_w, as described above, samples were taken and the amorphous lactose fraction measured using the two point moisture sorption isotherm method described in Section 4.5.3.1. The top surface to the slab apparatus was replaced and the contents were left to equilibrate for one day to ensure uniform water activity and temperature through the lactose slab.

A temperature gradient was applied across the lactose slab by pumping water at 50°C through the bottom plate from a water bath, while running tap water through the top plate at a constant temperature of 15°C. The temperature profiles through the slab and the relative humidity of each surface were recorded using a FIX data logger work station. Figure 6.19 and Figure 6.20 show the temperature and surface relative humidity profiles for the lactose slab

Once the surface relative humidity reached steady state, the apparatus was disassembled. Samples were taken from the top and bottom surfaces as well as midway

through the slab. These samples were tested for amorphous lactose fraction using the two point moisture sorption isotherm method. It should be noted that in obtaining these samples, it was not possible to gather sufficient powder at exactly one depth. Rather each sample was an average of material covering approximately 10-15 mm of the lactose bed.

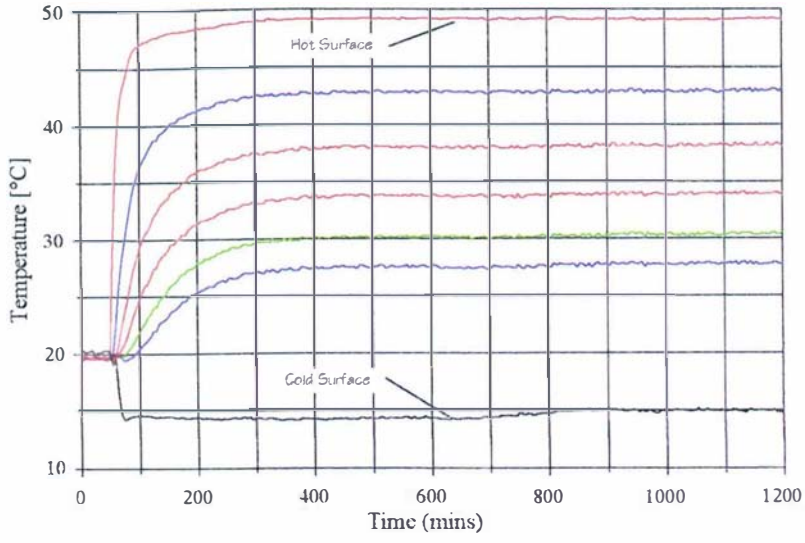

Figure 6.19 - Experimental temperature profiles for 78 mm lactose slab containing 4.5% amorphous lactose.

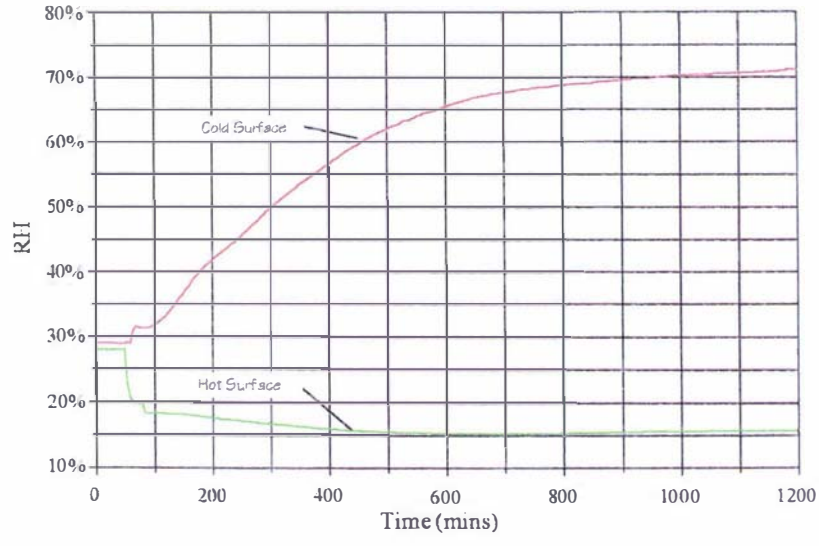

Figure 6.20 - Experimental surface relative humidity profiles for a 78 mm lactose slab with 4.5% amorphous lactose initially present.

The two point moisture sorption isotherms for these samples are shown as Figure 6.21. These measurements show that 4.5% amorphous lactose was present on the lactose prior to commencement of the experiment. There was good agreement between replicates for these samples.

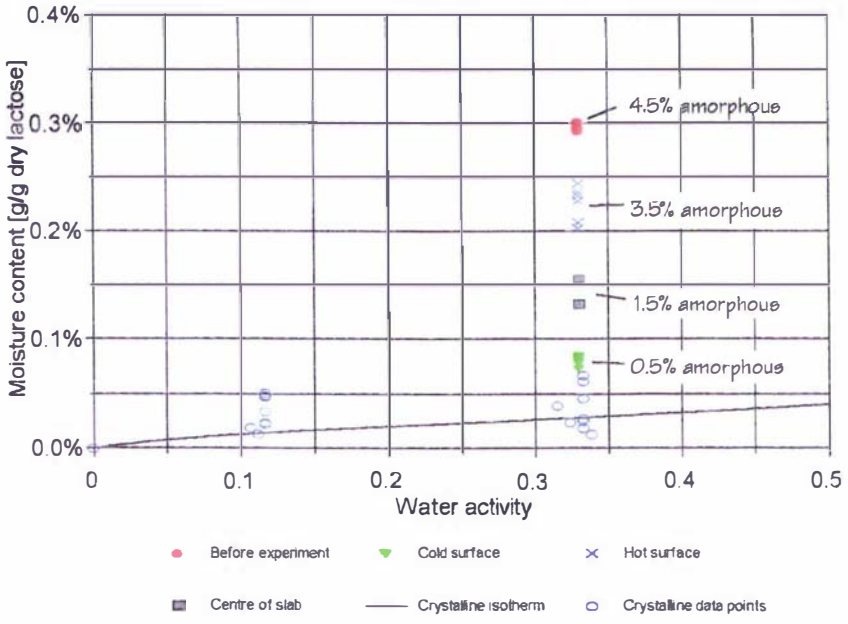

Figure 6.21 - Two-point isotherm results for lactose samples taken before and after the slab experiment.

After the experiment, the amount of amorphous lactose present at the cold surface was reduced. This is demonstrated by the fact that the amount of free moisture that could be held by the lactose at 0.33 a_w was much lower than that observed for the lactose samples analysed prior to the experiment. The moisture content measured at this water activity is slightly higher than the isotherm value for purely crystalline lactose also shown on the plot. This can be explained in two ways. There is some scatter in the purely crystalline isotherm data. This scatter could include the isotherm points measured for these samples. Alternatively, the apparent difference in moisture content could be due to the fact that the samples were taken as an average of the material present in the first 10-15 mm of the lactose surface. It is possible that some of the powder at lower depths still contained small amounts of amorphous lactose even if the top surface was completely crystalline. Either way, the results clearly show that there was amorphous lactose present before the experiment which was absent after the experiment was completed. This result is reinforced by the fact the cold surface relative humidity reached 73% at which amorphous lactose is most unlikely to be stable.

The hot surface amorphous lactose content measurements show that 3.5% amorphous lactose is present after the experiment was completed. It is unlikely that any crystallisation occurred in the conditions that this surface experienced. The glass transition temperature for amorphous lactose at a water activity of 0.2 a_w is 55°C as given from Figure 3.19. This means that the glass transition temperature was never exceeded and so crystallisation should never have occurred at this surface. Using Figure 3.31 and Figure 3.19 it was calculated that for crystallisation to occur in the time frame

studied (20 hours) then the water activity of the product must exceed 0.35 a_w at 50°C. It follows that while crystallisation was unlikely to have occurred at the hot surface itself, it is conceivable that limited crystallisation could have occurred just in from the hot surface. This could explain the apparent decrease in amorphous lactose content because the sampling included a range of depths of up to 15 mm from the hot plate.

The samples taken from the centre of the slab indicate that approximately half of the amorphous lactose originally present on the powder surface was crystallised during the course of the experiment.

It is interesting to note that while it is definite that amorphous lactose crystallisation has taken place in the lactose slab, there is no evidence of the rapid increase in surface relative humidity predicted by the model assuming either a hydrous or anhydrous crystallisation product. Reasons for this are discussed subsequently, after direct comparisons between the model and experimental conditions are presented.

6.3.6 Model Prediction Accuracy

The collected experimental data was compared against the transport model predictions. The temperature data for both surfaces were saved as text files and used to represent the temperature history for the surface nodes in the model. This accounted for the slight variations in plate temperature and the gradual change in plate temperature that occurred at the start of the experiment (see Figure 6.19).

Figure 6.22 shows the predictions of the temperature profiles through the lactose slab.

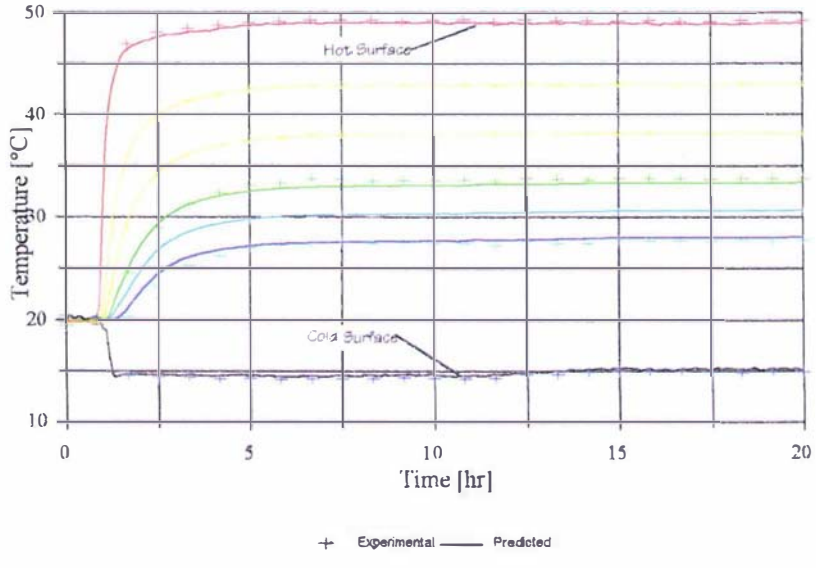

Figure 6.22 - Comparison of experimental and predicted temperature profiles with amorphous lactose present.

Figure 6.22 shows that good correlation between the predicted and experimentally measured temperature profiles was achieved. Figure 6.23 shows predictions of the hot and cold surface relative humidity profiles for the experiment.

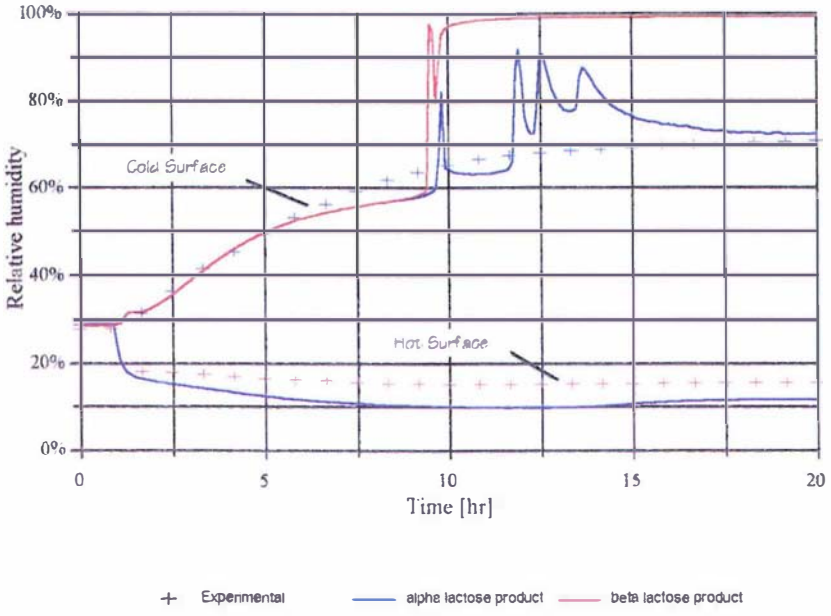

Figure 6.23 - Comparison of experimental and predicted surface relative humidity profiles with amorphous lactose present.

The comparison given between the experimentally measured results and the model predictions for crystallisation to both α-lactose Mono-hydrate and β-lactose shown in Figure 6.23 illustrates several points for discussion.

The experimentally measured hot surface relative humidity profile is different from the predicted hot surface profiles by approximately 5%. The relative humidity probes used (Hycal) in the experiment were generally well behaved. The probe however was not so stable in conditions of very low relative humidity, especially at high temperature (50°C) as present in this case. Because of this effect the 5% systematic offset evident in Figure 6.23 was assumed to be caused by measurement error and not due to any inadequacy of the transport model.

Another observation that can be seen in Figure 6.23 is that a dramatic release in moisture is predicted on the cold surface by the model irrespective of which crystallisation product was assumed. The experimental results indicate that this was not observed in practise. The two-point moisture sorption isotherm results presented in Figure 6.21 clearly showed that crystallisation did occur over the course of the experiment. The cold surface relative humidity profiles for the experimental and predicted results begin to deviate from each other at approximately 50% RH.

One explanation for the inconsistencies between the experimental and predicted results is that the assumption equilibrium is always found between the solid and gaseous phases of the bulk lactose. The model predictions show that when a specific relative humidity condition was reached, a rapid crystallisation takes place due to the release of moisture associated with the crystallisation. Because this rapid release of moisture was not experimentally observed it follows that either the rate of crystallisation is much less dependent on moisture than the Avrami model, fitted in Section 3.7.4.2.2.3, predicts, or the rate the moisture is released is not crystallisation controlled.

There is some evidence from the work carried out by O'Donnell (1997) and Cressey (1997) that the product of amorphous lactose crystallisation is difficult to dry. This suggests a fine porous structure which might trap moisture within it. It is not difficult to explain how such a structure could form as a result of crystallisation. Amorphous lactose exists as a unstructured matrix of lactose molecules. This matrix is very super saturated with respect to both α and β lactose and therefore there is a strong driving force for spontaneous nucleation and crystal growth. In conditions where the glass transition temperature is not exceeded, the high viscosity and hence low mobility of the lactose molecules prevent crystallisation taking place. When conditions change to allow movement of the lactose to form nuclei and for growth to occur, the matrix collapses and crystallisation takes place. Because the degree of super-saturation of lactose in the amorphous matrix is so high, it is likely that numerous point nuclei form and these nuclei grow and run into each other. Because the density of amorphous matrix (758 kg/m^3) is much lower than the crystalline form (1535 kg/m^3) the amount of space required for the crystal form is much lower than for the amorphous matrix. It follows that the structure resulting from the crystallisation has large pockets which can entrap moisture.

If a such a surface structure is formed on the surface of the particle due to the amorphous lactose crystallisation then it could limit the rate that moisture can escape the particle into the void spaces of the bulk powder where it is available for diffusion to other parts of the slab. In the experimental measurement of amorphous lactose crystallisation rate outlined in Section 3.7.4.2.2.3, the rate of crystallisation was slow (20 days) compared to the rate that such moisture release through the resulting crystalline structure. The crystallisation rate experiment therefore can be consistent with the above explanation.

For this explanation to be valid, crystallisation must proceed at a water activity corresponding to the point at which the experimental and predicted cold surface relative humidity profiles deviate (~50% RH). This indicates that crystallisation occurred at a significant rate at a lower water activity than is predicted using the Avrami model with the constants fitted in this work. The predicted water activity for crystallisation to occur within the time frame of this work was 0.57 a_w. This demonstrates a need for further investigation into the kinetics of amorphous lactose crystallisation. At faster crystallisation rates it is likely that consideration must be given to the rate that moisture can escape the crystallising structure.

The oscillating increase of cold surface relative humidity upon crystallisation, particularly evident for the α-lactose Mono-hydrate product, suggests an alternative explanation for the apparent lack of fit of the model. This oscillation is caused by the surface node reaching conditions conducive to crystallisation and subsequent release of moisture. This moisture then is free to diffuse back to the second node until this is able to crystallise. This process is then repeated onwards through the lactose slab until all of the nodes have crystallised or not enough moisture is available. In the real situation the concept of the discrete element that the node represents is not applicable and the oscillatory relative humidity fluctuations do not occur. This suggests that the simulation requires more nodes to accurately model the crystallisation phenomena compared for the prediction of moisture migration through the lactose slab.

The model was therefore run assuming a α-lactose mono-hydrate crystallisation product using 50 nodes instead of the regular 20 and the comparisons can be seen in Figure 6.24. It was found that a lower time step (0.5 s) was required to make the

simulation stable and this combined with the increased number of calculations required due to more nodes being present resulted in very long simulation times (15 hrs).

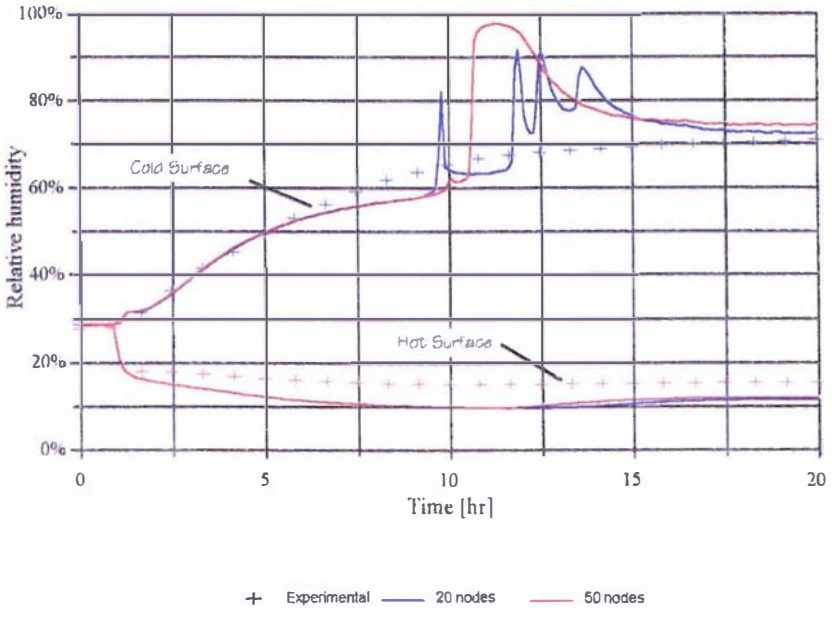

Figure 6.24 - Comparison of predictions for crystallisation to α-lactose Mono-hydrate with 20 and 50 nodes.

Figure 6.24 shows that a much smoother release of moisture results when more nodes are used. This suggests that a large number of nodes is required to accurately model the amorphous lactose crystallisation. Because the crystallisation still occurred rapidly, this effect can not be used to explain the differences between the model predictions and the experimental results. Because the experimental results showed that the release of moisture is relatively slow, 20 nodes should be sufficient to obtain accurate predictions once the correct moisture release mechanism and crystallisation rates are included into the model.

It is clear from Figure 6.20 that the inadequacies of the model are not influenced by the choice of crystallisation product. This is not to say that the product of crystallisation is not important. It is an integral part of determining the rate of crystallisation and degree of moisture release. It will also strongly effect the amount of free moisture contained inside the bulk lactose after crystallisation has proceeded.

It is also clear from this discussion that more accurate data for the amorphous lactose crystallisation process must be available before accurate prediction of amorphous lactose related caking in bulk lactose is possible.

6.3.7 Avoidance of Amorphous Lactose Related Caking in Bulk Lactose

In spite of the shortcomings of the model, the investigations carried out with the inclusion of amorphous lactose into the transport model, highlight several points concerning the effect of amorphous lactose in the caking of bulk lactose. It has been shown that the extra moisture holding capacity of the amorphous lactose means that the

total amount of free moisture contained within a bag is higher than that for completely crystalline lactose at the same water activity. Secondly this extra moisture holding capacity acts as a buffer and slows the rate of migration of moisture under the influence of a temperature gradient. This is of industrial importance as it means that the time required to achieve conditions conducive to amorphous lactose crystallisation at a particular local position within the slab, will increase with increasing amorphous lactose content. As the moisture migration is driven by a temperature gradient driving force, this means that bulk lactose with large amounts of amorphous lactose (~>3%) are less likely to crystallise under the influence of swinging temperature gradients than powders with low levels of amorphous lactose (~0.5-3%).

The transport model has shown that more research must be undertaken into the amorphous lactose crystallisation phenomena. This includes the kinetics of crystallisation, the rate moisture is released from the resulting crystalline structure and the product of crystallisation. Until better understanding of these phenomena are available it is not possible to accurately model caking in bulk lactose powders when amorphous lactose is present and crystallisation occurs.

The amorphous lactose crystallisation rate experiments (Section 3.7.4.2.2.3) have shown that the time required for crystallisation at a water activity of 0.435 is of the order of 20 days. This suggests that the rate of crystallisation at lower water activities is very slow. It is therefore possible to prescribe a maximum water activity level that must not be exceeded to ensure that the extent of amorphous lactose crystallisation will be negligible. If it is considered that this maximum water activity will exist only as long as the maximum temperature gradient to which the bag is exposed to is maintained, then it can be seen that a upper limit of 0.4 a_w is sensible until a better estimate can be obtained once complete understanding of the crystallisation process is available.

Figure 6.13 indicates that a maximum water activity of 0.4 a_w is achieved on the cold surface of a lactose slab when a 20°C temperature gradient is applied to product with an initial water activity of 0.25 a_w. This suggests that if lactose powders are packed at a water activity below 0.25 a_w in the industrial production of lactose powders, then amorphous lactose crystallisation will not occur under expected storage conditions.

6.4 CLOSURE

This section of the work covered the inclusion of the microscopic scale processes that are contributory to caking phenomena (liquid bridging, amorphous lactose crystallisation) into the overall transport model. This has highlighted several areas where more research is needed to provide complete understanding of the causes of caking especially concerning the transitions of amorphous lactose in the bulk powder. These include the rate of crystallisation, the rate of moisture release from the crystallising amorphous structure and the product of crystallisation.

The resulting models have allowed the assessment of appropriate guidelines for product water activity upon packing in industrial lactose production. A maximum water activity of 0.575 a_w is suggested for the case where no amorphous lactose is present, while a maximum of 0.25 a_w is suggested when amorphous lactose is present in small amounts.

This suggests two possible courses of action to avoid caking in industrial situations.

The first is to bag at a water activity of 0.25 a_w or lower. This will eliminate the possibility of any amorphous lactose present in the powder reaching conditions where crystallisation can occur, and allowing moisture to be released to facilitate liquid bridging and subsequent caking.

The second option is to ensure there is no amorphous lactose present in the powder when it is bagged. This relaxes the maximum water activity requirement from 0.25 to 0.575 a_w at the time of packing. This could be achieved by the inclusion of a conditioning step into the manufacturing process, downstream of the milling operations. Such conditioning could be achieved by contacting the powder with an elevated relative humidity air stream to encourage amorphous lactose crystallisation. This would then be followed by a drying step to ensure a final product water activity of less than 0.575 a_w. The technical feasibility of such an conditioning operation was the subject of another research study by O'Donnell (1997).

CHAPTER 7

CONCLUSIONS AND SUGGESTIONS FOR FUTURE WORK

7.1 CONCLUSIONS

This work has identified the mechanisms for lumping and caking in bulk lactose and the conditions under which these mechanisms occur. Liquid bridge formation was found to give lactose powders significant strength if the powder is subjected to conditions above 0.85 a_w. If these conditions are maintained for long periods of time (up to one month) then shrinkage and increased powder strength result. This is thought to be due to the dissolution of small asperities in the porous matrix, enabling adjacent particles to pack closer together. If the powder is subsequently dried, then crystalline bridges of greater strength than the originating liquid bridges result.

The mechanism of amorphous lactose flow in conditions above the glass transition temperature, has been shown to be insignificant with respect to caking in bulk crystalline lactose when the level of amorphous lactose is < 5%. Amorphous lactose is important, acting as a moisture sink. If conditions are favourable, crystallisation will occur, resulting in the release of moisture which contributes to caking by the liquid bridging mechanism. The effect of applied pressure on caking was not investigated

A model which describes the transport of moisture in one dimension as a result of temperature gradients was developed and validated. The microscopic scale processes of liquid bridging and amorphous lactose moisture relations were included into this model. The model agreed well with experimental trials for the case where the lactose powder was completely crystalline. Comparison of the model predictions with experimental trials for the case when amorphous lactose was present showed that some inadequacies of the model exist. These are to do with the rate of crystallisation, the rate that moisture is released from the crystallising amorphous matrix and the product of amorphous lactose crystallisation.

In spite of the inability to accurately model crystallisation of the amorphous matrix, it was possible to prescribe limits, which, if not exceeded will allow the production of caking free lactose powder. It was shown that under expected ambient conditions the product should be stored with a water activity below 0.57 a_w if no amorphous lactose is present and below 0.25 a_w if it is present.

These figures show that if no amorphous lactose is present in the packed samples, then the critical water activity limit is not as strict as for when it is present. This offers two alternative process philosophies which can be followed to achieve the goal of producing caking free lactose. These are to bag the product at low water activity, or to remove the amorphous lactose prior to packing. The conditioning of lactose is the subject of continuing research from this work.

7.2 SUGGESTED FUTURE RESEARCH

This work has highlighted several areas which require further research before a complete understanding of caking in bulk lactose can be achieved. These are listed below;

- Improved amorphous lactose crystallisation kinetics.
- Investigation into the products of amorphous lactose crystallisation.
- Investigation into structural changes during amorphous lactose crystallisation and the influence of the resulting structure on the rate of moisture release.
- The rate of the solid state conversion of β to α-lactose mono-hydrate.
- The feasibility of conditioning of lactose to eliminate amorphous lactose prior to packing.

REFERENCES

Abdel-Ghani M., Petri J.G., Seville J.P.K., Clift R. and Adams M.J. (1991). Mechanical properties of cohesive particulate solids. *Powder Technol.*, **65**, 113-123.

Adamson A.W. (1963). Physical chemistry of surfaces. John Wiley and Son, New York.

Aguilera J.M. and Stanley D.W. (1990). Microstructural principles of food processing and engineering. Elsevier Applied Science, London.

Aguilera J.M., del Valle J.M. and Karel M. (1995). Caking phenomena in amorphous food powders. *Trends Food Sci. Technol.*, **6**, 149-155.

Al-Duri B. and McKay G. (1992). Pore diffusion: Dependence of the effective diffusivity on the initial sorbate concentration in single and multisolute batch adsorption systems. *J. Chem. Tech. Biotechnol.*, **55**, 245-250.

Anderson R.B. (1946). Modifications of the Brunauer, Emmett and Teller equation. *J. Am Chem. Soc.*, **68**, 686-691.

Anonymous (1990a). The latest in fertilizer cake prevention. *Nitrogen*, **187**, 20-27.

Anonymous (1990b). Sugar storage in concrete silos. *Int. Sugar Jnl.*, **92**, 7-15.

ASHRAE (1993). ASHRAE Handbook. Fundamentals 1993. American Society of Heating, Refigeration and Air-conditioning Engineers Inc., Atlanta.

Audu T.O.K., Loncin M. and Weisser H. (1978). Sorption isotherms of sugars. *Lebensm. Wiss. u. Technol.*, **11**, 31-34.

Avrami M. (1941). *J. Chem. Phys.*, **9**, 177.

Avrami M. (1939). *J. Chem. Phys.*, **7**, 1103.

Avranitoyannis I. and Blanshard J.M.V. (1994). Rates of crystallization of dried lactose-sucrose mixtures. *J. Food Sci.*, **59**, 197-205.

Bagster D.F. (1970a). Cause, prevention and measurement of the caking of refined sugar - a review. Part I. *Int. Sugar Jnl.*, **72**, 263-267.

Bagster D.F. (1970b). Cause, prevention and measurement of the caking of refined sugar - a review. Part II. *Int. Sugar Jnl.*, **72**, 298-302.

Baker C.J. and Mai I.(1982). Physical effects of direct drilling equipment on undisturbed soils and techniques for measuring soil compaction in the vicinity of drilled grooves. *NZ. J. Agr. Res.*, **25** (1) 43-49.

Bauer T.H. (1993). A general analytical approach toward the thermal conductivity of porous media. *Int. J. Heat & Mass Transfer*, **36**, 4181-4191.

Bear J. and Bachmat Y. (1991). Introduction to modelling of transport phenomena in porous media. Kluwer Academic Publishers, Dordrecht. .

Berlin E., Anderson B.A. and Pallansch M.J. (1968). Comparison of water vapour sorption by milk powder components. *J. Dairy Sci.*, **51**, 1912-1915.

Berlin E., Kilman P.G., Anderson B.A. and Pallansch M.J. (1971). Calorimetric measurement of the heat of desorption of water vapour from amorphous and crystalline lactose. *Thermochim. Acta.*, **2**, 143-152.

Berlin E., Anderson B.A. and Pallansch M.J. (1973). Effect of hydration and crystal form on the surface area of lactose. *J. Dairy Sci.*, **55**, 1396-1399.

Biliaderis C.G. (1990). Thermal analysis of food carbohydrates. In *Thermal analysis of foods*. (Harwalkar V.R. and Ma C.Y. Eds). Elsevier Applied Science. New York. 168-220.

Bird R.B., Stewart W.E. and Lightfoot E.N. (1960). Transport phenomena. John Wiley and Sons., New York. .

Boon J. (1966). PhD dissertation, Delft University, Netherlands.

Boon J., Challa G. and Van Krevelen D.W. (1968). *J. Polymer Sci. A2.*, **6**, 1791,1835.

Bruin S. and Luyben K.C.A.M. (1980). Drying of food materials: A review of recent developments. In *Advances in drying, Vol 1.* (Mujumda A.S. Eds). Hemisphere Publishing, New York. 155-215.

Brunauer S., Emmett P.H. and Teller E. (1938). Adsorption of gases in multimolecular layers. *J. Am. Chem. Soc.*, **60**, 309-319.

Buckton G. and Darcy P. (1995). The use of gravimetric studies to assess the degree of crystallinity of predominantly crystalline powders. *Int. J. Pharm.*, **123**, 265-271.

Buma T.J. (1965). The true density of spray milk powders and of certain constituents. *Neth. Milk Dairy J.*, **19**, 249.

Bushill J.H., Wright W.B., Fuller C.H.F. and Bell A.V. (1965). The crystallisation of lactose with particular reference to its occurrence in milk powder, *J. Sci. Food Agric.*, **16**, 622.

Carslaw H.S. and Jaeger J.C. (1959). Conduction of heat in solids. Oxford University Press. London. .

Chirife J., Timmermann E.O., Iglesias H.A. and Boquet R. (1992). Some features of the parameter k of the GAB equation as applied to sorption isotherms of selected food materials. *J. Food Eng.*, **15**, 75-82.

Chuy L.E. and Labuza T.P. (1994). Caking and stickiness of dairy based food powders as related to glass transition. *J. Food Sci.*, **59**, 43-46.

Cleland D.J., Cleland A.C. and Jones R.S. (1994). Collection of accurate experimental data for testing the performance of simple methods for food freezing time prediction. *J. Food Proc. Eng.*, **17**, 93-117.

Collin M. and Rasmuson A. (1988). A comparison of gas diffusivity models for unsaturated porous media. *Soil Sci. Am. J.*, **52**, 1559-1565.

Cooper J.G. and Le Fever E.N. (1969). Thermophysical properties of water substance. Edward Arnold Ltd., London. .

Cornerlius M. (1991). RADS Refrigeration analysis design and simulation package. Release 3.1. Massey University, Palmerston North. .

Crank J. (1975). The mathematics of diffusion. Oxford University Press., London. .

Currie J.A. (1961). Gaseous diffusion in porous media. Part 3. Wet granular materials. *Br. J. Appl. Phys.*, **12**, 275-281.

De Boer J.H. (1953). The dynamical character of adsorption. Clarendon Press, Oxford. .

Deng Y., Fedler C.B. and Gregory J.M. (1992). Predictions of thermal characteristics for mixed porous media. *J. Mat. Civil Eng.*, **4**, 185-195.

Downton G.E., Flores-Luna J.L. and King C.J. (1982). Mechanism of stickiness in hygroscopic, amorphous powders. *Ind. Eng. Chem. Fund.*, **21**, 447-451.

Duckworth R.B. (1972). The properties of water around the surfaces of food colloids. *Proc. Inst. Food Sci. Technol. (UK).*, **5**, 60.

Fish B.P. (1958). Diffusion and thermodynamics of water in potato starch gel. In *Fundamental aspects of the dehydration of foodstuffs.* (Society of Chemical Industry. Eds). Metchim and Son Ltd. London. 143-157.

Flink J.M. (1983). Structure and structure transitions in dried carbohydrate materials. In *Physical properties of foods.* (Peleg M. and Bagley E. Eds). AVI Publishing, Connecticut. .

Franks F. (1991). Hydration phenomena: an update and implications for the food processing industry. In *Water relationships in food.* (Levine H. and Slade L. Eds). Plenum Press. New York. 1-19.

Gal. (1975). Recent advances in techniques for the determination of sorption isotherms. In *Water relations in foods.* (Duckworth R.B. Eds). Academic Press, London. .

Gekas V. (1992). Transport phenomena of foods and biological materials. CRC Press, Boca Raton. .

Gerhartz W. (1988). Ullmann's encylopedia of industrial chemistry. VCH. Verlagsgesellschaft, Weinheim,

Gillis J. (1920). Nouvelles recherches sur le sucre de lait. *Rec. trav. chim. Pays-Bas.*, **39**, 88-125.

Grayson M. (1979). Kirk-Othmer Encylopedia of chemical technology 3rd Edition. John Wiley and Sons, New York. 116-123.

Greenspan L. (1977). Humidity fixed points of binary saturated aqueous solutions. *J. Res. Nat. Bur. Stand. Sect. A.*, **81A**, 89-96.

Guggenheim E.A. (1966). Applications of statistical mechanics. Clarendon Press, Oxford. .

Hardesty J.O. and Kumagai R. (1952). Factors influencing the efficiency of flow conditioners. *Agr. Chem.*, **7**, 38-39,115.

Hargreaves J. (1995). Characterisation of lactose in the liquid and solid state using nuclear magnetic resonance and other methods. PhD Thesis, Massey University, Palmerston North.

Harnby N., Hawkins A.E. Opalinsk I. (1996). Measurement of the adhesional force between individual particles with moisture present. 1. - a review. *Chem Eng. R.* **74** (A6) 605-615.

Harper W.J. (1992). Lactose and lactose derivatives. In *Whey and lactose processing.* (Zadow J.G. Ed). Elsevier Applied Science. Essex. England. 317-360.

Hasegawa M., Saito K., Hong K., Tomiyasu H. and Watanabe K. (1985). Measurement and utilization of dynamic properties of powder beds. *Bulk Solids Handling*, **5**, 641-645.

Herrington B.L. (1934). Some physico-chemical properties of lactose. I. The spontaneous crystallisation of supersaturated solutions of lactose. *J. Dairy Sci.*, **17**, 501-518.

Hodges G.E. Lowe E.K. and Paterson A.H. (1993). A mathematical model of lactose dissolution. *Chem Eng. J.* **53** (2) B25-B33.

Hodges G. (1992). Lactose in bulk bags, study of moisture migration and caking mechanisms. Lactose Company of New Zealand., Hawera, New Zealand.

Hollenbach A.M., Peleg M. and Rufner R. (1983). Interparticle surface affinity and bulk properties of conditioned powders. *Powder Technol.*, **35**, 51-62.

Hollenbach A.M., Peleg M. and Rufner R. (1982). Effect of four anticaking agents on the characteristics of ground sugar. *J. Food Sci.*, **47**, 538-544.

Irani R.R., Callis C.F. and Lin T. (1959). How to select flow conditioning and anticaking agents. *Ind. Eng. Chem.*, **51**, 1285-1288.

Jenike A.W. (1970). *Storage and flow of solids.* Bulletin No 123 of the Utah Engineering Experiment Station. Utah.

Jenness R. and Patton S. (1959). Principles of dairy chemistry. Chapman and Hall, London.

Johari G.P., Hallbrucker A. and Mayer E. (1987). The glass transition of hyperquenched water. *Nature*, **330**, 552-553.

Jouppila K. and Roos Y.H. (1993). Glass transitions and physical state of dehydrated milk products. In *Proceedings of the sixth International Congress on Engineering and Food.* (Eds). Elsevier, Tokyo. .

Jouppila K. and Roos Y.H. (1994). Water sorption and time-dependent phenomena of milk powders. *J. Dairy Sci.*, **77**, 1798-1808.

Jouppila K., Kansikas J. and Roos Y.H. (1997). Glass transitions, water plasticization and lactose crystallisation in milk powder. *Submitted to J. Dairy Sci.*

Karel M. and Saguy I. (1991). Effects of water on diffusion in food systems. In *Water relationships in foods.* (Levine H. and Slade L. Eds). Plenium Press, New York. 157-173.

Karel M. (1975). Water activity and food preservation. In *Principles of food science: Part II, Physical principles of food preservation.* (Karel M., Fennema O.R. and Lund D.B. Eds). Marcel Dekker Inc., New York. 237-263.

Kawamura M. (1991). Moisture. In *Powder technology handbook.* (Linoya K., Gotoh K. and Higashitani K. Eds). Marcel Dekker Inc., New York. 183-192.

Kawashima Y. (1991). Adhesion and cohesion of powder. In *Powder technology handbook.* (Linoya K., Gotoh K. and Higashitani K. Eds). Marcel Dekker Inc., New York. 99-115.

Kent M., Christianson K., van Haneghem I.A., Holtz E., Morley M.J., Nesvadba P. and Poulsen K.P. (1984). Cost 90 collaborative measurements of thermal properties of foods. *J. Food Eng.*, **3**, 117-150.

King C.J. (1968). Rates of moisture sorption and desorption in porous, dried foodstuffs. *Food Technol.*, **22**, 509-515.

Kono H.O. Aksoy E. and Itani Y. (1994). Measurement and application of the rheological parameters of aerated fin powders - a novel characterisation approach to powder flow properties. *Powder Tech.*, **89**, 177-188.

Kumagai R. and Hardesty J.O. (1956). Relative effectiveness of granule coating agents. *Agr. Food Chem.*, **4**, 132-135.

Labrousse S., Roos Y. and Karel M. (1992). Collapse and crystallisation in amorphous matrices with encapsulated compounds. *Sciences Des Aliments.*, **12**, 757-769.

Labuza T.P. (1968). Sorption phenomena in foods. *Food Technol.*, **22**, 15-24.

Ladd M.F.C. and Lee W.H. (1965). The thermodynamics of crystalline hydrates. *J. Phys. Chem.*, **69**, 1840-1843.

Ladd M.F.C. and Lee W.H. (1969). Studies on crystalline hydrates. *J. Phys. Chem.*, **73**, 2033-2035.

Lazar M.E., Brown A.H., Smith G.S., Wong F.F. and Lindquist F.E. (1956). Experimental production of tomato powder by spraydrying. *Food Technol.*, **10**, 129-137.

LeMeste M., Voilley A. and Colas B. (1991). Influence of water on the mobility of small molecules dispersed in a polymeric system. In *Water relationships in food.* (Levine H. and Slade L. Eds). Plenum Press. New York. 123-138.

Leslie R.B., Carillo P.J., Chung T.Y., Gilbert S.G., Hayakawa K., Marousis S., Saravacos G.D. and Solberg M. (1991). Water diffusivity in starch-based systems.

Linko P., Plooari T., Harju M. and Heikonen M. (1981). Water sorption properties and the effect of moisture on structure of dried milk products. *Lebensm. Wiss. u. Technol.*, **15**, 26-30.

Lloyd R.J., Chen X.D. and Hargreaves J.B. (1996). Glass transition and caking of spray-dried lactose. *Int. J. Food Sci. Tech.*, **31**, 305-311.

Loncin M., Bimbenet J.J. and Lenges J. (1968). Influence of the activity of water on the spoilage of foodstuffs. *J. Food Technol.*, **3**, 131-142.

Lowe E.K. (1993). The dissolution of alpha lactose monohydrate: a mathematical model for predicting dissolution times. Masterate Thesis, Massey University, Palmerston North.

Luikov A.V. (1980). Heat and mass transfer. MIR Publishers, Moscow.

Luyben K.C.A.M., Olieman J.J. and Bruin S. (1980). Concentration dependent diffusion co-efficients derived from experimental drying curves. In *Drying '80. Volume 2: Proceedings of the second international symposium.* (Mujumdar A.S. Eds). Hemisphere Publishing Corporation. Washington. 233-243.

Lyle O. (1957). Technology for sugar refinery workers. Chapman Hall. London. .

MacCarthy D.A. and Fabre N. (1989). Thermal conductivity of sucrose. In *Food Properties and computer-aided engineering of food processing systems.* (Singh R.P. and Medina A.G. Eds). Kluwer Academic Publishers. 105-111.

Madamba P.S., Driscoll R.H. and Buckle K.A. (1996). The thin-layer drying characteristics of garlic slices. *J. Food Eng.*, **29**, 75-97.

Maroulis Z.B., Kiranoudis C.T. and Marinos-Kouris D. (1995). Heat and mass-transfer modelling in air drying of foods. *J. Food Eng.*, **26**, 113-130.

Mayer E. (1988). Hyperquenching of water and dilute aqueous solutions into their glassy states: an approach to cryo-fixation. *Cryoletters*, **9**, 66-77.

McCabe W.L. and Smith J.C. (1984). Unit operations in chemical engineering. McGraw Hill, New York.

McClellan A.L. and Hansberger H.F. (1967). Cross-sectional areas of molecules adsorbed on solid surfaces *J. Colloid Interface Sci.*, **23**, 577-599.

McGinnis R.A. (1971). Beet sugar technology. Beet Sugar Development Foundation, Colorado. .

McGuire K. (1997). Personal communication. Dept Plant Science, Massey University, Palmerston North.

McLaren R.G. and Cameron K.C. (1990). Soil science: An introduction to the properties and management of New Zealand Soils. Oxford University Press, Auckland. .

Meade G.P. (1963). Cane sugar handbook. Wiley and Sons Inc., New York. .

Mikhailov M.D. and Ozisik M.N. (1985). Unified analysis and solutions of heat and mass diffusion. John Wiley and Sons Ltd., New York. .

Millington R.J. and Shearer R.C. (1971). Diffusion in aggregated porous media. *Soil Sci.*, **111**, 372-378.

Moreyra R. and Peleg M. (1981). Effect of equilibrium water activity on the bulk properties of selected food powders. *J. Food Sci.*, **46**, 1918-1922.

Morishima K., Kawashima Y., Kawashima Y., Takeuchi H., Niwa T. and Hino T. (1993). Micrometric characteristics and agglomeration mechanisms in the spherical crystallization of bucillamine by the spherical agglomeration and the emulsion solvent diffusion methods. *Powder Technol.*, **76**, 57-64.

Moss H.V., Schilb T.W. and Warning W.G. (1933). Tricalcium phosphate as a caking inhibitor in salt and sugar. *Ind. Eng. Chem.*, **25**, 142-147.

Murakami E.G. and Okos M.R. (1989). Measurement and prediction of thermal properties of foods. In *Food properties and computer-aided engineering of food processing systems*. (Singh R.P. and Medina A.G. Eds). Kluwer Academic Publishers. 3-48.

Nash J.H., Leiter G.G. and Johnson A.P. (1965). Effects of antiagglomerant agents on physical properties of finely divided solids. *Ind. Eng. Chem. Fund.*, **4**, 140-145.

Niediek E.A. and Babernics L. (1979). Aroma sorption properties of amorphous sucrose and lactose. *Gordian*, **2**, 35-44.

Niediek E.A. (1982). Differences in properties between the crystalline and amorphous forms of lactose. *Zeitschrift Lebenssmittel-Technol. Verfrenstichnik*, **33**, 173-185.

Nelson T.J. (1949). Hygroscopicity of sugar and other factors affecting retention of quality. *Food Technol.*, **3**, 347-351.

Nichol W.M. (1990). The carbohydrate - sucrose. In *Handbook of sweeteners.* (Marie S. and Piggot J.G. Eds). Blackie and Son Ltd., Glasgow. .

Nickerson T.A. (1974). In *Fundamentals of dairy chemistry.* (Webb B.H., Johnson A.H. and Alford J.A. Eds). AVI Publishing, Connecticut. .

Nimick F.B. and Leith J.G. (1992). A model for thermal conductivity of granular porous media. *J. Heat Transfer*, **114**, 505-508.

Noel T.R., Parker R. and Ring S.G. (1995). Kinetic processes in highly viscous, aqueous carbohydrate liquids. In *Food macromolecules and colloids.* (Dickinson E. and Lorient D. Eds). The Royal Society of Chemistry. 543-551.

Notter G.K., Taylor D.H. and Downes N.J. (1959). Orange juice powder -factors affecting storage stability. *Food Technol.*, **12**, 113-118.

O'Donnell A. (1997). Conditioning of lactose powders. Masterate Thesis, Massey University, Palmerston North.

Olano A., Corzo N. and Matinez-Castro I. (1983). Studies on beta-lactose crystallisation. *Milchwissenschaft.*, **38**, 471-474.

Pancoast H.M. and Junk W.R. (1980). Handbook of sugars. AVI Publishers Inc., Connecticut.

Paterson A.H.J., Bronlund J.E. and O'Donnell A. (1997). Amorphous lactose determination in lactose powders by absorption. In *CHEMECA 97.* CHEMECA, Rotorua.

Pel L., Ketelaar A.A., Adan O.C.G. and Vanwell A.A. (1993). Determination of moisture diffusivity in porous media using scanning neutron radiography. *Int J Heat & Mass Transfer*, **36** 1261-1267.

Peleg M. (1983). Physical characterisation of food powders. In *Physical properties of foods.* (Peleg M. and Bagley E.B. Eds). AVI Publishing. Westport, Connecticut 293-324.

Peleg M. (1992). On the use of the WLF model in polymers and foods. *Crit. Rev. Food Sci. Nutrition.*, **32**, 59-66.

Peleg M. (1993). Glass transitions and the physical stability of food powders. In *Glass transitions in foods.* (Blanshard J.M.V. and Lilliford P.J. Eds). Nottingham University Press, Nottingham. 435-451.

Peleg M. and Mannheim C.H. (1969). Caking of onion powder. *Powder Technol.*, **4**, 157-160.

Peleg M. and Mannheim C.H. (1977). The mechanism of caking of powdered onion. *J. Food Proc. Pres.*, **1**, 3-11.

Perry H.P. and Green D.W. (1984). Perry's Chemical engineering handbook.6th Edition. McGraw Hill, Singapore. .

Peschl I.A.S.Z. (1989). Equipment for the measurement of mechanical properties of bulk materials. *Powder Handling & Processing.*, **1**, 73-81.

Pham Q.T. and Willix J. (1989). Thermal conductivity of fresh lamb meat, offals and fat in the range -40 to +30°C: Measurements and correlations. *J. Food Sci.*, **54**, 508-515.

Pietsch W., Hoffman E. and Rumpf H. (1969). Tensile strength of moist agglomerates. *Ind. Eng. Chem. Fund.*, **8**, 58-62.

Plinke M.A.E., Lithe D. and Loffler F. (1994). Cohesion in granular materials. *Bulk Solids Handling*, **14**, 101-106.

Pritzwald-Stegmann B.F. (1986). Lactose and some of its derivatives. *J. Soc. Dairy Tech.*, **39**, 91-97.

Reid R.C., Prausnitz J.M. and Sherwood T.K. (1987). The properties of gases and liquids. McGraw Hill, New York. .

Richardson G.M. and Malthus R.S. (1955). Salts for static control of humidity at relatively low levels. *J. App. Chem.*, **5**, 557-567.

Riepma K.A., Dekker B.G. and Lerk C.F. (1992). The effect of moisture sorption on the strength and internal surface area of lactose tablets. *Int. J. Pharm.*, **87**, 149-159.

Ristic M.M.and Drajojevic-Nesic M.J.(1987). A new approach for the description of the initial-stage kinetics during amorphous materials sintering. *Powder Technol.*, **49** 189-190.

Rockland L.B. (1960). Saturated salt solutions for static control of relative humidity between 5° and 40°C. *Anal. Chem.*, **32**, 1375-1376.

Roos Y. (1993). Melting and glass transitions of low molecular weight carbohydrates. *Carbohydr. Res.*, **238**, 39-48.

Roos Y. and Karel M. (1990). Differential scanning calorimetry study of phase transitions affecting the quality of dehydrated materials. *Biotechnol. Prog.*, **6**, 159-163.

Roos Y. and Karel M. (1991a). Plasticizing effect of water on thermal behaviour and crystallisation of amorphous food models. *J. Food Sci.*, **56**, 38-43.

Roos Y. and Karel M. (1991b). Applying state diagrams to food processing and development. *Food Technol.*, **45**, 66-71,107.

Roos Y. and Karel M. (1991c). Amorphous state and delayed ice formation in sucrose systems. *Int. J. Food Sci.Tech.*, **26**, 553-566

Roos Y. and Karel M. (1992). Crystallisation of amorphous lactose. *J. Food Sci.*, **57**, 775-777.

Roos Y. and Karel M. (1993). Effects of glass transitions on dynamic phenomena is sugar containing food systems. In *Glass transitions in foods.* (Blanshard J.M.V. and Lilliford P.J. Eds). Nottingham University Press, Nottingham. 207-222.

Rosenzweig N. and Narkis M. (1981). Sintering rheology of amorphous polymers. *Polym. Eng. Sci.*, **21**, 1167-1170.

Roth D. (1976). Amorphous icing sugar produced during crushing and recrystallisation as the cause of agglomeration and procedures for its avoidance. (in German) PhD thesis, University of Karlsruhe, Karlsruhe.

Rumpf H. (1961). In *Agglomeration.* (Knepper W. Eds). Chapman and Hall, London. .

Rumpf H. (1975). Particle Technology. Carl Hanser Verlag. Munich.

Rutland D.W. (1991). Fertilizer caking: mechanisms, influential factors, and methods of prevention. *Fert. Res.*, **30**, 99-114.

Saito Z. (1985). Particle structure in spray dried whole milk and in instant skim milk powder as related to lactose crystallisation. *Food Microstructure*, **4**, 333-340.

Schubert H. (1975). Tensile strength of agglomerates. *Powder Technol.*, **11**, 107-119.

Schubert H., Herrmann W. and Rumpf H. (1975). Deformation behaviour of agglomerates under tensile stress. *Powder Technol.*, **11**, 121-131.

Schubert H. (1987). Food particle technology Part I: Properties of particles and particulate food systems. *J. Food Eng.*, **6**, 1-32.

Schubert H. (1984). Capillary forces - modeling and application in particle technology. *Powder Technol.*, **37**, 105-116.

Scotter D.R. and Horne D.J. (1985). The effect of drainage on soil temperatures under pasture. *J. Soil Sci.*, **36**, 319-327.

Scoville E. and Peleg M. (1981). Evaluation of the effects of liquid bridges on the bulk properties of model powders. *J. Food Sci.*, **46**, 174-177.

Seville J.P.K. and Clift R. (1984). The effect of thin layers on fluidisation characteristics. *Powder Technol.*, **37**, 117-129.

Shah D.J., Ramsey J.W. and Wang M. (1984). An experimental determination of the heat and mass transfer coefficients in moist unsaturated soils. *Int. J. Heat & Mass Transfer*, **27**, 1075-1085.

Sharp P.F. (1938). Seeding test for crystalline beta lactose. *J. Dairy Sci.*, **21**, 445-449.

Sharp P.F. and Doob H. (1941). Quantitative determination of alpha and beta lactose in dried milk and dried whey. *J. Dairy Sci.*, **24**, 589.

Sharp P.F. and Hand D.B. (1939). U.S. Patents 2.182.618 and 2.182.619.

Shrotriya A.K., Verma L.S., Singh R. and Chaudhary D.R. (1991). Thermal diffusion through moist porous systems at different temperatures. *J. Energy Heat Mass Transfer*, **13**, 77-85.

Sinnott R. (1983). Chemical Engineering Vol 6, An introduction to chemical engineering design. Pergamon Press, Oxford.

Slade L. and Levine H. (1991). Beyond water activity: recent advances based on an alternative approach to the assessment of food quality and safety. *CRC Crit. Rev. Food Sci. Nutr.*, **30**, 115-360.

Smith D.S., Mannheim C.H. and Gilbert S.G. (1981). Water sorption isotherms of sucrose and glucose by inverse gas chromatography. *J. Food Sci.*, **46**, 1051-1053.

Soesanto T. and Williams M.C. (1981). Volumetric interpretation of viscosity for concentrated and dilute sugar solutions. *J. Phys. Chem.*, **85**, 3338-3341.

Stecher P.G. (1968). The Merck Index., Merck and Co. Inc., Rathway, New Jersey.

Steele B. (1989). *Is the water in your food too active?* CSIRO Food Research, Sydney.

Stitt F. (1958). Moisture equilibrium and the determination of water content of dehydrated foods. In *Fundamental aspects of the dehydration of foodstuffs.* (Society of Chemical Industry. Eds). Metchim and Son Ltd. London. 67-87.

Sweat V.E. (1986). Thermal properties of foods. In *Engineering properties of foods.* (Rao M.A. and Rizvi S.S.H. Eds). Marcel Dekker Inc., New York. 49-87.

Taylor A.A. (1961). Determination of moisture equilibria in dehydrated foods. *Food Technol.*, **15**, 536-540.

Thorne S. (1989). Local measurement of thermal diffusivity of foodstuffs. In *Food properties and computer-aided engineering of food processing systems.* (Singh R.P. and Medina A.G. Eds). Kluwer Academic Publishers. 113-116.

Thurby J.A. and Nickerson T.A. (1976). Crystallisation kinetics of alpha lactose. *J. Food Sci.*, **41**, 38-42.

Timmermann E.O. (1989). A BET like three sorption stage isotherm. *J. Chem. Soc., Faraday Trans. J.*, **85**, 1631-1645.

Timmermann E.O. and Chirife J. (1991). The physical state of water sorbed at high activities in starch in terms of the GAB sorption equation. *J. Food Eng.*, **13**, 171-179.

To E.C. and Flink J.M. (1978a). Collapse, a structural transition in freeze dried carbohydrates - I. an evaluation of analytical methods. *J. Food Technol.*, **13**, 551-565.

To E.C. and Flink J.M. (1978b). Collapse, a structural transition in freeze dried carbohydrates - II. effect of solute composition. *J. Food Technol.*, **13**, 567-581.

To E.C. and Flink J.M. (1978c). Collapse, a structural transition in freeze dried carbohydrates - III. Prerequisite of recrystallisation. *J. Food Technol.*, **13**, 583-594.

Tong C.H. and Lund D.B. (1990). Effective moisture diffusivity in porous materials as a function of temperature and moisture content. *Biotechnol. Prog.*, **6**, 67-75.

Tong C.H. and Lund D.B. (1990). Effective moisture diffusivity in porous materials as a function of temperature and moisture content. In *Engineering and Food. Volume 1. Physical properties and process control.* (Spiess W.E.L. and Schubert H. Eds). Elsevier Applied Science, London. 482-492.

Troller J. (1983). Methods to measure water activity. *J. Food Protection*, **46**, 129-134.

Troy H.C. and Sharp P.F. (1930). Alpha and Beta lactose in some milk products. *J. Dairy Sci.*, **13**, 140-157.

Tsourouflis S., Flink J.M. and Karel M. (1976). Loss of structure in freeze-dried carbohydrate solutions: Effects of temperature, moisture content and composition. *J. Sci. Food Agric.*, **27**, 509-519.

Vagenas G.K. and Karathanos V.T. (1991). Prediction of moisture diffusivity in granular materials, with special applications to foods. *Biotechnol. Prog.*, **7**, 419-426.

Van Brake J. and Heertjes P.M. (1974). Analysis of diffusion in micro-porous media in terms of a porosity, a tortuosity and a contrictivity factor. *Int. J. Heat & Mass Transfer*, **17**, 1093-1103

Van Krevelen D.W. (1990). Properties of polymers. Elsevier Applied Science. Amsterdam.

Voudouris N. and Hayakawa K. (1994). Simultaneous determination of thermal conductivity and diffusivity of foods using a point heat source probe: a theoretical analysis. *Lebensm. Wiss. u. Technol.*, **27**, 522-532.

Vrentas J.S. and Duda J.L. (1979). Molecular diffusion in polymer solutions. *A. I. Ch. E. J.*, **25**, 1-24.

Vuataz G. (1988). Preservation of skim-milk powders: role of water activity and temperature in lactose crystallization and lysine loss. In *Food preservation by moisture content.* (Seow C.C. Eds). Elsevier Applied Science. New York. .

Wade A. and Weller P.J. (1994). Handbook of pharmaceutical excipients. American Pharmaceutical Association, Washington. .

Walker D.M. (1967). A basis for bunker design. *Powder Technol.*, **1**, 228-236.

Wallack D.A. and King C.J. (1988). Sticking and agglomeration of hygroscopic, amorphous carbohydrate and food powders. *Biotechnol. Prog.*, **4**, 31-35.

Walstra P. and Jenness R. (1984). Dairy chemistry and physics. Wiley. New York. .

Wang B.X. and Fang Z.H. (1988). Water absorption and measurement of the mass diffusivity in porous media. *Int. J. Heat & Mass Transfer*, **31**, 251-257.

Warburton S. and Pixton S.W. (1978). The moisture relations of spray dried skimmed milk. *J. Stored Prod. Res.*, **14**, 143-158.

Weast R.C. and Astle M.J. (1979). CRC handbook of chemistry and physics. CRC Press, Cleveland, Ohio.

Welty J.G., Wicks C.E. and Wilson R.E. (1984). Fundamental of momentum, heat and mass transfer. John Wiley and Sons., New York. .

Whynes A.L. and Dee T.P. (1957). The caking of granular fertilizers: an investigation on a laboratory scale. *J. Sci. Food Agric.*, **8**, 577-591.

Williams M.L., Landel R.F. and Ferry J.D. (1955). The temperature dependence of relaxation mechanisms in amorphous polymers and other glass forming liquids. *J. Am. Chem. Soc.*, **77**, 3701-3707.

Willix J. (1996). Personal communication. Meat Industry Research Institute of New Zealand. Hamilton.

Willix J. and Lovatt S.J. (1997). Further thermal conductivity values of foods measured by a guarded hot plate. Submitted for publication to *J. Food Eng.*

Wursch P., Rosset J., Kollreutter B. and Klein A. (1984). Crystallization of Beta-lactose under elevated storage temperature in spray-dried milk powder. *Milchwissenschaft*, **39**, 579-582.

Xiong S., Narismhan G. and Okos M.R. (1991). Effect of composition and pore structure on binding energy and effective diffusivity of moisture in porous food. *J. Food Eng.*, **15**, 187-208.

Zsigmondy R. (1911). Uber die struktur des gels der kieselsaure. Theorie der ententwasserung. *Z. Anorg. Chem.*, **71**, 356.

APPENDIX A1

NOMENCLATURE

a	Amorphous lactose content	kg/kg
a_w	Water activity	
A	Cross sectional area	m^2
A_s	Specific surface area	m^2/m^3
c	BET constant	
c_{pa}	Specific heat capacity of air	J/kg°C
c_{pv}	Specific heat capacity of vapour	J/kg°C
c_{ps}	Specific heat capacity of solid	J/kg°C
C	Concentration	kg/m^3
C_a	Ambient concentration	kg/m^3
C_b	Bulk concentration	kg/m^3
C_i	Initial concentration	kg/m^3
$C_{1,2,3}$	Constants for WLF model	
D	Moisture diffusivity	m^2/s
D'	1st order absorption constant into amorphous lactose	s^{-1}
D_{eff}	Effective moisture diffusivity	m^2/s
E	Molar enthalpy	J/mol
E_L	Molar latent heat	J/mol
E_D	Molar heat of diffusion	J/mol
f	GAB constant	
Fo	Fourier number	
h	Third stage sorption isotherm constant	
H'	Third stage sorption isotherm intermediate	
H	Absolute humidity (except in Ch 3 where it is a tss isotherm constant)	kg H_2O/kg dry air
h_c	Surface heat transfer coefficient	$W/m^2°C$
h_g	Enthalpy in gas phase	J/kg
h_{lv}	Latent heat of vaporisation of water	J/kg
h_s	Enthalpy of solid phase	J/kg
h_v	Enthalpy of water vapour	J/kg
i	General node number	
I	Number of nodes	
j_{vs}	Moisture flux by adsorption onto solid	kg/s
J	Bessels function	
k	Constant for Gordon Taylor equation	
k'	General proportionality constant	
k''	General proportionality constant	
$k_{1,2}$	First order muta-rotation rate constants	s^{-1}
k_{cryst}	α-Lactose crystallisation rate constant	$s^{-0.5}$
K	Avrami rate constant	s^{-3}
L	Slab thickness	m
l	Length	m
m	Counter	
M	Moisture content of solid phase	kg H_2O/kg dry solid

N°	Number of nuclei per unit volume	m^{-3}
M_o	BET mono-layer moisture content	kg H_2O/kg dry solid
n	Avrami co-efficient	
p_v	Vapour pressure	Pa
p_w	Saturated vapour pressure	Pa
p_T	Total pressure	Pa
Q	Total enthalpy in porous matrix	J
r	Radius	m
r_b	Bridge radius	m
r_K	Kelvin radius	m
R	Universal gas constant	J/K/mol
RH	Relative humidity	%
S	Level of saturation	
t	Time	s
t_d	Delay time	s
T	Temperature	°C
T_a	Ambient temperature	°C
T_g	Glass transition temperature	°C
T_0	Characteristic temperature at $M = 0$	°C
T_r	Reference temperature	°C
v	Linear crystal growth rate	m/s
v_o	Linear crystal growth rate at T_g	m/s
V	Volume	m^3
V_O	Molar volume	m^3/mol
w	Weight fraction	kg/kg
W	Total moisture in porous matrix	kg H_2O
W^*	Work	J/mol
x	Axial space dimension	m
$x_{amorphous}$	Thickness of amorphous layer	m
Y	Fraction unaccomplished change	
Y_{av}	Average fraction unaccomplished change	
z	Height	m
R_p	Particle radius	m

Greek letters

α	Thermal diffusivity	m^2/s
β	Beta co-efficient	
γ	Constant relating moisture content to air vapour conc	
δ	Constrictivity in porous media	
Δ	Change	
ϵ	Porosity	
ζ	Roots of $J_{-1}(\mu) = 0$	
η	Viscosity	Pa.s
κ	Boltzmann constant	J/K
θ	Contact angle	rad
λ	Effective thermal conductivity of porous matrix	W/m°C
λ_g	Thermal conductivity of gas phase	W/m°C
λ_s	Thermal conductivity of solid phase	W/m°C
μ	Intermediate in analytical solution	
ξ	Mass average moisture content in amorphous phase	kg/m^3
ρ	Density	kg/m^3
ρ_a	Air density	kg dry air/m^3
ρ_{am}	Amorphous lactose particle density	kg/m^3
ρ_c	Lactose crystal particle density	kg/m^3
ρ_s	Solid phase particle density	kg/m^3
σ	Surface tension	N/m

τ_2	Tortuosity in porous media	
τ_c	Relaxation time for caking	s
ϕ	Caking index	

APPENDIX A2

PSYCHROMETRIC PROPERTIES OF AIR

Using 0°C as a datum for enthalpy the following relations have been used (ASHRAE 1993);

A2.1 DRY AIR ENTHALPY (J/kg dry air)

$$h_a = c_{pa} T \tag{A2.1}$$

A2.2 WATER VAPOUR ENTHALPY (J/kg water vapour)

$$h_v = c_{pv} T + h_{fg} \tag{A2.2}$$

A2.3 DRY AIR DENSITY (kg dry air/m^3)

$$\rho_a = \frac{273.15}{22.4(273.15+T)\left(\frac{1}{29}+\frac{H}{18}\right)} \tag{A2.3}$$

A2.4 VAPOUR PRESSURE (Pa)

$$p_v = \frac{29 H p_T}{18 + 29H} \tag{A2.4}$$

A2.5 SATURATED WATER VAPOUR PRESSURE (Pa)

$$p_w = e^{23.4795 - \frac{3990.56}{T+233.833}} \tag{A2.5}$$

A2.6 SURFACE VAPOUR PRESSURE (Pa)

$$p_s = a_W p_w \tag{A2.6}$$

A2.7 RELATIVE HUMIDITY (%)

$$H_R = \frac{p_v}{p_w} \qquad \text{(A2.7)}$$

A2.8 ABSOLUTE HUMIDITY (kg/kg dry air)

$$H = \frac{18 p_v}{29(p_T - p_v)} \qquad \text{(A2.8)}$$

APPENDIX A3

TRANSPORT MODEL FORMULATION

A3.1 ENTHALPY CONSERVATION EQUATIONS:

A3.1.1 ENTHALPY BALANCE IN THE GAS PHASE

An enthalpy balance in the gas phase of the porous lactose matrix can be written as;

$$\begin{bmatrix}\text{Rate of accumulation}\\ \text{of heat in gas phase}\end{bmatrix} = \begin{bmatrix}\text{Rate of inflow of heat}\\ \text{in diffused vapour}\end{bmatrix} - \begin{bmatrix}\text{Rate of outfow of heat}\\ \text{in diffused vapour}\end{bmatrix} + \begin{bmatrix}\text{Rate of inflow of heat by}\\ \text{conduction in gas phase}\end{bmatrix} - \begin{bmatrix}\text{Rate of outflow of heat by}\\ \text{conduction in gas phase}\end{bmatrix} - \begin{bmatrix}\text{Rate of outflow of heat}\\ \text{in condensing vapour}\end{bmatrix} \tag{A3.1}$$

When converted into equation form this gives;

$$\frac{\partial[h_g.\epsilon.V.\rho_a]}{\partial t} = \left[D.\epsilon.A.\frac{\partial[H.\rho_a.h_v]}{\partial x}\right]_{-ve} - \left[D.\epsilon.A.\frac{\partial[H.\rho_a.h_v]}{\partial x}\right]_{+ve} + \left[\lambda_g.\epsilon.A.\frac{\partial T}{\partial x}\right]_{-ve} - \left[\lambda_g.\epsilon.A.\frac{\partial T}{\partial x}\right]_{+ve} - j_{v\text{-}l}.h_{lv} \tag{A3.2}$$

A3.1.2 ENTHALPY BALANCE IN THE SOLID PHASE

An enthalpy balance in the solid phase of the porous lactose matrix can be written as;

$$\begin{bmatrix}\text{Rate of accumulation}\\ \text{of heat in solid phase}\end{bmatrix} = \begin{bmatrix}\text{Rate of inflow of heat}\\ \text{by conduction}\end{bmatrix} - \begin{bmatrix}\text{Rate of outfow of heat}\\ \text{by conduction}\end{bmatrix} + \begin{bmatrix}\text{Rate of inflow of heat}\\ \text{in condensing vapour}\end{bmatrix} \tag{A3.3}$$

When converted into equation form this gives;

$$\frac{\partial[h_s.(1-\epsilon).V.\rho_s]}{\partial t} = \left[\lambda_s.(1-\epsilon).A.\frac{\partial T}{\partial x}\right]_{-ve} - \left[\lambda_s.(1-\epsilon).A.\frac{\partial T}{\partial x}\right]_{+ve} + j_{v\text{-}s}.h_{lv} \tag{A3.4}$$

A3.1.3 TOTAL ENTHALPY BALANCE

A total enthalpy balance for the whole porous lactose matrix can be written as;

$$\begin{bmatrix} \textit{Total enthalpy} \\ \textit{in bulk lactose} \end{bmatrix} = \begin{bmatrix} \textit{Enthalpy of} \\ \textit{gas phase} \end{bmatrix} + \begin{bmatrix} \textit{Enthapy of} \\ \textit{solid phase} \end{bmatrix} \tag{A3.5}$$

When written as an equation this gives;

$$Q = ([h_g.\epsilon.V.\rho_a)] + ([h_s.(1-\epsilon).V.\rho_s)] \tag{A3.6}$$

Differentiating with respect to time gives;

$$\frac{\partial Q}{\partial t} = \frac{\partial[h_g.\epsilon.V.\rho_a]}{\partial t} + \frac{\partial[h_s.(1-\epsilon).V.\rho_s]}{\partial t} \tag{A3.7}$$

The parallel model for effective thermal conductivity of porous materials is written as;

$$\lambda = \epsilon.\lambda_g + (1-\epsilon).\lambda_s \tag{A3.8}$$

When Eq's (A3.2), (A3.4), (A3.7) and (A3.8) are combined this gives;

$$\frac{\partial Q}{\partial t} = D.\epsilon.V.\frac{\partial^2[H.\rho_a.h_v]}{\partial x} + \lambda.V.\frac{\partial^2 T}{\partial x^2} \qquad \textit{for } t>0 \textit{ and } 0<x<L \tag{A3.9}$$

A3.2 MOISTURE CONSERVATION EQUATIONS:

A3.2.1 MOISTURE BALANCE IN THE GAS PHASE

A moisture balance for the gas phase of the porous lactose matrix can be written as;

$$\begin{bmatrix} \textit{Rate of accumulation of} \\ \textit{moisture in gas phase} \end{bmatrix} \begin{bmatrix} \textit{Rate of inflow of} \\ \textit{moisture by diffusion} \end{bmatrix} \begin{bmatrix} \textit{Rate of outflow of} \\ \textit{moisture by diffusion} \end{bmatrix} - \begin{bmatrix} \textit{Rate of outflow of} \\ \textit{moisture by condensation} \end{bmatrix} \tag{A3.10}$$

When expressed as an equation this results in;

$$\frac{\partial[\epsilon.V.H.\rho_a]}{\partial t} = \left|D.\epsilon.A.\frac{\partial H.\rho_a}{\partial x}\right|_{xw} - \left|D.\epsilon.A.\frac{\partial H.\rho_a}{\partial x}\right|_{xw} - j_{v,s} \tag{A3.11}$$

A3.2.2 MOISTURE BALANCE IN THE SOLID PHASE

A moisture balance for the solid phase of the porous lactose matrix can be written as;

$$\begin{bmatrix} \textit{Rate of accumulation of} \\ \textit{moisture in solid phase} \end{bmatrix} = \begin{bmatrix} \textit{Rate of inflow of} \\ \textit{moisture by condensation} \end{bmatrix} \tag{A3.12}$$

When written in equation form this gives;

$$\frac{\partial[(1-\epsilon).V.M.\rho_s]}{\partial t} = j_{v.s} \tag{A3.13}$$

A3.2.3 TOTAL MOISTURE BALANCE

A total moisture balance for the combined porous lactose matrix can be written as;

$$\begin{bmatrix} \textit{Total moisture} \\ \textit{in bulk lactose} \end{bmatrix} = \begin{bmatrix} \textit{Moisture in} \\ \textit{gas phase} \end{bmatrix} + \begin{bmatrix} \textit{Moisture in} \\ \textit{solid phase} \end{bmatrix} \tag{A3.14}$$

Expressed in equation form this gives;

$$W = [\epsilon.V.H.\rho_a] + [(1-\epsilon).V.M.\rho_s] \tag{A3.15}$$

Differentiating with respect for time gives;

$$\frac{\partial W}{\partial t} = \frac{\partial[\epsilon.V.H.\rho_a]}{\partial t} + \frac{\partial[(1-\epsilon).V.M.\rho_s]}{\partial t} \tag{A3.16}$$

Combining Eq's (A3.11), (A3.13) and (A3.16) gives;

$$\frac{\partial W}{\partial t} = D.\epsilon.V.\frac{\partial^2 H.\rho_a}{\partial x^2} \qquad \textit{for } t>0, \textit{ and } 0<x<L \tag{A3.17}$$

A3.3 INITIAL CONDITIONS:

$$T = f(T_{initial}) \qquad \textit{for all } x \textit{ at } t = 0 \tag{A3.18}$$

$$W = f(RH_{initial}) \qquad \textit{for all } x \textit{ at } t = 0 \qquad \text{(A3.19)}$$

From these initial conditions all other initial values in the model can be calculated (ie. T, RH, M, H, ρ_a).

A3.4 BOUNDARY CONDITIONS:

A third kind of boundary condition (heat conduction) over both the top and bottom boundaries is used to describe heat transfer over the boundaries. This is more consistent with the experimental apparatus than assuming a constant boundary temperature (first kind of boundary condition) as the plates take some time to heat up after a step change has been applied.

$$h_c (T - T_a) = 0 \qquad \textit{for } t \geq 0 \textit{ at } x = 0, L \qquad \text{(A3.20)}$$

No moisture diffusion occurs over the top and bottom boundaries so a symmetry (fifth kind of boundary condition) is used to describe transport of moisture at the boundaries.

$$\frac{\partial (H\rho_a)}{\partial x} = 0 \qquad \textit{for } t \geq \textit{ at } x = 0, L \qquad \text{(A3.21)}$$

APPENDIX A4

FINITE DIFFERENCE EQUATIONS

A4.1 DEFINITION OF FINITE DIFFERENCE GRID:

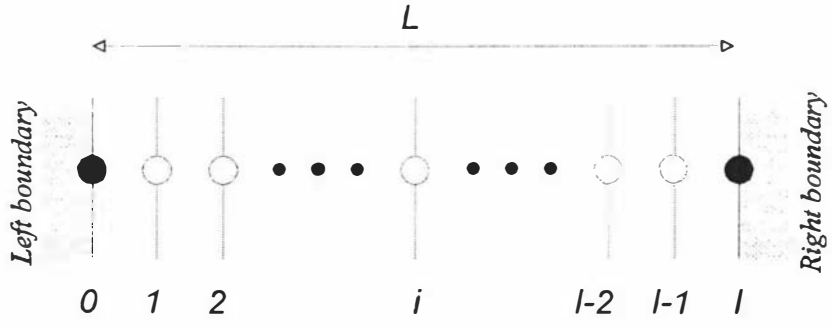

Figure A4.1 - Finite difference grid for transport model solution.

A4.2 FINITE DIFFERENCE APPROXIMATIONS:

A4.2.1 GENERAL INTERNAL NODES ($1 \le i \le I-1$):

$$Q_i^{new} = Q_i + \frac{V\Delta t}{\Delta x^2}\left[\lambda(1-\epsilon)[T_{i-1}-2T_i+T_{i+1}] + D\epsilon h_v(T_{i-1})[(H\rho_a)_{i-1}-(H\rho_a)_i] - D\epsilon h_v(T_i)[(H\rho_a)_i-(H\rho_a)_{i+1}]\right] \quad \text{(A4.1)}$$

$$(H\rho_a)_i^{new} = (H\rho_a)_i + \frac{D\Delta t}{\Delta x^2}\left[(H\rho_a)_{i-1}-2(H\rho_a)_i+(H\rho_a)_{i+1}\right] \quad \text{(A4.2)}$$

$$T_i = \frac{(Q_i - Hh_v(T_i)\epsilon V\rho_a)}{\epsilon V\rho_a(c_{p_a}+Hc_{p_v})+(1-\epsilon)V\rho_s(c_{p_s}+Mc_{p_w})} \quad \text{(A4.3)}$$

$$H_0 = \frac{W_0-(1-\epsilon)V\rho_s M_0}{\epsilon V\rho_a} \quad \text{(A4.4)}$$

$$M_i = f(H) \qquad \textit{(moisture sorption isotherm)} \tag{A4.5}$$

$$Y_i^{new} = Y_i + \Delta t\, n(1-Y_i)[-\ln(1-Y_i)]^{\frac{n-1}{n}} K^{\frac{1}{n}} \tag{A4.6}$$

A4.2.2 LEFT HAND BOUNDARY NODE (i = 0):

$$Q_0^{new} = Q_0 + \frac{2V\Delta t}{\Delta x^2}\left[h_c \Delta x[T_{a1} - T_0] - \lambda(1-\epsilon)[T_0 - T_1] - D\epsilon h_v(T_0)[(H\rho_a)_0 - (H\rho_a)_1] \right] \tag{A4.7}$$

$$(H\rho_a)_0^{new} = (H\rho_a)_0 - \frac{2D\Delta t}{\Delta x^2}\left[(H\rho_a)_0 - (H\rho_a)_1\right] \tag{A4.8}$$

$$T_0 = \frac{(2Q_0 - Hh_v(T_0)\epsilon V\rho_a)}{\epsilon V\rho_a(c_{p_a} + Hc_{p_v}) + (1-\epsilon)V\rho_s(c_{p_s} + Mc_{p_w})} \tag{A4.9}$$

$$H_0 = \frac{2W_0 - (1-\epsilon)V\rho_s M_0}{\epsilon V\rho_a} \tag{A4.10}$$

$$M_0 = f(H) \qquad \textit{(moisture sorption isotherm)} \tag{A4.11}$$

$$Y_0^{new} = Y_0 + \Delta t\, n(1-Y_0)[-\ln(1-Y_0)]^{\frac{n-1}{n}} K^{\frac{1}{n}} \tag{A4.12}$$

A4.2.3 RIGHT HAND BOUNDARY NODE (i = I):

$$Q_I^{new} = Q_I + \frac{2V\Delta t}{\Delta x^2}\left[\lambda(1-\epsilon)[T_{I-1} - T_I] + D\epsilon h_v(T_{I-1})[(H\rho_a)_{I-1} - (H\rho_a)_I] - h_c \Delta x[T_{a2} - T_I] \right] \tag{A4.13}$$

$$(H\rho_a)_I^{new} = (H\rho_a)_I + \frac{2D\Delta t}{\Delta x^2}\left[(H\rho_a)_{I-1} - (H\rho_a)_I\right] \tag{A4.14}$$

$$T_I = \frac{(2Q_I - Hh_v(T_I)\epsilon V\rho_a)}{\epsilon V\rho_a(c_{p_a} + Hc_{p_v}) + (1-\epsilon)V\rho_s(c_{p_s} + Mc_{p_w})} \tag{A4.15}$$

$$H_I = \frac{2W_I - (1-\epsilon)V\rho_s M_I}{\epsilon V \rho_a} \qquad \text{(A4.16)}$$

$$M_I = f(H) \qquad \textit{(moisture sorption isotherm)} \qquad \text{(A4.17)}$$

$$Y_I^{new} = Y_I + \Delta t\, n(1-Y_I)[-\ln(1-Y_I)]^{\frac{n-1}{n}} K^{\frac{1}{n}} \qquad \text{(A4.18)}$$

APPENDIX A5

PROGRAM SOURCE CODE

A5.1 PROGRAM DESCRIPTION:

The model was subdivided into its constituent objects. The program as a whole is represented as the unit LactCake.cpp. This includes initialisation of variables, functions for printing out results, finite difference equations and the code which controls the model solution.

The Node unit specifies the declaration of four classes. The class Node, is a generalised node which contains the commonalities that exist for all the nodes in the finite difference solution. The Node is made up of Air and Lactose objects. The classes InternalNode, LeftNode and RightNode are derived from class Node with the addition of a function describing the transport of heat and moisture from each node.

The Lactose unit declares a class describing the properties of lactose, including moisture relations, glass transitions etc.

The AirProps unit declares a class which describes air. The air state is defined by setting the pressure, temperature and humidity. From these three variables all of the other properties of air are calculated. It is in a form suitable for adding to any C++ program requiring an air object.

A5.2 LACTCAKE UNIT:

A5.2.1 LACTCAKE.CPP:

```
//. ***************************************************************************
//.              Program "LactCake.cpp"    © John Bronlund 1997
//. ***************************************************************************

#include <iostream.h>
#include <fstream.h>
#include <string.h>
#include "Node.h"
#include "Lactose.h"
#include "AirProps.h"

enum {size = 200};
char filename[13];
```

```
ofstream outfile_RH;
ofstream outfile_Am;
ofstream outfile_Temp;
ofstream outfile_Tg;

InternalNode Inside[size];
LeftNode BottomNode;
RightNode TopNode;
Ambient BottomAmbient("Bottom"),TopAmbient("Top");

int NumberNodes;
double Tfinish,Tprint;
enum OutType {Temp,MC,RH,Humidity,Hrhoa,Tg,Amorph,Strength};

void PrintOut(OutType x) {

    if (x==Hrhoa) {cout << Node::Time << "  ";}
    int i;
    switch(x) {
        case Temp:
      cout << Node::Time << "   ";
          cout << BottomNode.L.Temperature << "  ";
          outfile_Temp << Node::Time << "  ";
          outfile_Temp << BottomNode.L.Temperature << "  ";
          for (i=1;i<NumberNodes;i=i+1) {
            cout << Inside[i].L.Temperature << "  ";
            outfile_Temp << Inside[i].L.Temperature << "  ";
          };
          cout << TopNode.L.Temperature << endl;
          outfile_Temp << TopNode.L.Temperature << endl;
          break;

    case Hrhoa:
          //cout << BottomNode.L.PercentAmorph << "  ";
          outfile_RH << Node::Time << "  ";
          outfile_RH << BottomNode.L.Humidity/* *BottomNode.L.AirDensity()*/ << "  ";
          for (i=1;i<NumberNodes;i=i+1) {
            // cout << Inside[i].L.PercentAmorph << "  ";
            outfile_RH << Inside[i].L.Humidity/* *Inside[i].L.AirDensity()*/ << "  ";
          };
          //cout << TopNode.L.RH << endl;
          outfile_RH << TopNode.L.Humidity/* *TopNode.L.AirDensity()*/   << endl;
          break;

    case Strength:
      cout << Node::Time << "   ";
          cout << BottomNode.L.LumpingStrength() << "  ";
          outfile_Temp << Node::Time << "  ";
          outfile_Temp << BottomNode.L.LumpingStrength() << "  ";
          for (i=1;i<NumberNodes;i=i+1) {
            //cout << Inside[i].L.LumpingStrength << "  ";
            outfile_Temp << Inside[i].L.LumpingStrength() << "  ";
          };
          cout << TopNode.L.LumpingStrength() << endl;
          outfile_Temp << TopNode.L.LumpingStrength()  << endl;
```

```
            break;

          case Amorph:
         //cout << Node::Time << "  ";
            //cout << BottomNode.L.RateConstant() << "  ";
            outfile_Am << Node::Time << "  ";
            outfile_Am << BottomNode.L.PercentAmorph << "  ";
            for (i=1;i<NumberNodes;i=i+1) {
              //cout << Inside[i].L.RateConstant() << "  ";
              outfile_Am << Inside[i].L.PercentAmorph << "  ";
            };
            //cout << TopNode.L.RateConstant() << endl;
            outfile_Am << TopNode.L.PercentAmorph << endl;
            break;

          case RH:
            outfile_RH << Node::Time << "  ";
            //cout << BottomNode.L.RH() << "  ";
            outfile_RH << BottomNode.L.RH() << "  ";
            for (i=1;i<NumberNodes;i=i+1) {
              //cout << Inside[i].L.RH() << "  ";
              outfile_RH << Inside[i].L.RH() << "  ";
            };
            //cout << TopNode.L.RH() << endl;
            outfile_RH << TopNode.L.RH() << endl;
            break;

       case MC:
         outfile_Temp << Node::Time << "  ";
         outfile_Temp << BottomNode.L.MoistureContent() << "  ";
         for (i=1;i<NumberNodes;i=i+1) {
           outfile_Temp << Inside[i].L.MoistureContent() << "  ";
         };
         outfile_Temp << TopNode.L.MoistureContent() << endl;
          break;

          case Tg:
          //cout << Node::Time << "  ";
         //cout << (BottomNode.L.Temperature-BottomNode.L.TGlass()) << "  ";
            outfile_Tg << Node::Time << "  ";
         outfile_Tg << (BottomNode.L.Temperature-BottomNode.L.TGlass()) << "  ";
            for (i=1;i<NumberNodes;i=i+1) {
              //cout << (Inside[i].L.Temperature-Inside[i].L.TGlass()) << "  ";
           outfile_Tg << (Inside[i].L.Temperature-Inside[i].L.TGlass()) << "  ";
            };
            //cout << (TopNode.L.Temperature-TopNode.L.TGlass()) << endl;
         outfile_Tg << (TopNode.L.Temperature-TopNode.L.TGlass()) << endl;
          }

};

void main() {

OutType X1=Amorph;
OutType X2=RH;
```

```
OutType X3=Tg;
OutType X4=Temp;
cin.width(sizeof(filename));
cout << "Results file name                " << '\t';
cin >> filename;
cout << endl;
char fname[13];
char gname[13];
char hname[13];
strncpy(fname,filename,13);
strncpy(gname,filename,13);
strncpy(hname,filename,13);

outfile_RH.open(strcat(fname,".RH"));
if(!outfile_RH) cerr<<"couldn't open RH outfile"<<endl;

outfile_Am.open(strcat(filename,".amf"));
if(!outfile_Am) cerr<<"couldn't open amf outfile"<<endl;


outfile_Temp.open(strcat(gname,".tmp"));
if(!outfile_Temp) cerr<<"couldn't open temp outfile"<<endl;

outfile_Tg.open(strcat(hname,".tg"));
if(!outfile_Tg) cerr<<"couldn't open TG outfile"<<endl;

Node::Time = 0;

cout << "Time step                        " << '\t';
cin >> Node::dt;
cout << "Print out interval        " << '\t';
cin >> Tprint;
cout << "Total Simulation time          "       << '\t';
cin >> Tfinish;

//*****************************************************************************
// Setup Lactose Conditions
//*****************************************************************************

cout << "Number of nodes         " << '\t';
cin >> NumberNodes;

double Thickness;
cout << "Slab thickness                  " << '\t';
cin >> Thickness;
Node::dx = (Thickness/NumberNodes);

char answer;
cout << "Initialise each node seperately?   " << '\t';
cin >> answer;
if (answer == 'n') {
    double IntA,IntB,IntC,IntD,IntE;
    cout << "Initial Lactose Temperature (°C)" << '\t';
    cin >> IntA;
    cout << "Initial Lactose Water Activity  " << '\t';
```

```
cin >> IntB;
cout << "Initial Percent Amorphous       " << '\t';
cin >> IntC;
cout << "Initial Crystallinity of Amorphous" << '\t';
cin >> IntD;
cout << "Porosity          " << '\t';
cin >> IntE;

BottomNode.L.SetAirProps("Temperature",IntA,"RH",IntB);
if (IntD == 0) {
    BottomNode.L.SetAmorphous("PercentAmorph",IntC);}
else {
    BottomNode.L.SetAmorphous("PercentAmorph",IntC,"Crystallinity",IntD);};
if (IntE == 0) {}
else {BottomNode.L.SetPorosity(IntE);};
BottomNode.Water = BottomNode.L.Porosity*BottomNode.Vol*BottomNode.L.Humidity
    *BottomNode.L.AirDensity()+(1-BottomNode.L.Porosity)*BottomNode.Vol
    *BottomNode.L.ParticleDensity*BottomNode.L.MoistureContent();
BottomNode.Heat = (BottomNode.L.DryAirSpecHeat*BottomNode.L.Temperature
    +BottomNode.L.Humidity*(BottomNode.L.WaterVapSpecHeat
    *BottomNode.L.Temperature+BottomNode.L.LatentHeat))*BottomNode.L.Porosity
    *BottomNode.Vol*BottomNode.L.AirDensity()+(BottomNode.L.LactoseSpecHeat
    *BottomNode.L.Temperature+BottomNode.L.WaterSpecHeat*BottomNode.L.Temperature
    *BottomNode.L.MoistureContent())*(1-BottomNode.L.Porosity)*BottomNode.Vol
    *BottomNode.L.ParticleDensity;

TopNode.L.SetAirProps("Temperature",IntA,"RH",IntB);
if (IntD == 0) {
    TopNode.L.SetAmorphous("PercentAmorph",IntC);}
else {
    TopNode.L.SetAmorphous("PercentAmorph",IntC,"Crystallinity",IntD);};
if (IntE == 0) {}
else {TopNode.L.SetPorosity(IntE);};
TopNode.Water = TopNode.L.Porosity*TopNode.Vol*TopNode.L.Humidity
    *TopNode.L.AirDensity()+(1-TopNode.L.Porosity)*TopNode.Vol
    *TopNode.L.ParticleDensity*TopNode.L.MoistureContent();
TopNode.Heat = (TopNode.L.DryAirSpecHeat*TopNode.L.Temperature
    +TopNode.L.Humidity*(TopNode.L.WaterVapSpecHeat
    *TopNode.L.Temperature+TopNode.L.LatentHeat))*TopNode.L.Porosity
    *TopNode.Vol*TopNode.L.AirDensity()+(TopNode.L.LactoseSpecHeat
    *TopNode.L.Temperature+TopNode.L.WaterSpecHeat*TopNode.L.Temperature
    *TopNode.L.MoistureContent())*(1-TopNode.L.Porosity)*TopNode.Vol
    *TopNode.L.ParticleDensity;

for (int i = 1;i < NumberNodes;i=i+1) {
    Inside[i].L.SetAirProps("Temperature",IntA,"RH",IntB);
    if (IntD == 0) {
      Inside[i].L.SetAmorphous("PercentAmorph",IntC);}
    else {
      Inside[i].L.SetAmorphous("PercentAmorph",IntC,"Crystallinity",IntD);};
    if (IntE == 0) {}
    else {Inside[i].L.SetPorosity(IntE);};
    Inside[i].Water = Inside[i].L.Porosity*Inside[i].Vol*Inside[i].L.Humidity
      *Inside[i].L.AirDensity()+(1-Inside[i].L.Porosity)*Inside[i].Vol
      *Inside[i].L.ParticleDensity*Inside[i].L.MoistureContent();
```

```
        Inside[i].Heat = (Inside[i].L.DryAirSpecHeat*Inside[i].L.Temperature
          +Inside[i].L.Humidity*(Inside[i].L.WaterVapSpecHeat
          *Inside[i].L.Temperature+Inside[i].L.LatentHeat))*Inside[i].L.Porosity
          *Inside[i].Vol*Inside[i].L.AirDensity()+(Inside[i].L.LactoseSpecHeat
          *Inside[i].L.Temperature+Inside[i].L.WaterSpecHeat*Inside[i].L.Temperature
          *Inside[i].L.MoistureContent())*(1-Inside[i].L.Porosity)*Inside[i].Vol
          *Inside[i].L.ParticleDensity;
    };
}
else {};

//*****************************************************************************
// Setup Ambient Conditions
//*****************************************************************************

BottomAmbient.GetAndSetValues();
TopAmbient.GetAndSetValues();
cout << endl;cout << endl;
PrintOut(X1);
PrintOut(X2);
PrintOut(X3);
PrintOut(X4);

//*****************************************************************************
// Start of program proper
//*****************************************************************************
double Telapsed;

while (Node::Time <= Tfinish) {
    Node::Time = Node::Time + Node::dt;
    Telapsed = Telapsed + Node::dt;
    BottomAmbient.UpdateAmbient(Node::Time);
    TopAmbient.UpdateAmbient(Node::Time);

    BottomNode.Transport(BottomAmbient,Inside[1]);
    Inside[1].Transport(BottomNode,Inside[2]);
    for(int i=2;i < (NumberNodes-1);i=i+1) {
        Inside[i].Transport(Inside[i-1],Inside[i+1]);
    };
    Inside[NumberNodes-1].Transport(Inside[NumberNodes-2],TopNode);
    TopNode.Transport(Inside[NumberNodes-1],TopAmbient);

    BottomNode.UpdateAir();
    for (int i=1;i<NumberNodes;i=i+1) {
        Inside[i].UpdateAir();
    };
    TopNode.UpdateAir();

    if (Telapsed >= Tprint) {
        PrintOut(X1);
        PrintOut(X2);
    PrintOut(X3);
    PrintOut(X4);
        Telapsed = 0;
        };
```

```
};
PrintOut(X1);
PrintOut(X2);
};
```

A5.3 NODE UNIT:

A5.3.1 NODE.H:

```
#ifndef Node_H_
#define Node_H_

#include <iostream.h>
#include <stdlib.h>
#include "Lactose.h"
#include "AirProps.h"

enum Boolean {Yes, No};

class Ambient {
public:
char label[10];
Boolean ConstantTemperature;
double Temperature;
double TempArray[400];
double TimeInterval;
double htc;
friend iostream;
friend fstream;

Ambient(char* nm);
void SetAmbient(double temp,double h);
void GetAndSetValues();
void UpdateAmbient(double t);
};

class Node {

public:

Lactose L;
static double Time;
static double dt;
static double dx;
double Heat;
double Water;
double Vol;
double Tempnew,EffMCnew;
Node();
void SetNode(char inA[],double ina,char inB[],double inb,char inC[],double inc,
     char inD[] = "None",double ind = 42,char inE[] = "None",double ine = 42);
void GetAndSetValues();
void UpdateAir();
```

```
};

class InternalNode : public Node {
public:
void Transport(Node L_Node, Node R_Node);

};

class LeftNode : public Node {
public:
void Transport(Ambient L_Node,Node R_Node);
};

class RightNode : public Node {
public:
void Transport(Node L_Node,Ambient R_Node);
};

#endif   //Node_H_
```

A5.3.2 NODE.CPP:

```
#include <string.h>
#include <math.h>
#include <iostream.h>
#include <fstream.h>
#include "Lactose.h"
#include "AirProps.h"
#include "Node.h"


double Node::dt=0;
double Node::dx=0;
double Node::Time=0;

double aow=0.0;//526;

Ambient::Ambient(char* nm) {
    strcpy(label,nm);
    SetAmbient(20,60);
    TimeInterval=300;
};

void Ambient::SetAmbient(double temp,double h) {
    int I=0;
    while(!(I>300)) {
        TempArray[I]=temp;
        I++;
    }
    htc = h;
};

void Ambient::GetAndSetValues() {
```

```
    double IntA,IntB;
    char answer;
    cout << "Use constant temperature for " << label << " (y/n)?" << '\t';
    cin >> answer;
    if (answer == 'n') {
        char filename[13];
        cout << "Enter temperature history filename ";
        cin >> filename;
        ifstream infile(filename);
        int I=0;
        while(!infile.eof()) {
          infile >> TempArray[I];
          I++;
        }
        infile.close();
        cout << "Enter time interval for file" << filename;
        cin >> TimeInterval;
        cout << "Enter heat transfer coefficient          ";
        cin >> htc;
    }
    else {
        cout << label << " Boundary Temperature (°C)   " << '\t';
        cin >> IntA;
        cout << label << " Boundary HTC              " << '\t';
        cin >> IntB;
        SetAmbient(IntA,IntB);
        }
};

void Ambient::UpdateAmbient(double t) {
    double fract;
    double Int;
      fract = modf((t/TimeInterval),&Int);
    int I=(int)Int;
      Temperature = TempArray[I]+(TempArray[I+1]-TempArray[I])*fract/TimeInterval;
};

Node::Node() {
    Vol = 1e-5;
    Water = 0;
    Heat = 0;
};

void Node::GetAndSetValues() {
    double IntA,IntB;
    cout << "Initial Lactose Temperature (°C)" << '\t';
    cin >> IntA;
    cout << "Initial Lactose Water Activity  " << '\t';
    cin >> IntB;
    L.SetAirProps("Temperature",IntA,"RH",IntB);
    cout << "Initial Percent Amorphous                    " << '\t';
    cin >> IntA;
    cout << "Initial Crystallinity of Amorphous" << '\t';
    cin >>IntB;
    if (IntB ==0) {L.SetAmorphous("PercentAmorph",IntA);}
```

```
    else {L.SetAmorphous("PercentAmorph",IntA,"Crystallinity",IntB);};
    cout << "Porosity                                    " << '\t';
    cin >> IntB;
    if (IntB == 0) {L.SetPorosity();}
    else {L.SetPorosity(IntB);};
};

void Node::UpdateAir() {
    L.SetAirProps("Temperature",Tempnew,"RH",L.RH("EffectiveMC",EffMCnew));
};

void InternalNode::Transport(Node L_Node, Node R_Node) {
double Tempmin = (L.Temperature+L_Node.L.Temperature)/2;
double Tempmax = (L.Temperature+R_Node.L.Temperature)/2;
Heat = Heat+dt*Vol/pow(dx,2)*L.TConduct*(L_Node.L.Temperature
          -2*L.Temperature+R_Node.L.Temperature)
          +L.Diffusivity("Temperature",Tempmin)*(L.WaterVapSpecHeat*Tempmin
          +L.LatentHeat)*(L_Node.L.Humidity*L_Node.L.AirDensity()
          -L.Humidity*L.AirDensity())
          -L.Diffusivity("Temperature",Tempmax)*(L.WaterVapSpecHeat*Tempmax
          +L.LatentHeat)*(L.Humidity*L.AirDensity()
          -R_Node.L.Humidity*R_Node.L.AirDensity());
double PAmorphOld=L.PercentAmorph;
L.NewAmorphState(dt);
Water = Water+dt*Vol/pow(dx,2)*(L.Diffusivity("Temperature",Tempmin)
          *(L_Node.L.Humidity*L_Node.L.AirDensity()-L.Humidity*L.AirDensity())
          -L.Diffusivity("Temperature",Tempmax)*(L.Humidity*L.AirDensity()
          -R_Node.L.Humidity*R_Node.L.AirDensity()));
Water = Water-Vol*(1-L.Porosity)*L.ParticleDensity*aow*(PAmorphOld-L.PercentAmorph);

double diffMC = L.MoistureContent();
double diffT = L.Temperature;
double EffMC = L.MoistureContent();
double Temp = L.Temperature;
while ((fabs(diffMC)>1e-50) && (fabs(diffT)>1e-2)) {
    Tempnew = (Heat-Vol*L.Porosity*L.AirDensity("Temperature",Temp)*L.LatentHeat
        *L.AirHumidity("RH",L.RH("EffectiveMC",EffMC),"Temperature",Temp))
        /(Vol*L.Porosity*L.AirDensity("Temperature",Temp)*(L.DryAirSpecHeat
        +L.AirHumidity("RH",L.RH("EffectiveMC",EffMC),"Temperature",Temp)
        *L.WaterVapSpecHeat)+(1-L.Porosity)*Vol*L.ParticleDensity
        *(L.LactoseSpecHeat+EffMC*L.WaterSpecHeat));
    EffMCnew = (Water-L.Porosity*Vol*L.AirHumidity("RH",L.RH("EffectiveMC"
        ,EffMC),"Temperature",Temp)*L.AirDensity("Temperature",Temp))
        /((1-L.Porosity)*Vol*L.ParticleDensity);
    diffT = Temp-Tempnew;
    diffMC = EffMC-EffMCnew;
    Temp = Tempnew;
    EffMC = EffMCnew;
}
};

void LeftNode::Transport(Ambient L_Node, Node R_Node) {
double Tempmax = (L.Temperature+R_Node.L.Temperature)/2;

Heat = Heat+2*dt*Vol/dx*(L_Node.htc*(L_Node.Temperature
```

```
        -L.Temperature)-L.TConduct/dx*(L.Temperature-R_Node.L.Temperature)
        -L.Diffusivity("Temperature",Tempmax)/dx*(L.WaterVapSpecHeat*Tempmax
        +L.LatentHeat)*(L.Humidity*L.AirDensity()
        -R_Node.L.Humidity*R_Node.L.AirDensity()));
double PAmorphOld=L.PercentAmorph;
L.NewAmorphState(dt);
Water = Water+2*dt*Vol/pow(dx,2)*(-L.Diffusivity("Temperature",Tempmax)
        *(L.Humidity*L.AirDensity()-R_Node.L.Humidity*R_Node.L.AirDensity()));
Water = Water-Vol*(1-L.Porosity)*L.ParticleDensity*aow*(PAmorphOld-L.PercentAmorph);

double diffMC = L.MoistureContent();
double diffT = L.Temperature;
double EffMC = L.MoistureContent();
double Temp = L.Temperature;
while ((fabs(diffMC)>1e-50) && (fabs(diffT)>1e-2)) {
    Tempnew = (Heat-Vol*L.Porosity*L.AirDensity("Temperature",Temp)*L.LatentHeat
        *L.AirHumidity("RH",L.RH("EffectiveMC",EffMC),"Temperature",Temp))
        /(Vol*L.Porosity*L.AirDensity("Temperature",Temp)*(L.DryAirSpecHeat
        +L.AirHumidity("RH",L.RH("EffectiveMC",EffMC),"Temperature",Temp)
        *L.WaterVapSpecHeat)+(1-L.Porosity)*Vol*L.ParticleDensity
        *(L.LactoseSpecHeat+EffMC*L.WaterSpecHeat));
    EffMCnew = (Water-L.Porosity*Vol*L.AirHumidity("RH",L.RH("EffectiveMC"
        ,EffMC),"Temperature",Temp)*L.AirDensity("Temperature",Temp))
        /((1-L.Porosity)*Vol*L.ParticleDensity);
    diffT = Temp-Tempnew;
    diffMC = EffMC-EffMCnew;
    Temp = Tempnew;
    EffMC = EffMCnew;
}
};

void RightNode::Transport(Node L_Node,Ambient R_Node) {
double Tempmin = (L.Temperature+L_Node.L.Temperature)/2;
Heat = Heat+2*dt*Vol/dx*(-R_Node.htc*(L.Temperature-R_Node.Temperature)
        +L.TConduct/dx*(L_Node.L.Temperature-L.Temperature)
        +L.Diffusivity("Temperature",Tempmin)/dx*(L.WaterVapSpecHeat*Tempmin
        +L.LatentHeat)*(L_Node.L.Humidity*L_Node.L.AirDensity()-L.Humidity*L.AirDensity()));
double PAmorphOld=L.PercentAmorph;
L.NewAmorphState(dt);
Water = Water+2*dt*Vol/pow(dx,2)*(L.Diffusivity("Temperature",Tempmin)
        *(L_Node.L.Humidity*L_Node.L.AirDensity()-L.Humidity*L.AirDensity()));
Water = Water-Vol*(1-L.Porosity)*L.ParticleDensity*aow*(PAmorphOld-L.PercentAmorph);

double diffMC = L.MoistureContent();
double diffT = L.Temperature;
double EffMC = L.MoistureContent();
double Temp = L.Temperature;
while ((fabs(diffMC)>1e-50) && (fabs(diffT)>1e-2)) {
    Tempnew = (Heat-Vol*L.Porosity*L.AirDensity("Temperature",Temp)*L.LatentHeat
        *L.AirHumidity("RH",L.RH("EffectiveMC",EffMC),"Temperature",Temp))
        /(Vol*L.Porosity*L.AirDensity("Temperature",Temp)*(L.DryAirSpecHeat
        +L.AirHumidity("RH",L.RH("EffectiveMC",EffMC),"Temperature",Temp)
        *L.WaterVapSpecHeat)+(1-L.Porosity)*Vol*L.ParticleDensity
        *(L.LactoseSpecHeat+EffMC*L.WaterSpecHeat));
    EffMCnew = (Water-L.Porosity*Vol*L.AirHumidity("RH",L.RH("EffectiveMC"
```

```
        ,EffMC),"Temperature",Temp)*L.AirDensity("Temperature",Temp))
        /((1-L.Porosity)*Vol*L.ParticleDensity);
    diffT = Temp-Tempnew;
    diffMC = EffMC-EffMCnew;
    Temp = Tempnew;
    EffMC = EffMCnew;
}
};
```

A5.4 LACTOSE UNIT:

A5.4.1 LACTOSE.H:

```
// ********************************************************
//
// ************************ lactose.h *********************
//
// A class for characterisation of lactose in equilibrium with air.
//
// This class defines the fundamental properties of lactose as
// amorphous content, water activity all other properties are obtained
// through function calls.
// ********************************************************

#ifndef Lactose_H_
#define Lactose_H_

#include "airprops.h"

class Lactose : public AirProps {

    public:

    double Porosity;            // voidage fraction
    double PercentAmorph;       // amount of amorphous material
    double Crystallinity;       // crystallinity of amorphous portion

    double TConduct;                // effective thermal conductivity

    const double ParticleDensity;  // lactose particle density kg/m3
    const double LactoseSpecHeat;  // lactose specific heat capacity J/kg°C
    const double WaterSpecHeat;    // liquid water specific heat capacity J/kg°C

    //constructor
    Lactose();              // sets porosity, airspace,PercentAmorph and Crystallinity

    void SetAmorphous(char INa[],double a,char INb[]="Crystallinity",double b = 1e-15);
    void SetPorosity(double epsilon = 0.4);

    void NewAmorphState(double timestep);
    double NewCrystallinity(double timestep);
    double RateConstant();
    double TGlass();
    double MoistureContent(char IN[]="None",double in=42,
```

```
            char INb[]="None",double inb=42);
            // effective moisture content f(RH) kg/kg dry lactose
    double MC_Alpha(char IN[]="None",double in=42);
            // moisture content of crystalline lactose kg/kg dry lactose
    double MC_Amorphous(char IN[]="None",double in=42);
            // moisture content of amorphous lactose kg/kg dry lactose
    double Diffusivity(char IN[]="None",double in=42);
  double RH();
    double RH(char INa[],double a,char INb[]="None",double b = 42);
  double LumpingStrength();

};

#endif   //Lactose_H_
```

A5.4.2 LACTOSE.CPP:

```
// ********************************************************
//
// ********************** lactose.cpp *********************
//
// A class for characterisation of lactose in equilibrium with air.
//
// This class defines the fundamental properties of lactose as
// amorphous content, water activity all other properties are obtained
// through function calls.
// ********************************************************

#include "airprops.h"
#include "lactose.h"
#include <string.h>
#include <math.h>

Lactose::Lactose() :
    AirProps("Humidity",0.011,"Temperature",20),
    ParticleDensity(1540),
    LactoseSpecHeat(1250),
    WaterSpecHeat(4180) {
    SetPorosity();
    TConduct = 0.175;
    SetAmorphous("PercentAmorph",0.05,"Crystallinity",1e-18);
};

void Lactose::SetPorosity(double epsilon) {
    Porosity = epsilon;
};

void Lactose::SetAmorphous(char INa[],double a,char INb[], double b) {
    if (stricmp(INa,"Crystallinity") == 0) {
        char * INc = INa;
        double c = a;
        INa = INb;
        a = b;
```

```
        INb = INc;
        b = c;
    }
    if (stricmp(INa,"PercentAmorph") == 0) {
        PercentAmorph = a;
    }
    if (stricmp(INb,"Crystallinity") == 0) {
        Crystallinity = b;
    }
};

void Lactose::NewAmorphState(double timestep) {
    if ((1-Crystallinity)>0) {
    PercentAmorph = PercentAmorph/(1-Crystallinity)*(1-NewCrystallinity(timestep));
    Crystallinity = NewCrystallinity(timestep);
  }
  else Crystallinity=1;
};

double Lactose::NewCrystallinity(double timestep) {
    const double Avrami_m = 3;

    double dummy_Cry;
    if ((PercentAmorph > 0) && (RateConstant() > 0) && (Crystallinity < 1)) {
        dummy_Cry = Crystallinity+timestep*Avrami_m*(1-Crystallinity)*
            pow((-log(1-Crystallinity)),(Avrami_m-1)/Avrami_m)*
            pow(RateConstant(),(1/Avrami_m));
    }
    else {dummy_Cry = Crystallinity;}

    if (dummy_Cry > 1) { dummy_Cry = 1;}
    return dummy_Cry;
};

double Lactose::RateConstant() {
    const double Avrami = 3;
  const double C1 = 35.43;
  const double C2 = 108.38;
  const double C3 = 3e27;
  double K;
  if (Temperature > TGlass()) {
    K=C3*pow(exp(-C1/(8.314e-3*(C2+Temperature-TGlass()))),Avrami);
  }
    else {K = 0;};
  return K;
};

double Lactose::TGlass() {
    const double Tg1 = 101;
    const double Tg2 = -135;
    const double K = 6.7;
    return ((1-MC_Amorphous())*Tg1+K*MC_Amorphous()*Tg2)/
            ((1-MC_Amorphous())+K*MC_Amorphous());
};
```

```
double Lactose::MoistureContent(char INa[],double ina,char INb[],double inb) {

    if (stricmp(INa,"None") == 0) {
        INa = "RH";
        ina = RH();
    }
    if (stricmp(INb,"None") == 0) {
        inb = PercentAmorph;
    }
    return MC_Alpha(INa,ina)+MC_Amorphous(INa,ina)*inb;
};

double Lactose::MC_Alpha(char IN[],double in) {
    const double Vmtss = 2.5e-4;
    const double ctss = 8.8;
    const double ktss = 0.92;
    const double htss = 30;

    if (stricmp(IN,"None") == 0) {
        IN = "RH";
        in = RH();
    }

    double HH = 1+(1-ktss)/ktss*exp(htss*log(ktss*in))/(1-in);
    double HHH = 1+(HH-1)/HH*(1-ktss*in)/(1-in)*(htss+(1-htss)*in);
    return Vmtss*ctss*ktss*in*HH*HHH/((1-ktss*in)*(1+(ctss*HH-1)*ktss*in));
};

double Lactose::MC_Amorphous(char IN[],double in) {
    const double VmGAB = 0.0488;                    //0.048;
    const double cGAB =  3.23;                      //2;
    const double kGAB = 1.159;                      //1.25;

    if (stricmp(IN,"None") == 0) {
        IN = "RH";
        in = RH();
    }
    return VmGAB*cGAB*kGAB*in/((1-kGAB*in)*(1+(cGAB-1)*kGAB*in));
};

double Lactose::Diffusivity(char IN[],double in) {

    if (stricmp(IN,"None") == 0) {
        IN = "Temperature";
        in = Temperature;
    }

    return 1*Porosity*(0.0017255*(in+273.15)-0.2552)/10000;
};

double Lactose::RH() {
    return AirProps::RH();
};

double Lactose::RH(char INa[],double a,char INb[],double b){
```

```
    if ((stricmp(INa,"EffectiveMC") == 0) || (stricmp(INb,"EffectiveMC")==0)) {
        if ((stricmp(INb,"EffectiveMC") == 0)) {
          char * INc = INb;
          double c;
          c = b;
          INb = INa;
          b = a;
          INa = INc;
          a = c;
        }
        if ((stricmp(INb,"None")==0)) {
          INb = "PercentAmorph";
          b = PercentAmorph;
        }
        if ((stricmp(INa,"EffectiveMC") == 0) && (stricmp(INb,"PercentAmorph")==0)) {
          double Try1=0,Try2=1,MCalc=1,aw;
          while (fabs(MCalc-a)>1e-15) {
            aw=(Try1+Try2)/2;
            MCalc = MoistureContent("RH",aw,INb,b);
            if ((MCalc-a)<0) {Try1 = aw;}
            else {Try2 = aw;}
          }
          return aw;
        }
    }
    else return AirProps::RH(INa,a,INb,b);
};

double Lactose::LumpingStrength() {
    return 15929.447*MoistureContent();
};
```

A5.5 AIRPROPS UNIT:

A5.5.1 AIRPROPS.H:

```
//*************************************************************************
//
//***** ****************** AirProps.H ************************************
//
// A class for characterisation of air properties at atmospheric pressure.
//
// This class defines the fundamental properties of air as Temperature,
// Pressure and Absolute humidity. All other properties are obtained
// through function calls.
// ************************************************************************

#ifndef AirProps_H_
#define AirProps_H_

class AirProps {

public:
```

```
double  Temperature;                // °C
double  Humidity;                   // kg/kg dry air
const   double     Pressure;        // = 101300 Pa
const   double DryAirSpecHeat;      // = 1006 J/kg°C
const   double WaterVapSpecHeat;    // = 1875 J/kg°C
const    double GasConstant;        // = 8.413 J/mol°C
const    double LatentHeat;         // = 2.5e6 J/kg

AirProps(char[],double,char[],double); // Class AirProps constructor
void SetAirProps(char ina[], double aa, char inb[], double bb);
                                    //  Sets the Temperature and Humidity
double AirTemperature(char INa[],double a,char INb[]="None",double b=42);
double AirHumidity(char INa[],double a,char INb[]="None",double b=42);
double AirDensity();                // Dry air density kg/m3
double AirDensity(char INA[],double A,char INB[]="None",double B=42);
double VapPressure();               // Vapour Pressure (Pa) from Humidity
double VapPressure(char INA[],double A,char INB[]="None",double B=42);
double SatVapPressure();            // Saturated Vapour Pressure (Pa) from AirTemp
double SatVapPressure(char INA[],double A,char INB[]="None",double B=42);
double RH();                        // RH from Humidity and AirTemp
double RH(char INA_RH[],double A_RH,char INB_RH[]="None",double B_RH=42);
double AirEnthalpy();               // Air Enthalpy J/kg dry air
double AirEnthalpy(char INA[],double A,char INB[]="None",double B=42);

};

#endif   //AirProps_H_
```

A5.5.2 AIRPROPS.CPP:

```
// ***********************************************************
//
// ************************** AirProps.cpp *******************
//
// A class for characterisation of air properties at atmospheric pressure.
//
// This class defines the fundamental properties of air as Temperature,
// Pressure and Absolute humidity. All other properties are obtained
// through function calls.
// ***********************************************************

#include <string.h>
#include <math.h>
#include "Airprops.h"

// ***********************************************************
//
//              AirProps Constructor
//
// ***********************************************************

AirProps::AirProps(char INA[], double A, char INB[], double B) :
    Pressure(1013e2),               // Pa
    DryAirSpecHeat(1006),           // J/kg°C
```

```
    WaterVapSpecHeat(1875),     // J/kg°C
    GasConstant(8.413),         // Nm/mol°C
    LatentHeat(2.5e6) {         // J/kg

    SetAirProps(INA,A,INB,B);

};

void AirProps::SetAirProps(char ina[], double aa, char inb[], double bb) {

    Temperature = AirTemperature(ina,aa,inb,bb);
    Humidity = AirHumidity(ina,aa,inb,bb);
};

// ************************************************************
//
//              Air Humidity Functions
//
// ************************************************************

double AirProps::AirHumidity(char INa[], double a, char INb[] ,double b) {

    double dummyH;

    //******************** Sorting code ************************

    //. rearranges arguments so "Humidity" is last if it is present.
    if (stricmp(INa,"Temperature") == 0) {
        char * INc = INb;
        double c;
        c = b;
        INb = INa;
        b = a;
        INa = INc;
        a = c;
    }

    //. sets INb to "Temperature" if second argument is not given
    if (stricmp(INb,"None") == 0) {
        INb = "Temperature";
        b = Temperature;
    }


    //. checks if INb = "Humidity" and changes it so INa = "Humidity
    if (stricmp(INb,"Humidity") == 0) {
        INa = INb;
        a = b;
    }



    //******************** Calculation code ************************

    //. Humidity
```

```
    if (stricmp(INa,"Humidity") == 0) {
        dummyH = a;
    }

    //. RH and Temperature
    if ((stricmp(INa,"RH") == 0) && (stricmp(INb,"Temperature") == 0)) {
        dummyH = 18.0*a*exp(23.4795-3990.56/(b+233.833))
                /(29.0*(Pressure-a*exp(23.4795-3990.56/(b+233.833))));
    }

    //. AirDensity and Temperature
    if ((stricmp(INa,"AirDensity") == 0) && (stricmp(INb,"Temperature") == 0)) {
        dummyH = 18.0*(273.15/(22.4*(273.15+b)*a)-1/29.0);
    }

    //. Air Enthalpy and Temperature
    if ((stricmp(INa,"AirEnthalpy") == 0) && (stricmp(INb,"Temperature") == 0)) {
        dummyH = (a-DryAirSpecHeat*b)/(WaterVapSpecHeat*b+LatentHeat);
    }

    return dummyH;
};



// ************************************************************
//
//              Temperature Functions
//
// ************************************************************


double AirProps::AirTemperature(char INa[],double a,char INb[] , double b) {

    double dummyTemp;

    //******************* Sorting code ***********************

    //. rearranges arguments so "Humidity" is last if it is present.
    if (stricmp(INa,"Humidity") ==0) {
        char * INc = INb;
        double c;
        c = b;
        INb = INa;
        b = a;
        INa = INc;
        a = c;
    }

    //. sets INb to "Humidity" if second argument is not given
    if (stricmp(INb, "None") == 0) {
        INb = "Humidity";
        b = Humidity;
    }
```

```
    //. checks if INb = "Temperature" and changes it so INa = "Temperature"
    if (stricmp(INb,"Temperature") == 0) {
        INa = INb;
        a = b;
    }

    //****************** Calculation code ***********************

    //. Temperature
    if (stricmp(INa,"Temperature") == 0)  {
        dummyTemp = a;
    }

    // .RH and Humidity imputed from user
    else if ((stricmp(INa,"RH") == 0) && (stricmp(INb,"Humidity") == 0)) {
        dummyTemp = 3990.56/(23.4795-log(29*b*Pressure/(18+29*b)/a))-233.833;
    }

    //. AirEnthalpy and Humidity from user
    else if ((stricmp(INa,"AirEnthalpy") == 0) && (stricmp(INb,"Humidity") == 0)) {
        dummyTemp = (a-b*LatentHeat)/(DryAirSpecHeat+b*WaterVapSpecHeat);
    }

    //. AirDensity and Humidity from user
    else if ((stricmp(INa,"AirDensity") == 0) && (stricmp(INb,"Humidity") == 0)) {
        dummyTemp = (273.15/(a*22.4*(1/29.0+b/18.0)))-273.15;
    }

    //. room for more functions here

    return dummyTemp;
};

// ************************************************************
//
//          AirDensity Functions
//
// ************************************************************

double AirProps::AirDensity() {
    return 1/(22.4*(273.15+Temperature)*(1/29.0+Humidity/18.0)/273.15);
};

double AirProps::AirDensity(char INA[],double A,char INB[],double B) {

    double Humidity_int = AirHumidity(INA,A,INB,B);
    double Temperature_int = AirTemperature(INA,A,INB,B);
    return 1/(22.4*(273.15+Temperature_int)*(1/29.0+Humidity_int/18.0)/273.15);
};


// ************************************************************
//
//          Vapour Pressure Functions
//
```

```
// ********************************************************

double AirProps::VapPressure() {
    return 29*Humidity*Pressure/(18+29*Humidity);
};

double AirProps::VapPressure(char INA[],double A,char INB[],double B) {
    double Humidity_int = AirHumidity(INA,A,INB,B);
    return 29*Humidity_int*Pressure/(18+29*Humidity_int);
};

// ********************************************************
//
//          Saturated Vapour Pressure Functions
//
// ********************************************************

double AirProps::SatVapPressure() {
    return exp(23.4795-3990.56/(Temperature+233.833));
};

double AirProps::SatVapPressure(char INA[],double A,char INB[],double B) {
    double Temperature_int = AirTemperature(INA,A,INB,B);
    return exp(23.4795-3990.56/(Temperature_int+233.833));
};

// ********************************************************
//
//          Relative Humidity Functions
//
// ********************************************************

double AirProps::RH() {
    return VapPressure()/SatVapPressure();
};

double AirProps::RH(char INA_RH[],double A_RH,char INB_RH[],double B_RH) {
    return VapPressure(INA_RH,A_RH,INB_RH,B_RH)
                /SatVapPressure(INA_RH,A_RH,INB_RH,B_RH);
};

// ********************************************************
//
//          Air Enthalpy Functions
//
// ********************************************************

double AirProps::AirEnthalpy() {
    return DryAirSpecHeat*Temperature+Humidity
                *(WaterVapSpecHeat*Temperature+LatentHeat);
};


double AirProps::AirEnthalpy(char INA[],double A,char INB[],double B) {
```

```
    double Temperature_int = AirTemperature(INA,A,INB,B);
    double Humidity_int = AirHumidity(INA,A,INB,B);

    return DryAirSpecHeat*Temperature_int+Humidity_int
                *(WaterVapSpecHeat*Temperature_int+LatentHeat);
};
```